

Novel Methods of Detection and Treatment of *Pseudomonas aeruginosa* Infection in Cystic Fibrosis

**Thesis submitted for the degree of
Doctor of Philosophy
September 2015**

Dr. Rishi Pabary

**MBBS BSc (Hons) MSc MRCPCH
National Heart and Lung Institute
Imperial College, London**

Abstract

Although advances in the management of cystic fibrosis (CF) have led to a significant extension of life expectancy, the disease remains life-limiting. Successive pulmonary infections are the primary cause of morbidity, leading eventually to respiratory failure. *Pseudomonas aeruginosa* (Pa) is the dominant respiratory pathogen but difficulties in detection and increasing failure of conventional treatments to combat established infection mean that an urgent need exists for non-invasive techniques that screen for Pa, particularly in non-expectorating patients, and for novel antimicrobial therapies.

The first part of this thesis aimed to determine whether markers in exhaled breath, measured using selected ion-flow tube mass spectrometry (SIFT-MS), could distinguish between CF patients with and without chronic Pa infection. In what is the largest study to date of well-phenotyped CF patients, I demonstrated that a fingerprint that differentiates according to Pa status does appear to be present in exhaled breath, although the technique is not sufficiently sensitive at present to be used on an individual patient basis.

The second part of this thesis studies the potential of using bacteriophage in the treatment of Pa infection. I have shown that novel bacteriophage cocktails are efficacious *in vitro* against laboratory and clinical Pa strains isolated from CF patients. In a murine model of acute infection, I demonstrate that bacteriophage not only hasten clearance of Pa from the lung but also diminish the associated inflammatory response under certain conditions. Efficacy was demonstrated when bacteriophage was given prophylactically and after established infection, indicating potential utility in a clinical scenario. That bacteriophage remain viable following nebulisation, the preferred route of administration for future human trials, was also ascertained.

Whilst the results are promising, with potential to improve patient outcomes, both strands of work only demonstrate proof-of-concept for the studied strategies. A significant amount of additional work, some already underway, is necessary before either approach can be used in a clinical setting.

Acknowledgements

It has been an absolute privilege to be given the opportunity to undertake my PhD at Imperial College, London and the experience is something that will remain with me for many years to come. I would like to thank my four supervisors, Professor Jane Davies, Professor Andrew Bush, Professor Eric Alton and Professor George Hanna for their steadfast patience, support and guidance throughout the various challenges of this work. I must reserve a special mention for Jane, a true friend, who has shown unswerving belief in my abilities and ideas and is quite simply an inspiration from whom I have learnt an incredible amount in such a short space of time.

I would also like to thank all the staff in the Department of Gene Therapy for creating such a welcoming work environment that was a delight to be a part of. Special mentions must go to Dr. Charanjit Singh, who taught me the technical skills required for the murine experiments, and Dr. Amelia Shoemark who shared her experience and knowledge of electron microscopy techniques so that I could finally visualise the phage with which I had been working for so long. In the Department of Surgery and Cancer at St. Mary's Hospital, Dr. Sacheen Kumar and Dr. Juzheng Huang provided a wealth of knowledge in mass spectrometry which was invaluable.

Clinical studies are not possible without patients. As a paediatrician, it was a new experience and a real pleasure getting to know the adults with cystic fibrosis who showed genuine interest and demonstrated rare altruism in giving up their time for the purposes of my research, even on occasions when they were extremely unwell in hospital, and for this I am extremely appreciative.

I would also like to thank my friends for all their encouragement and for bringing exuberance and fun into my life during the course of this work. Finally and most importantly, I am eternally grateful to my parents for their unwavering support throughout my life; sadly my father passed away during this research and it is a source of great sorrow that he is not here to witness its completion.

Declaration of Originality

I declare that all the work within this thesis is my own unless stated otherwise and that all external sources are appropriately acknowledged.

Table of Contents

Abstract.....	2
Acknowledgements.....	3
Declaration of Originality.....	4
List of Figures	11
List of Tables	17
List of Abbreviations	21
Chapter 1: Introduction.....	24
Section 1.1: Chronic Suppurative Lung Disease and Bronchiectasis.....	24
Section 1.2: Cystic Fibrosis	25
1.2.1: Historical Perspective.....	25
1.2.2: CFTR Structure and Function	26
1.2.3: Classes of CFTR Mutation.....	27
1.2.4: Pathogenesis and Clinical Manifestations of CF	30
1.2.4.1: Sinonasal Disease.....	30
1.2.4.2: Gastrointestinal (GI) Disease	31
1.2.4.2.1: Meconium Ileus and Distal Intestinal Obstruction Syndrome (DIOS).....	31
1.2.4.2.2: Gastro-oesophageal Reflux Disease (GORD)	32
1.2.4.2.3: Pancreatic Disease	32
1.2.4.2.4: Other GI Manifestations in CF.....	33
1.2.4.3: Bone Disease.....	33
1.2.4.4: Other Manifestations of CF.....	34
Section 1.3: Host Defence of the Human Respiratory System	35
1.3.1: Biomechanical Defence and the Mucociliary Escalator	35
1.3.2: Cells of the Innate Immune Response	36
1.3.3: Adaptive Immune Defence of the Lung	37
Section 1.4: Mechanisms of Impaired Host Defence in the CF Lung	38
Section 1.5: Infection in the CF Lung	43
1.5.2: <i>Pseudomonas aeruginosa</i> (Pa).....	45
1.5.2.1: Mucoïd Pa and Biofilms	45
1.5.2.2: Pa and Antibiotic Resistance.....	47

1.5.2.3: Pa, Innate Immunity and CF.....	47
Section 1.6: Diagnosis of Pa Infection in CF.....	49
Section 1.7: Management of CF Lung Disease.....	49
1.7.1: Infection Control.....	50
1.7.2: Airway Clearance Therapies (ACTs).....	50
1.7.3: Mucolytics.....	50
1.7.4: Anti-Inflammatory Approaches.....	51
1.7.5: Antibiotic Strategies.....	52
1.7.6: Licensed Small Molecule Therapy.....	53
1.7.7: Lung Transplantation.....	53
Section 1.8: New and Experimental Therapies for CF.....	54
1.8.1: Gene Therapy.....	54
1.8.2: Experimental Small Molecule Therapy.....	55
1.8.3: Inhibition of Pa Adherence.....	55
1.8.3: Inhibition of Quorum Sensing.....	55
1.8.4: Inhibition of Biofilm Formation.....	56
1.8.5: Attenuation of Inflammatory Response.....	57
1.8.6: pH Restoration of CF Airways.....	58
1.8.7: Vaccination and antibody-based approaches.....	59
1.8.8: Other Novel Strategies for Pa Treatment in CF.....	60
Section 1.9: Context of Experimental Work.....	60
Part I: Novel Detection Methods for <i>Pseudomonas aeruginosa</i> Infection in CF.....	61
Chapter 2: Background.....	61
2.1: Volatile Organic Compounds in Exhaled Breath.....	61
2.2: Endogenous Volatile Organic Compounds and CF.....	62
2.3: Exogenous Volatile Organic Compounds produced by Pa.....	63
2.3.1: 2-Aminoacetophenone (2-AA).....	63
2.3.2: Hydrogen Cyanide (HCN).....	64
2.3.3: Sulphide Compounds.....	66
2.3.4: Other Exogenous VOCs Associated with Pa Infection.....	66
2.4: Exhaled Breath Analysis.....	67
2.4.1: Selected Ion-Flow Mass Spectrometry (SIFT-MS).....	68
2.4.2: Other Techniques for Exhaled Breath Analysis.....	70

2.4.3: Sampling of Exhaled Breath	71
2.4.4: Collection of Exhaled Breath.....	71
2.5: Rationale for Experimental Work, Hypothesis and Aims.....	72
2.5.1: Rationale	72
2.5.2: Hypothesis.....	73
2.5.3: Aims.....	73
Chapter 3: General Materials and Methods	74
3.1: Construction of Sampling Bags	74
3.2: SIFT-MS Analysis of Bag Samples	74
3.3: SIFT-MS Maintenance	75
3.4: Statistical Analysis.....	75
Chapter 4: SIFT-MS – Development of Exhaled Breath Analysis Protocol.....	76
4.1: Pilot Sputum Study.....	76
4.1.1: Materials and Methods.....	76
4.1.2: Results	78
4.1.3: Rationale for Next Stage of Assay Development	80
4.2: Bacterial Culture Experiments – Solid Media	80
4.2.1: Materials and Methods.....	80
4.2.2: Results	82
4.2.3: Rationale for Next Stage of Assay Development	82
4.3: Bacterial Culture Experiments – Liquid Media.....	83
4.3.1: Materials and Methods.....	83
4.3.2: Results	84
4.3.3: Rationale for Next Stage of Assay Development	87
4.4: Quantification of Pure Butanol	87
4.4.1: Materials and Methods.....	87
4.4.2: Results	88
4.4.3: Rationale for Next Stage of Assay Development	89
4.5: Repeatability and Reproducibility of Exhaled Breath Analysis using SIFT-MS.....	90
4.5.1: Materials and Methods.....	90
4.5.2: Results	90
4.5.3: Rationale for Next Stage of Assay Development	96
Chapter 5: Exhaled Breath Analysis of CF Patients and Healthy Controls	97
5.1: Materials and Methods.....	97

5.2: Statistical Analysis.....	100
5.3: Results.....	102
5.3.1: Subject Characteristics.....	102
5.3.2: Full Scan Analysis.....	105
5.3.3: Heatmap.....	106
5.3.4: CFPa+ vs. CFPa-.....	107
5.3.5: CF Patients vs. Healthy Controls.....	111
5.3.6: Exacerbating CF Patients vs. Stable CF Patients.....	114
Chapter 6: Discussion.....	116
6.1: Pilot Sputum Study.....	116
6.2: Bacterial Culture Experiments – Solid and Liquid Media.....	120
6.3: Repeatability and Reproducibility of Exhaled Breath Analysis using SIFT-MS.....	122
6.4: Exhaled Breath Analysis of CF Patients and Healthy Controls.....	124
6.4.1: Conclusions from Breath Study.....	129
Part II: Novel Treatment Approach for <i>Pseudomonas aeruginosa</i> Infection in CF	130
Chapter 7: Bacteriophage Therapy – Background.....	130
7.1: Historical Perspective.....	130
7.2: Bacteriophage Biology.....	131
7.2.1: Classification and Morphology.....	131
7.2.2.: Life Cycle.....	132
7.3: Clinical Applications.....	133
7.4: Bacteriophage and <i>Pseudomonas aeruginosa</i> Infection.....	134
7.5: Advantages and Disadvantages of Phage Therapy.....	135
7.6: Hypothesis and Aims.....	137
7.6.1: Hypothesis.....	137
7.6.2: Aims and Objectives.....	137
Chapter 8: General Materials and Methods.....	138
8.1: Pa Storage.....	138
8.2: Pa Culture.....	138
8.3: Semi-Solid Agar.....	138
8.4: Standard Plaque Assays.....	138
8.5: Phage Cocktails.....	139

Chapter 9: Characterisation of Phage Cocktails.....	140
9.1: Materials and Methods.....	140
9.1.1: Electron Microscopy	140
9.1.2: Transmission Electron Microscopy (TEM).....	140
9.1.3: Negative Staining of Bacteriophage.....	142
9.2: Results.....	143
9.2.1: Phage Cocktails Alone	143
9.2.2: Pa Alone	147
9.2.3: Pa and Phage Cocktail 1	148
9.3: Discussion.....	152
Chapter 10: <i>In vitro</i> Efficacy of Phage Cocktails.....	154
10.1: Materials and Methods.....	154
10.2: Results.....	155
10.3: Discussion.....	157
Chapter 11: Preparation for Non-Invasive Monitoring of Response	158
11.1: Materials and Methods.....	158
11.1.1: Luminescence of Pa Alone	158
11.1.2: Luminescence of Pa and Bacteriophage	159
11.1.3: Fluorescent Pa and Response to Bacteriophage Cocktail	159
11.2: Results.....	161
11.2.1: Luminescence vs. Optical Density.....	161
11.2.2: Luminescence following Bacteriophage Treatment	162
11.2.3: Fluorescence vs. Optical Density.....	168
11.2.4: Fluorescence following Bacteriophage Treatment	170
11.3: Discussion.....	172
Chapter 12: <i>In vivo</i> Efficacy of Phage Cocktail	178
12.1.1: Ethics Statement	178
12.2: Materials and Methods.....	178
12.2.1: Preparation of Pa for Murine Infection.....	178
12.2.2: Dose-Finding Methodology.....	178
12.2.3: Murine Infection Protocol.....	179
12.2.4: Processing of Samples.....	180
12.2.5: Cytokine Analysis	182
12.2.6: Statistical Analysis	183

12.3: Results.....	183
12.3.1: Simultaneous Administration of Bacteriophage and Pa	183
12.3.2: Delayed Administration of Bacteriophage (Post Pa-Infection).....	191
12.3.3: Prophylactic Administration of Bacteriophage	193
12.3.4: Administration of Bacteriophage Cocktails Alone	197
12.3.5: Cytokine Comparisons	199
12.3.6: Cytokine Correlations.....	200
12.4: Discussion.....	202
12.5: Conclusions from <i>in vivo</i> Work	209
Chapter 13: <i>In vitro</i> Efficacy of Phage Cocktails Following Nebulisation.....	210
13.1: Materials and Methods.....	210
13.2: Results.....	214
13.3: Discussion.....	217
Chapter 14: Efficacy of Phage Cocktails against CF Sputum	219
14.1: Materials and Methods.....	219
14.2: Results.....	221
14.3: Discussion.....	223
Summary and Future Directions	227
References.....	236
Appendix	270
A1: Consent form for Collection of Exhaled Breath and Sputum (Version 4 – 04/FEB/2014).....	270
A2: Graphs of Absorbance and Fluorescence (starting optical densities 0.25, 0.5 and 1.0)	271
A3: Insert from MesoScale Discovery Multiplex Kit for Cytokine Measurements.....	274
A4: Examples of Standard Curves Generated from MesoScale Discovery Plates October 2012....	287
A5: SOP for Absolute Quantification of Bacteriophage Following Nebulisation	294
A6: Abstracts arising from Thesis.....	299
A7: Papers arising from Thesis.....	300

List of Figures

Figure 1.2.2.1:	Schematic of CFTR	26
Figure 1.2.3.1	Schematic showing classes of CFTR mutation	30
Figure 1.3.2.1:	Schematic showing cascade of events by which bacteria induce neutrophil sequestration	37
Figure 1.5.1:	Changing prevalence of common respiratory pathogens in CF with age	44
Figure 1.5.2.1.1:	Schematic showing probable steps of biofilm formation	46
Figure 2.4.1.1:	Schematic of SIFT-MS	69
Figure 3.1.1:	Schematic showing construction of Nalophan™ bags	74
Figure 4.1.1:	Inoculation of a streak plate	77
Figure 4.1.2:	Graphs showing significant differences in four VOCs in headspace above plated sputum when compared to empty PSA plates	79
Figure 4.2.1.1:	Structure of copper ethylacetoacetate and 4,4'-methylenebis (N,N-dimethylaniline)	80
Figure 4.2.1.2:	Chemical reactions observed with cyanide detection paper	81
Figure 4.2.1.3:	Example of cyanide detection paper kept over a 96-well plate to detect differing amounts of cyanogenesis by various strains of Pa	81
Figure 4.3.2.1:	VOCs detected in headspace above different strains of Pa cultured in liquid media compared to VOCs in headspace above TSB alone	85
Figure 4.3.2.2:	VOCs detected in headspace above PA12B-4973 cultured in liquid media compared to VOCs in headspace above TSB alone	86
Figure 4.3.2.3:	Sequential rise in HCN detected in headspace above TSB and SM buffer	87
Figure 4.4.2.1:	Detection of butanol by SIFT-MS above sequentially increasing concentrations of >99.1% 1-butanol	88
Figure 4.4.2.2:	Sequentially increasing butanol detection in headspace above successive control samples	89
Figure 4.5.2.1:	CoV for VOCs measuring in sequentially exhaled breaths using SIFT-MS	92

Figures 4.5.2.2a/b:	Measured VOC concentrations in sequential exhaled breaths on four different days	93
Figure 4.5.2.3a:	Measured VOC concentrations in sequential exhaled breath samples taken following an overnight fast and thirty minutes after the fast was broken	94
Figure 4.5.2.3b:	Measured VOC concentrations in sequential exhaled breath samples taken following an overnight fast and thirty minutes after the fast was broken	95
Figure 5.1.1:	Photograph of exhaled breath collection from a control subject	99
Figure 5.3.1.1:	Box-and-whisker plot (Tukey) showing significant reduction in % predicted FEV ₁ in CFPa+ subjects compared to CFPa- subjects	103
Figure 5.3.1.2:	Box-and-whisker plot (Tukey) showing significant reduction in BMI in CFPa+ subjects compared to healthy controls	104
Figure 5.3.2.1:	Full scan spectra from a CF patient analysed using (a) H ₃ O ⁺ precursor ion, (b) NO ⁺ precursor ion and (c) O ₂ ⁺ precursor ion	105
Figure 5.3.3.1:	Heatmap showing VOC concentrations for each subject	106
Figure 5.3.4.1:	Box-and-whisker plots (Tukey) demonstrating significant differences in butanol, dimethyl disulphide and 2-AA in the exhaled breath of CFPa+ and CFPa- patients. No difference demonstrated in mouth-exhaled HCN	108
Figure 5.3.4.2:	Box-and whisker plot (Tukey) showing significantly lower FEV ₁ in CFPa- patients receiving nebulised therapy	109
Figure 5.3.4.3a:	ROC curve for CFPa+ vs. CFPa- patients with only three VOCs that differed significantly between groups used in the binary regression model	109
Figure 5.3.4.3b:	ROC curve for CFPa+ vs. CFPa- patients with all twelve analysed VOCs used in the binary regression model	109
Figure 5.3.5.1:	Box-and-whisker plots (Tukey) demonstrating significant differences in acetone, hydrogen sulphide, isoprene and pentanol in exhaled breath of CF patients and healthy controls	112
Figure 5.3.5.2a:	ROC curve for healthy controls vs. CF patients with only four VOCs that differed significantly between groups used in the binary regression model	113
Figure 5.3.5.2b:	ROC curve for healthy controls vs. CF patients with all twelve analysed VOCs used in the binary regression model	113

Figure 5.3.6.1:	Box-and-whisker plots (Tukey) demonstrating differences in ethanol, HCN, 2-AA and isoprene in exhaled breath of exacerbating and stable CF patients	115
Figure 6.1.1:	Human metabolic pathway for ethanol	118
Figure 7.2.1.1:	Schematic showing morphological classification of bacteriophage	131
Figure 7.2.2.1:	Schematic showing replication cycles of lytic and lysogenic phage	133
Figure 9.1.1.1:	Schematic of a transmission electron microscopy	141
Figure 9.1.1.2:	Photograph of transmission electron microscope at RBH	141
Figure 9.2.1.1:	Morphological differences in head and tail on TEM of phage cocktail 1	144
Figure 9.2.1.2:	TEM of multiple phage from cocktail 1	144
Figure 9.2.1.3:	Morphological differences in head and tail on TEM of phage cocktail 2	145
Figure 9.2.1.4:	TEM of differing morphology and multiple phage from cocktail 2	145
Figure 9.2.1.5:	Morphological differences in head and tail on TEM of phage cocktail 3	146
Figure 9.2.1.6:	TEM of differing morphology and multiple phage from cocktail 3	146
Figure 9.2.2.1:	TEM of clinical strain of Pa selected for <i>in vivo</i> use	148
Figure 9.2.2.2:	TEM of PAO1 at lesser magnification than phage from cocktail 1	148
Figure 9.2.3.1:	TEM of PAO1 and phage cocktail 1, 2hrs after being mixed	149
Figure 9.2.3.2:	TEM at higher magnification at 2hrs; phage particles visible within PAO1	149
Figure 9.2.3.3:	Further TEM of PAO1 and phage cocktail 1, 2hrs after being mixed	150
Figure 9.2.3.4:	High magnification TEM at 2hrs with phage congregated around indistinct bacterial cell and at 4hrs with multiple phage visible inside and outside the cell wall	150
Figure 9.2.3.5:	TEM of PAO1 and phage cocktail 1, 4hrs after being added together	151
Figure 9.2.3.6:	TEM showing pouching out of bacterial cell wall	151
Figure 10.2.1:	Photographs showing inhibition of Pa growth with bacteriophage cocktails	156
Figure 11.2.1.1:	Example of IVIS LivingImage picture produced when photographing 24-well plates containing luminescent PAO1	161
Figure 11.2.1.2:	Linear relationship between luminescence and optical density for a genetically modified strain of PAO1	162

Figure 11.2.2.1:	Graph showing luminescence of PAO1 (initial OD of 1), 6hrs after treatment with three bacteriophage cocktails at three concentrations	163
Figure 11.2.2.2:	Graph showing luminescence of PAO1 (with an initial OD of 1), 24hrs after treatment with three bacteriophage cocktails at three concentrations	163
Figure 11.2.2.3:	Graph showing luminescence of PAO1 at different optical densities prior to addition of 50µl of neat bacteriophage cocktails	165
Figure 11.2.2.4:	Graph showing luminescence of PAO1 at differing optical densities after 24hrs incubation at 37°C	166
Figure 11.2.2.5:	Graph showing luminescence of PAO1 at differing optical densities after 48hrs incubation at 37°C	166
Figure 11.2.2.6:	Graph showing luminescence of PAO1 at different optical densities 24hrs after addition of 50µl of three bacteriophage cocktails	167
Figure 11.2.2.7:	Graph showing luminescence of PAO1 at different optical densities 48hrs after addition of 50µl of three bacteriophage cocktails	168
Figure 11.2.3.1:	Standard plaque assay for iRFP PAO1	169
Figure 11.2.3.2:	Linear relationship between fluorescence and optical density for a genetically modified strain of PAO1 (iRFP)	169
Figure 11.2.4.1:	Graphs showing absorbance and fluorescence over time for wild-type and iRFP PAO1 with starting optical densities of 0.05 and 0.1, with and without treatment with bacteriophage cocktail	171
Figure 11.3.1:	Bacterial growth curve	174
Figure 12.2.4.1:	Schematic of Neubauer haemocytometer	181
Figure 12.3.1.1:	Differential cell counts from BAL performed at 48hrs in mice inoculated with 2.5×10^6 of a clinical strain of Pa and simultaneously treated with 20µl bacteriophage cocktail or SM buffer	184
Figure 12.3.1.2:	Differential cell counts from BAL performed at 48hrs in mice inoculated with 2.5×10^6 of PAO1 and simultaneously treated with 20µl bacteriophage cocktail or SM buffer	185
Figure 12.3.1.3:	Example of mouse BALF under 40x light magnification	185

Figure 12.3.1.4:	Differential cell counts from BAL performed at 48hrs in mice inoculated with 5×10^6 of PAO1 and simultaneously treated with 20 μ l bacteriophage	186
Figure 12.3.1.5:	Pro-inflammatory cytokines from BAL at 48hrs in mice inoculated with 2.5×10^6 of a clinical strain of Pa and simultaneously treated with 20 μ l bacteriophage cocktail or SM buffer	188
Figure 12.3.1.6:	Colony counts/ml from BAL performed at 24hrs in mice inoculated with 2.5×10^7 PAO1 and simultaneously treated with 20 μ l bacteriophage cocktail or SM buffer	189
Figure 12.3.1.7:	Differential cell counts from BAL performed at 24hrs in mice inoculated with 2.5×10^7 of PAO1 and simultaneously treated with 20 μ l bacteriophage cocktail or SM buffer	190
Figure 12.3.1.8:	Significant difference in two pro-inflammatory cytokines from BAL at 24hrs in mice inoculated with 2.5×10^7 of PAO1 and simultaneously treated with 20 μ l bacteriophage cocktail or SM buffer	192
Figure 12.3.2.1:	Colony counts/ml from BAL performed at 48hrs in mice inoculated with 2.5×10^7 PAO1 and treated with 20 μ l bacteriophage cocktail or SM buffer (controls) 24hrs post-infection	191
Figure 12.3.2.2:	Differential cell counts from BAL performed at 24hrs in mice inoculated with 2.5×10^7 of PAO1 and treated with 20 μ l bacteriophage cocktail or SM buffer (controls) 24hrs post-infection	192
Figure 12.3.2.3:	Significant difference in two pro-inflammatory cytokines from BAL at 24hrs in mice inoculated with 2.5×10^7 of PAO1 and treated with 20 μ l bacteriophage cocktail or SM buffer (controls) 24hrs post-infection	193
Figure 12.3.3.1:	Colony counts/ml from BAL performed at 24hrs in mice inoculated with 2.5×10^7 PAO1 following pre-treatment with 20 μ l bacteriophage cocktail or SM buffer (controls) 48hrs prior to infection	194
Figure 12.3.3.2a:	PSA plates following BALF culture	195
Figure 12.3.3.2b:	Positive splenic cultures for samples C9-C11 (controls) but not growth from spleen of mouse T12	195

Figure 12.3.3.3:	Differential cell counts from BAL performed at 24hrs in mice inoculated with 2.5×10^7 PAO1 following pre-treatment with 20 μ l bacteriophage cocktail or SM buffer (controls) 48hrs prior to infection	196
Figure 12.3.3.4:	Significant reduction in KC from BAL performed at 24hrs in mice inoculated with 2.5×10^7 PAO1 following pre-treatment with 20 μ l bacteriophage cocktail or SM buffer (controls) 48hrs prior to infection	197
Figure 12.3.4.1:	Differential cell counts from BAL performed at 48hrs in mice inoculated with 20 μ l bacteriophage cocktail 1, 2 or 3 or SM buffer (controls)	199
Figure 12.3.5.1:	Pro-inflammatory cytokines from BAL performed at 48hrs in mice inoculated with either 2.5×10^6 or 5×10^6 PAO1 and simultaneously treated with 20 μ l bacteriophage cocktail or SM buffer (controls)	200
Figure 13.1.1:	Flowchart showing nebuliser protocol for Pari LC Plus and Aeroeclipse II	212
Figure 13.1.2:	Experimental nebuliser set-up	212
Figure 13.1.3:	Flowchart showing nebuliser testing protocol for eFlow rapid	213
Figure 13.2.1a/b:	Sensitivity of PAO1 to phage 2 and phage 3	216
Figure 13.2.2:	Box-and-whiskers plot (Tukey) showing change in phage 3 titres over time with nebulisation	218
Figure 14.2.1:	Ongoing efficacy of phage cocktail 1 against PAO1 when given with RhDNase	221
Figure 14.3.1:	Photograph showing difference in phage efficacy when used in conjunction with RhDNase	224
Figure A2.1:	Graphs showing absorbance and fluorescence over time for wild-type and iRFP PAO1 with starting optical densities of 0.25, with and without treatment with bacteriophage cocktail	271
Figure A2.2:	Graph showing absorbance and fluorescence over time for wild-type and iRFP PAO1 with starting optical densities of 0.5, with and without treatment with bacteriophage cocktail	272
Figure A2.3:	Graph showing absorbance and fluorescence over time for wild-type and iRFP PAO1 with starting optical densities of 1.0, with and without treatment with bacteriophage cocktail	273

List of Tables

Table 2.3.4.1:	Selected VOCs that are associated with Pa infection	67
Table 2.4.2.1:	Advantages and disadvantages of experimental techniques used for exhaled breath analysis	70
Table 4.1.2.1:	Summary of pilot data with VOCs measured using the H ₃ O ⁺ precursor ion	78
Table 4.1.2.2:	Summary of pilot data with VOCs measured using the NO ⁺ precursor ion	79
Table 4.1.2.3:	Summary of pilot data with VOCs measured using the O ₂ ⁺ precursor ion	79
Table 4.2.2.1:	Levels of HCN detected in headspace above three strains of Pa	82
Table 4.3.2.1:	Levels of ammonia, butanol, HCN and 2-AA detected in headspace above different strains of Pa cultured in liquid media compared to controls	84
Table 4.3.2.2:	Levels of ammonia, butanol, HCN and 2-AA detected in headspace above PA12B-4973 cultured in liquid media compared to controls	85
Table 4.3.2.3:	Levels of ammonia, butanol, HCN and 2-AA detected in headspace above TSB alone (controls) in different experiments	86
Table 4.4.2.1:	Butanol detection by SIFT-MS above increasing concentrations	88
Table 4.5.2.1:	Median CoV [range] for VOCs in exhaled breath measured using SIFT-MS	91
Table 4.5.2.2:	Median [range] of VOC concentrations in ppbv in five sequentially exhaled breaths taken from a healthy control subject before and after breaking an overnight fast	94
Table 4.5.3.1:	Raw data for five sequential breath samples (taken pre- and post-lunch) analysed using SIFT-MS	96
Table 5.1.1:	Analytical chemistry information of VOCs analysed in exhaled breath	100
Table 5.3.1.1:	Subject characteristics of 100 subjects who provided exhaled breath samples for analysis using SIFT-MS	103
Table 5.3.4.1:	Median [IQR] of 12 VOCs in ppbv measured in the exhaled breath of CF patients with and free of Pa infection	107

Table 5.3.4.2:	Median [IQR] of 12 VOCs in ppbv in exhaled breath of CF patients free of Pa infection (CFPa-) who were either not on any anti-Pa therapy or were receiving regular nebulised treatment	108
Table 5.3.5.1:	Median [IQR] of 12 VOCs in ppbv measured in exhaled breath of CF patients and healthy controls	111
Table 5.3.6.1:	Median [IQR] of 12 VOCs measured in exhaled breath of exacerbating and stable CF patients	115
Table 6.2.1:	Magnitude of 2-AA detection using SIFT-MS in bacterial culture work compared to previous headspace analysis studies using SIFT-MS	121
Table 10.2.1:	Dilutions at which bacteriophage cocktails were effective <i>in vitro</i> against five clinical and one laboratory strain of Pa	155
Table 10.3.1:	<i>In vitro</i> antibiotic susceptibility of five clinical strains of Pa used for phage sensitivity assays	157
Table 11.2.1.1:	Luminescence readings at each optical density for PAO1 (n=6)	161
Table 11.2.2.1:	Colony counts after plating serially diluted PAO1 broths with an initial OD of 1 onto PSA, 24hrs after treatment with bacteriophage cocktail	164
Table 11.2.3.1:	Fluorescence readings at each optical density for PAO1 (n=6)	169
Table 12.3.1.1:	Inflammatory cells and differential in BALF at 48hrs of mice infected with 2.5×10^6 PAO1 or a clinical strain of Pa and simultaneously administered either bacteriophage or SM buffer (controls)	184
Table 12.3.1.2:	Inflammatory cells and differential in BALF at 48hrs of mice infected with 5×10^6 PAO1 and simultaneously administered either bacteriophage or SM buffer (controls)	186
Table 12.3.1.3:	Levels of pro-inflammatory cytokines in BALF at 48hrs from mice infected with 2.5×10^6 PAO1 or a clinical strain of Pa and simultaneously administered either bacteriophage or SM buffer (controls)	187
Table 12.3.1.4:	Levels of pro-inflammatory cytokines in BALF at 48hrs from mice infected with 5×10^6 PAO1 and simultaneously administered either bacteriophage or SM buffer (controls)	188

Table 12.3.1.5:	Inflammatory cells and differential in BALF at 24hrs from mice infected with 2.5×10^7 PAO1 and simultaneously administered either bacteriophage or SM buffer (controls)	189
Table 12.3.1.6:	Levels of pro-inflammatory cytokines in BALF at 24hrs from mice infected with 2.5×10^7 PAO1 and simultaneously administered either bacteriophage or SM buffer (controls)	190
Table 12.3.2.1:	Inflammatory cells and differential in BALF at 48hrs from mice infected with 2.5×10^7 PAO1 and administered either bacteriophage or SM buffer (controls) 24hrs post-infection	192
Table 12.3.2.2:	Levels of pro-inflammatory cytokines in BALF at 48hrs from mice infected with 2.5×10^7 PAO1 and administered either bacteriophage or SM buffer (controls) 24hrs post-infection	192
Table 12.3.3.1:	Inflammatory cells and differential in BALF at 24hrs from mice infected with 2.5×10^7 PAO1 following administration of either bacteriophage or SM buffer (controls) 48hrs prior to infection	195
Table 12.3.3.2:	Levels of pro-inflammatory cytokines in BALF at 24hrs from mice infected with 2.5×10^7 PAO1 following administration of either bacteriophage or SM buffer (controls) 48hrs prior to infection	196
Table 12.3.4.1:	Inflammatory cells and differential in BALF at 48hrs from mice inoculated with 20 μ l bacteriophage cocktail 1, 2 or 3 or SM buffer (controls)	198
Table 12.3.4.2:	Levels of pro-inflammatory cytokines in BALF at 48hrs from mice inoculated with 20 μ l bacteriophage cocktail 1, 2 or 3 or SM buffer (controls)	199
Table 12.3.6.1:	Spearman r correlation co-efficients (cytokines and inflammatory cell counts)	201
Table 12.5.1:	Key results from BALF in phage-treated mice when compared to control mice under five different infection conditions	209
Table 13.2.1:	Dilutions down to which bacteriophage cocktail efficacy was demonstrated following passage through three different nebuliser systems	214
Table 13.2.2:	Change in phage titres after 15 minutes nebulisation (for LCP/AE) or at the end of nebulisation (eFlow)	216

Table 14.2.1:	Organisms isolated from sputa of inpatients (n=40) on Foulis Ward	221
Table 14.2.2:	Sensitivity of CF sputa treated with SM buffer alone, bacteriophage cocktail alone and of Pa strains isolated from these sputa on plaque assay	222
Table 14.2.3:	Sensitivity of CF sputa treated with SM buffer alone, bacteriophage cocktail alone or bacteriophage cocktail + RhDNase and of Pa strain isolated from these sputa on plaque assay	223

List of Abbreviations

2-AA	2-Aminoacetophenone
AAT	α 1-antitrypsin
ABC	ATP-binding cassette
ACT	Airway clearance therapy
ANOVA	Analysis of variance
ASL	Airway surface liquid
ATP	Adenosine triphosphate
AUC	Area under curve
BAL	Bronchoalveolar lavage
BALF	Bronchoalveolar lavage fluid
BSA	Bovine serum albumin
cAMP	Cyclic adenosine monophosphate
CBAVD	Congenital bilateral absence of the vas deferens
CFPa+	CF patients with chronic <i>Pseudomonas aeruginosa</i> infection
CFPa-	CF patients free of <i>Pseudomonas aeruginosa</i> infection
CO	Carbon monoxide
COPD	Chronic obstructive pulmonary disease
CoV	Coefficient of variation
CF	Cystic fibrosis
CFRD	CF-related diabetes
CFTR	Cystic fibrosis transmembrane conductance regulator
CFU	Colony forming units
CSLD	Chronic suppurative lung disease
DAMPs	Damage-associated molecular patterns
DIOS	Distal intestinal obstruction syndrome
DMDS	Dimethyl disulphide
DNA	Deoxyribonucleic acid

EBC	Exhaled breath condensate
ELISA	Enzyme-linked immunosorbent assay
EM	Electron microscopy/micrograph
ENaC	Epithelial sodium channel
FDA	US Food and Drug Administration
FEV ₁	Forced expiratory volume in one second
FS	Full scan
g	Gauge
GC-MS	Gas-chromatography mass spectrometry
GI	Gastrointestinal
GORD	Gastro-oesophageal reflux disease
HCN	Hydrogen cyanide
HRCT	High resolution computerised tomography
HS	Hydrogen sulphide
IFN	Interferon
IgG	Immunoglobulin G
IgM	Immunoglobulin M
IL	Interleukin
IQR	Interquartile range
KC	Keratinocyte chemoattractant
LPS	Lipopolysaccharide
LTB ₄	Leukotriene B ₄
MC+s	Microscopy, culture and sensitivity
MIM	Multiple ion monitoring
MIP-2	Macrophage inflammatory protein-2
mRNA	Messenger RNA
MSD	Membrane-spanning domain
<i>m/z</i>	Mass-to-charge ratio
NBD	Nucleotide-binding domain
NE	Neutrophil elastase

NK	Natural killer
nm	Nanometer
NO	Nitric oxide
ORCC	Outwardly rectifying chloride channel
Pa	<i>Pseudomonas aeruginosa</i>
PAMPS	Pathogen-associated molecular patterns
PCD	Primary ciliary dyskinesia
PCL	Periciliary layer
PEP	Positive expiratory pressure
PERT	Pancreatic enzyme replacement therapy
PFU	Phage forming units
PKA	Protein kinase A
ppbv	Parts-per-billion by volume
PSA	<i>Pseudomonas</i> -specific agar
PTR-MS	Proton transfer reaction mass spectrometry
RBH	Royal Brompton Hospital
RNA	Ribonucleic acid
ROC	Receiver operating characteristic
RSV	Respiratory syncytial virus
s	Seconds
SIFT-MS	Selected ion flow tube mass spectrometry
TEM	Transmission electron microscopy/micrograph
TGF- β	Transforming growth factor beta
TLR	Toll-like receptor
TNF	Tumour necrosis factor
Treg	T-regulatory
TSB	Tryptone soy broth
VOC	Volatile organic compound

Novel Methods of Detection and Treatment of Infection in Cystic Fibrosis

Chapter 1: Introduction

Section 1.1: Chronic Suppurative Lung Disease and Bronchiectasis

Chronic suppurative lung disease (CSLD) is the term applied to a number of respiratory conditions the unifying symptom of which is a persistent wet cough (1), often productive of sputum. CSLDs include cystic fibrosis (CF), primary ciliary dyskinesia (PCD) and non-CF bronchiectasis, which itself has a wide range of underlying aetiologies (2). A hallmark of CSLDs is increased susceptibility to chronic and recurrent respiratory infections which, if not treated promptly and aggressively, can subsequently lead to bronchiectasis, which is characterised by chronic neutrophilic inflammation (3).

Bronchiectasis is defined as “irreversible dilatation and thickening of the airways” (4) and results from destruction of bronchial and peribronchial tissue following bronchial obstruction and inflammation, which usually occurs secondary to successive respiratory infections or localised anatomical obstruction to an airway. It is a radiological diagnosis, which is confirmed by high resolution CT scan (HRCT) of the chest, usually performed because of persistently abnormal plain chest radiographs but, more controversially, as a routine means of monitoring disease progression in CSLD, particularly CF (5-9). Bronchiectasis was previously considered to be irreversible but there is increasing evidence that early changes suggestive of bronchiectasis in children (airway dilatation) can resolve (10); 26% of children had resolution of airway wall thickening and dilatation on serial HRCT scans in a recent study (11). Infective exacerbations in paediatric CSLD occur following periods of clinical stability. They are characterised by a constellation of symptoms including increased cough and sputum production, decreased exercise tolerance and reduced appetite (12) although attempts to establish a gold standard definition criteria have been unsuccessful and, as there remains no consensus, variability in reporting and clinical practice remains (13).

This is important as prompt recognition and aggressive treatment of infective exacerbations may reduce neutrophilic inflammation in the lungs, thereby decreasing incidence and preventing progression of bronchiectasis which in turn can achieve symptom control, maintain lung function (14, 15) and improve quality of life (16). However, even in cases where therapy is commenced, 25% of children with CF fail to recover baseline lung function after an exacerbation, with greater degree of decline in spirometry prior to hospital admission associated with worse outcomes (17). Similar findings are noted in adults with CF where female sex, malnourishment and time between exacerbations are identified as additional risk factors for failure to regain baseline lung function (18, 19). Decline in respiratory function over time is currently therefore inevitable in CSLD as, even with optimal care, risk of infection is both ubiquitous and unavoidable.

Section 1.2: Cystic Fibrosis

1.2.1: Historical Perspective

CF, as a multi-system disorder with a constellation of respiratory and gastrointestinal symptoms, was first described by Dorothy Andersen in 1938 (20) but it is thought that perhaps the first reference to the disease dates back to 1606 when Alonso y de los Ruyzes de Fonteca stated “woe to that child which kissed on the forehead tastes salty; he is bewitched and will soon die” (21). CF is the commonest autosomal recessive disease in the Northern European population with 1 in 2500 live births being affected in the UK (22) and 1 in 25 individuals being carriers (23) which equates to approximately 300 new cases per annum in the UK (24, 25). Since October 2007, newborn screening for CF by bloodspot analysis of immunoreactive trypsin has been offered to all babies born in the UK; if this is elevated, a further diagnostic algorithm is then followed (26). The protein encoded for by the CF gene, cystic fibrosis transmembrane conductance regulator (CFTR), was identified in 1989 (27-29), four years after the locus was mapped to chromosome 7q31 (30, 31). It is mutations in this *CFTR* gene, of which over 2000 have since been identified (although less than 200 are considered to be definitely disease-generating (32)), that are the molecular basis of CF (33-35).

1.2.2: CFTR Structure and Function

CFTR is a glycoprotein composed of 1480 amino acids (36) that belongs to the ATP-binding cassette (ABC) family of transmembrane proteins (37). ABC proteins facilitate active transport of molecules across cell membranes, a process that is driven by binding of adenosine triphosphate (ATP) to their nucleotide-binding domains (NBD) (38). All ABC transporters have two components; the NBD and the membrane-spanning domain (MSD). CFTR is unique in the ABC family because it has an additional R (regulatory) domain that contains multiple phosphorylation sites which can influence channel activity (39, 40). The R domain links two MSDs, which form a selective transmembrane chloride channel (38, 41), and two NBDs (42). This is schematically shown in Figure 1.2.2.1.

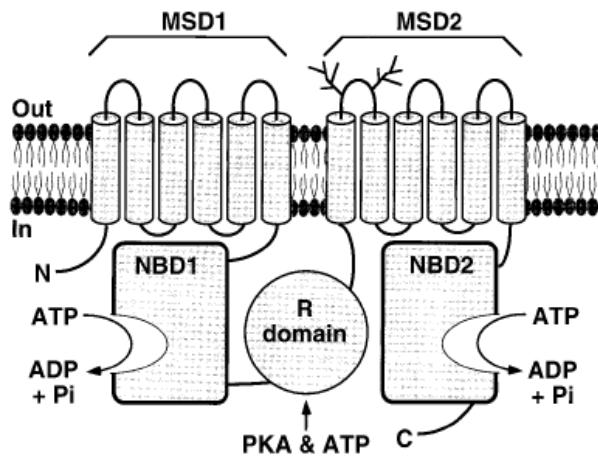


Figure 1.2.2.1: Schematic of CFTR. Two six-segment MSDs are linked to two NBDs by the R domain which is phosphorylated prior to channel opening by cyclic AMP (cAMP) dependent protein kinase A (PKA).

Protein phosphatases that dephosphorylate the R domain are responsible for returning CFTR to quiescence.

Image reproduced from (31)

Movement of chloride ions via CFTR is dependent on both phosphorylation of the R domain by protein kinase A (and, to a degree, protein kinase C) and CFTR-induced ATP hydrolysis (38, 43). CFTR also contributes to bicarbonate transport, both directly and indirectly (44, 45), and has indirect effects on cellular ion homeostasis through regulation of other ion channels within the cell membrane including the epithelial sodium channel (ENaC) (46, 47) and outwardly rectifying chloride channels (ORCC) (48). The pathophysiology of CF is therefore complex and, given the contrasting roles of epithelia in which CFTR is found, organ-specific manifestations of dysfunction exist. In the sweat glands for example, impaired chloride reabsorption leads to abnormally salty sweat with high chloride content; this is the basis of the pilocarpine-iontophoresis sweat test, first described by

Gibson and Cook (49). Sweat chloride >60mmol/L was historically considered pathognomonic but it is now known that CF is not an “all or nothing disease” (50) and, whilst making the diagnosis is usually straightforward, there are a number of patients with non-classical CF that present a diagnostic dilemma. This variation in CF phenotype is partly explained by the sheer number of mutations in the *CFTR* gene that have been identified, but exact mechanisms underlying certain disease manifestations remain unclear. Twin studies (51) suggest that modifier genes (52) or polymorphisms influence *CFTR* function, accounting for some of the discord that exists between CF genotype and phenotype (53-55), even in patients that have identical mutations, whilst polymorphisms in non-*CFTR* genes including α 1-antitrypsin (56) and mannose-binding lectin (57) have been associated respectively with milder and more severe CF pulmonary disease.

Environmental influences such as socioeconomic status and availability of specialist care (58) and chance effects such as acquisition of respiratory infections at a young age (59) also affect the development and progression of CF lung disease. Despite these factors, genotype is important as *CFTR* mutations can be classified into six groups, based on their molecular mechanisms and likely functional consequences of dysfunction (55, 60, 61) such as pancreatic dysfunction (which is more predictable from genotype than extent of respiratory disease) or a degree of residual ion transport being present. However, as only five of more than 2000 known mutations occur at a frequency of greater than 1% on at least one allele in patients diagnosed with CF (62), accurate inferences about likely clinical manifestations cannot always be made.

1.2.3: Classes of *CFTR* Mutation

I. Defective Biosynthesis

Class I (nonsense) mutations are large deletions or frameshifts that encode premature stop codons, resulting in production of truncated, unstable protein which is rapidly cleared from the cell by messenger RNA (mRNA) decay (63). As virtually no *CFTR* exists at the apical cell

membrane, these are severe mutations. Examples include G542X (p.Gly542x) (64, 65) and W1282X (p.Trp1282X), both of which are common in the Ashkenazi Jewish population (66).

II. Abnormal Processing and Trafficking

In class II mutations, CFTR is incorrectly folded (abnormal processing), most often due to abnormalities in glycosylation (55, 67), and degradation occurs prior to the protein arriving at the apical cell membrane (abnormal trafficking). Class II mutations include Δ F508 (Phe508Del), the commonest mutation worldwide (62), and are associated with a severe phenotype. Unlike class I mutations, some mutant CFTR may reach the apical cell membrane (68) and maintain residual function. Interventions that overcome abnormalities in processing, prevent degradation by the endoplasmic reticulum or improve trafficking of misfolded CFTR therefore appeal as potential therapeutic targets (69-71).

III. Defective Channel Regulation or Gating

Class III mutations affect ATP binding at the NBDs, preventing ATP hydrolysis which is necessary for the channel to function, although CFTR is processed and trafficked as normal to the apical cell membrane. The commonest class III mutation is G551D (p.Gly551Asp), accounting for around 3.1% of all mutations in the United Kingdom (62, 72). Compared to wild-type CFTR, the open probability of G551D is diminished to around 1% (73). The basic defect in class III mutations should theoretically be easier to correct than mutations where CFTR is not present at the cell membrane; this has been confirmed *in vitro* (74) and recent studies of the small molecule Ivacaftor have demonstrated efficacy in phase III clinical trials (75, 76). Class III mutations are generally associated with a severe phenotype.

IV. Defective Chloride Conductance

Class IV defects, some of which are due to missense mutations in MSD1, alter CFTR protein structure, leading to restricted movement of chloride ions through the channel (41). Like

class III mutations, there is a normal amount of CFTR but unlike class III mutations there is residual function; class IV mutations are thus associated with a milder phenotype and patients are often pancreatic sufficient (77). R117H (p.Arg117His) is an example of a class IV mutation; this affects splicing of exon 9 and is influenced by the polymorphic polythymidine sequence (5, 7 or 9 thymidines) that precedes the splicing receptor site (78). R117H only causes disease under certain circumstances even when another CF-causing mutation is present in *trans* (79) and has a particular association with isolated congenital bilateral absence of the vas deferens (CBAVD) (80).

V. Reduced Synthesis and Trafficking

Class V mutations are associated with atypical splicing of mRNA (81) or mutations that prevent full glycosylation and trafficking of CFTR (55, 82). As some residual CFTR is expressed in the apical membrane, these mutations typically display a milder phenotype. Examples of class V mutations are A455E (p.Ala455Glu) and P574H (p.Ile148LeufsX5), both of which are associated with pancreatic sufficiency (82).

VI. Increased Turnover

Class VI mutations have a truncation of the C-terminal of CFTR, leading to normal biosynthesis and trafficking but severe instability and accelerated degradation of the mature channel at the apical cell membrane (83). Examples of class VI mutations are Q1412X (p.Gln1412X) and 4326delTC (p.Cys1400X), both of which are associated with a severe CF phenotype (55, 83).

Many mutations belong to more than one class; for example Phe508del, whilst primarily considered a class II mutation, also demonstrates defective channel regulation (class III), explaining the rationale behind use of CFTR potentiators (Section 1.7.6) in treatment (84), and decreased stability (class VI).

A schematic diagram showing normal CFTR and the mutation classes is shown in Figure 1.2.3.1.

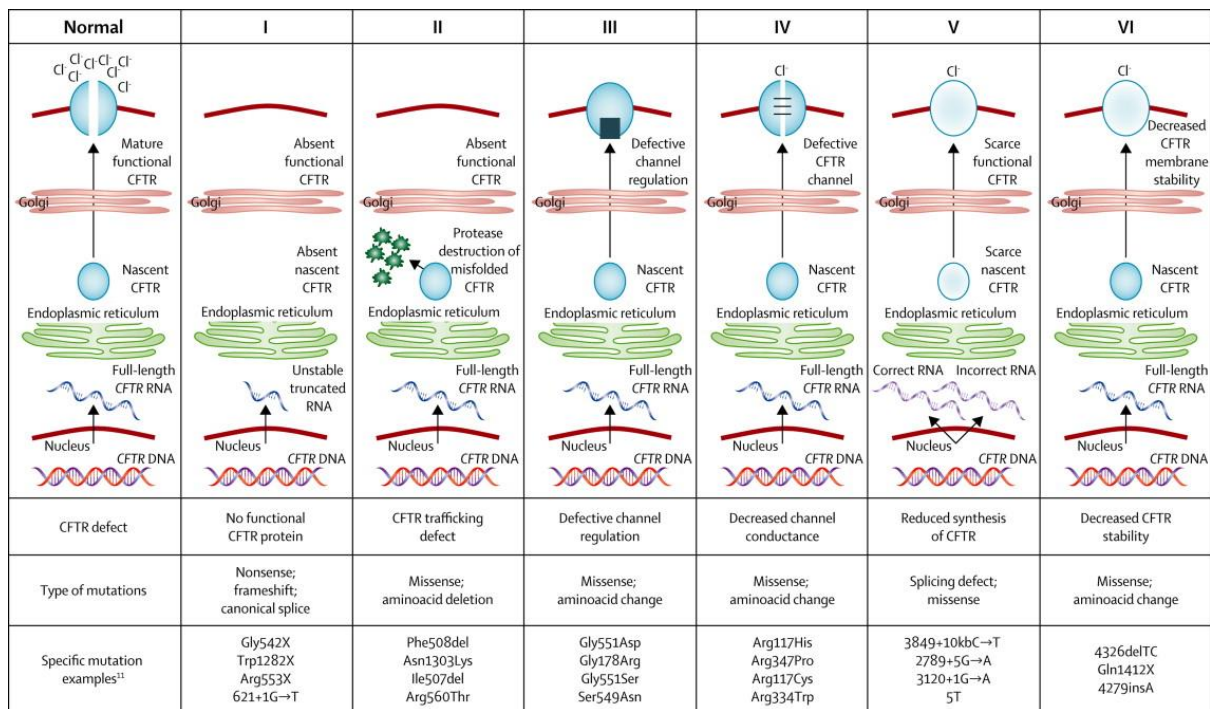


Figure 1.2.3.1: Schematic Diagram Showing Classes of CFTR Mutation. Reproduced from (85)

1.2.4: Pathogenesis and Clinical Manifestations of CF

CFTR mutations have variable expression, such that CF genotype does not accurately predict the pattern or severity of clinical disease. Most morbidity and mortality in CF is secondary to lung disease (86), the pathogenesis and management of which will be discussed in detail in subsequent sections.

1.2.4.1: Sinonasal Disease

Upper and lower airway epithelial surfaces are similar, suggesting that pathophysiology of lung and sinonasal disease may be related. However, prevalence of rhinosinusitis is more than twice as high in carriers of a CFTR mutation compared with the general population (87) and, as there is no increase in lower respiratory symptoms in this group, other mechanisms are likely involved. Sinus disease may precede lung disease in children with CF (88, 89) and recent studies using the CF pig model have demonstrated defective ion transport and sinus hypoplasia in newborn piglets (88, 90). This fits with the finding that radiological sinonasal disease is virtually ubiquitous in CF patients (91), although less

than 10% report symptoms (92), perhaps due to overriding gastrointestinal and respiratory features being present. Symptoms of sinonasal disease include nasal obstruction, chronic rhinorrhoea, recurrent headaches and anosmia (91). Nasal polyps occur in up to 48% of patients (93). As with lower respiratory pathogens, bacteria isolated from the sinuses vary with patient age, although concordance between the two sites is poor (94). Despite this, two-way exchange of bacteria between the sinuses and lungs has been demonstrated (95), suggesting that aggressive medical therapy or sinus surgery, particularly prior to lung transplantation, might prevent chronic infection, although this has not yet been proven (96).

1.2.4.2: Gastrointestinal (GI) Disease

1.2.4.2.1: Meconium Ileus and Distal Intestinal Obstruction Syndrome (DIOS)

Between 10-15% of CF patients present in the newborn period with meconium ileus (97) which may be detected antenatally from a second trimester antenatal ultrasound demonstrating echogenic bowel (98). The pathophysiology is not fully understood but likely related to CFTR dysfunction in the secretory intestinal epithelium causing dehydration of intraluminal contents and mechanical obstruction of the small bowel (97). Babies present with symptoms of bowel obstruction; conservative treatment with gastrograffin enema may be successful (99) but surgery is often required, though this does not usually affect long-term outcomes (100). A similar proportion of older CF patients develop faecal obstruction of the distal small bowel, termed distal intestinal bowel obstruction (DIOS), for which constipation is a differential diagnosis. Pathophysiology of DIOS is similar to meconium ileus although pancreatic insufficiency (97) and reduced intestinal motility (101) are also implicated and previous abdominal surgery is a risk factor (102). Management is usually medical (copious fluids and laxatives) with surgery indicated in non-responsive cases to prevent bowel perforation.

1.2.4.2.2: Gastro-oesophageal Reflux Disease (GORD)

GORD is up to eight times more common in patients with CF than in the general population (103), but the mechanisms remain unclear. Increased intrathoracic and abdominal pressure due to forced expiration and cough is a likely mechanical cause (104) but a high prevalence in babies without respiratory symptoms (105) suggests that GORD is also likely to be a primary phenomenon in CF (106) due to factors such as increased frequency of lower oesophageal sphincter relaxation and prolonged gastric emptying time (103). Standard CF treatments such as high fat diet, pancreatic enzymes and postural drainage (103, 107) may exacerbate GORD, although a study from our centre found no association with infant physiotherapy (108). Symptoms of GORD include vomiting, dysphagia, regurgitation, chronic cough and hiccups (107). GORD can aggravate respiratory symptoms in CF by inducing aspiration or bronchospasm. Management is usually medical but patients may require surgical intervention such as Nissen's fundoplication in severe cases.

1.2.4.2.3: Pancreatic Disease

In the pancreas, chloride secretion is impaired because CFTR function is defective and, due to the secondary effect on flow of sodium and water, thick mucus forms which blocks the pancreatic duct and prevents enzymes reaching the small intestine, causing nutrient malabsorption and, over time, destruction of pancreatic tissue (109). This leads to exocrine pancreatic insufficiency, affecting between 80-90% of patients with CF, that requires lifelong treatment with pancreatic enzyme replacement therapy (PERT). With progressive damage, inadequate bicarbonate secretion by the pancreas causes intraduodenal pH to become acidic, leading to inactivation of enzymes and denaturing of bile salts. This impairs lipid absorption and explains why supplementation of fat soluble vitamins (A, D, E and K) is essential in CF patients. Destruction of the pancreatic islet cells also causes insulin deficiency and the development of CF related diabetes (CFRD) over time; this is not usually present from birth but is increasingly being recognised due to improved survival (110) and routine screening from childhood (111). CFRD has features of both Type I and Type II diabetes

mellitus (112) as glucose metabolism is influenced by clinical factors unique to CF including chronic malnutrition and infection, liver dysfunction, insulin resistance and glucagon deficiency (110) whilst pancreatic destruction over time causes progressive insulin deficiency. 38% of asymptomatic adolescents demonstrate abnormal glucose metabolism and approximately 50% of adults will have CFRD by the age of 30 (113). CFRD is associated with deterioration in respiratory and nutritional status though improved screening and institution of aggressive early treatment with insulin has led to a narrowing of mortality differences in CF patients with and without diabetes (114). This is likely because, even in the pre-diabetic period when hyperglycaemia is minimal, respiratory and nutritional decline are well described (115).

Acute pancreatitis is also associated with CFTR dysfunction and has been described predominantly in patients without other manifestations of classical CF such as pancreatic insufficiency (116)

1.2.4.2.4: Other GI Manifestations in CF

20% of patients with CF develop rectal prolapse; other GI complications include intussusception and volvulus (117). Hepatobiliary manifestations include focal biliary fibrosis, fatty infiltration of the liver and macronodular cirrhosis (118) and there is an increased risk of GI malignancy, for reasons that are not yet completely clear (119). An iatrogenic complication is fibrosing colonopathy that has been associated with high-dose PERT (120). GI features of CF have been reviewed (121).

1.2.4.3: Bone Disease

Low bone mineral density in CF was first reported in 1979 and 20-34% of adults have age-adjusted standard deviation bone density scores of less than -2 z-scores which is associated with an increased risk of pathological fractures (122). Pathophysiology of bone disease in CF is multifactorial, likely related to glucocorticoid use, vitamin D and K malabsorption, physical inactivity and chronic systemic inflammation (122). Furthermore, counter to earlier studies, it is now thought that CFTR is expressed in bone (123); this indicates that bone disease is an intrinsic part of CF, explaining why even very young children can present with osteopaenia (124). With CF patients living longer, treatment with

oral and intravenous bisphosphonates that can increase bone mineral density is likely to become increasingly necessary (125).

1.2.4.4: Other Manifestations of CF

In addition to the systems described previously, like any other chronic disease, CF can have psychological manifestations, often from a young age (126). Fertility is affected; 98% of men with CF have CBAVD resulting in azoospermia but, with advances in assisted reproductive techniques, are able to father children (127). Suboptimal fertility in women with CF is multifactorial; increased tenacity of the cervical mucus and suboptimal nutrition are implicated but natural conception is possible, particularly if lung function, glycaemic control and nutrition are optimised (128). It is important to note that, despite increasing knowledge of the pathophysiology and significant advances in the management of all aspects of CF disease over the past thirty years, median age of survival is still only 43.5 years (129). As mentioned previously, although CF is a multisystem disorder, the vast majority of morbidity and mortality is due to lung disease which is predominantly the consequence of successive airway infections and the downstream consequences thereof. This is the focus of the next section and of the experimental work in this thesis.

Section 1.3 Host Defence of the Human Respiratory System

Before describing the pathophysiology of CF lung disease, it is important to first place this in context by briefly discussing normal host defence.

1.3.1: Biomechanical Defence and the Mucociliary Escalator

The human respiratory tract is responsible for conducting air from the atmosphere to the terminal bronchioles and alveoli where gas exchange takes place. Effective mechanical and biochemical barriers exist throughout the respiratory tract to protect it from the constant insults to which it is exposed from the environment. The majority of inhaled particles are filtered by the nose which also humidifies and warms air (130). Like much of the respiratory tract, pseudo-stratified columnar ciliated epithelium lines the nasal mucosa (131) and goblet cells, which secrete mucus, are found interspersed within this epithelium. Mucus is separated from the cilia by a periciliary layer (PCL) (132, 133); together these constitute the airway surface liquid (ASL). Whilst mucus is effective at trapping inhaled particles and contains antibacterial proteins such as IgA and lactoferrin that directly inactivate or destroy pathogens (130, 134), innate host defence also depends on movement of this mucus layer. Effective movement of the mucus requires not only co-ordinated beating of the cilia, which is compromised in conditions such as PCD and in smokers (135), but also homeostasis of the PCL; the optimal height of this is $\sim 7\mu\text{m}$, which is maintained by a combination of sodium reabsorption and chloride secretion (136). Newer research suggests that this model of the mucociliary escalator might be simplistic, as mucus exists as a tangled mesh above the cilia (137), rather than as a discrete layer, although its role in innate immunity of the respiratory tract remains indisputable. Working in conjunction with mucociliary clearance (MCC) are the actions of coughing and sneezing; both are initiated by sensory receptors in the nose, bronchi and trachea which, when stimulated by irritants, communicate with higher centres in the brain, to trigger the reflexes that propel mucus and foreign particles out of the airways at high velocity (138).

1.3.2: Cells of the Innate Immune Response

Pulmonary innate immunity is orchestrated by respiratory epithelial cells that line the conducting airways. In addition to creating a tight physical barrier with the underlying stroma, they also secrete a vast number of host defence molecules including β -defensins, cathelicidin LL37 and surfactant proteins A and D, both at baseline and when exposed to pathogens and toxins (139). Such responses can influence "professional" immune cells; for example, increased secretion of the protein Foxa3 by epithelial cells in response to rhinovirus infection has been shown to induce cytokines IL-33 and IL-17 (140) and enhance the adaptive immune response (Section 1.3.3), whilst dysregulation of this pathway is associated with recurrent infections in CF (139). The respiratory epithelium and innate immunity has been reviewed (139).

Mucosal defence in the human lung is augmented by cellular mechanisms. Alveolar macrophages are the resident immune cells that initiate phagocytosis and orchestrate host cellular defence by release of cytokines and chemokines. These signalling molecules include IL-8 and IL-12 that respectively simulate neutrophil recruitment and activate natural killer (NK) cells (141) in response to stimuli such as lipopolysaccharide (LPS) in bacterial cell walls or autocrine signals such as TNF- α (142). The neutrophil-mediated innate immune response to bacteria is critical to defence in the human lung and depends on a complex cascade of signalling, summarised in Figure 1.3.2.1. However, excessive accumulation of neutrophils can be detrimental, with ongoing inflammation resulting in lung injury (143) which is of particular relevance in CF. Other cells of pulmonary innate immunity are dendritic cells which are only weakly phagocytic but far more effective at antigen-presenting than alveolar macrophages; this is important for cell-mediated immunity as they bind antigen before migrating to regional lymph nodes where T-cell activation occurs and the humoral (acquired) response to pulmonary infection is initiated (141).

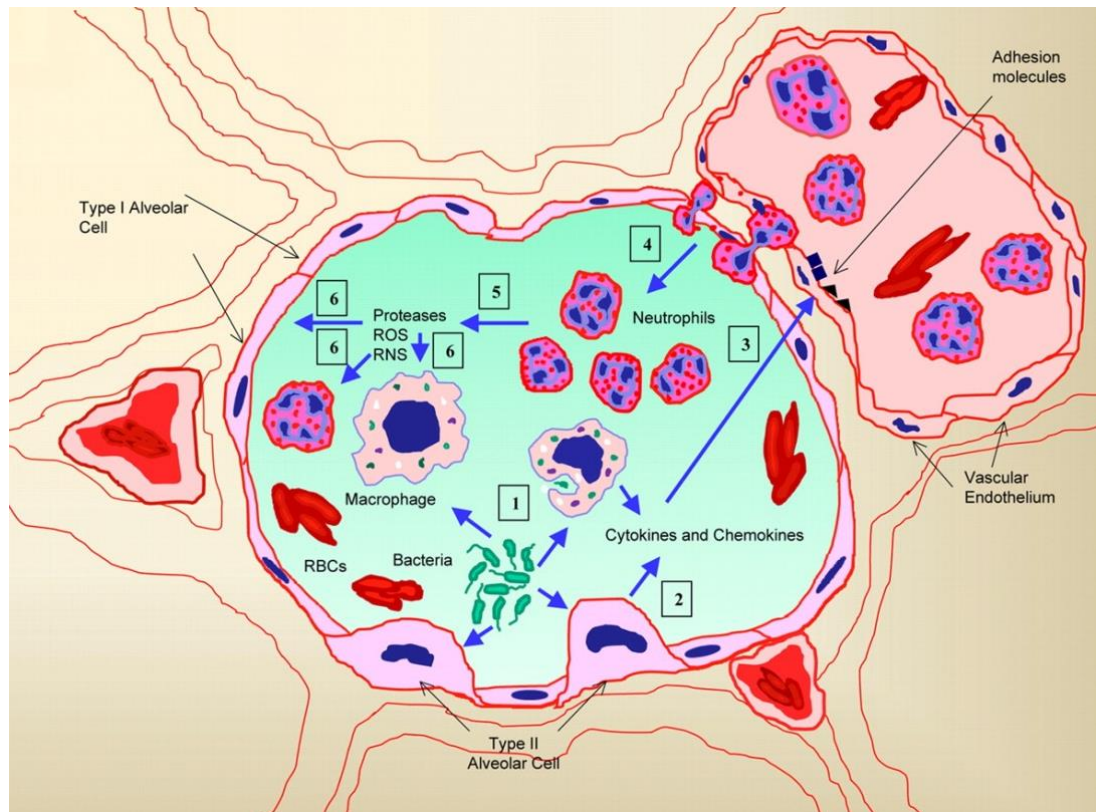


Figure 1.3.2.1: Schematic diagram showing cascade of events by which bacteria induce neutrophil sequestration. (1) Bacteria interact with alveolar macrophages and epithelium (2) inducing cytokine and chemokine production, (3) which upregulate expression of cell adhesion molecules on capillary endothelia (4) mediating migration of neutrophils into the alveolar spaces. (5) Neutrophils produce proteases, reactive oxygen species (ROS) and reactive nitrogen species (RNS) which act on infected cells (6) to cause necrotic cell death. These events eventually lead to extensive lung injury. Adapted from (143).

1.3.3: Adaptive Immune Defence of the Lung

The adaptive immune response depends on interactions between dendritic cells, NK cells and T-cells (144). Antigen presentation by dendritic cells to local lymph nodes leads to activation of naïve CD4 T-cells to either type 1 or 2 (Th1/Th2) responses, which forms the basis of immunological memory. The interaction of NK and dendritic cells, influenced by cytokines such as IL-12 and IL-4, determines which response predominates. Responses to previously encountered pathogens are accelerated in the healthy human lung due to formation of memory T-cells, which are able to directly migrate to infected tissues, and because prior exposure leads to an increased number of dendritic cells which are immediately able to respond to infection. This immune response is modulated by regulatory T-cells (Tregs) which are a subpopulation of T-cells that prevent autoimmunity and down regulate the

immune response once pathological organisms have been eradicated (145); the exact mechanisms by which Tregs function remain unclear but cytokines such as IL-10 and transforming growth factor β (TGF- β) have been implicated (146). Cell-mediated adaptive immunity in the lung has been reviewed (144).

Section 1.4: Mechanisms of Impaired Host Defence in the CF Lung

Although the exact mechanisms relating lung disease to CFTR dysfunction continue to be debated, it is clear that innate host defence mechanisms are impaired in the CF lung, leading to persistent infection and inflammation. Historically, the two prevailing theories for the mechanisms underlying CF lung disease were the low volume and high salt hypothesis, the former now being most widely favoured:

1. Low Volume Hypothesis (147, 148)

The PCL separates mucus from the cilia in the lung and has an optimum depth of 7 μ m, which is maintained by a combination of sodium reabsorption and chloride secretion (136). Cell culture experiments show that ASL absorption is increased in CF which depletes the PCL and allows penetration of mucus into it, thereby impairing transport, which has been confirmed by *in vivo* studies of mucociliary clearance (149). Defective CFTR mediates this due to: i) loss of chloride secretion and ii) increased sodium absorption via ENaC (usually regulated by CFTR) which together reduces ASL volume whilst maintaining normal tonicity (147). That ENaC over-expressing mice develop CF-like lung disease lends credence to this mechanism (150). In addition, cell cultures show that mucus rheology is also altered by increased ASL absorption, exacerbating retention in the airways and predisposing to infection. Whilst it has been suggested that inflammation may precede infection (151), post mortem findings of retained mucus in CF neonates who died within 48 hours of birth suggests that this is the primary pathologic lesion (148).

Although depletion of the PCL *in vitro* leads to complete failure of mucus transport (148), mucus clearance *in vivo* remains measurable in many CF patients (152), suggesting that other mechanisms exist that are not recapitulated in static culture models. In a novel culture system that mimics the phasic motion and shear stress in the lungs associated with normal tidal breathing, regulation (slowing) of sodium transport is maintained, not by CFTR but by release of ATP into the PCL where it interacts with purinergic receptors. The regulatory effects of phasic motion on adenosine concentration in the PCL also impact chloride secretion through upregulation of calcium-activated chloride conductance (153). Therefore, unlike in static culture models, CF airway epithelia in phasic motion are able to maintain PCL height at 7 μ m and mucus transport is preserved (153).

It is clear that the PCL has regulatory effects on clearance of CF mucus but, if this is in fact preserved by phasic motion, the mechanism for lung disease remains unclear. Lung disease in CF is characterised by exacerbations. Whilst changes in the bacterial microbiome are increasingly implicated in these exacerbations (154), 40% are attributed to viral infections which ultimately cause disease progression and decline in lung function (155). Respiratory viruses are isolated in over 50% of infants with CF who are admitted to hospital with respiratory symptoms, with a six-fold increase in the rate of acquisition of Pa at subsequent follow-up (156). Respiratory syncytial virus (RSV), the commonest respiratory pathogen in infancy that infects virtually all children by the age of two (157), damages respiratory epithelia both directly (to a limited extent) and indirectly, secondary to the effects of neutrophil influx into the airways (158). In addition, RSV depletes volume of the PCL in CF epithelial cells in phasic motion by upregulation of enzymes metabolising ATP (153). It is this "second hit", that knocks out the alternative ATP-driven mechanism for maintaining PCL depth in the CF lung, which is now thought to cause mucus stasis and adherence of bacteria to the airways.

Evidence against PCL depletion being attributable to sodium hyperabsorption is provided by animal models. In CFTR^{-/-} pig epithelia there is reduced chloride and bicarbonate transport but no increase in transepithelial sodium reabsorption or reduction in PCL depth and, in keeping with humans, CF pigs demonstrate a heightened response to amiloride due to lack of chloride conductance as opposed to increased sodium transport (159). Similarly, no difference in sodium transport in response to amiloride is observed in the CF ferret trachea (160) or in nasal or lower airways of CF rats when compared to wild-type animals although, unlike the CF pig, ASL depth in the CF rat and ferret is diminished (161, 162). Taken together, these studies suggest that CFTR, not ENaC, is the primary regulator of the PCL depth and that loss of anion transport rather than sodium hyperabsorption triggers airway disease.

Whilst the low volume hypothesis is now favoured, an important caveat is that, in freshly obtained airway biopsies from CF patients, although reduction in PCL height is observed ($4.52 \pm 0.47\mu\text{m}$ compared with $5.60 \pm 0.28\mu\text{m}$ in controls), $p = 0.06$), PCL height was not currently recommended as an endpoint in clinical trials as large sample sizes would be required for sufficient power to be achieved (163).

2. High Salt Hypothesis (164, 165)

The apical surfaces of epithelial cells cultured from CF subjects demonstrate a deficit in bacterial killing *in vitro* compared to cells cultured from healthy controls. As this is corrected by the addition of water, whilst bathing healthy cells in sodium chloride leads to a loss of bactericidal properties, it has been suggested that innate mucosal immunity, mediated by molecules such as lysozyme and β -defensin-1, is inhibited by high salt levels. It is postulated that CFTR in healthy airways favours sodium chloride reabsorption in excess of water, much like the normal sweat gland, such that the ASL is usually hypotonic, and that failure of this predisposes to infection in CF. However, airway epithelia are more permeable than sweat

glands and, although a number of theories have been suggested as to how ASL hypotonicity is achieved despite this, *in vivo* studies demonstrate that sodium concentration of ASL does not differ between CF infants and healthy controls (166) and that ASL in health is isotonic which would, according to the high salt hypothesis, inhibit defensin activity (148). For these reasons, this proposed mechanism for CF lung disease is now less widely accepted.

Aside from these two theories of the pathophysiology of pulmonary infection in CF, it has been demonstrated that CF airway epithelial cells are less effective in eliminating viral infections, allowing increased replication (167) and airway inflammatory changes that predispose to earlier acquisition of bacterial infections such as *Pseudomonas aeruginosa* (Pa) in children (156) and loss of pulmonary function. It is not clear whether this is a direct consequence of CFTR dysfunction or whether CFTR is a modifier gene for antiviral proteins (167); that there are no obvious defects in immune cell function at sites other than the lung where CFTR is also expressed means that any direct impact of dysfunction in human immunity is difficult to explain. Early animal models such as the CF mouse, although lacking typical lung disease, demonstrate that exaggerated inflammatory responses might be explained by abnormal macrophage signalling pathways (168) while recent work using β -ENaC over-expressing mice suggests airway surface dehydration and subsequent mucociliary dysfunction is associated with early onset airway neutrophilia (169). It has also been shown that low levels of CFTR mRNA are expressed in macrophages, neutrophils and dendritic cells; as these cells differ in CF and non-CF mice, as demonstrated by bone marrow transplant studies, a role in pathophysiology is suggested (170). This is supported by murine studies of conditional inactivation of CFTR in immune cells where prolonged inflammation and ineffective resolution of infection occurs despite these mice demonstrating no other phenotypic features associated with total absence of CFTR (170). These findings of an ongoing response to prior infection might explain why inflammation is seen in seemingly sterile bronchoalveolar lavage (BAL) samples taken from infants with CF (171).

Whilst neutrophils are vital for innate immunity, a persistent response can cause destruction of lung tissue (143) as demonstrated by the presence of neutrophil elastase (NE), a product of activated neutrophils, in BAL being associated with bronchiectasis (11) and decline in lung function in children (172) with CF. Although not always identified, it is likely that infection precedes this inflammatory response, demonstrated by the fact that BAL from neonatal CF pigs, which mimic CF lung disease in humans better than other animal models, does not contain activated neutrophils or inflammatory cytokines such as IL-8 at birth (173). It is likely that a defect in innate immunity exists within the CF lung that drives the inflammatory cascade; when bacteria are introduced into the lungs of CFTR^{-/-} pigs there is impaired clearance in comparison to wild-type pigs (173) which has been attributed to differences in ASL pH (174) inhibiting action of antimicrobial peptides such as human β -defensin-3 and LL-37 (175). ASL in CF pigs is more acidic compared to wild-type pigs; reducing the pH of ASL in wild-type pigs inhibits bacterial killing whilst increasing the pH of ASL in CFTR^{-/-} pigs reverses the defect, providing a causal link for loss of CFTR, which facilitates bicarbonate (HCO_3^-) transport, and deficient host defence (174). This fits with increasing evidence that abnormalities in HCO_3^- transport due to defective CFTR play a key role in the pathophysiology of CF; it has been suggested that loss of HCO_3^- secretion impairs removal of calcium from mucins, preventing normal expansion and leading to stasis of mucus in areas such as the ducts of the pancreas which, in health, secrete large quantities of bicarbonate (176). This theory is given credence by work using CF mice which shows a similar ileal phenotype to humans; it has been shown that ileal mucus in CF mice is denser and more adherent than that in wild-type mice and this can both be normalised by secretion into a higher concentrated sodium bicarbonate buffer and that addition of HCO_3^- to already formed CF mucus almost completely normalises mucus rheology (177).

By contrast, although a pilot study in neonates has demonstrated more acidic pH of nasal ASL in CF (178), this difference is not apparent in older children (aged 3-16) and an earlier study in adults also failed to find any difference between ASL pH in CF patients and healthy controls (179). Studies in CF ferrets also suggest that the role of pH in the pathophysiology of an innate immune defect in CF is

less clear-cut. In this model, ASL height is reduced at birth but mucociliary clearance only becomes impaired after one week. CF ferrets demonstrate reduced antimicrobial activity in bronchoalveolar lavage fluid (BALF) and impaired clearance of Pa (but not *Staphylococcus aureus*) which is not ameliorated by changes in pH or bicarbonate (162). BALF from CF ferrets shows abnormal signalling in various inflammatory and immune pathways including complement and macrophage function and contains elevated levels of IL-8 and TNF- α when compared to wild-type animals, despite BALF bacterial load being similar in both groups (162). These findings indicate that heightened inflammatory responses to bacteria occur shortly after birth and that a specific defect in innate immunity against Pa exists in CF, perhaps explaining why infection with this microorganism becomes so prevalent over time.

Section 1.5: Infection in the CF Lung

Abnormal MCC, mucus rheology and possible impairment of bacterial killing at mucosal surfaces due to CFTR dysfunction predispose to successive pulmonary infections, usually from infancy or early childhood, eventually leading to respiratory failure which is the primary cause of death in CF (180). Typically organisms such as *Staphylococcus aureus* and *Haemophilus influenzae* are associated with early CF infection and it is thought that these, and childhood viruses such as RSV (181), initiate inflammation and damage the epithelial surfaces of the lung, predisposing to increased attachment and infection with other organisms (180), primarily the opportunistic Pa, which is a chronic pathogen in approximately 80% of adult patients with CF (182). The change in prevalence of Pa and other common pathogens with increasing age in CF patients is shown in Figure 1.5.1 (overleaf).

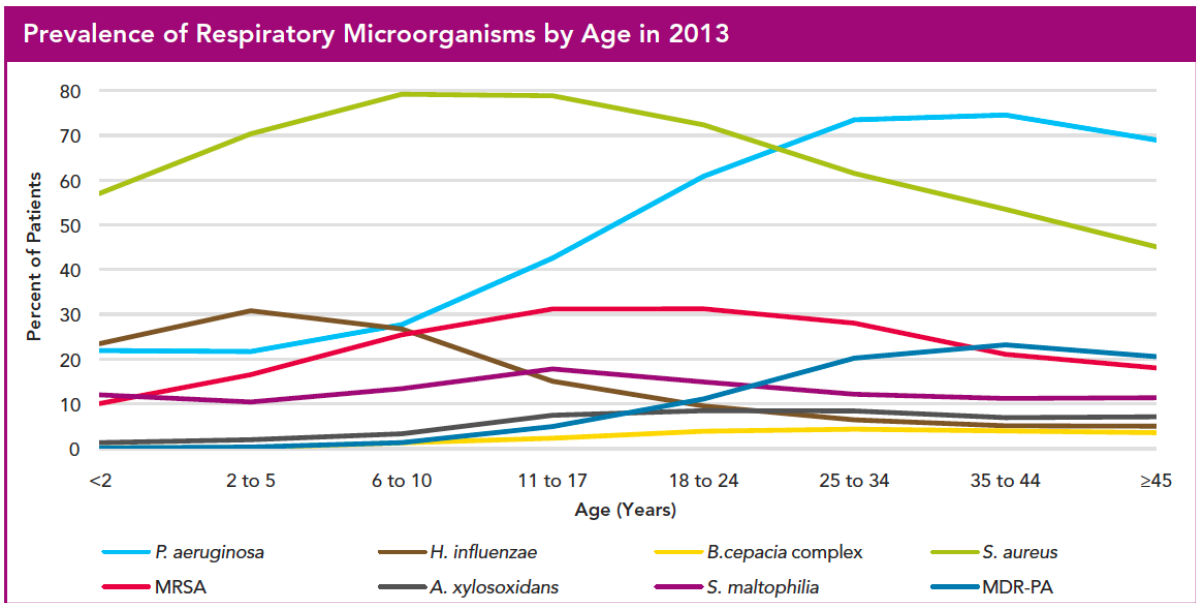


Figure 1.5.1: Changing prevalence of common respiratory pathogens in CF with age. Adapted from (183); UK figures are similar except for significantly higher MRSA prevalence in the USA

Although culture is the microbiological gold standard, only 1% of bacteria can be detected by this means (184); up to 41% of cultures during a pulmonary exacerbation are negative despite the presence of clinical signs and symptoms (185). New molecular sequencing techniques have increased our understanding of the respiratory microbiome such that, having once been considered sterile, it is now known that a diverse microbiota exists in the healthy human lung (186). In CF, loss of this microbial diversity, which likely coincides with ascendancy of pathological bacteria over time and the associated increase in antibiotic use, has recently been linked to decline in lung function (186). A role for bacterial diversity in health, which is still not fully understood, is given credence by the finding that enteral probiotics can reduce frequency of pulmonary exacerbations in CF (187); the mechanism for this remains unclear but may be secondary to translocation of bacteria into the airways or an indirect benefit of reduced inflammation of the intestinal wall.

1.5.2: *Pseudomonas aeruginosa* (Pa)

Pa is the dominant respiratory pathogen in adult CF patients and is associated with increased morbidity and mortality (188). It is a gram-negative rod ubiquitous in the environment, notably in soil and water, which opportunistically infects susceptible patients such as those with indwelling medical devices such as tracheostomies or catheters, immunodeficiency or burns in addition to patients with CF. Motile, planktonic strains of Pa transmitted either from an environmental reservoir or through contact from another carrier are the usual cause of initial infection in CF and can often be eradicated by timely, aggressive therapy (189) but, following a period of intermittent infection of variable duration, most patients ultimately become chronically infected. This is due in part to early detection of Pa infection being problematic in children and adults with mild disease as they are often unable to expectorate sputum and oropharyngeal cultures (for example cough swabs) have poor sensitivity for lower airways pathogens (190); a retrospective review of paediatric bronchoscopies at the Royal Brompton Hospital showed that 20% of children with previously negative microbial cultures isolated Pa on BAL (191). However, Pa infection can still be missed by single or even two-lobe BAL due to regional differences in bacterial infection (192, 193) and, because bronchoscopy is invasive, it cannot be performed repeatedly in children. Serum Pa antibodies can be measured but are generally low at time of first isolation and therefore not considered useful for early diagnosis in our centre, although may have a role in monitoring response to treatment (194). For these reasons, there is an urgent need for a non-invasive tool with which to screen for lower airways infection in CF but, even if this were available, the inherent characteristics of Pa indicate that the problem of chronic infection would remain unless better antibacterial strategies can be devised.

1.5.2.1: Mucoïd Pa and Biofilms

Persistent Pa infection in CF occurs when, in response to triggers such as hypoxia within the CF mucus, genomic mutations occur that induce synthesis of a mucoïd exopolysaccharide matrix (alginate) which shields the bacteria from both phagocytosis (195) and antibiotics (196). This matrix itself is highly pro-inflammatory and lung function in patients tends to be worse in patients who are

infected with mucoid strains of Pa (197). The transition from non-mucoid to mucoid infection is associated with a switch in Pa phenotype from planktonic to a biofilm mode of growth (198). This switch relies on quorum sensing, a complex process of signalling between bacteria which culminates in upregulation of genes necessary for the production of biofilms once a critical mass of bacteria are present (199). Pa in biofilms exist in sessile microcolonies, embedded in an extracellular polymeric matrix and differ from motile Pa in terms of gene transcription and growth rate; colonies tend to be larger, making mucociliary clearance difficult, and less metabolically active (197, 200). Biofilms shield bacteria from the host immune response and antibiotics and, even if antibiotics are effective against Pa in biofilms, highly resistant “persister cells” may remain which repopulate the polysaccharide matrix of the biofilm when antibiotic concentrations decline, leading to recrudescence of infection (201). For these reasons, eradication of mucoid Pa infection is often not possible using conventional therapy. A summary of the stages of biofilm formation is shown in Figure 1.5.2.1.1.

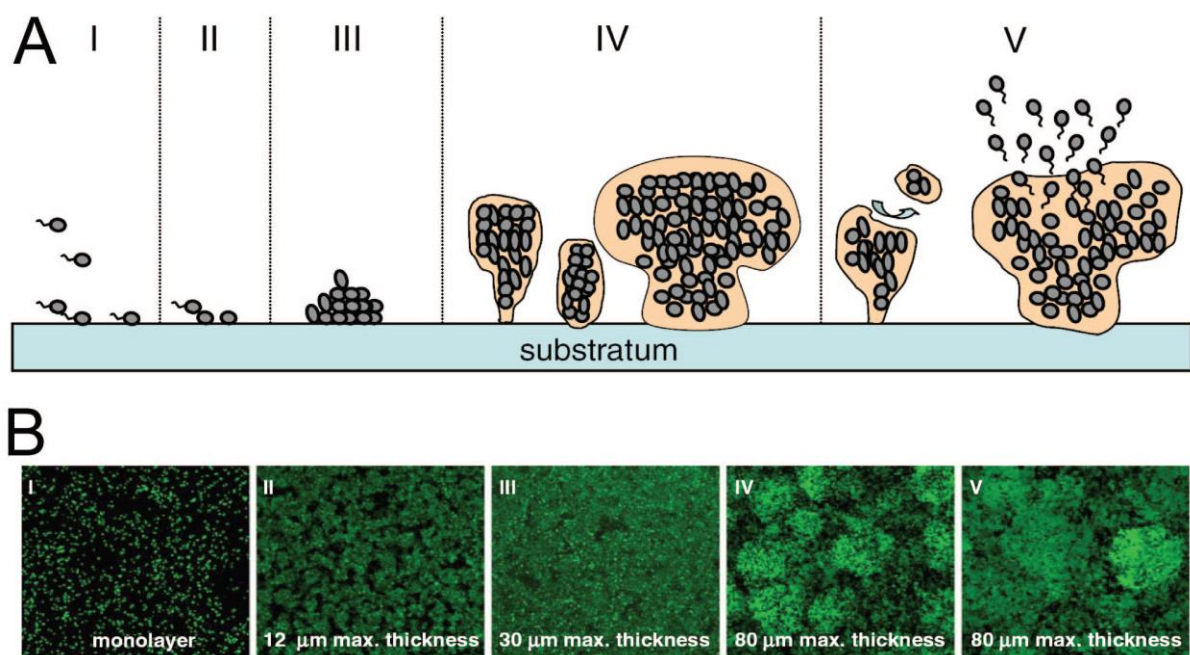


Figure 1.5.2.1.1: Probable steps of biofilm formation. Schematically shown in A with confocal microscopy of fluorescently labelled organisms in B. Single planktonic organisms are inhaled (I) and settle onto the respiratory mucosa (II) and multiple into microcolonies (III). When a critical mass is reached, quorum sensing switches on genes necessary for biofilm formation, which surrounds the now large microcolonies (IV). It is thought that respiratory exacerbations result when the biofilm intermittently breaks down and a shower of organisms is released (V). Reproduced and adapted from (197, 202).

1.5.2.2: Pa and Antibiotic Resistance

Antimicrobial resistance in general has been flagged as a major global health risk by the World Health Organisation (203) and, although initial infection can often be eradicated, Pa is inherently resistant to many classes of antibiotics due to drug efflux pumps that limit antibiotic accumulation within the cell (204, 205). Furthermore, Pa resistance can evolve in the presence of antimicrobial agents; for example, point mutations in the genes coding for deoxyribonucleic acid (DNA) gyrase and topoisomerase IV (target enzymes for quinolone antibiotics such as ciprofloxacin) reduce antibiotic susceptibility over time (206) which itself is often difficult to assess as *in vitro* sensitivity is not reflected *in vivo* (207). These factors, coupled with a decline in spending on research and development of novel antibiotics (208), mean that management of Pa infection in CF remains a challenge. For a full review of Pa and antibiotic resistance mechanisms see (209, 210)

1.5.2.3: Pa, Innate Immunity and CF

Whilst it is clear that an innate immune defect exists in CF, the reasons why Pa becomes the dominant organism in the CF airway remains largely unclear. Historically, it was thought that CFTR is itself an epithelial receptor for Pa that directly regulates infection (211). Recent work has looked at the direct dysregulation of signalling and phagocytosis due to interaction of Pa with CFTR-deficient airway cells and, whilst expression of CFTR in neutrophils remains controversial, a number of other possible pathways have been identified (212). These are discussed in this section; for a comprehensive review of the innate immune response to Pa infection see (213).

Although defective ASL homeostasis and abnormal airway pH in CF are likely to predispose to infection (Section 1.4), a causal link with CFTR dysfunction was only demonstrated recently using synchrotron-based imaging that allows visualisation of the ASL in pig trachea (214). In this study, ASL secretion by submucosal glands was triggered by Pa introduced into the lumen of the pig trachea. ASL secretion was CFTR dependent; in tracheas treated with a CFTR-blocker, no response was seen. As normal ASL secretion is required to wash antimicrobials and mucins from the submucosal glands

into the airway lumen, this might explain why there appears to be an impaired innate response to Pa infection in CF.

It has also been demonstrated that CFTR is expressed in monocytes and that phagocytosis of Pa is reduced in peripheral blood monocytes taken from CF patients and in those where CFTR is chemically inhibited. The underlying mechanism for this likely relates to impaired interaction of monocytes with Pa that has been opsonised by complement, which is thought to play a key role in Pa clearance (215); the alternative activation pathway and complement C3 are necessary for a protective immune response to Pa in mice (216) and an association with polymorphisms in C3 and risk of Pa infection in CF has been described (217). These findings indicate that there may be a direct cause and effect relationship between CFTR dysfunction and susceptibility to Pa infection.

Toll-like receptors (TLRs) have recently been found to play a key role in phagocytosis of Pa by alveolar macrophages (218). Although previously thought to be only a signalling receptor, TLR-5 activation was shown to be crucial for clearance of Pa by alveolar macrophages; non-flagellated Pa and mutants that do not bind to TLR-5 are resistant to phagocytosis. In addition, in TLR-5 knockout alveolar macrophages, there was a reduction in IL-1 β production (which is vital in regulation of endosomal pH and bacterial killing by alveolar macrophages) in response to Pa. TLRs are also expressed in epithelial cells and thus, rather than being an "innocent bystander", it is now thought that the epithelium itself plays a key role in the mucosal inflammatory response (219). Innate immune receptors within the epithelium are able to respond to endogenous damage-associated molecular patterns (DAMPs) such as β -defensin 2 or exogenous pathogen-associated molecular patterns (PAMPs) such as bacterial DNA (220). Murine studies have shown that TLR-4 dependent signalling in the respiratory epithelium is required for bronchoconstriction, neutrophil recruitment and cytokine release in response to Pa infection (221, 222). These TLR roles are thought to be independent of CFTR function but, because of the increased susceptibility to Pa infection in CF, TLR-5 has been proposed as a modifier gene and possible target for future novel therapies (223).

1.6: Diagnosis of Pa Infection in CF

Early identification of Pa infection enables timely aggressive therapy, with the aim of preventing or at least delaying chronic infection, but techniques such as oropharyngeal cultures are relatively insensitive in mild disease where bacterial load may be low (206). Molecular techniques such as polymerase chain reaction (PCR), although still predominantly a research tool, are becoming more widely available and can rapidly quantify Pa (224). However, these methods also identify other species not grown *in vitro*, the significance of which remains unclear. It is apparent that microbial diversity in the CF lung is reduced with increasing age (225), which might be linked to antibiotic treatment (226), and thus determining when and how to treat "infections" identified by these techniques is likely to raise as many questions as answers.

Other methods of diagnosing Pa, such as enzyme-linked immunosorbent assay (ELISA) to identify serum immunoglobulin G (IgG) and immunoglobulin M (IgM) antibodies (227), are effective in detecting chronic infection and response to treatment but no single antigen test detects an antibody response in all infected patients (228) and levels during early infection, although elevated, show a large degree of overlap with healthy controls (229). For these reasons, diagnosis in our centre continues to rely on conventional microbiological techniques with the addition of techniques such as sputum induction that may increase bacterial yield (230, 231).

1.7: Management of CF Lung Disease

Until recently, the aim of management of CF lung disease was to avert or alleviate downstream symptoms that result from retention of tenacious, dehydrated mucus and successive pulmonary infections. Over the past decade, focus has shifted towards targeting and correcting the basic CFTR defect which could, in theory, prevent complications of CFTR dysfunction prior to symptom onset. As a number of different classes of CFTR mutation cause disease (Section 1.2.3), treatments that target the underlying defect may not be applicable to all patients.

1.7.1: Infection Control

Molecular fingerprinting techniques first confirmed cross-infection of CF patients with resistant Pa strains in 1996 (232). Segregation of patients was initially not deemed necessary (233) but has since been associated with a reduction in person-to-person transmission (234). Genotypic surveillance of Pa to enable strict cohorting of patients attending outpatient clinics is recommended to halt spread of epidemic strains (235). In our centre, all CF inpatients are isolated in single cubicles and discouraged from mixing with one another; in practice, particularly with children and teenagers, this is impossible to police. Infection with transmissible Pa strains has been shown to increase rates of hospitalisation and antibiotic use (236) and hence strict infection control measures for all patients and healthcare professionals should always be observed.

1.7.2: Airway Clearance Therapies (ACTs)

ACTs to overcome the effects of dehydrated ASL and impaired mucociliary clearance are considered a fundamental tenet of CF management (237). Respiratory physiotherapists are an integral part of the multidisciplinary team (238), administering therapy directly (percussion and postural drainage) or instructing patients how to perform active breathing exercises and autogenic drainage. A variety of mechanical devices that create positive expiratory pressure (PEP) to aid clearance of secretions are available including Flutter™ and acapella™. No one PEP is demonstrated as being superior to others (239) and, as the techniques are intrusive and time-consuming, regimes should be individualised to maximise compliance (237). However, although attractive to many patients, high-frequency chest wall oscillation (vest) is inferior to PEP techniques and is not recommended as the primary form of ACT in CF (240). Exercise has additional health benefits (preserving bone density for example) and is recommended as an adjunct (not a substitute) for ACT (239).

1.7.3: Mucolytics

Aside from infants and those with very mild disease, most CF patients undertake ACT in conjunction with at least one inhaled mucolytic to maximise mucus clearance. Early studies demonstrated that

bovine deoxyribonuclease reduces viscosity of CF sputum (241) by cleavage of neutrophil DNA and it has since been shown that regular use of nebulised recombinant deoxyribonuclease (rhDNase or Pulmozyme™) improves mucus clearance and lung function and reduces exacerbations (242-244).

As impaired mucociliary clearance is associated with reduction in depth of the PCL of ASL (Section 1.4), rehydrating agents are also effective mucolytics. Inhalation of hypertonic saline creates an osmotic gradient that allows water to be drawn into the airway lumen from the epithelial interstitium, facilitating movement of secretions which is further enhanced by its inherent propensity to induce cough (245, 246). Unlike rhDNase there is no clear long-term clinically significant improvement in lung function although there are clear benefits in quality of life and reduction in pulmonary exacerbations (247), which might also be linked to osmotic sensitivity of mucoid Pa stains (245). Mannitol has a similar mechanism of action to hypertonic saline; it has also been shown to reduce pulmonary exacerbations and also improve lung function in adult patients with CF (248, 249).

1.7.4: Anti-Inflammatory Approaches

A hallmark of CF lung disease is persistent neutrophilic inflammation (Section 1.4) triggered by microbial infection and, although long-term anti-inflammatory therapy with ibuprofen has been shown to slow disease progression in CF (250), it requires careful control of serum levels and has known systemic side effects which mean ibuprofen is not widely used (251). Inhaled corticosteroids are often prescribed, primarily for those patients believed to have concomitant "CF asthma" (252), and were initially thought to have direct anti-inflammatory benefits for all patients with CF (251). However, the CF-WISE study showed that many CF patients were able to discontinue treatment with inhaled corticosteroids without any clinical change (253) and, *in vitro*, glucocorticoids have been shown to **prolong** neutrophil survival (254) which might paradoxically increase inflammation if recapitulated in the airways. Other safety concerns, notably that long-term use disrupts the lung microbiome and may increase incidence of non-tuberculous *Mycobacterium* (NTM) infection, also

exist (255, 256). Similar concerns exist over Azithromycin (257) which reduces pulmonary exacerbations and improves lung function in patients with chronic Pa infection (258, 259), presumably via anti-inflammatory mechanisms as it has no direct antibiotic action against planktonic Pa. It blocks quorum sensing (260) and impairs biofilm growth but a concern is that, once biofilms are established, it might upregulate bacterial adaptive resistance mechanisms (261). However, our own data (unpublished) and a CF registry study demonstrate no link between Azithromycin use and NTM infection (257). Another anti-inflammatory approach is the use of antioxidants such as glutathione (262) and N-acetylcysteine (263) to modulate oxidative stress, a hallmark of neutrophilic airway inflammation, though clinical efficacy has yet to be demonstrated.

1.7.5: Antibiotic Strategies

Prophylactic oral flucloxacillin to prevent infection with *Staphylococcus aureus* is recommended for babies diagnosed with CF in the United Kingdom (but not in USA or most of Europe) for at least the first three years of life (264) though concerns exist that this strategy may increase risk of Pa infection (265). No benefit has been shown with the use of prophylactic anti-pseudomonal antibiotics to prevent initial infection with this organism and the strategy has theoretical drawbacks such as risk of drug toxicity (206). Eradication of early Pa infection is possible and has economic and clinical benefits (266). There is currently a paucity of evidence for what the optimum treatment regimen might be (206, 267) with a multi-centre study currently ongoing in the United Kingdom (TORPEDO-CF, UKCRN ID 7543/EudraCT 2009-012575-10). For patients not recruited to TORPEDO, current paediatric policy in our centre is to treat first Pa isolates with three weeks of oral ciprofloxacin and three months of nebulised colistimethate. If subsequent microbiological cultures are negative, then nebulised treatment is stopped. When Pa is isolated on subsequent occasions, long-term nebulised or inhaled chronic suppressive therapy is initiated. Colistimethate or Promixin is used first-line, alternating monthly with tobramycin if patients have persistent symptoms or lung function decline. Aztreonam lysine for inhalation (AZLI) is a newer nebulised anti-pseudomonal that has been shown

to improve respiratory symptoms and lung function (268) but is less widely used in children, partly because dosing is thrice daily compared with twice daily.

Pulmonary exacerbations in patients who isolate Pa are treated with oral, or a combination of at least two intravenous antibiotics selected on the basis of several factors including sensitivity (though this can differ *in vitro* and *in vivo*), existing knowledge of local epidemic strains, patient characteristics (for example allergic status and individual patient preference) and cost (206). Intravenous therapy is typically for two weeks; due to psychosocial and economic benefits this is increasingly self-administered by adult patients within the home environment (269).

1.7.6: Licensed Small Molecule Therapy

The advent of high throughput screening has made it possible for thousands of small molecules to be rapidly tested in order to identify compounds that correct the basic CFTR defect. Ivacaftor, a CFTR potentiator that enhances opening of the channel, was the first small molecule to demonstrate efficacy in terms of improved lung and CFTR function (assessed by measuring sweat chloride) and is now licenced for use in patients aged six and over with at least one class III mutation (75, 270). A reduction in Pa burden in patients taking Ivacaftor has since been reported; this is likely secondary to improvements in mucociliary clearance with correction of the basic defect although no associated reduction in sputum biomarkers of inflammation was demonstrated (271).

1.7.7: Lung Transplantation

CF is now a leading indication for lung transplant despite historical concerns that systemic immunosuppression on a background of chronic Pa infection would be dangerous (272). Transplantation confers a survival benefit to patients with advanced CF lung disease (273-275) but is not curative. Recurrence of Pa infection is common in transplanted lungs (272), possibly secondary to chronic drainage of organisms from bacterial reservoirs elsewhere in the respiratory tract such as the sinuses (276) and is exacerbated by immunosuppression. In recent case series, five-year survival rates of up to 78% have been reported (273, 274).

1.8: New and Experimental Therapies for CF

The ultimate aim of CF therapy is to correct the basic defect which, theoretically, could ameliorate downstream consequences of CFTR dysfunction, including Pa infection. Whilst progress has been made towards this goal, a need remains for new therapies that target Pa directly; even when conventional antimicrobials are commenced eradication failure rates are high (277), leading to greater risk of subsequent exacerbation (278) and loss of respiratory function. 80% of current patients with CF are chronically infected by the age of 18 and, even if CFTR function could be restored in this group, it is unlikely that this would result in resolution of persistent Pa infection, for which there is currently no definitive cure.

1.8.1: Gene Therapy

Gene therapy which, like small molecules would correct the basic defect in CF but unlike small molecules is not mutation-specific, aims to deliver functional CFTR protein to the respiratory epithelium. As CF is a single gene disorder, gene therapy was an obvious strategy for treatment once the *CFTR* gene was discovered in 1989. Progress has been slow however since early murine studies demonstrated approximately 50% of CFTR function could be restored by nebulised gene transfer (279), due to host defence mechanisms hampering effective gene delivery (280) and concerns about immunogenicity of viral vectors (281). Efficacy of a non-viral cationic lipid vector (GL67A, Genzyme, USA) has been demonstrated (282) and safety using a different CFTR plasmid was established by the UK CF Gene Therapy Consortium in 2011. A recent trial of gene therapy nebulised monthly for one year using this plasmid demonstrated a statistically significant benefit in forced expiratory volume in one second (FEV_1), with stabilisation demonstrated in the treatment group compared to decline in those subjects receiving placebo (283). Studies investigating the potential benefits of using gene transfer vectors with more potency are ongoing.

1.8.2: Experimental Small Molecule Therapy

Ivacaftor (Section 1.7.6) provides proof-of-concept that the basic defect can be overcome and, if this can be achieved early enough in life, the hope is that downstream consequences, including chronic Pa infection, might be averted altogether. However, small molecules targeting non-gating CFTR mutations have so far been less successful. Ataluren (PTC₁₂₄) showed initial promise for class I mutations (284) but a phase III trial failed to reach the primary end-point. CFTR correctors such as VX-809 (Lumacaftor) for class II mutations minimally reduce sweat chloride but with no associated improvement in clinical indices (285). Phase III trials using a combination of a CFTR potentiator and corrector (Ivacaftor and Lumacaftor) in Phe508del homozygotes aged 12 and over demonstrated a modest absolute improvement in lung function, improved weight gain and reduction in pulmonary exacerbations (286). This combination was recently approved under the name Orkambi by the US Food and Drug Administration but in the United Kingdom it is not currently recommended for routine use by the National Institute for Health and Care Excellence (NICE) due to concerns about cost and uncertainty about its long-term impact.

1.8.3: Inhibition of Pa Adherence

Initial Pa infection generally relies on adherence by piliated strains (287) and strategies that impair this, such as silver coating of urinary catheters (288) might inhibit formation of biofilms. β -linked acetylmannan (acemannan) is a polymer that inhibits binding of both mucoid and non-mucoid Pa strains to cultures of human lung epithelia (289). Phosphatidylglycerol, the phospholipid component of surfactant that contributes to mucus adhesiveness and is deficient in CF secretions (290), has also been shown to inhibit Pa adherence in cultured non-CF and CF respiratory epithelium although *in vivo* efficacy has not been demonstrated for either of these strategies.

1.8.4: Inhibition of Quorum Sensing

Quorum sensing, a complex mechanism of bacterial communication, regulates many Pa virulence pathways (291); it is thus a target for novel therapeutic strategies. Garlic, a potent inhibitor of

quorum sensing, increases susceptibility of Pa biofilms to tobramycin *in vitro* and improves clearance of infection in a murine model although is associated with initial inflammation and doses in this study are too high to be tolerated by human subjects (292). "Quorum quenching" activity has also been demonstrated in chamomile, components of algae and bacterial enzymes capable of degrading N-aceylhomoserine lactones, which are key components of quorum sensing signalling (291), though none of these are clinically applicable at present.

1.8.5: Inhibition of Biofilm Formation

In combination with gentamicin, alginate lyase has been shown to enhance elimination of mucoid Pa from biofilms in a continuous flow culture medium possibly representative of CF sputum (293). This was thought to be due solely due to enzymatic degradation of alginate in the biofilm matrix but a recent study indicates that biofilm dispersion is independent of catalysis and rather alginate lyase modulates Pa cellular metabolism, causing cellular detachment and enhancing susceptibility to tobramycin (294). This data suggests that studies of efficacy *in vivo* should investigate synergistic effects of alginate lyase with conventional antimicrobials.

Other substances may also inhibit biofilm formation. Seaweed extracts, particularly juglone, impair biofilm formation in a dose-dependent manner (295) and provided proof-of-concept for OligoG (Algipharma, Norway), a drug derived from Norwegian seaweed which reduces sputum viscosity and disrupts biofilms (296) *in vitro* and is currently in Phase IIb clinical trials as a dry powder for inhalation in patients with CF (ClinicalTrials.gov identifier NCT02157922). Sodium nitrite kills mucoid Pa in murine lungs (297) and reduces Pa biofilm formation in cultured human bronchial epithelial cells (298) at doses well tolerated and achieved by aerosolisation (299) though further work is necessary due to concerns about increased tobramycin and ciprofloxacin resistance (298). Growth of Pa biofilms requires iron (300) and down regulation of genes necessary for Pa biofilm production has been induced by iron chelators *in vitro* (301) which can be nebulised for delivery into the human lung (302). At present, no products specifically for inhibition of biofilm growth are commercially

available, although RhDNase has some effect in the presence of neutrophils (303) and under experimental conditions has been shown to act synergistically with poly(aspartic) acid (304).

1.8.6: Attenuation of Inflammatory Response

Neutrophilic response to chronic Pa infection in CF plays a key role in progressive lung parenchymal damage (143) and strategies that attenuate this response are attractive therapeutic options (Section 1.7.4). Efficacy of recombinant secretory leukoprotease inhibitor (rSLPI), a potent inhibitor of NE, has been demonstrated *in vivo* following aerosolisation. However, it does not accumulate on the surface of the respiratory epithelium and levels required to suppress the significant burden of NE in the CF lung are difficult to achieve (305). Like rSLPI, α 1-antitrypsin (AAT) is an endogenous inhibitor of NE in the human lung; when aerosolised in a small group of CF patients, anti-neutrophil elastase activity was enhanced and increased Pa killing, suggesting an additional benefit in augmenting host defence (306). However, a subsequent randomised controlled trial showed no significant reduction in sputum NE activity following treatment with recombinant AAT with concerns raised about drug delivery in patients with severe disease and possible inactivation of AAT within the proteolytic environment in the CF lung (307). Surprisingly, CF patients with AAT deficiency do not have more severe lung disease (308), suggesting the paradigm of adjunctive therapy to counteract excessive NE is over-simplistic; currently there is no clinical role for nebulised rSLPI or AAT in CF.

Interferon gamma (IFN- γ), a Th1 signature cytokine (309), changes the inflammatory response to Pa infection from neutrophil to macrophage predominant when given intraperitoneally in rats (310), suggesting a role for therapeutic immunomodulation in CF. However, no improvements in lung function or sputum inflammatory markers and bacterial density were seen following thrice weekly nebulisation for twelve weeks in patients \geq 12 years (311). There is increasing evidence of dysfunction in macrophage-pathogen interactions in CF; IFN- γ administered to monocytes derived from peripheral blood of CF patients has recently been shown to offset this by stimulating autophagy, a vital process in eliminating intracellular pathogens such as *Burkholderia cenocepacia*

(312) and attenuating the hyperinflammatory response in CF (313). Small numbers of CF patients with NTM infection currently receive subcutaneous or inhaled IFN- γ and, although there is no consistent benefit, reduction in need for intravenous antibiotics has been demonstrated (314).

An important caveat to the potential of anti-inflammatory strategies is shown by a study investigating inhibition of leukotriene B₄ (LTB₄), a potent neutrophil chemoattractant (315) which induces lung damage in CF. A large randomised controlled trial of BIIL 284 BS, an inhibitor of the LTB₄ receptor, was terminated early when highly significant increases in pulmonary exacerbations and pulmonary adverse events were noted in adults receiving the trial drug. The exact mechanisms for this were unclear but may relate to the fact that, as a consequence of reduced neutrophil chemotaxis in patients with established chronic lung infection, bacterial proliferation increased with a paradoxical elevation in peripheral neutrophil count (316). A murine study where animals infected with Pa and treated with BIIL 284 had higher rates of bacteraemia and pulmonary pro-inflammatory cytokine concentrations compared to those receiving placebo (317) is likely an analogous response. It is possible that suppression of inflammation in CF might only be beneficial at certain stages of disease, as demonstrated in a study of oral prednisolone which showed benefit only in patients who were chronically infected with Pa (318). Immunosuppression early in life could be detrimental as it might hasten onset of chronic infection (319) and this, coupled with concerns that systemic steroids may exacerbate complications such as bone disease and CFRD, explains why prednisolone is not used routinely in CF management.

1.8.7: pH Restoration of CF Airways

Abnormally low ASL pH has been demonstrated in cultured CF bronchial epithelium (320). This causes hyperactivity of ENaC channels in cultures of respiratory epithelium (321), exacerbating mucus dehydration, and inhibits bacterial killing in the porcine lung (174). Alkalinisation with bicarbonate has been shown to reverse these deficits (174, 321). A reduction in Pa density in CF sputum treated with alkalinised hypertonic saline has recently been reported, with stepwise

improvements demonstrated as pH of nebulised saline increased from 5.86 to 6.6 to 7.4 (322). Data from the only *in vivo* study of nebulised sodium bicarbonate therapy in CF has yet to be published (ClinicalTrials.gov identifier NCT00177645).

1.8.8: Vaccination and antibody-based approaches

Early studies of active vaccination for Pa infection in CF demonstrated no benefit (323, 324). This is not entirely surprising as most patients with persistent Pa infection have antibodies which do not confer any obvious benefit and may in fact be detrimental as marked antibody response correlates with poor outcome (325). However, a recent study suggests that four intramuscular vaccinations in patients aged 2-18 over a period of fourteen months reduces the relative risk of Pa acquisition by 33% (324). This vaccine, based on outer membrane proteins of Pa, enhances opsonophagocytosis (326) and impairs the ability of Pa to bind to interferon gamma (IFN- γ), which is thought to enhance virulence, and warrants further investigation (327).

Unlike active immunisation, passive monoclonal antibody prophylaxis provides immediate high titres with efficacy demonstrated in animal models of Pa infection; however, antibodies from healthy donors are variable in titre, expensive, have poor lung penetration and may even enhance inflammation (328). Newer techniques using i) transgenic mice to generate human monoclonal antibodies, ii) recombinant IgG human monoclonal antibodies (329) and iii) antibody phage libraries to select monoclonal antibodies against exopolysaccharide (330) have demonstrated efficacy in animal models. A phase 1 study of KB001-A, a PEGylated recombinant anti-Pa antibody that blocks a key Pa virulence mechanism, demonstrated good tolerability and reduction in sputum inflammatory markers but not Pa density in CF patient compared to controls (331); results of a phase 2 study are awaited (ClinicalTrials.gov identifier NCT01695343).

Immunoglobulin Y, derived from hens receiving intramuscular Pa immunisation, has been shown to inhibit growth of Pa (332). In a case report, oral immunotherapy with immunoglobulin Y was shown

to reduce Pa infection by over 80% in a single patient over a period of ten years; the treatment is available on a case-by-case basis in Sweden (333)

1.8.9: Other Novel Strategies for Pa Treatment in CF

Several other novel approaches to the treatment of Pa infection in CF are also being investigated including antimicrobial peptides (206) and inhibitors of efflux pumps (implicated in antibiotic resistance). A full review of these strategies can be found in the literature (291).

1.9: Context of Experimental Work

Although much current CF research is focusing on correction of the basic defect, strategies to treat the commonest class II mutation, Phe508Del, have so far been less successful than approaches to correcting class III defects. For this reason, and with increasing antibiotic resistance, there remains a pressing need for new methods by which to detect and treat Pa infection in CF. These two themes form the basis of experimental work undertaken for the two following sections of this thesis which are i) identification and detection of biomarkers associated with Pa infection that can be measured non-invasively and in real time using mass spectrometry and ii) use of bacteriophage therapy as an adjunct or alternative to current antibiotic approaches for the treatment of Pa infection.

These two themes are explored in more detail in the section-specific introductions to Parts I and II of this thesis. The context and rationale for my experimental work is further explained in these two sections, which are each followed by specific hypotheses, aims and objectives.

Part I: Novel Detection Methods for *Pseudomonas aeruginosa* Infection in CF

"By the sense of smell, we can recognise the peculiar perspiration of many diseases, which has an important bearing on their identification (334)"

Chapter 2: Background

2.1: Volatile Organic Compounds in Exhaled Breath

Volatile organic compounds (VOCs) are organic (carbon-based) atmospheric trace gases with a high vapour pressure and low solubility at room temperature (335). They are synthesised mainly by living organisms including trees, animals and bacteria (336) but can also be manmade, mainly as by-products of industrial processes, a source that has been associated with adverse respiratory health in children (337). Anecdotal reports, stretching back to Hippocrates (c460-370 BC) description of fetor oris in the ancient Greek era (338), hinted at the potential of breath odour as an aid to medical diagnosis and the subsequent identification of over two hundred distinct VOCs in exhaled breath using gas-chromatography mass spectrometry (GC-MS) in 1971 (339) demonstrated that quantification of subtle differences in breath profile might be feasible. Whilst this diversity is advantageous in terms of the potential for numerous differences to be detected in exhaled breath depending on the underlying pathology, it has also undermined the rate at which breath diagnostics has progressed due to difficulties of simultaneously sampling and analysing VOCs belonging to different chemical groups. The variable amount of water vapour and sheer number of different compounds present in exhaled breath, coupled with the need to appreciate the influence that the external environment might have on their concentration, makes understanding the interaction between biological mechanisms underlying production of each individual VOC a complex and time-consuming process (335). For these reasons, endogenous VOCs are not yet used widely in clinical settings for patient diagnosis and monitoring, although proof-of-concept research has shown that levels of breath ammonia are elevated in renal failure and fall during haemodialysis (340) and that patients with chronic liver disease can be identified through quantification of VOCs containing

sulphur (341, 342). It has also been demonstrated that electronic nose analysis of exhaled breath differentiates adult patients with chronic obstructive pulmonary disease (COPD) from those with asthma (343), GC-MS can distinguish breath from asthma patients from that of healthy controls and that VOC profile differs according to whether asthma patients display a neutrophilic or eosinophilic phenotype (344). The feasibility of using exhaled breath to directly influence patient care has been shown by: i) use of ^{13}C -labelled urea to diagnose *Helicobacter pylori* infection in children (345), although this requires patients to drink a radiolabelled isotope prior to breath sample analysis and ii) use of nitric oxide (NO) which, although not strictly a VOC due to the lack of carbon in its structure, is an endogenous marker produced by the human lung which can be measured either nasally to screen for primary ciliary dyskinesia (PCD) (346, 347) or exhaled to monitor eosinophilic airway inflammation using chemiluminescence or commercially-available fraction of nitric oxide (FeNO) monitors (348). All of this evidence suggests that processes such as infection and inflammation, which disrupt normal biological function, might induce biochemical abnormalities within the host that can be detected by methods other than established invasive techniques such as blood tests.

2.2: Endogenous Volatile Organic Compounds and CF

Most studies relating to endogenous breath biomarkers in CF have focused on NO or nitrites, either in exhaled breath or exhaled breath condensate (EBC), but neither has proven clinically useful. For this reason, and the fact that no association has previously been demonstrated with Pa infection (349), it will not be discussed further here. A review of the literature is available (350).

Carbon monoxide (CO), though toxic in high concentrations, is produced endogenously and is thought to have homeostatic importance in most tissue types of the human body (351). Levels in exhaled breath are higher in CF patients compared with healthy controls (352) (a difference that is more marked in those homozygous for the p.Phe508del mutation), increase with pulmonary exacerbations and decline following antibiotic therapy (353). These differences are thought to reflect oxidative stress in CF patients, which is higher than in healthy controls and increases further during

an exacerbation (354); such a mechanism is thought also to explain ethane (C₂H₆) being elevated in exhaled breath and correlating with CO levels in this group (355). However, the difficulty of using endogenous VOCs to monitor disease due to the complexity of interacting biological mechanisms, is highlighted by the finding that breath isoprene (CH₂=C(CH₃)CH=CH₂), also a marker of oxidative stress, did not differ in a small study of CF patients before and after they received treatment for infective exacerbations (356).

2.3: Exogenous Volatile Organic Compounds produced by Pa

As previously described, there is immense diversity of endogenous VOCs that can be detected in exhaled breath of human subjects but individual biological variability and lack of consistent findings due to understanding of the interactions between mechanisms means that clinical application has so far been limited. Of more interest as a diagnostic aid are exogenous VOCs that are not produced in health, as the presence of these would be strongly indicative of an underlying disease process. A recent study demonstrated that activation of the human immune system by lipopolysaccharide (bacterial endotoxin) resulted in a more aversive body odour than when subjects were exposed to a placebo, suggesting that a subconscious "behavioural immune response" based on smell has evolved to protect healthy individuals from contracting infection (357). However, as bacteria exist symbiotically within the healthy body, predominantly in the gastrointestinal tract (358) but also in the lungs (184, 359, 360), which were until recently considered to be sterile, it is clear that not all bacteria induce this response and that some VOCs in exhaled breath might be exogenous, but derived from organisms that are not harmful and live in the human host. The challenge is to identify specific VOCs that are produced by pathogenic bacteria which would facilitate rapid detection and early treatment of infection.

2.3.1: 2-Aminoacetophenone (2-AA)

Historically, microbiologists have described Pa growing in cultures or burn wounds as having a distinctive "grape-like" odour that serves as an aid to identification. In 1979, Cox identified 2-

aminoacetophenone (2-AA, $\text{H}_2\text{NC}_6\text{H}_4\text{COCH}_3$) as the VOC responsible for this characteristic smell (361) and, more recently, 2-AA has been quantified in the exhaled breath of subjects with CF using GC-MS (362). The appeal of 2-AA as a potential biomarker of infection is confirmed by *in vitro* work demonstrating that it is relatively specific for Pa; it is not detected in air above (headspace) cultures of other pathogens including *Haemophilus influenzae*, *Pseudomonas fluorescens*, *Burkholderia multivorans*, *Streptococcus pneumoniae* and *Aspergillus fumigatus*, although traces have been detected in the headspace above cultures of *Escherichia coli* and *Staphylococcus aureus* (362). However, a major disadvantage to consider when proposing 2-AA as a breath biomarker, in keeping with the main disadvantage of breath being used to diagnose disease, is that contamination may occur from external sources; it is detectable in beer and wine and ingestion of various foods, including corn chips and cheese, can lead to elevated levels in exhaled breath (363, 364).

2.3.2: Hydrogen Cyanide (HCN)

It has been shown that Pa synthesises hydrogen cyanide (HCN) under microaerobic conditions ($\text{FiO}_2 < 0.05$) but not at higher oxygen tensions or under anaerobic conditions (365, 366). Few other respiratory pathogens are cyanogenic (367) (though HCN has been detected *in vitro* and in exhaled breath of patients with *Helicobacter pylori* infection (368)). As cyanide is a potent toxin, this might explain why Pa, which is inherently cyanide-resistant due to expression of the enzyme rhodanese that detoxifies cyanide to thiocyanate (369), consistently becomes the predominant organism in the CF lung (370). For these reasons, HCN has potential as a relatively specific biomarker for Pa infection. However, as human neutrophils have been shown to produce it *in vitro* after being exposed to *Staphylococcus epidermidis* (371, 372) and sputum neutrophil concentration correlates with cyanide levels (373), it is possible that inflammation caused by Pa infection, rather than Pa infection itself, is responsible for cyanide production. Counter to this theory is the finding that, although HCN is detected in the sputum of CF patients infected with Pa, it is absent in sputum of patients infected with other organisms (374, 375), who would also have neutrophilic airway inflammation. That HCN in

exhaled breath originates from Pa rather than inflammation is further supported by the finding that patients with asthma and chronic obstructive pulmonary disease (COPD), both conditions that can also be associated with neutrophilic inflammation (376, 377), do not have elevated levels in exhaled breath (378, 379).

In addition to being detectable in the sputum of CF patients with Pa infection, where its presence is associated with significantly poorer indices of lung function (374, 375), HCN has been detected in the headspace above bacterial cultures using mass spectrometric techniques (380, 381); the degree of cyanogenesis has been noted to vary according to Pa strain (382, 383). It has been reported that children with CF have higher levels of HCN in exhaled breath than children with asthma (378), that it can differentiate between children with and without Pa infection in CF (384) and that nose-exhaled, but not mouth-exhaled, breath can differentiate between adult CF patients with and without Pa infection (385), although in all these studies the levels were very low and at the limits of detection for the technology being used for quantification. Like many other VOCs, other sources of HCN can confound exhaled breath quantification. HCN is present in the environment (cigarette smoke and car exhaust fumes) and may also be generated in the oral cavity of healthy human subjects by the oxidation of thiocyanate by salivary peroxidase (386), a theory given credence by studies demonstrating lower HCN concentrations in breath exhaled from the nose rather than the mouth (385, 387). However, given the almost universal presence of sinus disease in CF adults, and the common isolation of Pa from sinus lavage (in up to 73% of patients (388)), using nose-exhaled breath to measure HCN may not be truly representative of the lower airways, indicated by the fact that bacterial strains in one study were concordant between the upper and lower airways in less than 50% of cases (94). Whilst HCN clearly shows promise as an exhaled biomarker of infection, a recent study demonstrated no difference between concentrations in exhaled breath of subjects chronically infected with Pa and other organisms (389), so further study is warranted to elucidate whether it will be useful in a clinical setting.

2.3.3: Sulphide Compounds

Sulphide compounds have also been shown to be produced by Pa (390). Dimethyl disulphide (DMDS, CH_3SSCH_3), which has an odour similar to garlic, has been detected in the headspace above bacterial cultures using mass spectrometric techniques (380, 381) although is less specific than HCN and 2-AA, also being associated with presence of other species such as *Escherichia coli* (391) as well as being present in the exhaled breath of patients with liver disease (392) (a potential issue in CF) and hypermethioninemias (393). Surprisingly, given that sulphides are produced by a range of bacteria (394, 395), levels of a similar molecule, dimethyl sulphide ($(\text{CH}_3)_2\text{S}$), associated with a cabbage-like smell, are reported as being lower in CF patients compared to healthy controls (396), raising the possibility that consumption of VOCs by bacterial species may occur *in vivo*. Counter to this, elevated levels of dimethyl sulphide were reported in headspace above Pa in another study (397) and high levels have also been reported in extra-oral blood-borne halitosis (398, 399) which could potentially confound *in vivo* measurements.

2.3.4: Other Exogenous VOCs Associated with Pa Infection

Whilst 2-AA, HCN and sulphide compounds are most commonly cited in the literature, a number of other VOCs belonging to diverse chemical groups including alcohols, hydrocarbons, acids, aldehydes and ketones have also been suggested as being associated with Pa infection (397, 400). Some of these are summarised in Table 2.3.4.1; as over 60 have been described, only those with multiple citations with relevance to the proposed experimental techniques of this thesis (Section 2.4.1) are listed. The diversity of potential markers that might be associated with respiratory infections, summarised in comprehensive reviews (368, 400-402), coupled with studies that analysed VOC profile rather than individual compounds (400, 403, 404), leads me to hypothesise that an approach looking to identify a number of VOCs constituting a unique "bacterial fingerprint" might be more fruitful than searching for a single specific biomarker that is pathognomonic for Pa status. The

difficulty in identifying such a fingerprint is alluded to by the fact that different studies, often using contrasting methods of quantification, have directly conflicting results as shown in Table 2.3.4.1.

VOC	Increased (References)	Decreased (References)
Acetone ((CH ₃) ₂ CO)	(383, 405)	(406, 407)
Acetonitrile (CH ₃ CN)	(380, 408)	
Ammonia (NH ₃)*	(380, 407, 409)	(405, 406)
Butanol (C ₄ H ₉ OH)	(390, 394)	(408, 409)
Ethanol (CH ₃ CH ₂ OH)	(394, 408, 409)	(391, 406)
Methanol (CH ₃ OH)	(397)	(407)
Methyl-thiocyanate (CH ₃ SCN)	(383, 394)	
Methyl-mercaptan (CH ₃ SH)	(380, 394, 407)	(405, 406)
2-Nonanone (CH ₃ (CH ₂) ₆ COCH ₃)	(390, 394, 397, 404)	(408)
Toluene (C ₇ H ₈)	(390, 410)	

Table 2.3.4.1: Selected VOCs that have been associated with Pa infection in the literature. Over 60 VOCs have been cited as possibly being increased or reduced in the presence of Pa (in studies looking at bacterial cultures as well as breath, urine and sputum) using a variety of different analytical techniques (400). Those listed here have multiple citations although findings are often inconsistent across different studies.

2.4: Exhaled Breath Analysis

Exhaled breath consists of primarily of nitrogen, oxygen, carbon dioxide, inert gases and water, with a small fraction representing volatile organic compounds in concentrations as low as in the parts-per-trillion range (350). Until relatively recently, quantification of trace constituents was impossible and physicians relied on analysis of bodily fluids, tissue or imaging techniques, some of which are invasive or painful and have inherent problems associated with them such as the risk of spreading infection and logistics of sample storage and/or destruction following analysis. Breath analysis could circumvent many of these problems; it is non-invasive, breath would not ideally need to be stored or transported and, crucially, might be possible in real-time, thus reducing delays between sample collection and analysis. The identification and quantification of trace VOCs in exhaled breath using GC-MS (339) was considered the breakthrough required to make this a reality as it simultaneously separates and quantifies compounds within a complex mixture. Unfortunately the process is labour intensive, expensive and cannot be performed in real-time (411) and, as analysis of low molecular weight compounds (such as HCN) using GC-MS is difficult (412), a need remained for an alternative quantification technique.

2.4.1: Selected Ion Flow Tube Mass Spectrometry (SIFT-MS)

Selected ion flow tube mass spectrometry (SIFT-MS) offers potential for gaseous mixtures containing VOCs to be analysed in real-time (413). Precursor ions (H_3O^+ , NO^+ or O_2^+) are produced by a microwave discharge source and selected based on their mass/charge (m/z) ratio by an upstream quadrupole mass filter. Based on pre-existing knowledge of the kinetics and reactions of the VOCs that are to be quantified, the operator selects one of the three ion species to be injected into an inert carrier gas (usually helium) which convects VOCs as a thermalized swarm along a flow tube at a known flow rate. These ions do not react with the major compounds in air, instead selectively ionising only volatile and trace compounds present within a sample introduced upstream of the ion source to generate characteristic product (analyte) ions that are quantified downstream by a quadrupole detection mass spectrometer. The flow rate of the ion swarm/carrier gas determines the reaction time. By measuring the count rates of the precursor ions and the characteristic product ions downstream, real-time quantification can be achieved, giving absolute concentrations of VOCs present in the parts-per-billion by volume (ppbv) range (413). As the concentration of exhaled VOCs in the breath of healthy volunteers has been studied using SIFT-MS (414-419), differences associated with disease may be detected. Although sample preparation is not required, a drawback of SIFT-MS is that ion chemistry for each compound of interest needs to be known and included on the on-board kinetics library to facilitate quantification.

SIFT-MS has two different modes of analysis. In full-scan mode (FS), ambient air/breath is introduced at a known flow rate into the carrier gas and the downstream analytical mass spectrometer system will scan over a predetermined m/z range for a given time. Complete mass spectra will be produced that contain peaks relating to product ions which can then be identified using knowledge of ion chemistry and the on-board kinetics library. In multiple ion monitoring mode (MIM), the operator identifies which VOCs are to be quantified and the downstream analytical mass spectrometer switches between the m/z values that correspond to the targeted VOC species. By using the data obtained downstream in conjunction with the known rate co-efficients of the reactions between

precursor ions and VOC molecules from the kinetics library, simultaneous downstream quantification of several VOCs can be achieved. MIM provides more accurate quantification than using FS mode but both are used together to ensure that all mass spectra obtained have typical peaks, as this improves quality control, reducing likelihood of errors that might occur if using MIM alone. A detailed review of SIFT-MS can be found in the literature (413) and a schematic diagram, adapted from (413) is shown in Figure 2.4.1.1.

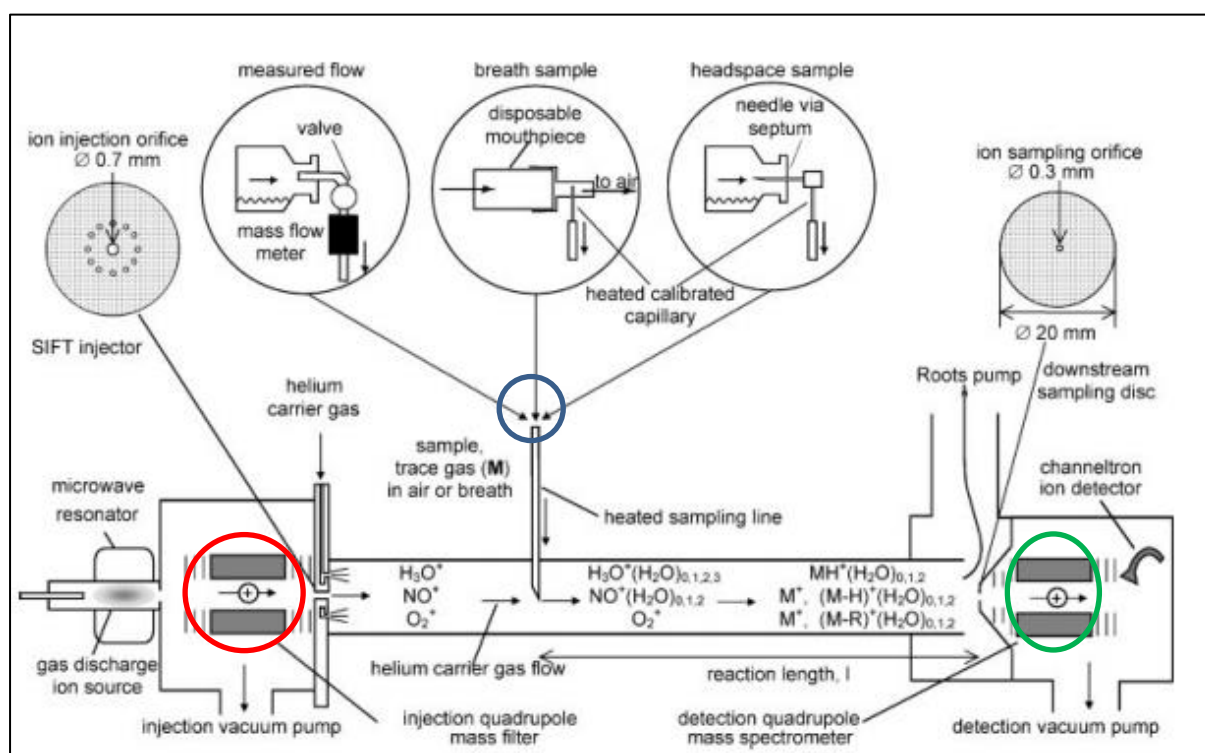


Figure 2.4.1.1: Schematic diagram of SIFT-MS. H_3O^+ , NO^+ or O_2^+ ions are selected by a downstream quadrupole mass filter (circled in red), and carrier along the flow tube in inert helium. Breath is introduced downstream (circled in blue). Constituent VOCs in the sample are quantified using existing knowledge of ion chemistry, stored in the kinetics library, by downstream quantification of characteristic product ions (circled in green).

2.4.2: Other Techniques for Exhaled Breath Analysis

In addition to GC-MS and SIFT-MS, other experimental techniques exist that might aid study of exhaled breath including electronic noses (420), proton-transfer-reaction mass spectrometry (PTR-MS) (421) and ion mobility spectrometry (422). If exhaled breath is passed via a cooling system, at temperatures in the region of 0-4°C, liquid exhaled breath condensate (EBC) is formed which can be collected and analysed not only for volatile biomarkers using mass spectrometric techniques (423, 424) but also pro-inflammatory cytokines with ELISA (425) or flow cytometry (426). Despite such diverse techniques being available, breath analysis has not become part of routine clinical practice because of technical issues, particularly with sampling, whilst inconsistent methodology across different platforms has given rise to contradictory data (427). Table 2.4.2.1 summarises advantages and disadvantages of some of the technology currently available for analysis of exhaled breath.

Method	Advantage	Disadvantage
GC-MS	Identification of unknown VOCs and profiling possible Highly reproducible Sensitivity in ppb range	System immobile Slow Pre-concentration needed Real-time measurements not possible Expensive Not suitable for clinical use
Ion Mobility Spectrometry	No pre-concentration needed Mobile Low cost Suitable for clinical use Sensitivity in ppm range	VOC chemical identification and profiling not possible Real-time measurements not possible
SIFT-MS	Measures VOCs in real-time Potential for online testing Fast Mobile system Sensitivity in ppb range	VOC chemical identification and profiling not possible
PTR-MS	Measures VOCs in real-time Potential for online testing Fast Sensitivity in ppb range	VOC chemical identification and profiling not possible
Electronic Noses	Easy to use Cheap, fast and portable Suitable for bedside use Sensitivity in ppb range	Sensors not designed for single VOCs Devices not compatible with each other

Table 2.4.2.1: Advantages and disadvantages of selected experimental techniques currently being used for exhaled breath analysis. Adapted from (368). ppb = parts-per-billion and ppm = parts-per-million.

2.4.3: Sampling of Exhaled Breath

A single tidal exhaled breath consists of anatomical dead-space gas (approximately 150mls in adults) from the upper part of the respiratory tract that does not participate in gas exchange and alveolar air (typically around 350mls) that originates from the deeper parts of the lung and contains VOCs from the blood (368, 428). Spontaneously breathing subjects can easily provide tidal breath samples directly into analytical equipment such as the SIFT-MS or into bags or canisters for off-line analysis; the benefit of this approach is that no additional equipment for collection is necessary but there is the downside that the dead space component might dilute VOC concentrations (427). Sampling purely alveolar air might improve accuracy of exhaled breath analysis, as VOC concentrations will be in equilibrium with those in the lung alveoli (429), but requires additional equipment and levels can vary according to the breath manoeuvres used during collection (430). For these reasons, and the fact that it has been shown that a single vital capacity (from maximum inspiration to expiration) exhalation contains levels of volatiles that correlate well with those in alveolar air (431), approaches that use tidal or easily reproducible breathing manoeuvres are preferable when devising methodology for breath analysis with the ultimate goal of it being widely applicable in a clinical setting. This is of particular relevance to the work in this thesis as the aim is to develop a screening tool that can be used in the paediatric setting.

2.4.4: Collection of Exhaled Breath

Samples can be collected in a number of ways, either directly into an instrument for immediate analysis which has benefits with regards to cost and reducing the risk of sample deterioration over time but also has implications for infection control, particularly in diseases such as CF where segregation to minimise cross-contamination of patients is imperative, or into containers for off-line analysis. For the purpose of analysis using SIFT-MS, these come in a number of forms:

- i. Tedlar™ bags: Made from polyvinyl fluoride and chemically inert. VOCs including methanol, acetone, isoprene and acetaldehyde have half-lives ranging from 5-13 days in

these bags and losses 52 hours after filling are less than 10% (432). Tedlar bags are expensive and single-use, although some studies have demonstrated stability for several uses provided they are washed between samples with pure nitrogen.

- ii. Nalophan™ bags: Made from polyethylene terephthalate, these are cheaper than Tedlar bags and can be made from rolls of Nalophan in-house. Even when made to double-thickness, these bags are slightly porous however, leading to loss of VOCs over time (433). Comparability of 20µm thick bags to Tedlar bags has been demonstrated for storage times of up to five hours (433) and, for HCN analysis, using thicker 70µm Nalophan to make collection bags gives rise to good correlation between online and offline measurements for storage times of up to 24hrs (384). Being cheap and easy to produce, Nalophan bags are single-use, which is preferable to reduce risk of cross-infection.
- iii. SUMMA™ canisters: Stainless steel containers with internal surfaces that have been electropolished, making them chemically inert. Advantages include durability, easy of transportation and stability of samples over time (434), although some studies have shown that loss of some VOCs can still occur due to physical adherence to the internal surface of the canisters as well as chemical decomposition (435). Although reusable, the canisters are expensive.

2.5: Rationale for Experimental Work, Hypothesis and Aims

2.5.1: Rationale

As discussed in Chapter 1, there is a clear need for a rapid, non-invasive technique with which to accurately diagnose infection, particularly Pa, as this can help to reduce morbidity and mortality (436-438). The availability of SIFT-MS as a tool for detecting VOCs in exhaled breath without the need for additional costly sample preparation is an attractive strategy by which this might be

achieved. Most work to-date has focused on single biomarkers of Pa infection, primarily HCN and 2-AA and, although some results have been promising, a clinically applicable test remains elusive. It is possible that, by broadening the scope of VOCs being analysed and using them in combination to make a "bacterial fingerprint" for Pa, more accurate discrimination might be achieved than by concentrating our search on a single pathognomonic marker.

2.5.2: Hypothesis

The presence of Pa infection in CF patients with chronic infection can be determined by analysis of a single, mixed alveolar/anatomical deadspace breath sample analysed offline within two hours of collection using SIFT-MS.

2.5.3: Aims

- To undertake a rudimentary pilot study analysing headspace above sputum from CF patients chronically infected with Pa. This aimed to: i) establish familiarity with the SIFT-MS instrument for ongoing work, ii) confirm whether findings from previous studies using SIFT-MS to analyse headspace above CF sputum (380, 439) could be replicated using our patient cohort and technology and iii) determine if other VOCs in addition to HCN and 2-AA might be of interest for later analysis in exhaled breath.
- To establish whether exhaled breath analysis using our SIFT-MS instrument was both repeatable and reproducible. This was necessary prior to recruitment of patients to ensure that any data produced from the final study was of sufficient quality.
- To recruit well-phenotyped adult patients, with and without chronic Pa infection as defined by Leeds Criteria (440), and healthy control subjects to provide exhaled breath samples for offline analysis of multiple VOCs (including HCN and 2-AA) using SIFT-MS in order to determine if discrimination can be achieved.

Chapter 3: General Materials and Methods

3.1: Construction of Sampling Bags

Nalophan™ (Kalle, UK) was used for collection of all samples in this study (Section 2.4.4). I constructed double-thickness bags using two A4-sided sheets of 25µm Nalophan inserted into one another and sealed at the top using a heat sealer for five seconds. A 1ml Luer-Lok™ syringe (Terumo, Belgium) was folded into the lower opening of the bag which was then also heat sealed to ensure that there were no leaks. This syringe acted as the conduit for sample collection for exhaled breath and also as the inlet for connection to the SIFT-MS for analysis for all experiments in this study. For sputum experiments, samples were put into the bags before sealing. A schematic diagram of the Nalophan bag construction is shown in Figure 3.1.1.

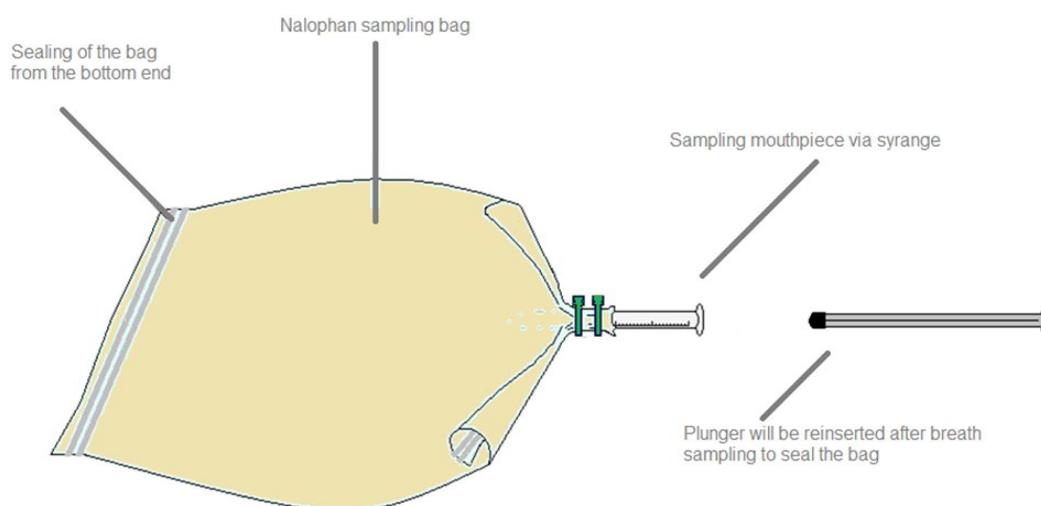


Figure 3.1.1: Schematic diagram of construction of bags for sample collection. Bags were made in-house using double-thickness 25µm Nalophan cut to A4 size as described above.

3.2: SIFT-MS Analysis of Bag Samples

All samples collected in Nalophan bags in this study (sputum or breath) were analysed by connecting the bags to a heated sampling line via the 1ml syringe (Section 2.4.1). Analysis was always over a period of 70 seconds (s), with the first 10s discarded from analysis to ensure sufficient headspace gas had passed down the sampling line prior to starting quantification. Measured VOC concentrations were averaged between the 10s-70s period. Bags were kept in an incubator at 37°C for the duration

of the analysis to minimise loss of water vapour during analysis, which would impact on the measured concentration of water-soluble compounds. This methodology and that for construction of the Nalophan bags had been validated in previous work by our group (441).

3.3: SIFT-MS Maintenance

Following each day of use, the flow rate of helium carrier gas was increased and the SIFT-MS left to sample ambient air for thirty minutes in order to flush the system of residual VOCs from previous experiments. Additional maintenance was undertaken when higher levels of 2-AA were detected during bacterial cultures experiments (Table 4.2.2.3), coinciding with other users of the instrument reporting inconsistencies in their data. This required fitting of a new sampling line and upstream gas discharge ion source, both of which are expected for wear-and-tear. A longer delay was experienced between September 2012 and January 2013 as other components of the SIFT-MS failed and external help had to be sought to resolve these problems.

3.4: Statistical Analysis

Sample sizes were opportunistic as there were no data to inform a power calculation. GraphPad Prism 6.0 (GraphPad, USA) and SPSS Statistics 21.0 (IBM, USA) were used for statistical analyses for all work in this part of the thesis. Specific statistical techniques for each experiment are described individually under the detailed materials and methods for that section of work.

Chapter 4: SIFT-MS – Development of Exhaled Breath Analysis Protocol

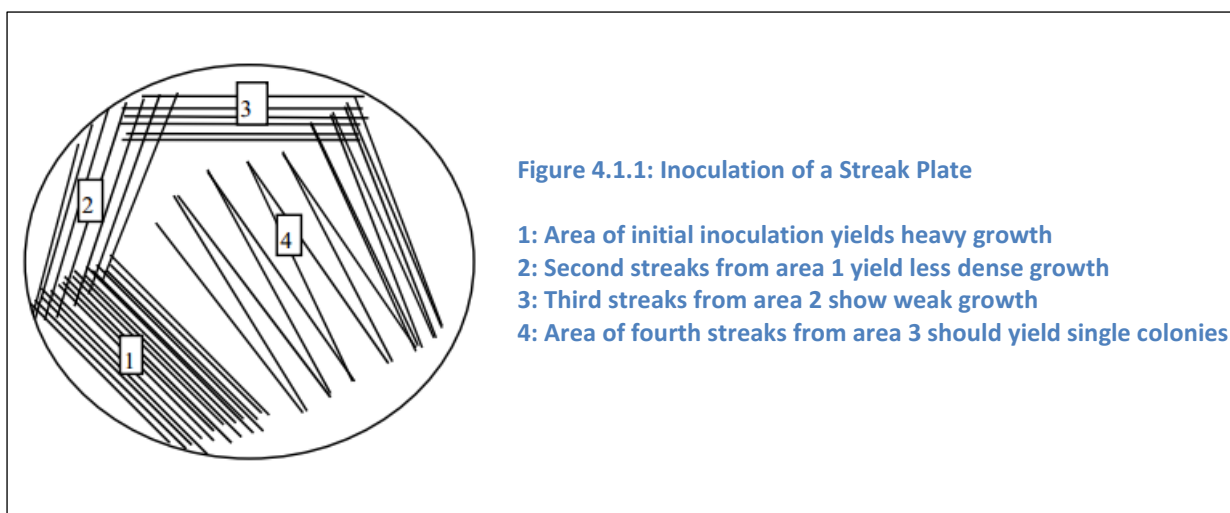
Starting with the first aim (Section 2.5.3), a pilot sputum study was initially undertaken to establish familiarity with the SIFT-MS instrument for ongoing work and to confirm if findings from previous studies could be replicated.

4.1: Pilot Sputum Study

4.1.1: Materials and Methods

Sputum from well phenotyped adult patients (n=13) with CF was collected after obtaining informed consent. All subjects were in-patients on Foulis Ward at the Royal Brompton Hospital (RBH) who were chronically infected with Pa, as defined by Leeds Criteria (440), and had a Pa-positive culture in the preceding two weeks. Adult patients were selected for the purposes of this chapter as, unlike many paediatric patients, they are more commonly able to expectorate spontaneously (442), particularly if having an acute exacerbation as may be expected during a hospital admission (443). Patients were asked to provide samples in the morning and typically produced these after their first physiotherapy session of the day.

Sputum was plated directly onto Pa-specific agar (PSA) plates (Oxoid, UK) using single-use disposable sterile inoculation loops (Fisher Scientific, UK) using a standard streak plating technique. A new inoculation loop was used at each step of the streaking in order to ensure that cross-contamination from previously streaked sectors did not occur and that the density of cells decreased during the procedure. This was to ensure that single colonies were yielded which could then be identified by our microbiology laboratory at the end of the experiment to determine whether the headspace analysis was from pure or mixed bacterial growth. This is shown in Figure 4.1.1. The sputum sample was then sent to our accredited CF microbiology laboratory for standard microscopy, culture and sensitivity testing.



Inoculated PSA plates (without lids) were placed in Nalophan bags (Section 3.1) before being sealed. Control bags (n=10) containing empty PSA plates that had not been inoculated with sputum were prepared in the same way. All bags were then incubated at 37°C for 48hrs to stimulate bacterial growth.

After 48hrs, following visual confirmation of bacterial growth on PSA, the bags were taken to our Profile 3 SIFT-MS instrument (Instrument Science, UK) and attached directly to the sampling port following removal of the plunger from the 1ml syringe. The gas within each bag (headspace above the plated sputum) was analysed as described in Section 3.2. A standard panel of 25 VOCs (n=23) was initially used and 2-AA (n=10) was also measured when the kinetics for this compound were added to the SIFT-MS kinetics library at a later date.

Pre-existing knowledge of the kinetics and reactions of VOCs that are to be quantified usually determines which one of the three precursor ions (H_3O^+ , O_2^+ and NO^+) should be selected for carriage in the inert helium carrier gas to allow downstream VOC quantification. However, the SIFT-MS kinetics library does allow more than one precursor ion to be used to quantify some, but not all VOCs; as I was familiarising myself with the technology and wished to see if detection varied if different precursors were used, some VOCs in sputum headspace were measured sequentially with two or even all three of the precursor ions, each time with the standard methodology described in Section 3.2.

Non-parametric Mann-Whitney U-test was used for data analysis as only some VOCs passed the D'Agostino-Pearson omnibus test for Gaussian distribution. As the pilot study was in part a “fishing” exercise to identify compounds that might be of interest in subsequent experiments, a multiple comparisons correction test was not used during this part of my work.

4.1.2: Results

A standard panel of 25 VOCs was measured (n=23) with 2-AA added to the analysis when the kinetics were available. Tables 4.1.2.1, 4.1.2.2 and 4.1.2.3 show VOC levels detected using H₃O⁺, O₂⁺ and NO⁺ precursor ions respectively. Figure 4.1.2.1 shows the four compounds that differed significantly between bags containing Pa and control bags, as measured with the H₃O⁺ precursor ion. Although a statistically significant difference is present, it is worth noting that there is significant overlap between the two groups.

VOC	Median ppbv Pa [IQR]	Median ppbv Control [IQR]	p
AcetaldehydeBAMOD	94.4 [44.1 – 470.2]	233.9 [129.5 – 403.1]	<0.05*
Acetic Acid	38.3 [29.7 – 53.8]	44.8 [40.1 – 65.6]	0.1007
Acetone	16.4 [11.6 – 23.3]	14.8 [12.3 – 20.3]	0.7118
Ammonia	111.5 [88.1 – 156.7]	133 [96.2 – 195.9]	0.5473
Butanol	0.0 [0.0 – 5.7]	13.5 [1.3 – 47.3]	<0.05*
Diethyl Ether	17.1 [12.5 – 12.8]	17.5 [9.5 – 26.8]	0.6809
Dimethyl Sulphide + Ethanol	44.5 [9.9 – 95.4]	81.7 [11 – 154.5]	0.1809
Ethanol	339.8 [228.8 – 417.0]	314.5 [240.7 – 725.0]	0.8435
Ethanol83	116.6 [71.3 – 196.4]	105.7 [75.8 – 483.4]	0.6330
Ethylphenol	12.8 [9.8 – 19.8]	19.3 [14.9 – 23.1]	0.0791
FormaldehydeBAMOD	60.9 [38.4 – 77.6]	50.9 [42.4 – 62.4]	0.4982
Hexanoic Acid	47.0 [20.5 – 58.4]	52.6 [47.5 – 59.2]	0.1652
Hydrogen Cyanide	4.2 [2.7 – 6.4]	3.4 [1.5 – 4.3]	0.4023
Hydrogen Sulphide	0.6 [0.3 – 1.3]	0.6 [0.2 – 1.1]	0.6119
Methanol	37.2 [30.25 – 44.4]	36.8 [32.3 – 133.1]	0.9999
Methylphenol	16.3 [11.1 – 23.0]	24.2 [21.8 – 27.6]	<0.05*
Propanol	7.2 [5.8 – 9.3]	10.1 [6.3 – 21.4]	0.2551
Pentanoic Acid	9.7 [8.1 – 17.3]	8.0 [6.7 – 13.3]	0.2138
Pentanol	27.1 [23.4 – 37.9]	44.8 [32.2 – 60.6]	<0.05*
Phenol	19.8 [17.8 – 21.1]	20.3 [17.2 – 23.8]	0.6508
Propanoic Acid	10.7 [9.4 – 15.6]	13.8 [7.2 – 20.1]	0.5938
2-AA	7.1 [5.5 – 9.4]	8.8 [7.5 – 12.8]	0.2134

Table 4.1.2.1: Summary of Pilot Data with VOCs measured using H₃O⁺ Precursor Ion on SIFT-MS

VOC	Median ppbv Pa [IQR]	Median ppbv Control [IQR]	p
Acetone	9.5 [7.3 – 11.4]	10.2 [7.9 – 12.1]	0.8316
Ethylphenol	8.3 [7.2 – 14.1]	11.7 [7.6 – 16.9]	0.4185
Isoprene	13.8 [2.4 – 16.2]	6.8 [1.5 – 14.2]	0.2378
Methylphenol	10.5 [7.4 – 14]	15.3 [11.3 – 21.0]	<0.05*
2-AA	8.3 [5.7 – 9.7]	7.7 [6.8 – 8.3]	0.6489

Table 4.1.2.2: Summary of Pilot Data with VOCs measured using NO⁺ Precursor Ion on SIFT-MS

VOC	Median ppbv Pa [IQR]	Median ppbv Control [IQR]	P
Acetone	37 [29.4 – 43.1]	32.1 [25.9 – 53.8]	0.9154
Ammonia	113.4 [96.5 – 175.6]	157.3 [81.6 – 189.4]	0.6408
Carbon Disulphide	49.8 [41.5 – 53.5]	48.8 [33.3 – 55.4]	0.5518
Ethylphenol	20.5 [16.4 – 30.2]	24.6 [22.4 – 29.9]	0.4785
Isoprene	15.5 [12.6 – 18.6]	15.2 [12.4 – 24.9]	0.5983
Methylphenol	12.9 [9.6 – 17.1]	14.0 [11.8 – 17.3]	0.5943
Nitric Oxide	418.7 [400.3 – 479.2]	409.6 [392.3 – 533.8]	0.6764

Table 4.1.2.3: Summary of Pilot Data with VOCs measured using O₂⁺ Precursor Ion on SIFT-MS

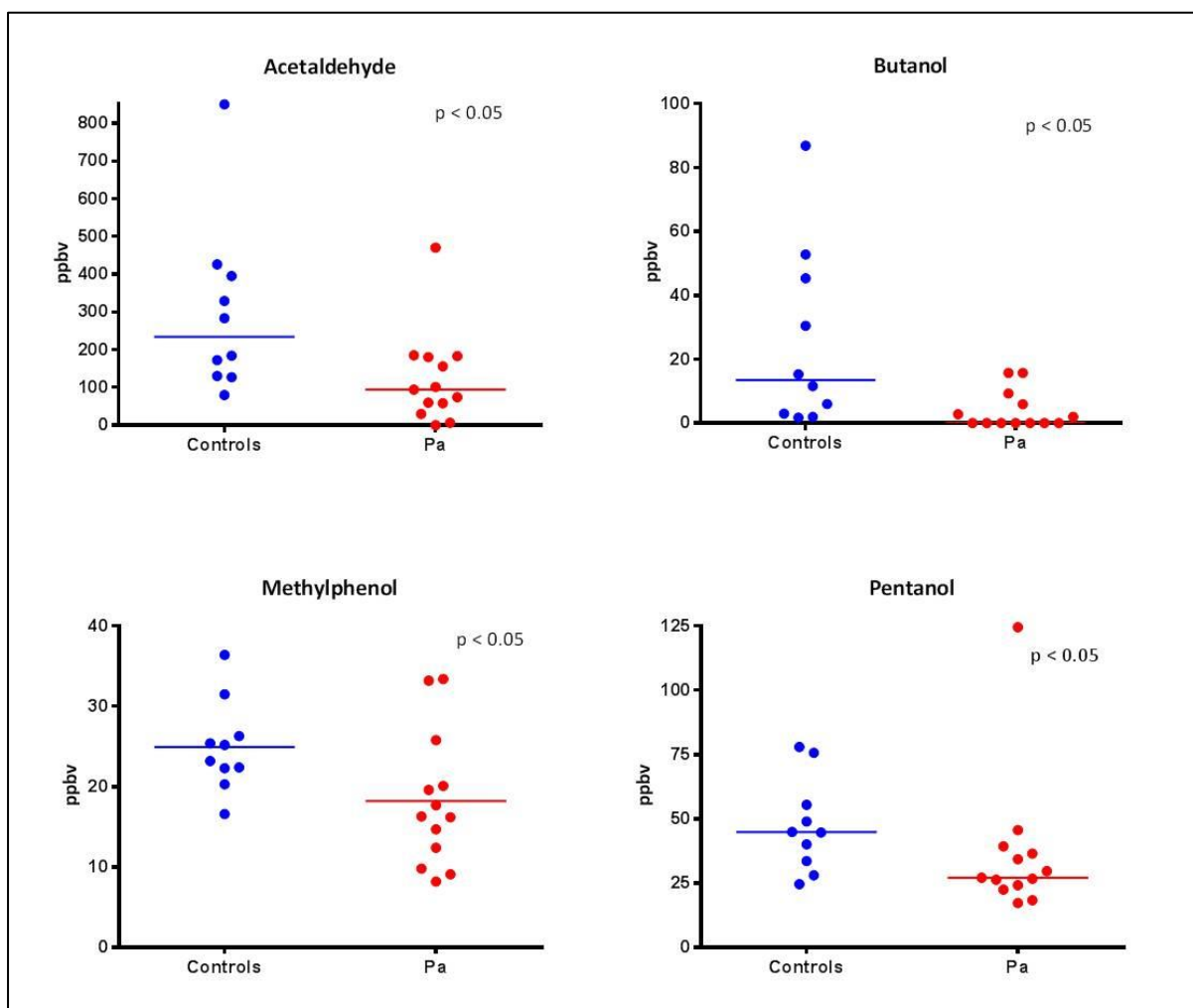


Figure 4.1.2: Graphs showing significant differences in four VOCs in headspace above plated sputum containing Pa compared with empty PSA plates as measured by SIFT-MS using the H₃O⁺ precursor ion. Whilst statistically significant differences were seen, note overlap between groups.

4.1.3: Rationale for Next Stage of Assay Development

The pilot data differed significantly from the work of Carroll et al (380) despite the only discernible difference in methodology being the volume of the Nalophan bags in which agar plates were incubated (200mls vs. 2000mls). Of most concern was that there was no difference in HCN detected in sputum and control bags whilst, in the Carroll study, levels of up to 17190 ppbv were present. I therefore formulated a series of experiments using pure bacterial cultures to determine if higher levels of HCN would be detected by the SIFT-MS in our facility.

4.2: Bacterial Culture Experiments – Solid Media

4.2.1: Materials and Methods

Three strains of Pa known to produce differing quantities of HCN (two naturally occurring, one genetically modified, kindly provided by Dr. Huw Williams, Reader in Microbiology, Imperial College London) were streak inoculated onto PSA plates (n=2 for each strain) from agar slopes and incubated in sealed Nalophan bags at 37°C for 48 hours as described in Section 4.1. Control bags containing empty plates (n=2) were also prepared.

In addition to measurement of HCN on SIFT-MS, I here utilised specific cyanide-detection paper: a validated, semi-quantitative and rapid method for detection of cyanogenic bacteria (444, 445). Cyanide detection solution was produced by dissolving 5mg copper ethylacetoacetate (Sigma, UK) and 5mg tetrabase 4,4'-methylenebis (N,N-dimethylaniline) (Sigma, UK) in 2mls chloroform (the chemical structure of these compounds is shown in Figure 4.2.1.1). Into this, 8cm x 12cm pieces of 3mm filter paper (Whatman, USA) were dipped, for a few seconds.

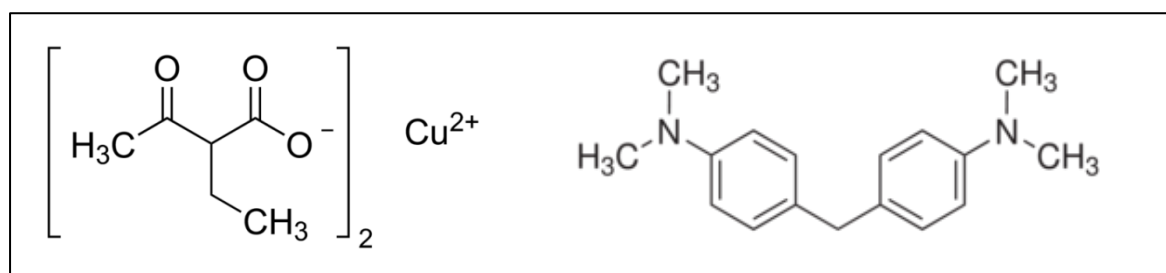
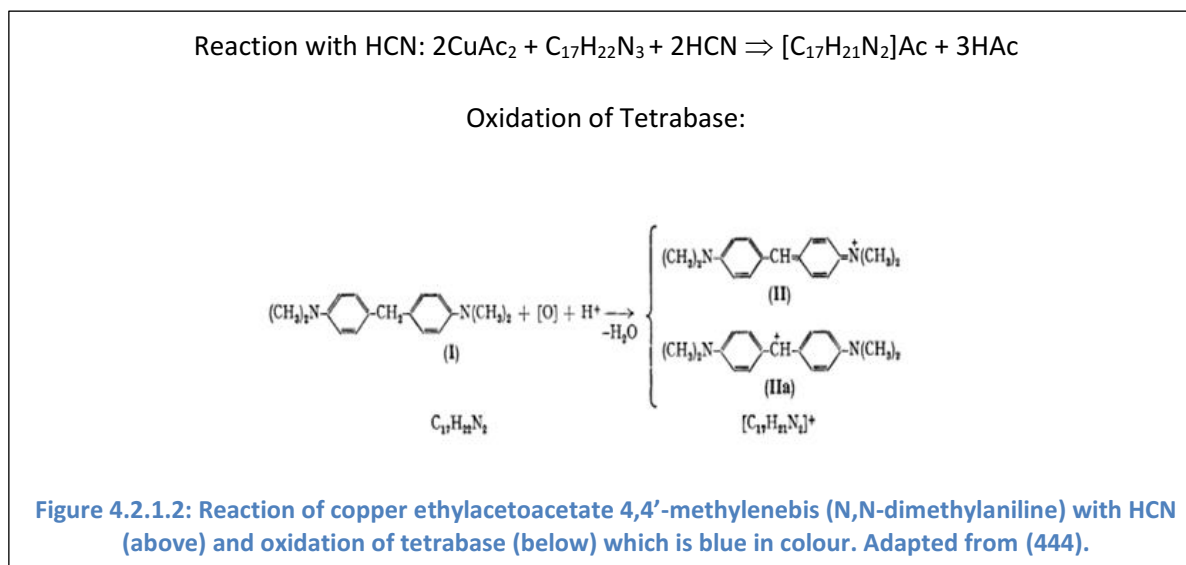


Figure 4.2.1.1: Copper ethylacetoacetate (left) and 4,4'-methylenebis (N,N-dimethylaniline) (right)

Cyanide detection paper turns blue when cyanide reacts with the copper (I) ion to produce copper cyanide (CuCN), following which tetrabase is oxidised by the copper (II) ion to form a stain (Figure 4.2.1.2).



A strip of cyanide detection paper was put into each bag prior to sealing and incubation. For each strain of Pa in this experiment, cyanide detection paper was both taped across the top of the open PSA streak plate (n=1) and left loose within the Nalophan bag (n=1) to determine whether diffusion throughout the headspace was taking place. After 48hrs, bacterial growth was confirmed by visual inspection and HCN was quantified by SIFT-MS as described in Section 3.2. The bags were then opened and the detection paper removed for examination: it is semi-quantitative – the darker the paper, the more cyanide has been detected. An example of a plate demonstrating assessment of cyanogenesis of bacterial strains cultured in a 96-well plate is shown in Figure 4.2.1.3.

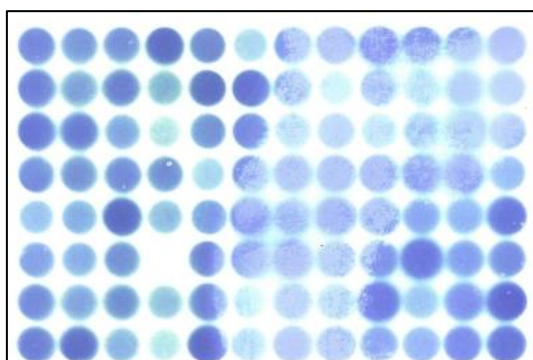


Figure 4.2.1.3: Example of detection paper kept over a 96-well plate to detect differing amounts of cyanogenesis by various strains of Pa. The darker the colour, the greater $[\text{CN}^-]$

4.2.2: Results

In the presence of Pa, cyanide detection paper in Nalophan bags changed from white to different shades of blue, confirming both the production of cyanide and the ability of the paper to detect HCN. The change in colour was consistent regardless of whether the paper was left loose in the Nalophan bag or taped across the open PSA plate on which the sputum was inoculated, demonstrating that HCN was diffusing freely throughout the headspace of the plate in the bag. When bags were connected to the SIFT-MS sampling port, HCN was detected at levels higher than that seen in the pilot sputum study and correlated both with i) the known cyanogenic properties of the cultured Pa strains (advised by Dr. Huw Williams) and ii) the degree of colour change noted in the cyanide-detection paper, confirming this to be semi-quantitative. These results are summarised in Table 4.2.2.1.





Pa Strain	Description	Cyanide Paper	SIFT-MS (ppbv)
Pa14	Wild type clinical strain Most common clonal group worldwide (446)		31.9 29.8
Δ hcnA	Mutant strain deficient in cyanide production Biosynthetic replacement gene for HCN synthase		6.1 8.3
gacS	Global activator dysregulated quorum-sensing Intermediate hydrogen cyanide production		20.0 14.0
Control	Empty Pa-specific plates Incubated concurrently with Pa samples		7.2 6.9

Table 4.2.2.1: Levels of HCN detected in the headspace above three strains of Pa (n=2 for each strain) cultured on PSA (and control plates (n=2) containing no Pa) in Nalophan bags, as measured with cyanide detection paper and SIFT-MS.

4.2.3: Rationale for Next Stage of Assay Development

Whilst HCN levels were i) detected in quantities appropriate to that expected based on known cyanogenic properties of the three Pa strains being tested and ii) correlated with the degree of colour change of the cyanide detection paper, concerns persisted as levels detected by SIFT-MS remained relatively low in comparison to previously published work. Therefore, liquid culture experiments were undertaken to determine if levels would be higher if i) volume of headspace was reduced and ii) density of bacterial growth was increased.

4.3: Bacterial Culture Experiments – Liquid Media

4.3.1: Materials and Methods

Two clinical Pa strains (laboratory numbers PA12B-4973 and PA12B-5001, kindly provided by Mr. Neil Madden, Senior Clinical Microbiologist, RBH) and two laboratory strains (PA14 and PA5539, the latter a mutant known to produce only small quantities of HCN, kindly provided by Dr. Huw Williams) were introduced from agar slopes into 10mls of tryptone soy broth (TSB) with a single-use plastic inoculation loop (Fisher Scientific, UK) and incubated overnight at 37°C with agitation. TSB was made in-house, adding 3g TSB powder (Sigma, UK) to 100mls deionised water and sterilising by autoclaving (Priorclave, UK) at 121°C. Following overnight incubation, optical density of the bacterial broths was adjusted using spectrophotometry (Spectronic, UK) at a wavelength of 620nm to 1.0 (equivalent to approximately 1×10^9 colony forming units (CFU)/ml) by dilution with sterile TSB. 100µl of this broth was added to 10mls sterile TSB in a 30ml Sterilin (Thermo Scientific, UK) and this was incubated overnight with agitation at 37°C (n=6 for each strain). 100µl SM buffer was introduced aseptically into 10mls of TSB and incubated overnight in the same way, to act as a control (n=6). Following incubation of these samples, analysis of headspace in the Sterilins was performed by connecting the SIFT-MS sampling port to a 21 gauge Microlance™ needle (BD, Ireland) via a narrow bore extension line (Vygon, UK). The needle was used to pierce double thickness Parafilm™ (Bemis, USA) that was applied over the Sterilin tubes immediately after the lids were removed (to prevent loss of VOCs). Headspace was analysed described in Section 3.1, with the H_3O^+ precursor ion (to quantify HCN, butanol and ammonia) and NO^+ precursor ion (for 2-AA quantification).

The entire liquid culture methodology was repeated at a later date using PA12B-4973 (n=6 with 6 control samples), the clinical strain identified for use in my bacteriophage work (see Part II, Section 8.2). This was because I was considering whether it might be possible to collect exhaled breath from mice that had been infected with this organism to see if: i) HCN could be detected in it using SIFT-MS and, if it could ii) whether levels were lower in mice receiving bacteriophage therapy who would, in theory have had a lower Pa load in their lungs. This was ultimately not feasible (single experiment

only, not discussed in this thesis) but additional data for this section of work was obtained opportunistically by repeating the culture experiment with this extra strain.

Where VOC production from more than two groups was being compared, one-way analysis of variance (ANOVA) assuming a non-parametric distribution (Kruskal-Wallis test) was used. Where only two groups were being compared, non-parametric t test (Mann-Whitney U test) was used for analysis. Median ppbv and range are given for all measurements in this section.

4.3.2: Results

Optical density of TSB inoculated with Pa and incubated overnight at 37°C ranged between 0.728 and 1.862, which is expected due to biological variability. It was demonstrated that: i) different strains of Pa produce different amounts of HCN, as described in the literature (367, 380-382) and ii) significant amounts of HCN could be detected using our SIFT-MS using this method, although levels were still lower than some other published studies. Although the methodology was identical, the two experiments (one with three Pa strains and controls and the other with a different Pa strain and controls) are summarised separately in Table 4.3.2.1 and Figure 4.3.2.1 and Table 4.3.2.2 and Figure 4.2.2.2. This is because there were marked differences between headspace VOCs above the control samples when the two experiments were compared. These differences are summarised in Table 4.3.2.3.

VOC	PA5539 (n=6)	PA14 (n=6)	PA12B-5001 (n=6)	Controls (n=6)	p
Ammonia	3997 [2525-5644]	4443 [1975 – 15764]	2323 [1506 – 5771]	1266 [1010 – 1465]	<0.01
Butanol	141.1 [13.8 – 400.3]	122.1 [36.1 – 322.6]	191.7 [58.8 – 487.4]	142.6 [21.9 – 221.2]	0.756
HCN	739.9 [442 – 938.8]	2257 [793 – 4455]	3155 [1404 – 4177]	8.9 [5.7 – 11.3]	<0.001
2-AA	11.4 [5.3 – 15.9]	10.9 [9.9 – 14.4]	9.1 [7.3 – 10.5]	6.6 [5.1 – 9.4]	<0.05

Table 4.3.2.1: Median [range] levels of ammonia, butanol, HCN and 2-AA detected in headspace above different strains of Pa cultured in liquid media and TSB alone (controls). Cells highlighted in red show groups that differ significantly from controls in post-hoc analysis (Dunn’s multiple comparisons test).

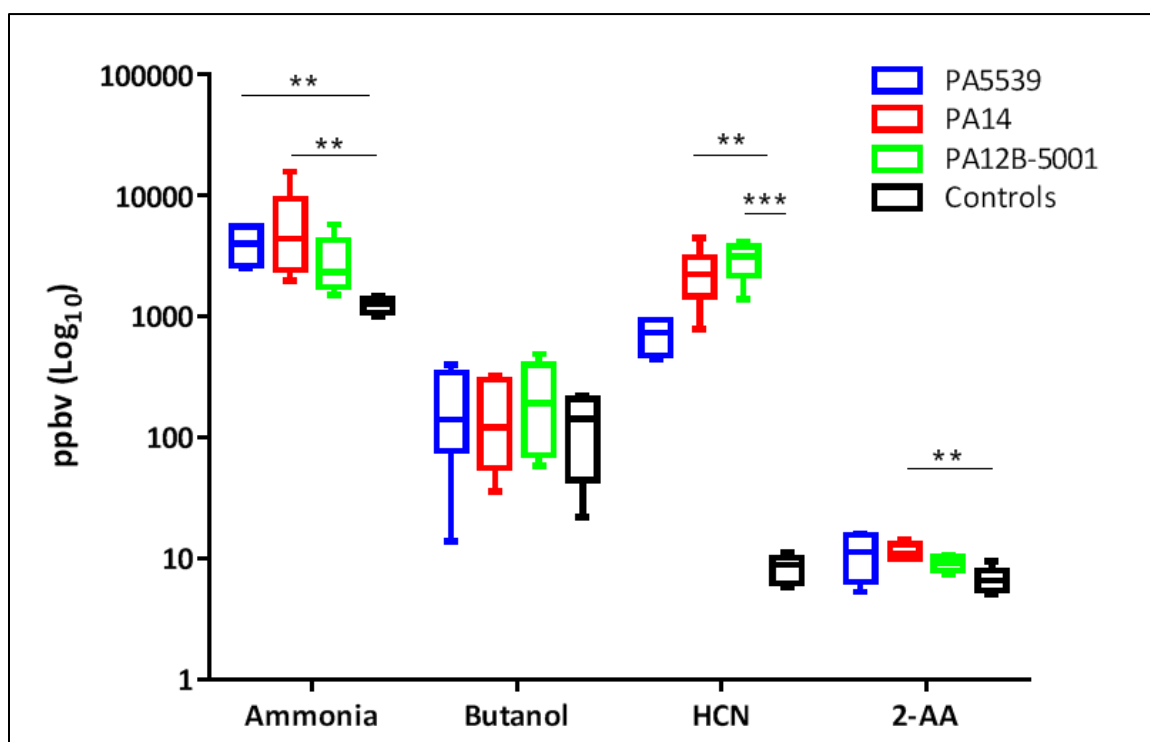


Figure 4.3.2.1: VOCs detected in headspace above different strains of Pa cultured in liquid media compared to VOCs in headspace above TSB alone (controls).

VOC	PA12B-4973 (n=6)	Controls (n=6)	p
Ammonia	1203 [794 – 1908]	1085 [655.6 – 2025]	0.571
Butanol	509.3 [445.7 – 729.2]	725.9 [578.5 – 807.2]	<0.05
HCN	5802 [4431 – 6547]	318.8 [69.9 – 561.4]	<0.01
2-AA	44.2 [35.0 – 71.4]	36.3 [16.1 – 49.3]	0.387

Table 4.3.2.2: Median [range] levels of ammonia, butanol, HCN and 2-AA detected in headspace above PA12B-4973 cultured in liquid media and TSB alone (controls).

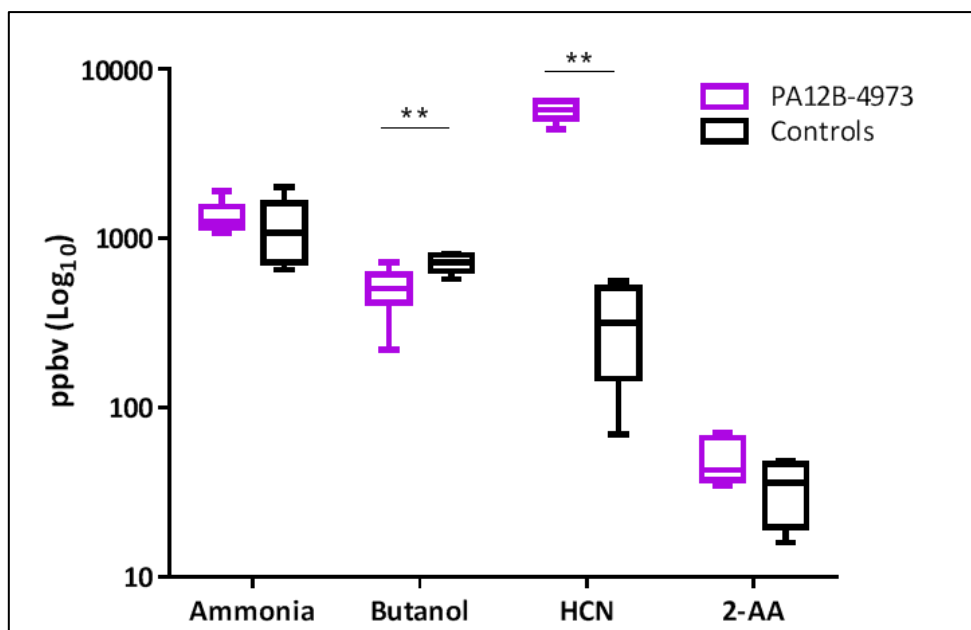


Figure 4.3.2.2: VOCs detected in headspace above PA12B-4973 cultured in liquid media compared to VOCs in headspace above TSB alone (controls).

VOC	Controls Experiment 1 (n=6)	Controls Experiment 2 (n=6)	p
Ammonia	1266 [1010 – 1465]	1085 [655.6 – 2025]	0.571
Butanol	142.6 [21.9 – 221.2]	725.9 [578.5 – 807.2]	<0.01
HCN	8.9 [5.7 – 11.3]	318.8 [69.9 – 561.4]	<0.01
2-AA	6.6 [5.1 – 9.4]	36.3 [16.1 – 49.3]	<0.01

Table 4.3.2.3: Median [range] levels of ammonia, butanol, HCN and 2-AA detected in headspace above TSB alone (controls) in different experiments.

Since the methodology for preparation of these controls (n=6 in each group) was identical, concerns were raised about the repeatability and reproducibility of SIFT-MS measurements. After further analysis, a methodological difference was noted; in the first experiment, where levels of headspace VOCs were consistently low, all six control samples were analysed **before** the bacterial samples whilst in the second experiment they were done at random, interspersed with bacterial samples containing large quantities of headspace VOCs. No clear pattern in readings was discernible for ammonia, butanol and 2-AA but there was an obvious sequential increase in HCN ppbv in the headspace above control samples, suggesting that carryover was taking place due to large amounts being detected in the headspace above bacterial cultures and complete washout from the system not being achieved. This is shown in Figure 4.3.2.3.

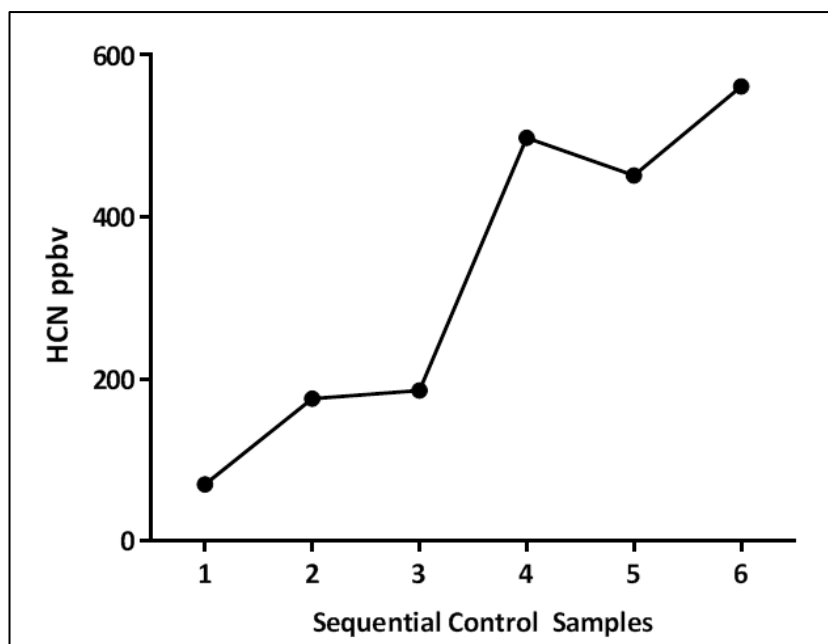


Figure 4.3.2.3: Sequential rise in HCN in ppbv (y-axis) detected in headspace above TSB inoculated with SM buffer (controls) when samples were analysed at random between bacterial samples rather than sequentially prior to bacterial samples being tested. Each point on the x-axis represents a control sample analysed at progressively later points during the experiment.

4.3.3: Rationale for Next Stage of Assay Development

As SIFT-MS sensitivity was noted to be compromised if high levels of HCN "flooded" the system, it was important to establish if this was also i) problematic for other compounds and ii) of any clinical relevance. As butanol was readily available in our laboratory, an experiment to quantify increasing concentrations was devised with the aim being to see if detection was compromised at higher concentrations and whether SIFT-MS detection was accurate enough to generate a standard curve.

4.4: Quantification of Pure Butanol

4.4.1: Materials and Methods

>99% 1-butanol (Sigma, UK) was serial log diluted with deionised water (concentrations from neat to 10^{-6}) and the headspace above 5mls of each concentration in a 30ml Sterilin was analysed for 70s as described in Section 3.1. The Sterilin was connected to the sample port using narrow bore extension tubing and a 21g needle as described in Section 4.3.1. Readings were taken sequentially and separated by sampling from headspace above 5mls deionised water.

4.4.2: Results

The hypothesis that high VOC concentrations can flood the SIFT-MS system and make subsequent readings inaccurate was further clarified by quantification of pure butanol. Whilst it was clear that accurate detection still occurs at high concentrations, as shown by the linear relationship between concentration and measured ppbv in Figure 4.3.1, carryover was evident (as shown in Figure 4.3.2) with increasing butanol detected in the headspace above sequential control samples of deionised water despite attempts to flush the system by allowing five minutes to elapse with helium carrier gas running and the sampling port only exposed only to room air. These results are summarised in Table 4.4.2.1.

Concentration	SIFT-MS ppbv	Control ppbv
0.000001	321.0	176.4
0.00001	1161.5	532.7
0.0001	6407.0	774.3
0.001	58235.5	1931.5
0.01	344325.2	2521.3
0.1	2041254.0	6364.7
1	2496020.0	10934.9

Table 4.4.2.1: Butanol detection by SIFT-MS in headspace above increasing concentrations of >99% 1-butanol. Note accumulation of butanol in headspace above deionised water (controls) after sequential analysis of increasing butanol concentrations.

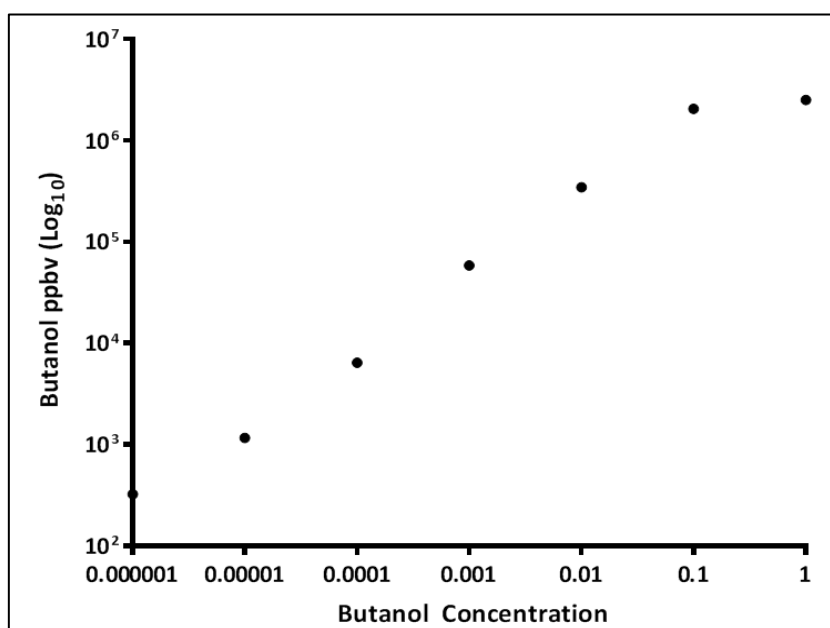


Figure 4.4.2.1: Detection of butanol by SIFT-MS above sequentially increasing concentrations of >99.1% 1-butanol. Note linear relationship between concentration and ppbv, indicating accuracy of detection.

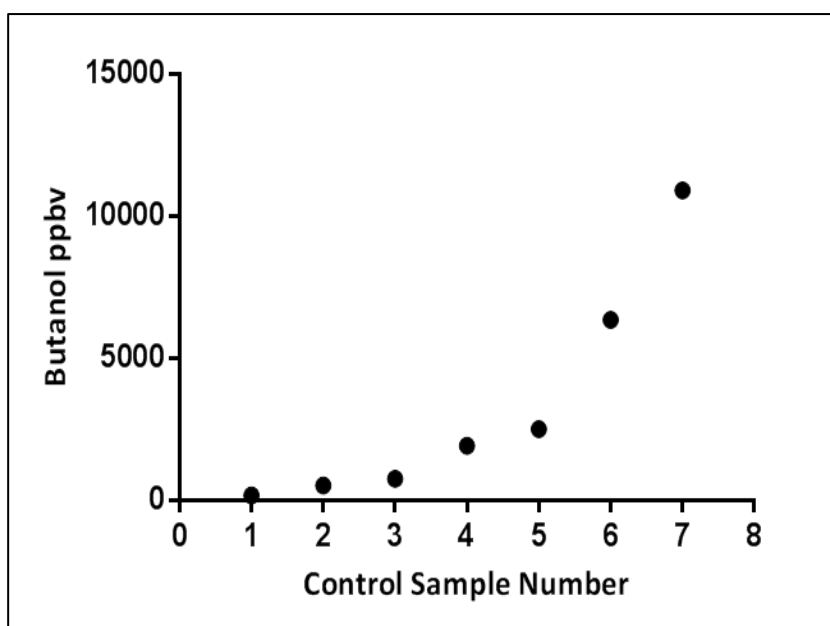


Figure 4.4.2.2: Sequentially increasing butanol detection in headspace above successive control samples, demonstrating that carryover of detection occurs when high VOC concentrations are detected by SIFT-MS.

4.4.3: Rationale for Next Stage of Assay Development

Results in this section confirm the finding that SIFT-MS may not accurately quantify VOCs in sequential samples if there has been a very high concentration of a particular VOC in the previous sample (this was demonstrated for HCN and butanol). However, based on published data, this is unlikely to be of relevance clinically; levels of HCN and butanol that caused significant carryover of signal were way in excess of anything previously published in the literature as being physiological in exhaled breath, even in patients with significant Pa infection. It was however important to perform these experiments to understand this limitation of the SIFT-MS system. In ongoing breath work, this informed additional vigilance in monitoring data from sequential samples to ensure there was no stepwise increase in detection of any given VOC over the course of successive breaths. The assay experiments until now demonstrate that SIFT-MS does accurately measure VOCs, with the butanol experiment particularly reassuring, as a standard curve was generated from analysis of samples of increasing concentration. With this established, it was important to investigate the repeatability and reproducibility of SIFT-MS quantification of exhaled breath VOCs.

4.5: Repeatability and Reproducibility of Exhaled Breath Analysis using SIFT-MS

4.5.1: Materials and Methods

Healthy, non-smoking controls (n=3) recruited from postgraduate students at Imperial College, London were initially investigated. Each provided vital capacity exhalations, into double thickness Nalophan bags that were flushed before use with dry synthetic air (BOC, UK). Subjects were asked to inhale fully through the nose (as close to total lung capacity as possible) and then exhale from the mouth into the bag via the 1ml Luer-Lok syringe, shown in Figure 3.1.1. Subjects were asked to exhale slowly as rapid exhalation i) can affect VOC profile (447) and ii) because healthy adults were likely to exceed the 2L capacity of the Nalophan bag within the first second of expiration (FEV₁) causing it to burst. Unlike with CF patients, there were no infection control concerns; samples were therefore collected at St. Mary's University Hospital where the SIFT-MS was based as opposed to being taken from patients at RBH and transported over to St. Mary's for testing as was necessary in later parts of this work. Sequential breath samples (between n=2 and n=5) were taken and VOC levels were measured as described in Section 3.1. On one day, five breath samples were measured sequentially following an overnight fast and then five breaths from the same subject were analysed thirty minutes after lunch had been consumed and the mouth rinsed with water. This was to see what effect fasting and ingestion of food had on VOC profile over the course of a single day. Results were displayed graphically and, where possible, co-efficients of variation (CoV) calculated.

4.5.2: Results

Reproducibility analysis of SIFT-MS measurements of VOC concentration in breath was carried out on six occasions. Two sequential exhaled breath samples were analysed on one occasion, three breaths on two occasions, four breaths on one occasion and five breaths on two occasions. CoV for each VOC was calculated when ≥ 3 breaths were analysed (n=5) which is shown in Figure 4.5.2.1. Median [range] CoV for each compound is shown in Table 4.5.2.1.

VOC	Median % CoV [range]
Ethanol83	13.6 [7.6 – 47.5]
Methanol	9.4 [3.7 – 12.2]
Propanol	25.5 [10.8 – 42.1]
Butanol	37.1 [25.8 – 51.5]
Pentanol	23.2 [10.7 – 30.0]
Dimethyl Disulphide	30.9 [15.8 – 62.0]
Hydrogen Sulphide	85.4 [49.1 – 148.2]
Hydrogen Cyanide	19.8 [7.2 – 41.6]
2-AA	49.9 [22.1 – 92.7]
Acetone	9.8 [3.9 – 25.2]
Isoprene	21.5 [10.7 – 27.3]
Ammonia	20.1 [6.8 – 29.5]

Table 4.5.2.1: Median CoV [range] for VOCs in exhaled breath (n=3-5) measured on five separate occasions using SIFT-MS.

Measured VOC concentrations in sequential breath samples measured on May 17th, May 22nd, May 24th and June 18th 2012 are shown in Figures 4.5.2.2a and 4.5.2.2b. On June 19th 2012, five breaths were analysed in the morning following an overnight fast and five breaths from the same subject were run thirty minutes after the fast was broken with lunch on the same day. Median [range] of VOC concentrations pre- and post-lunch are summarised in table 4.5.2.2. p values are calculated using non-parametric Mann-Whitney U-test. Each individual VOC measurement pre- and post-lunch is shown in Figures 4.5.2.3a and 4.5.2.3b.

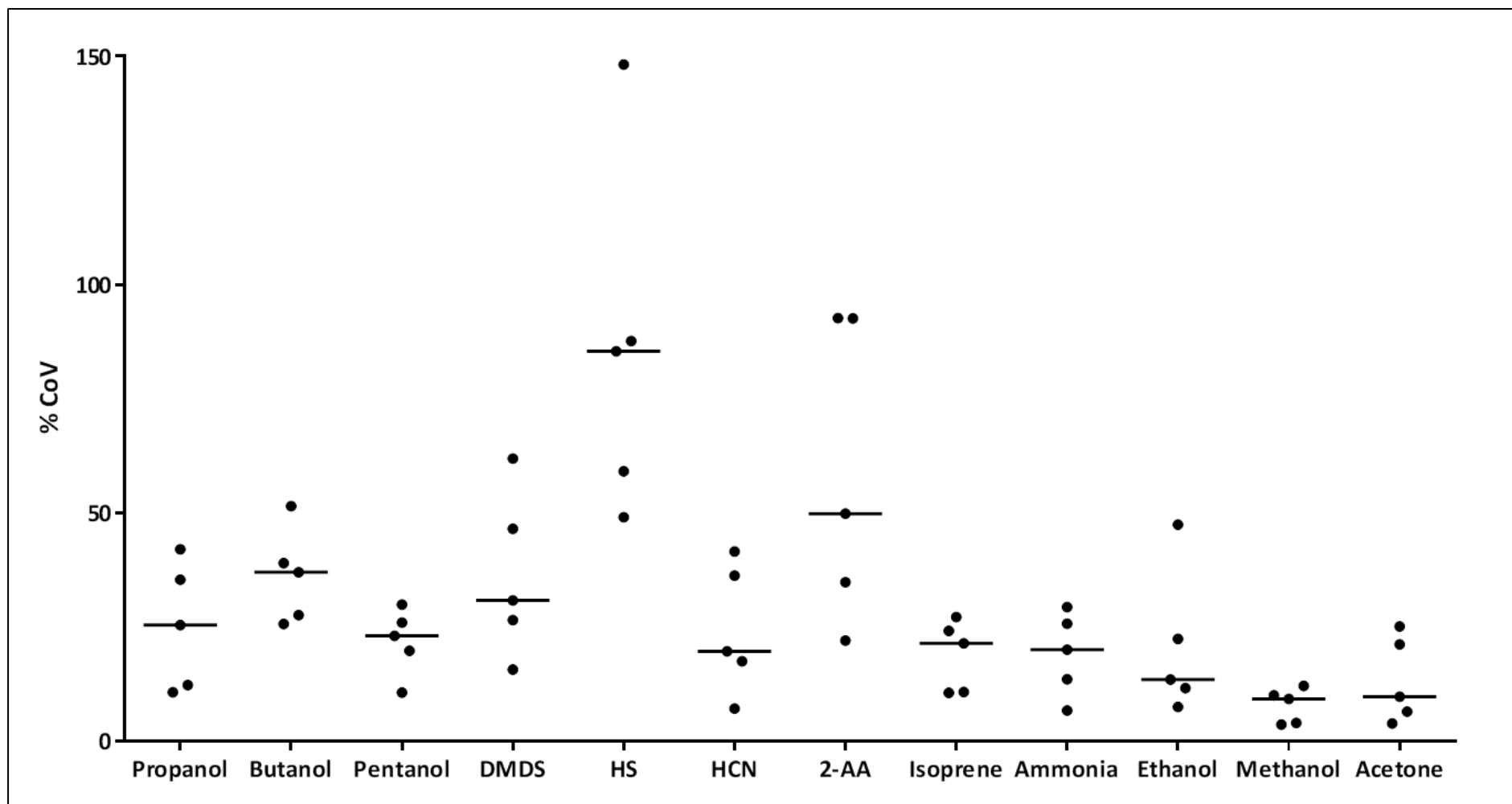
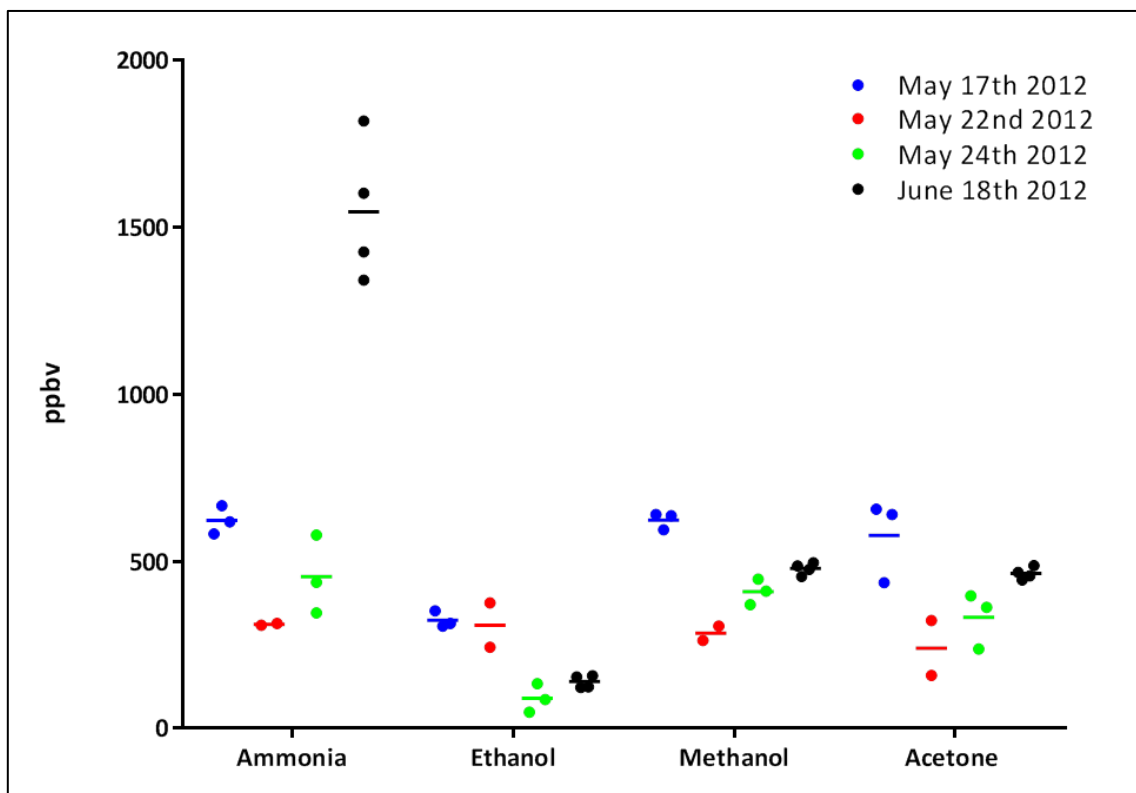
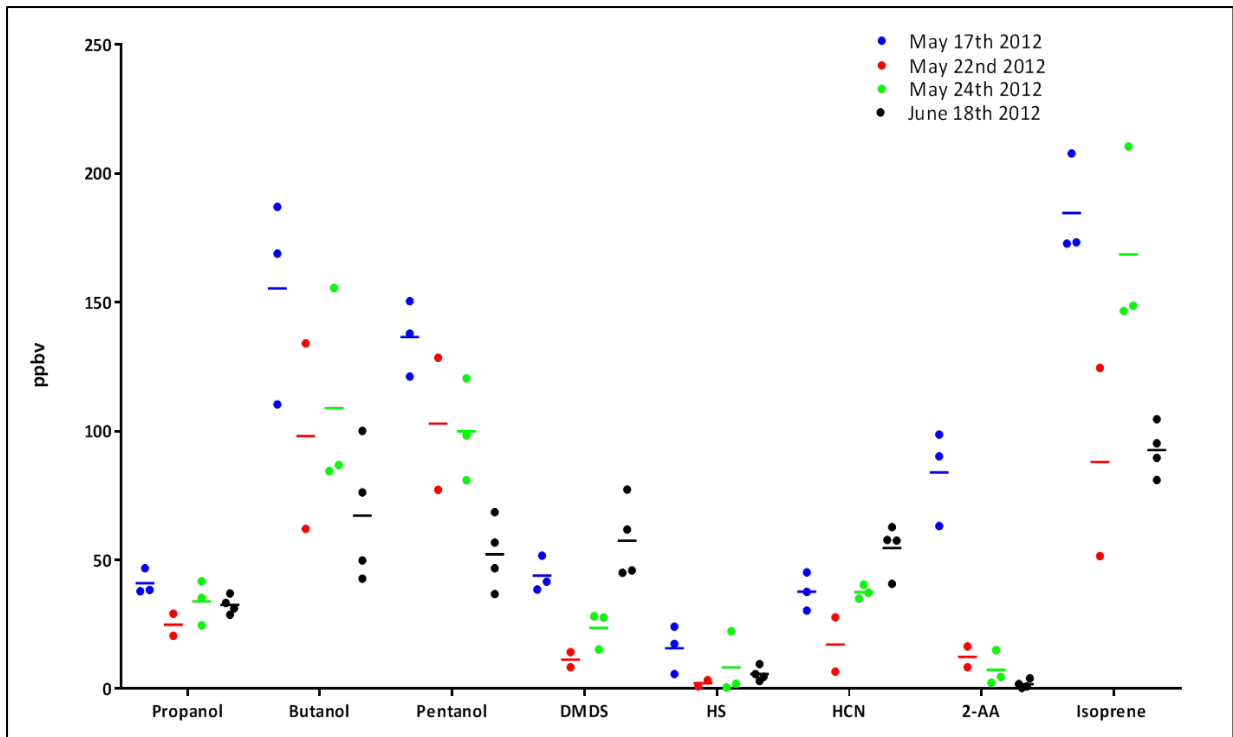


Figure 4.5.2.1: CoVs for VOCs measured in sequentially exhaled breaths (n=3-5) using SIFT-MS on five different occasions in 2012.

Lines are drawn at the median CoV.



Figures 4.5.2.2a and 4.5.2.2b: Measured VOC concentrations in sequential exhaled breath samples (n=2 to n=4) on four different days. Note significant day-to-day variability in concentration of some compounds and variation between individual measurements taken on the same day. Lines are marked at the mean measured concentration (in ppbv) on each day.

VOC	Pre-Lunch Median ppbv [range]	Post-Lunch Median ppbv [range]	p
Ethanol ⁸³	66.2 [51.7 – 71.0]	188.1 [167.9 – 273.4]	<0.01
Methanol	388.7 [340.8 – 434.6]	317.2 [297.8 – 397]	0.10
Propanol	20.2 [10.7 – 32.0]	18.3 [14.4 – 32.1]	0.94
Butanol	84.6 [15.7 – 99.8]	41.6 [25.8 – 58.5]	0.22
Pentanol	39.8 [34.5 – 64.9]	46.6 [38.7 – 66.3]	0.41
Dimethyl Disulphide	93.7 [24.8 – 101.7]	25.4 [11.2 – 59.6]	0.10
Hydrogen Sulphide	3.6 [3.2 – 14.0]	1.3 [0.4 – 4.3]	0.20
Hydrogen Cyanide	16.2 [9.3 – 24.2]	12.0 [6.2 – 16.9]	0.31
2-AA	1.7 [1.0 – 3.2]	4.3 [2.2 – 6.2]	<0.05
Acetone	823.1 [754.0 – 886.5]	463.6 [396.8 – 517.7]	<0.01
Isoprene	94.7 [85.1 – 140.8]	81.9 [66.9 – 122.1]	0.22
Ammonia	677.3 [413.0 – 853.0]	411.4 [344.8 – 569.3]	0.06

Table 4.5.2.2: Median [range] of VOC concentrations in ppbv in five sequentially exhaled breath samples taken from a healthy control subject before and after breaking an overnight fast.

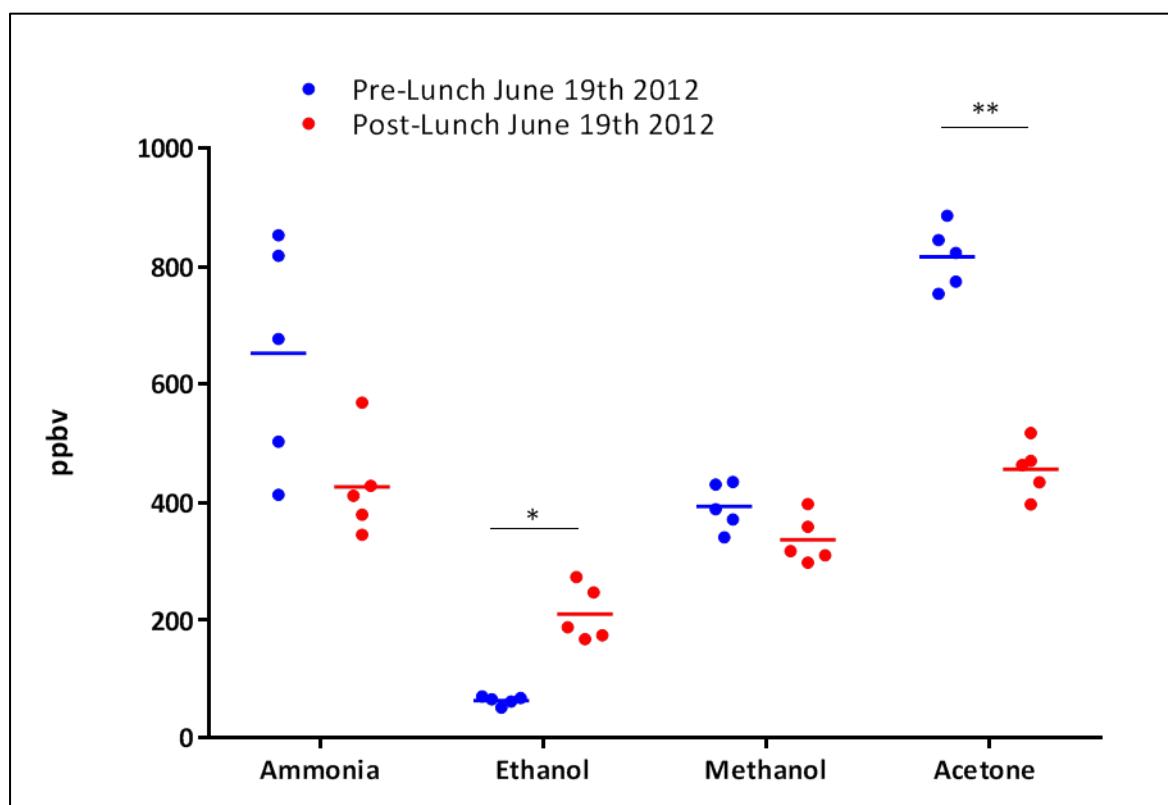


Figure 4.5.2.3a: Measured VOC concentrations in sequential exhaled breath samples (n=5) taken following and overnight fast and thirty minutes after the fast was broken with lunch. Note significant differences in ethanol and acetone levels, and a trend towards a difference in levels of detected ammonia.

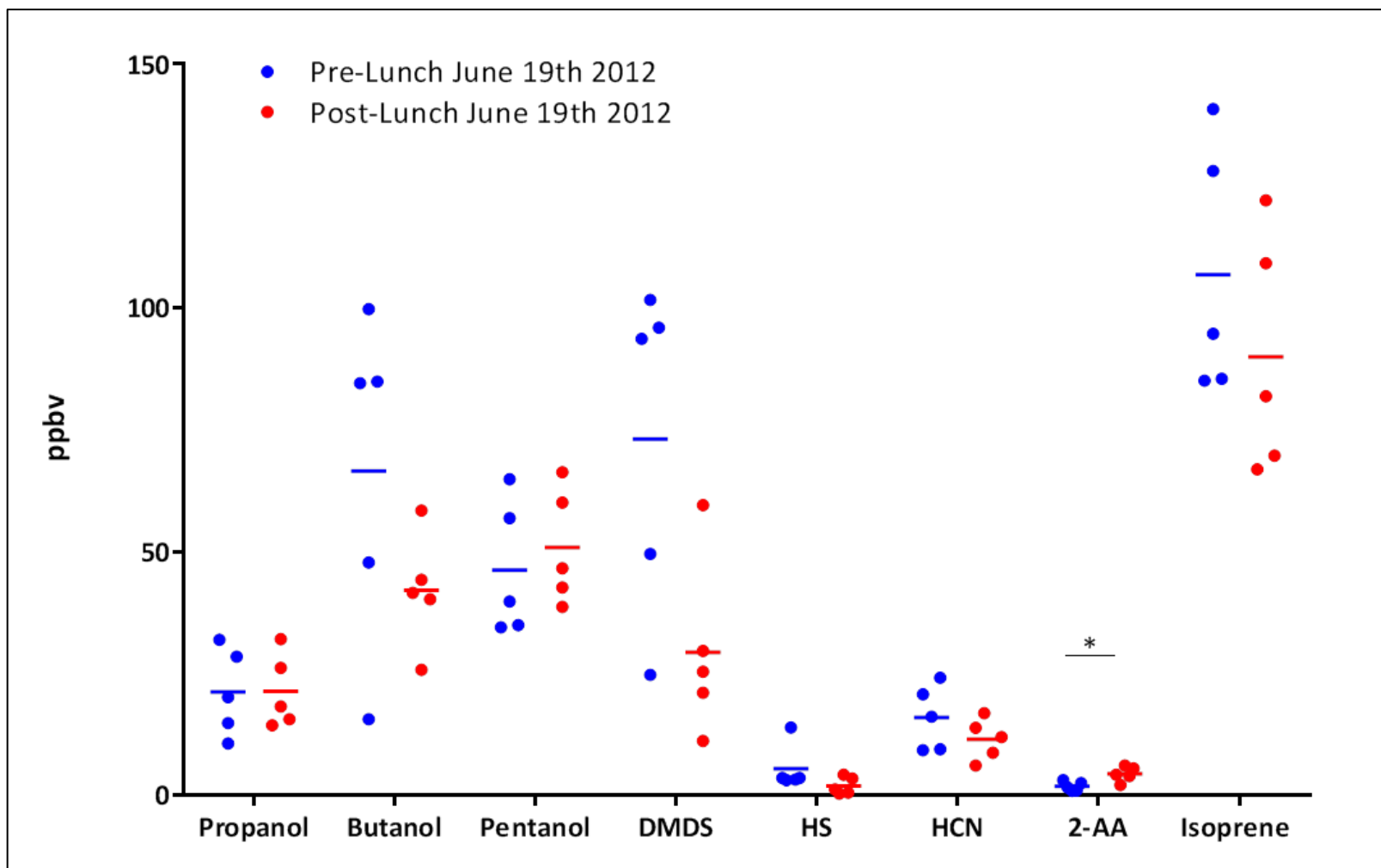


Figure 4.5.2.3b: Measured VOC concentrations in sequential exhaled breath samples (n=5) taken following and overnight fast and thirty minutes after the fast was broken with lunch. Note significant difference in 2-AA levels, with an increase noted after consumption of food.

4.5.3: Rationale for Next Stage of Assay Development

This section helped with a fuller understanding of reproducibility and repeatability of SIFT-MS measurements of exhaled breath. Furthermore, measured VOC levels were not in the range where carryover of signal had previously been noted to be problematic (for butanol and HCN) and no clear incremental pattern of rising VOC concentrations was noted in sequential breath samples; an example of this is shown by the raw data for the pre- and post-lunch experiment (Table 4.5.3.1). Given these findings, I felt that reliability and sensitivity of our SIFT-MS instrument to detect VOCs in exhaled breath had been sufficiently established such that the primary aim of this section, to determine whether discrimination of Pa status is possible by exhaled breath analysis, could be attempted.

VOC	Pre-Lunch (Breaths 1-5)					Post-Lunch (Breaths 1-5)				
	ppbv					ppbv				
Acetone	886.5	774.3	823.1	845.1	754.0	470.5	517.7	396.8	434.1	463.6
Ammonia	413.0	853.0	818.2	677.3	503.2	428.1	411.4	569.3	344.8	379.0
Ethanol	82.6	100.5	100.0	100.2	112.6	310.0	223.8	212.5	200.4	345.2
Methanol	430.2	388.7	371.1	434.6	340.8	358.8	397.0	297.8	317.2	310.2
Propanol	20.2	28.5	10.7	14.9	32.0	14.4	15.7	26.2	18.3	32.1
Butanol	84.6	47.8	99.8	84.9	15.7	44.3	25.8	41.6	58.5	40.3
Pentanol	39.8	34.5	64.9	56.9	35.0	38.7	46.6	42.7	60.1	66.3
DMDS	101.7	93.7	96.0	49.6	24.8	59.6	29.7	25.4	11.2	21.1
HS	3.6	3.6	3.3	3.2	14.0	0.4	1.3	4.3	3.5	0.6
HCN	9.5	9.3	20.8	24.2	16.2	13.9	12.0	6.2	8.8	16.9
2-AA	4.2	4.4	3.6	2.0	3.4	9.8	10.7	7.3	6.8	3.8
Isoprene	128.1	94.7	85.5	140.8	85.1	109.2	122.1	66.9	81.9	69.7

Table 4.5.3.1: Raw data for five sequential breath samples (taken pre- and post-lunch) analysed using SIFT-MS. Note that there is no obvious incremental increase in detected concentration in sequential samples for any VOC, indicating that concerns about signal carryover are unlikely to have clinical relevance.

Chapter 5: Exhaled Breath Analysis of CF Patients and Healthy Controls

5.1: Materials and Methods

Inpatients and outpatients with a confirmed diagnosis of CF were recruited opportunistically from Foulis Ward or the clinics at RBH. Patients were stratified into those with chronic Pa infection (CFPa+) and those free of infection (CFPa-) based on Leeds Criteria (440):

- CFPa+: Patients in whom airway culture results were Pa positive for $\geq 50\%$ of samples obtained in the preceding twelve months.
- CFPa-: Included patients falling under Leeds Criteria i) free of Pa (no isolates in the preceding year) and ii) never had a positive Pa culture.

All subjects were required to have had at least four microbiological culture samples (BAL, cough swabs or sputum) sent for analysis to the microbiological lab at RBH in the previous twelve months. Healthy, non-smoking control subjects were recruited from staff and students at RBH. All participants provided written informed consent and the study was approved by the local and national ethics committee. A copy of the consent form is included in the Appendix to this thesis.

Following a fast of at least four hours, each subject provided a single breath sample into a Nalophan bag, constructed as described in Section 3.1. This offline sampling of exhaled breath was necessary due to concerns about risk of cross-infection of CF patients at two stages: a) whilst waiting to be seen, due to lack of individual patient cubicles at the SIFT-MS laboratory facility and b) from the SIFT-MS instrument itself. RBH has criteria for keeping CFPa+ and CFPa- patients apart by scheduling outpatient clinics on different days. Increasing the risk of cross-infection of CF patients for the purposes of a research study, when the benefits of segregation are widely accepted (448), was deemed unethical. Furthermore, as it has been shown that measured concentrations of VOCs collected into secure double thickness Nalophan bags correlate well with online breath samples, with better correlation seen when sampling at 37°C, as in this study, rather than at 20°C (384), the

benefits to patients of offline sampling outweighed the risks (primarily sample loss in transit) and inconvenience of transporting samples across London.

All inpatient samples were collected at the time patients woke in the mornings, usually around 8am with the breakfast trolley, so the period of fasting was considerably longer, and these participants were also standardised in terms of not having undertaken physiotherapy overnight or having had any nebulised or inhaled therapy prior to providing the sample. It was more difficult to control for these possible confounding factors with outpatient samples; 5/29 of these patients came specifically to provide exhaled breath and therefore were under the same conditions as the inpatients but, for the remaining 24/29, the period of fasting was shorter (although at least four hours in all cases) and they had done physiotherapy and taken their morning inhaled and nebulised medications prior to providing the sample (at least four hours earlier). It was not considered ethical to ask that these treatments be withheld on the day of a clinic appointment as this might have affected clinical assessments such as spirometry. Healthy controls all provided samples at around 8am, so had fasted overnight, and none of them were taking regular inhaled or nebulised therapy or undertaking vigorous physical exercise before providing the sample. It was not possible to control accurately for the volume of exhaled air collected within the bag; use of a pneumotach was considered but felt to pose a risk that was unacceptable in terms of increased likelihood of cross-infection. The majority of subjects were able to fill the bag to capacity, which was assessed visually and by touch. As VOC concentration was reported in ppbv, small differences in the volume of exhaled breath collected were unlikely to influence results. Two subjects with severe CF lung disease were unable to fill the bag with a single exhalation and, although all bags were inspected for leaks after being filled, some samples demonstrated significant loss of volume on visual inspection between time of collection and arrival for analysis; in both these situations, samples were discarded.

Patient samples were collected either on Foulis Ward or the outpatient clinic whilst healthy controls provided samples in the treatment room on Rose Ward. Figure 5.1.1 shows a healthy control subject exhaling into a Nalophan bag. Bags were transported in a sealed plastic box at room temperature to St. Mary's University Hospital where analysis for 12 VOCs of interest was performed within two hours of sample collection as described in Section 3.1. Multiple ion monitoring (MIM) mode was used to quantify VOCs in ppbv and full scan (FS) mode used subsequently to ensure that full spectra were available for visual analysis of peaks if discrepant results from MIM quantification became apparent when the data was reviewed. The rationale behind this is described in Section 2.4.1. Analytical chemistry information for the 12 VOCs used in the final analysis and the precursor ions used for their quantification are shown in Table 5.1.1.



Figure 5.1.1: Photograph of exhaled breath collection from a control subject into a Nalophan bag. Informed consent to reproduce photograph obtained from subject.

	Molecular Formula	Precursor ion	<i>m/z</i>	Characteristic product ions	Ref
Methanol	CH ₄ O	H ₃ O ⁺	33, 51	CH ₅ O ⁺ , CH ₅ O ⁺ (H ₂ O)	(413)
Ethanol ⁸³	C ₂ H ₆ O	H ₃ O ⁺	83	C ₂ H ₇ O ⁺ (H ₂ O) ₂	(413)
Propanol	C ₃ H ₈ O	H ₃ O ⁺	43	C ₃ H ₇ ⁺	(413)
Butanol	C ₄ H ₁₀ O	H ₃ O ⁺	57	C ₄ H ₉ ⁺	(413)
Pentanol	C ₅ H ₁₂ O	H ₃ O ⁺	71	C ₅ H ₁₁ ⁺	(413)
Dimethyl disulphide	C ₂ H ₆ S ₂	H ₃ O ⁺	95	C ₂ H ₆ S ₂ H ⁺	(413)
Hydrogen sulphide	H ₂ S	H ₃ O ⁺	35	H ₃ S ⁺	(413)
Hydrogen cyanide	HCN	H ₃ O ⁺	28	H ₂ CN ⁺	(449)
Ammonia	NH ₃	O ₂ ⁺	17, 35	NH ₃ ⁺ , NH ₃ ⁺ (H ₂ O)	(413)
Acetone	C ₃ H ₆ O	NO ⁺	88	NO ⁺ ·C ₃ H ₆ O	(413)
Isoprene	C ₅ H ₈	NO ⁺	68	C ₅ H ₈ ⁺	(413)
2-AA	C ₈ H ₉ NO	NO ⁺	135	C ₈ H ₉ NO ⁺	(450)

Table 5.1.1: Analytical chemistry information of the VOCs analysed in exhaled breath in this study including the molecular formula, mass to charge ratio (*m/z*), the precursor ions, and characteristic product ions used for their analysis by SIFT-MS.

The choice of precursor ions for each VOC of interest was based on results from previous studies (414-419) and the SIFT-MS kinetics library that prevents certain combinations of precursor and VOC for detection being selected on the basis of pre-existing knowledge about ion chemistry. This theoretically ensured that accurate analysis was possible without interference from other VOCs.

5.2: Statistical Analysis

As no data was available to inform sample size, recruitment for this part of the study was opportunistic. Statistical analysis was performed using SPSS Statistics 21.0 (IBM, USA) and Prism 6.0 (GraphPad, USA). Subject characteristics were explored using Kruskal-Wallis test (with Dunn's multiple comparison test where applicable) for age, body mass index (BMI), FEV₁, immunoglobulin E (IgE) and specific IgE to *Aspergillus fumigatus* and χ^2 test for gender, genotype, pancreatic exocrine status, CF-related diabetes (CFRD) and CF liver disease. Mann-Whitney U-test was used to compare

concentrations of measured VOCs between 2 groups; comparisons were made between CFPa+ and CFPa- patients and between healthy controls and all CF patients.

All 12 VOCs in the study were incorporated into a binary logistic regression model to discriminate between i) CFPa+ and CFPa- and ii) CF patients and healthy controls. Linear combination of VOC concentrations was compared to a variable threshold in order to construct a Receiver Operating Characteristic (ROC) curve. Binary logistical regression analysis, where the disease condition was the dependent variable and VOC concentration the independent variable, was used to obtain optimum weights of concentration for each individual VOC providing the maximal area under the curve (AUC) value. Using a linear combination of significant VOCs, the predicted probability (p) obtained from the binary logistical regression analysis is:

$$\ln (p/1-p) = \text{coefficient}_n \times \text{VOC}_n + \text{constant}$$

This statistical methodology has previously been validated in SIFT-MS studies of VOCs in exhaled breath of patients with Crohn's disease (451) and upper GI cancer (452).

Graphs of subject characteristics and individual VOCs in this part of the study are shown as Tukey box-and-whisker plots. In these, values are plotted as outliers if they are above the 75th centile plus 1.5 times the interquartile range (IQR) or less than the 25th centile minus 1.5 times the IQR. Whiskers are therefore stopped at the largest value less than the sum of the 75th percentile plus 1.5 times the IQR or the smallest value minus 1.5 times the IQR.

5.3: Results

5.3.1: Subject Characteristics

111 subjects were recruited opportunistically from patients, students and staff at RBH between August 2012 and August 2013. Due to technical difficulties with the SIFT-MS, there was a pause in recruitment as no samples could be analysed between September 2012 and January 2013. One sample from 8th March 2013 and four samples collected on 10th April 2013 were transported to St. Mary's Hospital but could not be used due to VOC measurements and full spectra that appeared anomalous, most likely due to headspace above bacterial cultures having earlier been analysed using the SIFT-MS, resulting in carryover of signal as discussed in Section 4. Butanol and ethanol levels on two samples collected in January 2013 were unusually high (levels not considered physiologically possible), thought to be related to use of disinfectants in the lab over the holiday period, and these samples were also excluded from the analysis. When such issues became apparent the SIFT-MS was flushed by increasing the flow rate of helium carrier gas and allowing the machine to sample room air (≥ 6 hrs); only when VOCs returned to expected background levels was any further breath analysis attempted. Two subjects with severe CF lung disease were unable to fill a Nalophan bag with a single exhalation of breath and these samples were also not analysed. Finally, on reviewing the clinical data, two subjects classified as CFPa- were excluded as single growths of Pa were detected in both at nine and eleven months prior to sample collection respectively. Therefore, 100 subjects were included in the final analysis; there were no significant differences in baseline demographics or clinical parameters between CFPa+ and CFPa- patients, aside from in FEV₁ which, as expected (453, 454), was lower in subjects chronically infected with Pa. The only clinical data collected from healthy controls was age, BMI and gender; BMI was significantly higher in control subjects compared to CFPa+ patients with no other differences apparent between groups.

A summary of subject characteristics is shown in Table 5.3.1.1. Figure 5.3.1.1 shows the difference in FEV₁ between CFPa+ and CFPa- patients and Figure 5.3.1.2 shows BMI across the three groups.

	CFPa+ (n=44)	CFPa- (n=29)	Controls (n=27)	p
Median Age [IQR]	27 [22.3-34]	24 [18.5-32.5]	31 [28-34]	0.12
Male [%]	19 [43.2]	11 [37.9]	11 [40.7]	0.90
Median BMI [IQR]	20.8 [18-23.8]*	22.3 [19.8-24]	23 [21.8-26]*	<0.05
p.Phe508del Homozygous [%]	21 [47.7]	16 [55.2]		0.63
p.Phe508del Heterozygous [%]	17 [38.6]	11 [37.9]		
Pancreatic Insufficiency [%]	40	26		0.86
CFRD [%]	17 [38.6]	10 [34.5]		0.72
Liver Disease [%]	8 [18.2]	7 [24.1]		0.54
Median FEV ₁ [IQR]	45 [28.3-61.8]	57 [46.0-74.5]		<0.05
Median IgE [IQR]	37 [8.3-187.5]	76 [30.5-380]		0.16
Median Aspergillus IgE [IQR]	0.46 [0.05-4.3]	0.36 [0.65-7.8]		0.73
Median % Water Levels in Exhaled Breath [IQR]	4.2 [3.8 – 5.1]	4.5 [3.8 – 4.9]	4.3 [3.7 – 5.0]	0.84

Table 5.3.1.1: Subject characteristics of 100 participants who provided exhaled breath samples for analysis using SIFT-MS. CF-related liver disease was defined as abnormal ultrasound scan with independent physician decision to treat with ursodeoxycholic acid therapy ± deranged LFTs. No patients had LFTs ≥3x the normal range or fulminant liver disease.

* indicates the groups across which a significant difference was evident using Dunn's multiple comparison test.

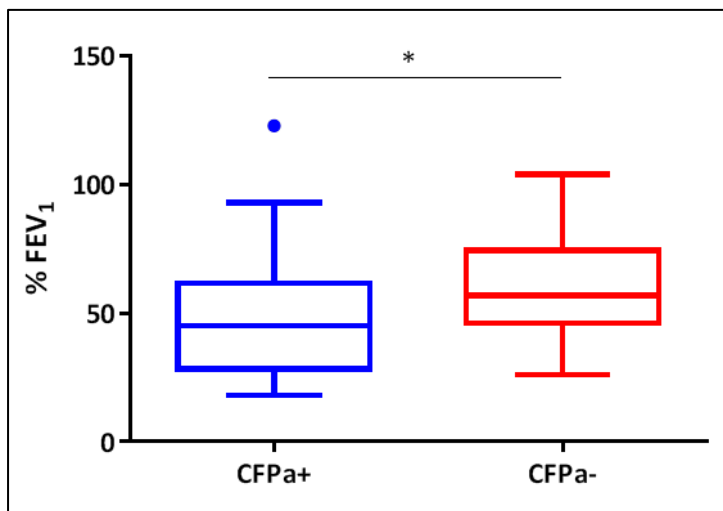


Figure 5.3.1.1: Box-and-whisker plot (Tukey) showing significant reduction in % predicted FEV₁ in CFPa+ subjects compared to CFPa- subjects (p < 0.05).

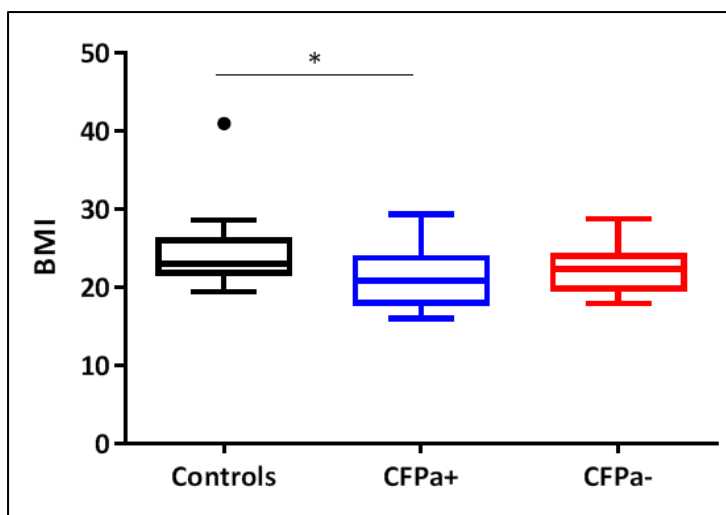


Figure 5.3.1.2: Box-and-whisker plot (Tukey) showing significant reduction in BMI in CFPa+ subjects compared to healthy controls ($p < 0.05$)

In the CFPa- group, the median [IQR] number of culture samples (BAL, sputum or cough swabs) negative for Pa growth over the preceding 12 months was 8 [5-11]. Going back further, the median [IQR] of negative samples in this group was 18 [14-38]; one non-expectorating patient had no sputum samples on the hospital electronic database but 20 cough swabs negative for Pa. 4/27 of the CFPa- subjects had no pathogen growth in the preceding twelve months; the other patients in this group isolated a number of other organisms including bacteria (*Staphylococcus aureus*, methicillin resistant *Staphylococcus aureus*, *Stenotrophomonas maltophilia* and *Haemophilus influenzae*), fungi (*Aspergillus fumigatus*, *Candida albicans* and *Scedosporium apiospermum*) and non-tuberculous mycobacteria (NTM; *Mycobacterium avium-intracellulare* and *Mycobacterium abscessus*). For the CFPa+ group, the median [IQR] of culture samples in the year prior to the breath sample was 9 [7 – 17]. Both mucoid and non-mucoid strains were isolated from 24 (54.5%) patients, non-mucoid strains alone from 14 patients (31.8%) and mucoid strains alone from 6 patients (13.6%). Subgroup analysis of mucoid compared with non-mucoid VOC profiles were not done as the numbers were too small to interpret with confidence. There was no statistically significant difference in FEV₁ between subjects only growing mucoid or non-mucoid Pa (median [IQR] % FEV₁ 56.5 [23.5 – 76.5] vs. 40.5 [22.5 – 62.5], $p = 0.483$).

5.3.2: Full Scan Analysis

Full scan analysis of all samples was performed after quantification of VOCs in MIM mode in order to identify the presence of various compounds in exhaled breath. This was a quality control measure that allowed complete spectra to be reviewed if concerns arose in subsequent data analysis regarding accuracy of measurements in MIM mode. A representative example of a spectrum from a CF patient is shown in Figure 5.3.2.1.

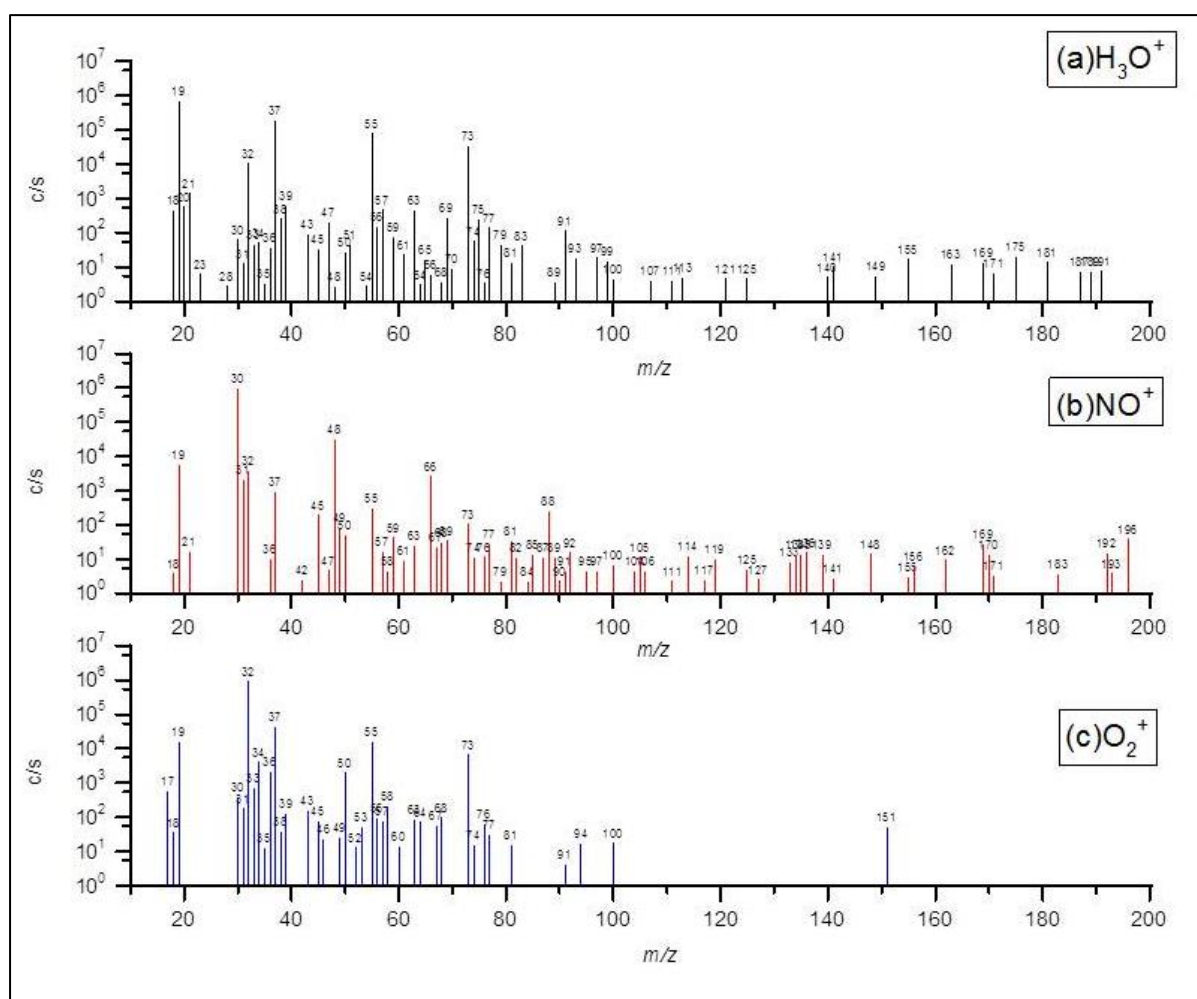


Figure 5.3.2.1: Full scan spectra of exhaled breath from a CF patient analysed using (a) H₃O⁺ precursor ion, (b) NO⁺ precursor ion and (c) O₂⁺ precursor ion. The individual characteristic product ions and their hydrates were assigned to the analysed molecules. In (a), *m/z* 19, 37, 55 and 73 are H₃O⁺ (H₂O) 0, 1, 2, 3; *m/z* 33, 51 is methanol; *m/z* 47 is ethanol; *m/z* 43 is propanol; *m/z* 57 is butanol; *m/z* 71 is pentanol; *m/z* 35 is hydrogen sulphide; *m/z* 28 is hydrogen cyanide; dimethyl disulphide was not detected in this sample, *m/z* 95. In (b) *m/z* 30, 48, 66 and 84 are NO⁺ (H₂O) 0, 1, 2, 3; *m/z* 68 is isoprene; *m/z* 88 is acetone; *m/z* 135 is 2-AA. In (c) *m/z* 32, 50, 68 are O₂⁺ (H₂O); *m/z* 17, 35 are ammonia. (c/s = counts per second).

5.3.3: Heatmap

The concentration of each VOC detected in every subject, expressed as a percentage of the highest recorded value, is shown in Figure 5.3.3.1. High concentrations are shown on the heatmap in red with low concentrations in green, as indicated by the adjacent key.

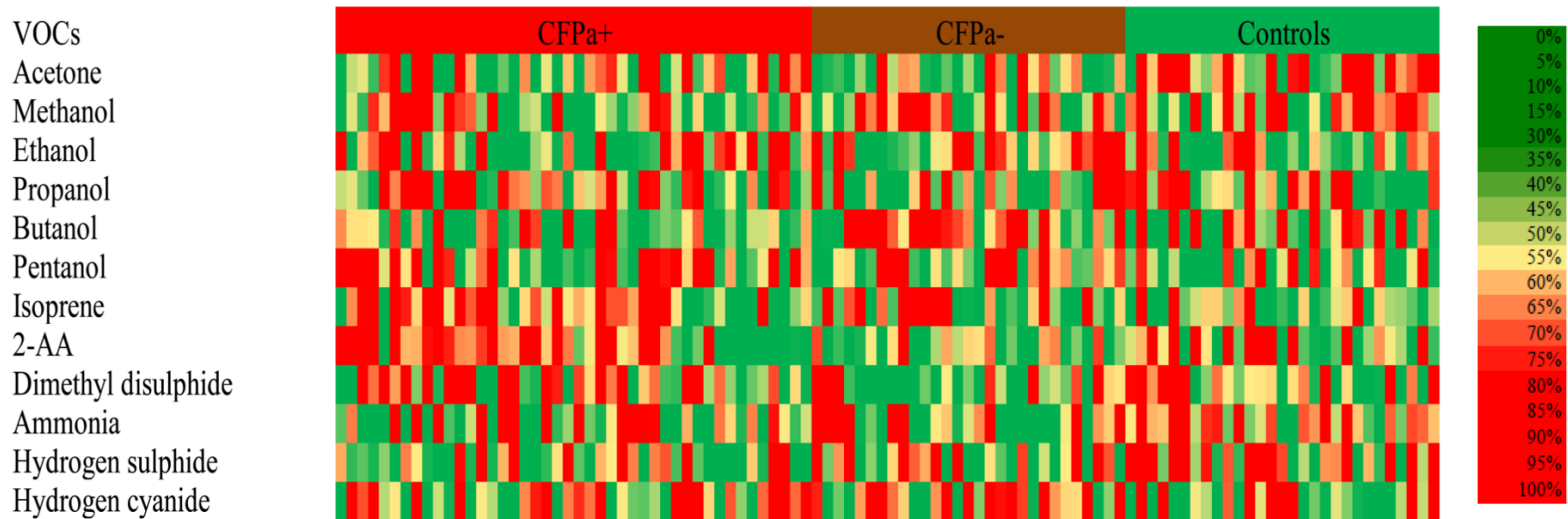


Figure 5.3.3.1: Heatmap showing VOC concentrations for each subject (n=100). The highest concentration of a particular VOC across the entire group is considered as 100% (signified by the darkest shade of red). Concentrations in all other subjects are shown as a proportion of this maximum value, with lowest readings in dark green (0%), as shown in the adjacent key.

Each column represents the VOC profile of each individual subject. If there was definite separation in any VOC across the groups, it would be expected that large blocks of red would coalesce in one of the groups (CFPa+ for example) with large blocks of green under the others. This would be seen, for example, if BALF neutrophils were being depicted in a similar way for these three subject groups. That no clear separation of red and green is seen for any VOC demonstrates that, although a signal might be present, there is marked overlap between groups and no single VOC from those measured here can be used clinically as a biomarker for Pa infection.

5.3.4: CFPa+ vs. CFPa-

Significant differences were noted in 3 of the 12 measured VOCs according to Pa status of CF patients. Dimethyl disulphide ($p < 0.05$) and 2-AA ($p < 0.001$) were significantly higher in the CFPa+ group whilst butanol ($p < 0.01$) was lower. No difference was detected in HCN or any of the other measured VOCs. These results are summarised in Table 5.3.4.1. Box-and-whisker plots (Tukey) of the VOCs that differed between groups and of HCN are shown in Figure 5.3.4.1.

VOC	CFPa+ (n=44)	CFPa- (n=29)	p
Ethanol ⁸³	171.8 [106.5 – 392.0]	181.2 [121.2 – 328.3]	0.782
Methanol	267.2 [209.1 – 328.4]	288.9 [208.9 – 349.9]	0.289
Propanol	145.5 [67.3 – 207.6]	87.1 [47.4 – 188.6]	0.136
Butanol	40.4 [26.3 – 79.3]	91.0 [41.2 – 181.4]	<0.01
Pentanol	47.6 [31.3 – 69.2]	46.3 [33.3 – 56.7]	0.359
Dimethyl Disulphide	81.1 [42.0 – 149.6]	51.9 [26.2 – 88.9]	<0.05
Hydrogen Sulphide	1.0 [0.4 – 2.7]	1.7 [0.3 – 3.8]	0.608
Hydrogen Cyanide	9.0 [5.5 – 12.8]	10.1 [6.2 – 12.9]	0.869
2-AA (NO)	3.6 [1.2 – 6.0]	1.8 [0.0 – 3.3]	<0.001
Acetone (NO)	270.0 [164.0 – 360.6]	232.2 [167.4 – 309.2]	0.324
Ammonia (O ₂)	321.7 [147.8 – 541.2]	364.2 [192.3 – 623.2]	0.585
Isoprene (NO)	91.2 [64.8 – 141.8]	73.8 [57.6 – 192.7]	0.710

Table 5.3.4.1: Median [IQR] of 12 VOCs in ppbv measured in the exhaled breath of CF patients with (CFPa+) and free (CFPa-) of Pa infection; p values calculated using the Mann-Whitney U test.

A subgroup analysis of CFPa- patients was undertaken to see whether VOC profile was affected by being on chronic suppressive therapy (nebulised Colomycin, Tobramycin or Aztreonam). This was to help determine whether differences seen in CFPa+ subjects might be attributable to the effects of inhaled treatment rather than Pa infection itself. Ten patients were not receiving nebulised treatment, all of whom had not Pa isolated for at least two years, whilst nineteen patients were having regular nebulised therapy. VOC profile did not differ across these groups although FEV₁ was lower in the group receiving nebulised therapy. Median [IQR] % FEV₁ was 74.0 [50.1 – 89.5] in patients not receiving nebulised treatment compared to 53.0 [35.0 – 61.0], $p < 0.05$, in subjects on nebulised therapy. These findings are summarised in Table 5.3.4.2 and Figure 5.3.4.2.

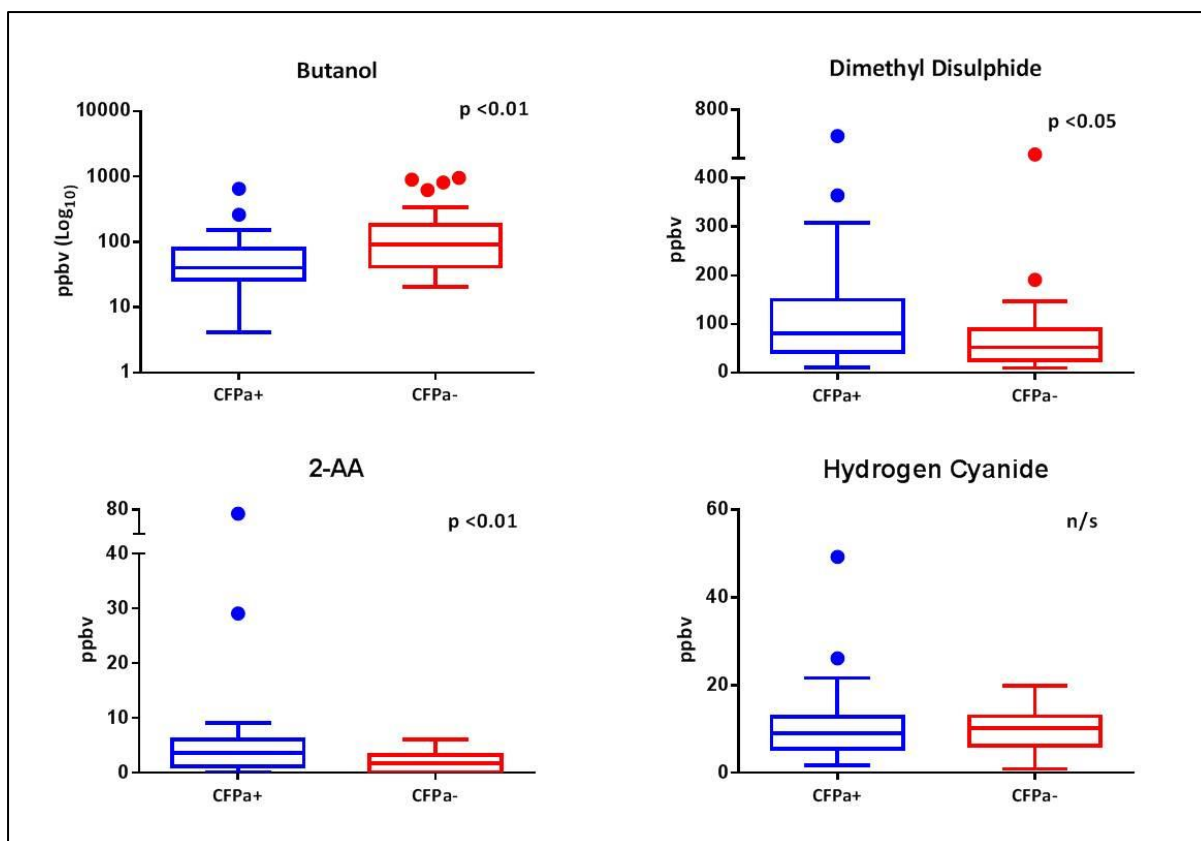


Figure 5.3.4.1: Box-and-whisker plots (Tukey) demonstrating statistically significant but clinically unimportant differences in butanol, dimethyl disulphide and 2-AA in the exhaled breath of CFPa+ and CFPa- patients. No difference is demonstrated in mouth-exhaled hydrogen cyanide (HCN) between the groups.

VOC	No Nebulised Therapy (n=10)	On Nebulised Therapy (n=19)	p
Ethanol ⁸³	188.3 [149.7 – 381.2]	168.9 [114.8 – 305.3]	0.437
Methanol	282.7 [192.9 – 349.0]	288.9 [211.0 – 353.5]	0.500
Propanol	80.2 [46.2 – 274.9]	91.3 [43.7 – 173.6]	0.910
Butanol	43.5 [35.8 – 97.8]	98 [55.3 – 198.4]	0.167
Pentanol	49.0 [35.2 – 52.1]	45.6 [25.0 – 58.9]	0.372
Dimethyl Disulphide	67.8 [46.0 – 111.7]	36.2 [22.7 – 69.7]	0.112
Hydrogen Sulphide	1.6 [0.4 – 3.7]	1.8 [0.0 – 4.2]	0.847
Hydrogen Cyanide	9.6 [6.9 – 13.1]	10.2 [5.3 – 13.1]	0.990
2-AA (NO)	1.5 [0.0 – 3.6]	1.8 [0.0 – 3.0]	0.864
Acetone (NO)	282.0 [195.3 – 327.8]	225.3 [167.5 – 307.3]	0.406
Ammonia (O ₂)	287.4 [168.6 – 484.9]	373 [194.4 – 631.3]	0.367
Isoprene (NO)	72.8 [55.7 – 97.1]	96.5 [58.3 – 208.7]	0.417

Table 5.3.4.2: Median [IQR] of 12 VOCs in ppbv in exhaled breath of CF patients free of Pa infection (CFPa-) who were either not on any anti-Pa therapy (n=10) or were receiving regular nebulised treatment (n=19). No difference in any of the 12 VOCs was demonstrated; p values calculated using Mann-Whitney U test.

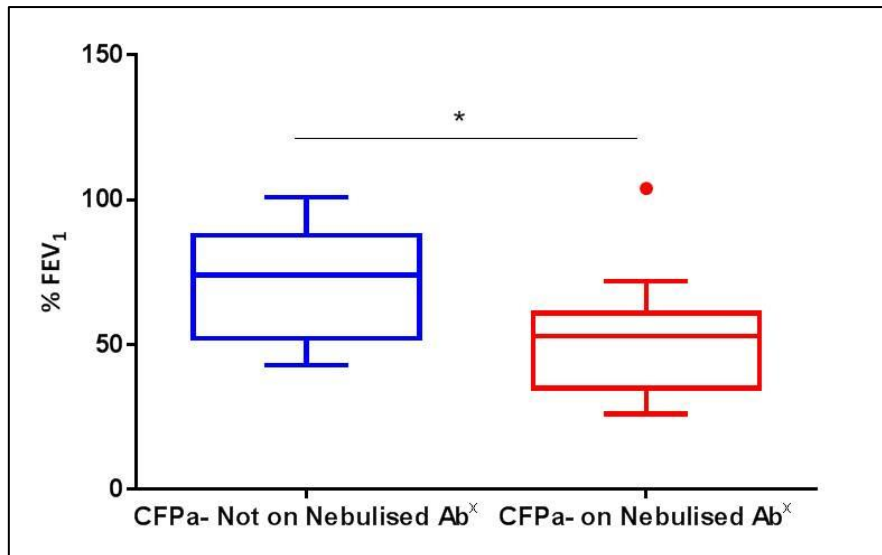


Figure 5.3.4.2: Box-and-whisker plot (Tukey) showing significantly lower FEV₁ in CFPa- patients receiving nebulised therapy (p < 0.05). This is expected as subjects with more severe disease are more likely to be kept on chronic suppressive therapy despite the increased treatment burden.

A diagnostic prediction model (ROC analysis) constructed using binary regression of butanol, 2-AA and dimethyl disulphide (the three VOCs that differed significantly across the groups) gave an AUC of 0.774 (95% Confidence Interval (CI) 0.667 – 0.882) with a sensitivity and specificity of 0.828 and 0.649 respectively. AUC was higher if all 12 analysed VOCs were used in the diagnostic prediction model at 0.842 (95% CI 0.753 – 0.930) with a sensitivity of 0.828 and specificity of 0.705. The ROC curves are shown in Figures 5.3.4.3a and 5.3.4.3b.

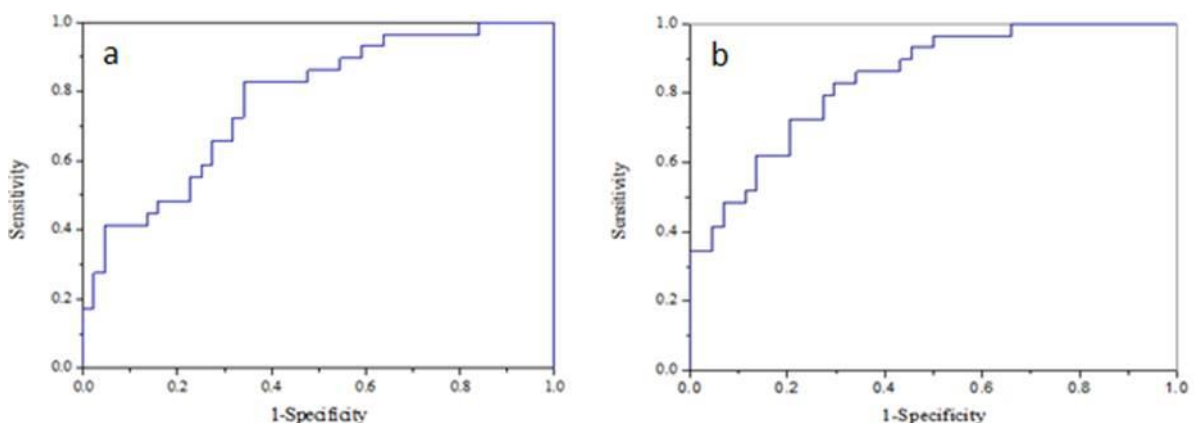


Figure 5.3.4.3a (left) and 5.3.4.3b (right): ROC curves for CFPa+ vs. CFPa- patients with (a) only the three VOCs (2-AA, butanol and dimethyl disulphide) that were significantly different between groups and (b) with all 12 analysed VOCs used in the binary regression model.

FEV₁ was the only clinical parameter that differed between CFPa+ and CFPa- groups ($p < 0.05$). Linear regression analysis, assessing influence of FEV₁ on VOC concentrations, demonstrated that, although propanol and dimethyl disulphide correlated with FEV₁, r^2 values were extremely low (0.066 and 0.097 respectively), suggesting that FEV₁ was unlikely to be confounding these results.

5.3.5: CF Patients vs. Healthy Controls

Though not the primary focus of this study, exhaled breath from CF patients, irrespective of Pa status, and healthy controls was also compared as, although a new diagnostic test for CF is not required, any differences in breath profile between CF patients and healthy controls might provide information about underlying pathological mechanisms in CF. 4 out of the 12 quantified VOCs were significantly different; isoprene and pentanol were both increased (both $p < 0.05$) in CF patients whilst acetone ($p < 0.01$) and hydrogen sulphide ($p < 0.05$) were lower in CF patients compared with healthy controls. These results are summarised in Table 5.3.5.1. Box-and-whisker plots (Tukey) of the VOCs that differed between CF patients and healthy controls are shown in Figure 5.3.5.1.

VOC	CF (n=73)	Controls (n=27)	p
Ethanol ⁸³	177.2 [111.6 – 352.4]	145.3 [97.6 – 224.4]	0.185
Methanol	275.2 [209.6 – 335.4]	294.3 [239.2 – 424.2]	0.230
Propanol	126.1 [54.0 – 201.5]	112.4 [46.8 – 201.3]	0.672
Butanol	55.7 [29.0 – 101.8]	41.0 [26.2 – 139.7]	0.856
Pentanol	46.4 [32.5 – 62.7]	36.4 [22.0 – 50.4]	<0.05
Dimethyl Disulphide	63.1 [35.5 – 120.2]	73.5 [38.2 – 120.2]	0.744
Hydrogen Sulphide	1.2 [0.4 – 3.1]	2.6 [0.8 – 6.8]	<0.05
Hydrogen Cyanide	10 [5.6 – 12.7]	7.1 [4.6 – 12.7]	0.156
2-AA (NO)	2.9 [0.9 – 4.9]	2.5 [1.1 – 5.7]	0.968
Acetone (NO)	258.6 [167.4 – 328.6]	341.7 [236.9 – 572.1]	<0.01
Ammonia (O ₂)	340.6 [189.1 – 585.1]	432.7 [332.4 – 522.8]	0.058
Isoprene (NO)	88.2 [58.5 – 151.0]	74.1 [50.0 – 89.3]	<0.05

Table 5.3.5.1: Median [IQR] of 12 VOCs in ppbv measured in exhaled breath of CF patients and healthy controls; p values calculated using Mann-Whitney U test.

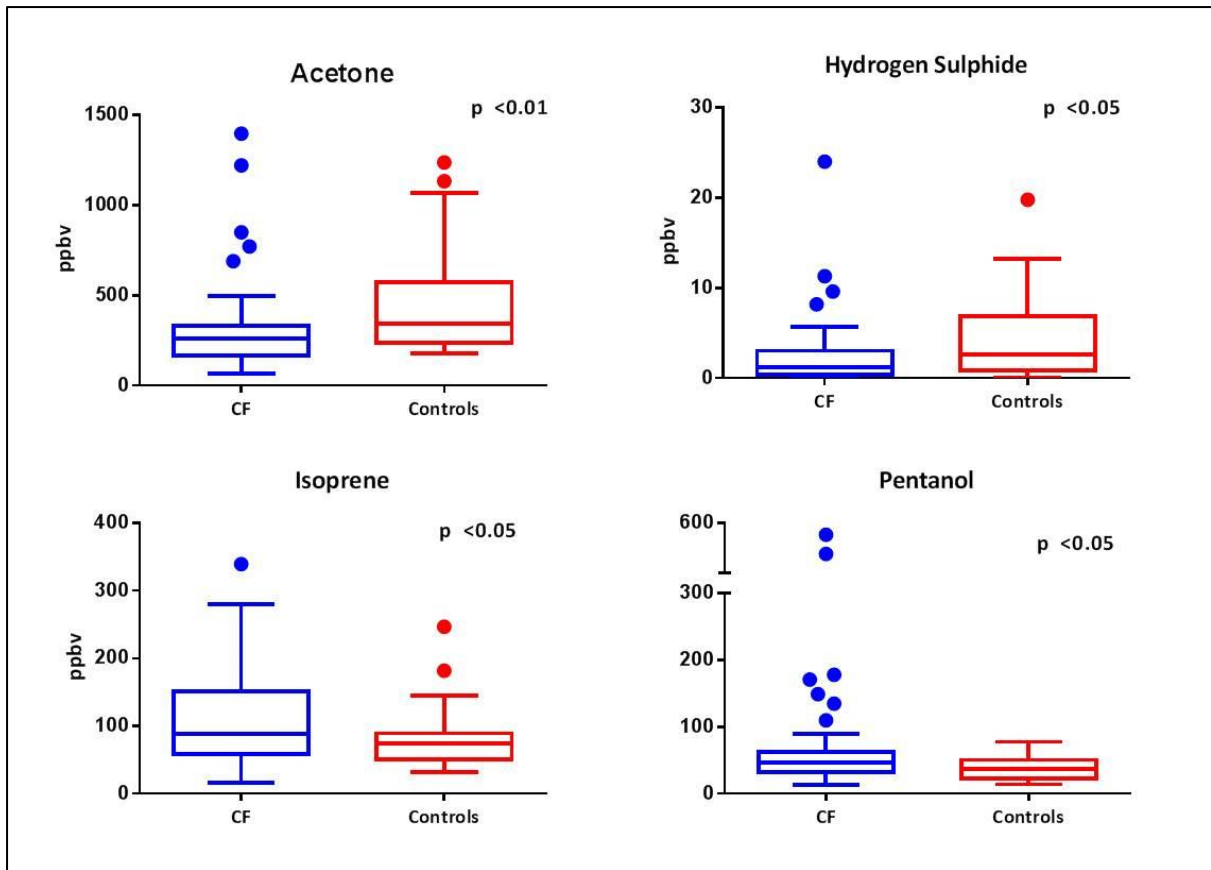


Figure 5.3.5.1: Box-and-whisker plots (Tukey) demonstrating significant differences in acetone, hydrogen sulphide, isoprene and pentanol in the exhaled breath of CF patients and healthy controls.

ROC analysis using only the 4 VOCs that were statistically different across the two groups gave an AUC of 0.811 (95% CI 0.725 – 0.897), with sensitivity of 0.852 and specificity of 0.671. If all 12 VOCs were used in the diagnostic prediction model, discrimination was again superior; AUC increased to 0.884 (95% CI 0.809 – 0.959), with sensitivity of 0.815 and specificity of 0.877. The ROC curves are shown in Figures 5.3.5.2a and 5.3.5.2b.

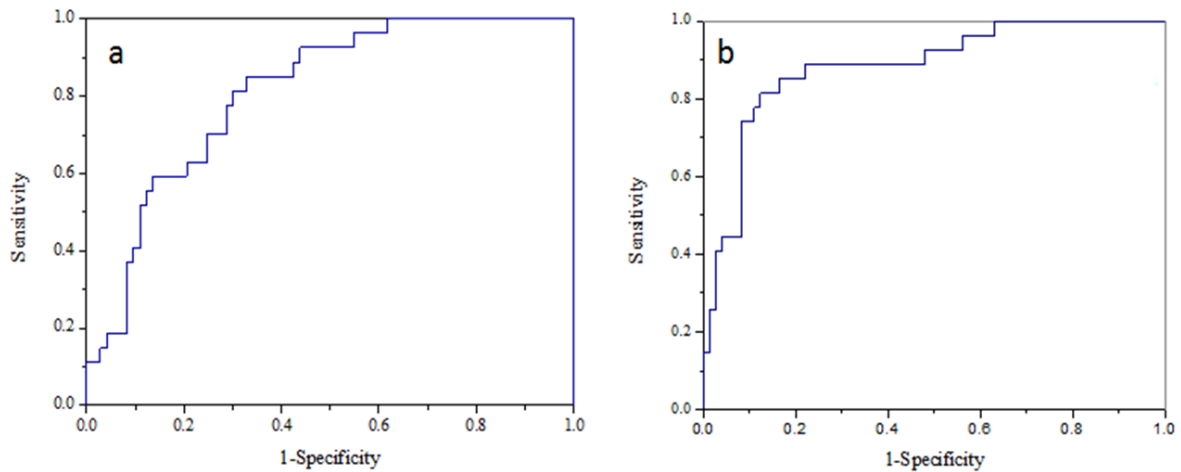


Figure 5.3.5.2a (left) and 5.3.5.2b (right): ROC curves of healthy controls vs. CF patients with (a) only the four VOCs (acetone, hydrogen sulphide, isoprene and pentanol) that were significantly different between groups and (b) with all 12 analysed VOCs used in the binary regression model.

Of possible confounders, BMI was significantly different lower in CFPa+ patients when compared with healthy controls ($p < 0.05$) on univariate analysis. When BMI of all CF patients in the study was compared to that of healthy controls, it was significantly lower ($p < 0.05$). No significant differences were found between the CFPa- patients and control subjects. Linear regression analysis to investigate influence of BMI on VOC concentration demonstrated that there was no direct correlation of any single VOC with BMI.

5.3.6: Exacerbating CF Patients vs. Stable CF Patients

Post-hoc comparison of CF patients who were exacerbating or stable, regardless of Pa status, was also undertaken. Classification of these groups was:

- Exacerbating: Patients experiencing a physician-diagnosed increase in pulmonary symptoms (n=43). These patients had been admitted to Foulis Ward and were receiving intravenous antibiotics; unfortunately the day of treatment could not be standardised as this was a post-hoc analysis. For any future study, VOC profile would be measured at pre-defined times during an exacerbation (for example, admission, day 7 and day 14 of treatment).
- Stable: Patients who attended hospital specifically to provide an exhaled breath sample (n=5) or outpatients recruited opportunistically from the CF clinic (n=25) who did not require an immediate emergency admission for an increase in symptoms.

Significant differences were seen in ethanol⁸³ ($p < 0.05$), HCN, 2-AA and isoprene (all $p < 0.01$). This is summarised in Table 5.3.6.1 (overleaf). Box-and-whisker plots (Tukey) of the VOCs that differed between exacerbating and stable patients are shown in Figure 5.3.6.1. The most striking difference was in exhaled isoprene ($p < 0.001$), which was lower in non-exacerbating patients. However, there was no difference in isoprene when stable CF patients and healthy controls were compared suggesting that differences observed previously between all CF patients and healthy controls (Section 5.3.5) was mainly attributable to the exacerbating CF patients. Detecting differences between exacerbating and stable CF patients was not a primary outcome measure of this work and confounding factors, such as effects of treatment, exist as a consequence. Data should therefore be interpreted with caution in the absence of a well-designed prospective study.

VOC	Exacerbating (n=43)	Stable (n=30)	p
Ethanol ⁸³	145.6 [87.5 – 261.3]	202.1 [125.6 – 388.6]	<0.05
Methanol	276.4 [217.9 – 346.9]	267.2 [197.2 – 322.6]	0.334
Propanol	149.3 [78.0 – 211.4]	87.1 [50.4 – 169.1]	0.060
Butanol	49.4 [26.1 – 114.3]	55.9 [33.3 – 91.1]	0.652
Pentanol	45.6 [29.0 – 59.4]	49.8 [35.3 – 64.9]	0.229
Dimethyl Disulphide	85.3 [36.2 – 186.9]	56.3 [28.5 – 80.0]	0.063
Hydrogen Sulphide	1.7 [0.7 – 3.0]	1.0 [0.3 – 3.2]	0.305
Hydrogen Cyanide	7.8 [4.8 – 11.9]	11.4 [9.1 – 14.3]	<0.01
2-AA (NO)	3.7 [2.2 – 5.6]	1.1 [0.5 – 2.9]	<0.001
Acetone (NO)	231.3 [161.1 – 309.8]	292.2 [210.7 – 364.4]	0.061
Ammonia (O ₂)	306.8 [194.4 – 634.8]	356.8 [169.9 – 448.5]	0.349
Isoprene (NO)	108.0 [84.3 – 208.7]	64.0 [47.5 – 88.2]	<0.001

Table 5.3.6.1: Median [IQR] of 12 VOCs in ppbv measured in exhaled breath of exacerbating and stable CF patients; p values calculated using Mann-Whitney U test.

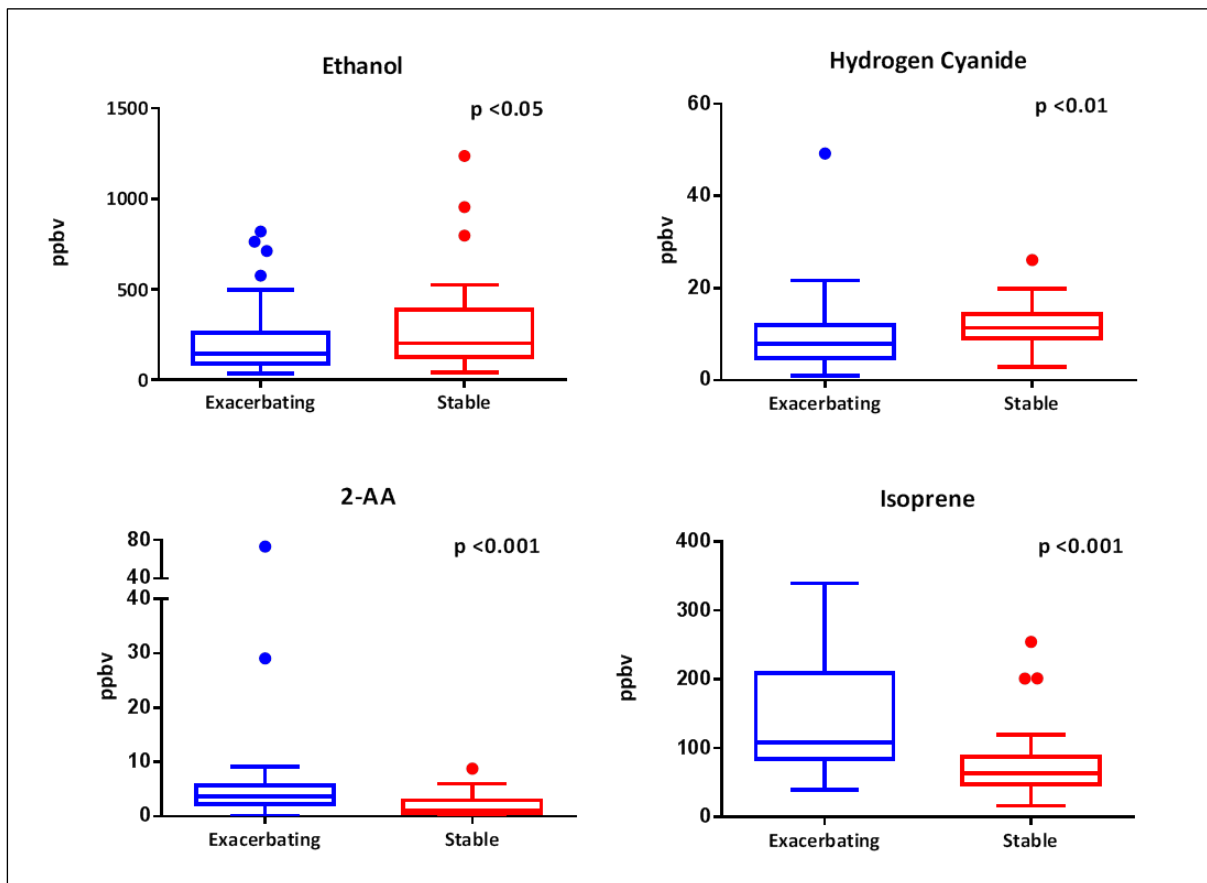


Figure 5.3.6.1: Box-and-whisker plots (Tukey) demonstrating significant differences in ethanol, hydrogen cyanide, 2-AA and isoprene in the exhaled breath of exacerbating and stable CF patients.

Chapter 6: Discussion

The ultimate aim of the experimental work in Part I was to determine whether SIFT-MS could differentiate between subjects on the basis of Pa status. However, several concerns became apparent during the period when I was trying to become familiar with the technology which needed to be addressed prior to commencing recruitment and which require further discussion.

6.1: Pilot Sputum Study

The pilot study was undertaken to ensure familiarity with SIFT-MS and the protocol for collection and analysis of samples in Nalophan bags and also to determine whether previously published work could be replicated using the instrument available in our facility. The most important finding of this study was that HCN was not detected above Pa sputum, which meant bacterial culture experiments were devised to ensure that this was not due to instrument malfunction.

Pilot data differed significantly from the work of Carroll et al (380) despite the only discernible difference in methodology being the volume of the Nalophan bags in which agar plates were incubated (200mls vs. 2000mls). In Carroll's study, headspace ammonia was 0-760 ppbv above sterile PSA plates (n=4) and 850-18840 ppbv above Pa-positive sputum (n=9) whilst HCN was undetectable above sterile plates and levels were as high as 3540 ppbv above the Pa cultured sputum, although levels were zero above two of the nine samples. It has been demonstrated that cyanogenesis by Pa differs according to strain (367) but all strains (n=26) in a SIFT-MS study of headspace produced at least 15 ppbv (IQR 30 – 1327 ppbv) after 48hrs incubation on blood agar (382). There was a non-significant trend towards non-mucoid strains producing more HCN. Although it is possible that all thirteen sputa in my pilot study only contained mucoid Pa, coming as they did from chronically infected adult patients, it is extremely unlikely that all of these strains produced no HCN whatsoever, such that no difference was apparent when headspace above cultured sputa was compared to that above blank plates. This raised concerns about the ability of our SIFT-MS (which to my knowledge was identical and set up in the same way to those in the literature) to accurately

detect HCN. In retrospect, I would have utilised Pa isolated from these sputa for bacterial culture experiments, as described in Section 4.2, to see whether this made a difference to detected levels but samples were no longer available in the clinical microbiology lab at RBH by the time I had concerns that there might be a detection issue; this is a weakness of my assay development experimental methodology.

In addition to low HCN, levels of sputum headspace 2-AA were also negligible in my pilot study. Concentrations were around the SIFT-MS detection limit of 1 ppbv and no difference was noted between the headspace above blank PSA plates and those containing sputa. In a previous study that used GC-MS to detect VOCs, 2-AA was produced by all twenty clinical isolates of Pa that were cultured in liquid media (362) at significantly higher levels than that detected here by SIFT-MS. Although the production of 2-AA by Pa, like HCN, appears to be strain specific (381) and there were differences in experimental methodology (quantification performed using GC-MS that has a pre-concentration step rather than SIFT-MS being the most obvious), these factors alone are unlikely to be responsible for such large discrepancies. A more recent study investigating production of 2-AA above Pa cultures using SIFT-MS (455) detected levels that were of similar magnitude to that seen in my pilot work (range 0.1 – 13.8 ppbv) and concurred that levels varied according to Pa strain; this group were also unable to explain why detected levels were much lower than previously published.

In general, SIFT-MS studies aiming to identify volatile fingerprints have focused on VOCs that might be produced during Pa metabolism. A novel finding of my pilot study is that several compounds were significantly lower in the headspace above cultured Pa sputum, suggesting **consumption** (or inhibition of a production pathway) rather than **production** itself. Most striking was the observation that median butanol in the headspace above Pa sputa was 0 ppbv vs. 13.5 ppbv above blank PSA plates ($p < 0.05$) and was undetectable above 7/13 (54%) sputum samples. Although there are no published data for *P. aeruginosa*, another *Pseudomonas* strain, *P. butanovara*, expresses two butanol dehydrogenases (456, 457) that allow butanol to be utilised as a metabolic substrate (457,

458). This provides a plausible physiological explanation for this reduction in butanol, which has also been reported in a secondary electrospray ionisation mass spectrometry (SESI-MS) study; a relative lack of butanol was seen in association with Pa cultures when compared to other species including *Salmonella typhimurium* and *Escherichia coli* (408). Counter to this is GC-MS work suggesting **production** of butanol in cases of ventilator-associated Pa pneumonia, albeit at a far slower rate than respiratory infections caused by other bacterial species (394). Levels of butanol in that study were minute and detection only occurred after 24hrs. There are no reports in the literature of butanol production by human hosts but environmental contamination is a possible source of the butanol that was seen; it is used in the manufacture of pharmaceuticals, occurs naturally in lentils and pulses and has been reported as contributing to apple and pear aromas (459). Although no consensus can be reached from the literature regarding butanol, further experiments to determine SIFT-MS detection capacity for butanol were devised due to the striking finding of undetectable butanol in over 50% of samples from my pilot data and also due to later concerns about the potential effects of signal carryover.

Acetaldehyde was also reduced in the headspace above plated Pa sputa. Although consumption of this by Pa has been described in the literature (394) production by bacterial pathogens, including Pa (albeit to a lesser degree than other organisms), has also been demonstrated (400). Acetaldehyde is an intermediate in the metabolic pathway for ethanol, as shown in Figure 6.1.1, indicating that both host and environment could affect levels in exhaled breath. For this reason, it was not taken forward into the final diagnostic prediction model although I did measure it in all subjects in the final exhaled breath study; no differences were demonstrated according to Pa status or between CF and healthy controls (data not shown).

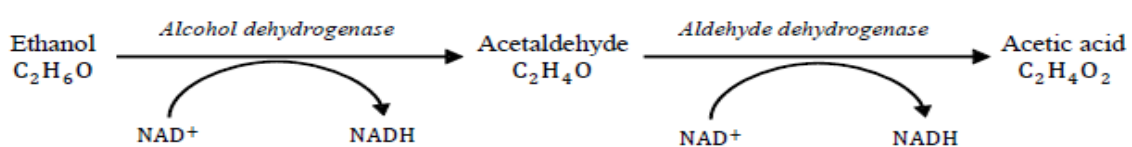


Figure 6.1.1: Human metabolic pathway for ethanol

Reduction in pentanol has not previously been associated with the presence of Pa. Levels detected in my pilot study were low and there was significant overlap between groups. In view of this, the relatively small number of samples in the study and the fact that pentanol contamination might occur from environmental sources (cleaning products, polishes), the robustness of finding reduced levels in association with Pa is questionable. However, it is thought that alcohols such as pentanol, methanol and propanol are more prominently (but not exclusively) produced by *Escherichia coli* (which is not a common CF pathogen) (460) and there are no reports of it being produced by human metabolism. Hence, although pentanol might not be a specific marker of Pa infection *per se*, quantification of this (and other alcohol groups) might still be of use in distinguishing Pa from other infections through different VOC fingerprints. For these reasons, alcohols were taken forward into ongoing breath experiments and incorporated into my diagnostic prediction model.

Methylphenol was the fourth compound that was significantly reduced in the headspace above Pa sputa. Methylphenol is a derivative of phenol which is produced endogenously from aromatic amino acid metabolism and found in drinking water, foods and is used in manufacturing (461). There are no reports in the literature indicating either production or consumption of this VOC by Pa (or other bacterial species). As levels were so low, which would potentially make measurements much more sensitive to the effects of contamination from the environment (where methylphenol is widespread), I considered other VOCs to be of more relevance and it was not used for ongoing work.

In summary, the pilot data highlighted that VOC consumption as well as production might be useful in establishing a fingerprint for the presence of Pa. This helped guide selection of VOCs for later breath work but, before this could be commenced, concerns about the integrity of our SIFT-MS instrument had to be addressed. These arose because HCN, which according to the existing body of literature is the most promising biomarker for Pa infection, was not significantly increased in the headspace above Pa sputum compared to headspace above blank PSA plates.

6.2: Bacterial Culture Experiments – Solid and Liquid Media

Only low levels of HCN and 2-AA, the two VOCs most associated with Pa infection in the literature, were detected during my pilot study. Bacterial culture experiments were thus performed to demonstrate whether our SIFT-MS machine could accurately detect these compounds. Measured HCN correlated with expected quantities, based on pre-existing knowledge of capacity for HCN production by strain, when three strains were cultured on solid media and also with degree of change in cyanide detection paper. This confirmed detection capability of our instrument, although absolute levels of HCN being detected remained lower than in previous studies of headspace above Pa cultures on solid media (382). By culturing Pa in liquid media, larger quantities of HCN, 2-AA and ammonia were detected in headspace with strain-dependent differences again observed. Although this indicates that presence of Pa *in vitro* can be demonstrated using our SIFT-MS instrument, a concern is that high VOC concentrations are able to flood the system and that carryover of signal occurs. This was seen with HCN and when the headspace above laboratory-grade butanol was sampled; although a standard curve was achieved in the latter experiment, suggesting accurate quantification, it was evident that headspace concentrations in each sequential control sample were increasing. The study on headspace above CF sputum that used a similar methodology to my pilot sputum study (380) does not indicate whether samples were analysed sequentially according to type (sterile vs. upper respiratory tract flora vs. Pa), or whether they were run in random order, and how much time elapsed between running each sample. From the data, it is likely that samples in that study were separated by sample type as all sterile plates had no HCN detected and, had these been run in random order following large quantities of HCN being detected previously, some degree of signal would be expected unless there was a substantial washout period between samples. For this reason, although my data from bacterial cultures supports the conclusion by Carroll that >100ppb HCN is highly specific as a biomarker for Pa growth, I have methodological concerns about that study and comparability to my pilot data should not be assumed. These results were not considered to have problematic implications for HCN and butanol as non-invasive biomarkers for Pa infection as

quantities reported in exhaled breath are far lower than that above bacteria (378, 384, 385, 419, 462) and the likelihood of carryover between samples was therefore not felt to be significant, although was still looked for in all subsequent work.

2-AA contributes to the characteristic odour of Pa (361). It has previously been readily detected in the headspace above Pa cultures using GC-MS but not SIFT-MS (362, 455) for reasons that remain unclear but may be related to differences in production according to Pa genotype and phenotype (390, 455) and experimental methodology. GC-MS has quantified 2-AA at up to one million ppbv in headspace above liquid cultures (362); the magnitude of the difference between this and what was detected in my experiments suggests that strain-specific differences in production are unlikely to be accountable and that the pre-concentration step required for GC-MS analysis is more likely to be responsible. Data from my bacterial cultures (Section 4.3.2) are inconsistent but show some similarities to that reported in the SIFT-MS literature (455). There was a significant difference in headspace 2-AA above cultured PA14 (but not two other strains of Pa) compared with sterile TSB, with levels comparable to two of three previously published studies. However, levels were far higher in a second experiment where no difference was seen between headspace above PA12B-4973 and sterile TSB. These findings are summarised in Table 6.2.1.

Experiment/Reference	Pa 2-AA (Median [range] ppbv)	Controls 2-AA (Median [range] ppbv)
1: PA14	10.9 [9.9 – 14.4]	6.6 [5.1 – 9.4]*
2: PA12B-4973	44.2 [35.0 – 71.4]	36.3 [16.1 – 49.3]
Gilchrist (455)	1.8 [0.1 – 13.8]	<0.5
Shestivska (381)	< 14	
Thorn (409)	1.06 – 1.38	

Table 6.2.1: Magnitude of 2-AA detection using SIFT-MS in bacterial culture experiments compared to previous headspace analysis studies using SIFT-MS
*indicates significant difference between two groups.

PA12B-4973 and control headspace data was of concern given the magnitude of 2-AA detection; it was around this time that other users of our SIFT-MS instrument reported inconsistencies with their results. A full service of the instrument was subsequently undertaken (Section 3.3) after which time background levels of 2-AA normalised and exhaled breath studies could commence.

6.3: Repeatability and Reproducibility of Exhaled Breath Analysis using SIFT-MS

With capacity for our SIFT-MS to detect several VOCs of interest established, accuracy of repeated measurements required investigation prior to recruitment of subjects for breath analysis. Key findings from this section are: i) there is significant individual breath-to-breath variability for some VOCs which is marked for some trace compounds such as 2-AA and hydrogen sulphide but lower for more abundant compounds such as acetone, ii) breath-to-breath variability also varies daily, as shown by wide range of CoVs measured on different days for some VOCs (for example, 22.1 – 92.7% for 2-AA) and iii) some VOC measurements are highly repeatable on any individual day but disparity exists in measured quantities from day-to-day, as shown in Figure 4.5.2. Understanding biological mechanisms for breath-to-breath and day-to-day variation in individual subjects is difficult given the complexity of human metabolism and it is unlikely that these processes could be modified for tighter standardisation of breath collection. However, there is accumulating evidence that there are diurnal variations in hormone secretion (463-465) which may differ between individuals and it is conceivable that these might affect exhaled breath profile. Furthermore, oral contamination of exhaled breath analysed using SIFT-MS has previously been described (387) and the potential of EBC in non-invasive diagnosis has also been hampered by concerns about contamination from the mouth, GI tract and nose (466, 467). For these reasons, sampling for repeatability and reproducibility was undertaken following overnight fast with breath collected between 8 and 9am but day-to-day variability persisted despite these measures. The impact of food ingestion on breath profile is demonstrated by repeatability testing pre- and post-lunch following an overnight fast, with significant increases in ethanol⁸³ and 2-AA, found in foods such as bread, fizzy drinks and corn chips (364, 468), all of which were consumed prior to post-fast breath sampling. Acetone was noted to be significantly lower after breaking the fast, likely due to reduction in ketogenesis; this has previously been reported following oral glucose tolerance testing (469). Finally, there was a trend towards reduced ammonia ($p = 0.06$) when an overnight fast was broken; this can be explained by studies that demonstrate significant

correlation of plasma ammonia with glucagon (470), the hormone responsible for raising glucose concentrations in the bloodstream, which becomes elevated during a fasting state.

In view of circadian differences in metabolism and differences before and after fasting, for which there are plausible biological mechanisms, breath samples from all inpatients and control subjects in the exhaled breath analysis study were collected in the morning following an overnight fast to ensure a degree of standardisation. Outpatient sampling could not be performed identically as adult CF clinics at RBH take place in the afternoon. All outpatients were also fasted for at least four hours but 24/29 of these samples were taken i) in a different part of the hospital, ii) at a different time of day and iii) after routine treatments such as physiotherapy and inhaled antibiotics and corticosteroids, all of which had potential to be confounding if inpatients (exacerbating) and outpatients (stable) were compared. Detecting differences in VOC profile between these two groups was not a primary outcome of the exhaled breath study and hence the post-hoc analysis (Section 5.3.6) was considered hypothesis-generating rather than definitive.

In summary, it is evident that significant intra-subject variability exists when measuring exhaled VOCs in breath of healthy control subjects. This is a concern as gold standard medical investigations should be sensitive, specific and reproducible. However, the ultimate aim of this work was to distinguish between patients with and without infection on the basis of volatiles either being produced or consumed by Pa. The expectation was that differences between infected and non-infected patients would be sufficiently significant (when a number of VOCs were combined) such that, even with a high degree of individual breath-to-breath variability, differences would remain apparent. For example, median CoV of HCN in my data was 19.8%; on the basis of previous work, children with asthma had lower exhaled HCN than those with CF and Pa infection (median ppbv [IQR] 2.0 [0.0 – 4.8] vs. 13.5 [8.1 – 16.5]) and, even with 19.8% variability, differences in that study would have remained apparent, as there was clear separation between groups (378). For this reason, it was deemed appropriate at this juncture to begin patient recruitment. Ideally, I would also

have liked to undertake repeatability and reproducibility experiments in CF patients; due to previously described logistical issues and concerns about infection control, as well as difficulties for patients with severe lung disease to provide more than one exhaled breath sample, this was not done and is another relative weakness of this study.

6.4: Exhaled Breath Analysis of CF Patients and Healthy Controls

The exhaled breath analysis data demonstrates proof-of-concept that a signal is present in exhaled breath that differentiates CF patients according to Pa infection status. It is the most comprehensive breath profiling study in CF patients to date. VOCs were selected for analysis based on the pilot sputum study, their presence in exhaled breath of the general population and previously reported associations with bacterial infections and oxidative stress (390, 413, 415, 416, 462, 471, 472).

Amongst analysed VOCs, 2-AA, dimethyl disulphide and butanol differed across CFPa+ and CFPa- groups but with considerable overlap suggesting that, on an individual patient basis, none of these VOCs alone are accurate biomarkers of infection and that single VOCs are only useful for inter-group analyses. The heatmap (Figure 5.3.3.1) shows all 100 subjects and, whilst clustering occurs across subject groups for some VOCs, complete separation is not apparent in any column, indicating that none of the VOCs individually are likely to be pathognomonic biomarkers. When combined in a diagnostic prediction model, the twelve VOCs discriminate between CFPa+ and CFPa- with a sensitivity and specificity of 0.828 and 0.705 respectively. Whilst encouraging, with sensitivity for Pa greater than oropharyngeal culture (473, 474), this does not compare favourably to the [¹³C] urea breath test that is used clinically to diagnosed *Helicobacter pylori* infection, which has a sensitivity of 93.8% and specificity of 99.1% in children (475). It is possible that adding other VOCs to this "Pa fingerprint" might increase discriminatory capacity to a more clinically useful level or that improving SIFT-MS sensitivity (several VOCs in this study including 2-AA and HCN are trace compounds found at levels around the current detection limit of 1ppbv) may amplify differences; recent work has demonstrated detection in the parts-per-trillion range is now achievable with SIFT-MS (476).

As previously discussed, 2-AA is readily detected above bacterial cultures with GC-MS but results have been variable with SIFT-MS (362, 455). It has also been detected in exhaled breath of patients with Pa infection (362), although median levels were less than in our CFPa+ group (0.242 ppbv vs. 3.6 ppbv). This might be attributable to production of 2-AA varying according to Pa genotype (390, 455) with strains likely to have been different in this study compared to previous work undertaken in New Zealand (362). In contrast to major abundant VOCs such as acetone, median CoV of 2-AA was higher (35.4%) in reproducibility experiments. Using SIFT-MS, 2-AA can be analysed using both the H_3O^+ and NO^+ precursor ions to produce characteristic product ions m/z 136, 154 and 135 respectively (450). In this study, NO^+ was employed as it produces a single downstream ion. Analysis of 2-AA using H_3O^+ was also conducted for additional validation; good consistency was demonstrated (median concentration of 2-AA using H_3O^+ 3.3 vs. 3.6 ppbv using NO^+). Although differences between CFPa+ and CFPa- were observed, low levels around the SIFT-MS detection limit, considerable overlap between groups and CoV of 92.7% on one occasion means that clinical applicability cannot be assumed at this stage, with biological variability likely contributing to some of the differences seen.

Like 2-AA, DMDS has been detected in the headspace above bacterial cultures of Pa (381, 477) although this is less specific, being associated with the presence of other species such as *Escherichia coli* (391). As exhaled breath samples have high humidity level, the characteristic product ion of DMDS using H_3O^+ precursor ions (m/z 97) might overlap with dihydrate ions of propanol (m/z 97). This potential influence was assessed, with no correlation found between DMDS and propanol concentrations (correlation data not shown). I have detected higher levels for the first time in exhaled breath of CFPa+ patients. The concentration of DMDS detected in this study is orders of magnitude higher than 2-AA but significant overlap remains between groups with a median CoV of 30.9% again indicating that, although a difference was detected according to Pa status, it is not sufficiently sensitive to be a unique infection biomarker.

Butanol was the third compound that differed significantly according to Pa status. In keeping with preliminary *in vitro* work measuring VOC concentrations in headspace above CFPa+ sputum, levels were significantly reduced in CFPa+ subjects, suggesting consumption by the bacteria. As previously stated, other strains of *Pseudomonas* possess enzymes that metabolise butanol (458). It is feasible that Pa, a facultative anaerobe, uses alternative metabolic substrates when under microaerobic conditions such as the CF airway. This has been demonstrated with nitrate-driven respiration (478) and might explain why butanol was lower in infected subjects. However, the findings contradict other *in vitro* studies suggesting that Pa produces butanol, albeit at a lesser rate than other bacteria (390), most of which produce very low concentrations (479). There was less overlap between groups compared to 2-AA and DMDS, although median CoV remained high at 37.1%.

Of potential breath biomarkers of Pa infection, HCN has been previously thought to have the most potential. Raised HCN levels in Pa-infected sputum have been detected using a cyanide-sensitive electrode (375) and *in vitro* above bacterial cultures of Pa with mass spectrometry (380, 381). In exhaled breath studies, HCN has differentiated between CFPa+ children and children with asthma (378) and children with and without Pa infection in CF (384). However, in another study (389) and in our cohort, no difference was observed, although there was a trend towards elevated HCN in the CF group compared to non-CF controls. Detected levels in our study were similar to those reported in the literature. HCN production varies with Pa phenotype and genotype (455), which may account for differences in measured concentrations in exhaled breath between studies. A recent study suggests that the oral cavity is the main contributor to mouth-exhaled HCN (480); as oral bacterial contamination in adult subjects may be greater than in children (385), nasally-exhaled HCN is postulated as a more accurate biomarker in this group which might explain why no difference has been observed in our study. However, given the almost universal presence of sinus disease in CF adults, and common isolation of Pa from sinus lavage (in up to 73% of patients (388)), this approach to exhaled breath sampling may not be fully representative of the lower airways; bacterial strains in

one study were concordant between upper and lower airways in less than 50% of cases. For a comprehensive review of the SIFT-MS and HCN literature, see reference (481).

Differences in VOCs patterns were also seen between controls and CF patients. The sensitivity and specificity of the VOC profile to differentiate between the groups were 0.815 and 0.877 respectively; whilst this is of interest as it gives a hint of quantifiable mechanistic differences that might be contributing to disease in the CF airway, a new diagnostic test for CF using VOCs is clearly not needed. A test that relates either to degree or severity of lung disease or could provide a sensitive biomarker for pulmonary exacerbations would have more clinical value. In a post-hoc analysis comparing exacerbating and stable patients (irrespective of Pa status), isoprene was higher in exacerbating subjects with almost complete separation between groups (Figure 5.3.6.1) although there was no direct correlation between exhaled isoprene and FEV₁. This finding might be explained by the fact that isoprene, the most abundant hydrocarbon in exhaled breath (387), is a marker of oxidative stress, which is increased in CF patients at the time of exacerbation (354). This has been investigated previously in a small pilot study of CF subjects before and after treatment for worsening symptoms (356) with no differences demonstrated in exhaled isoprene, although this might be attributable to the small sample size (n=24).

Individually, none of the 12 VOCs significantly correlated with FEV₁. However, other VOCs in addition to isoprene did also differ between exacerbating and stable patients (Table 5.3.6.1). Samples were taken opportunistically during exacerbations rather than at standardised time-points, so drawing firm conclusions is difficult and the findings are considered hypothesis generating, not definitive. ROC analysis gives an AUC of 0.940 (95% CI 0.885 – 0.995) and a sensitivity and specificity of 0.876 and 0.893 respectively. A large prospective longitudinal study stratifying patients into groups based on pathogens isolated (by culture or, ideally using molecular sequencing techniques) and evaluating breath profile sequentially at pre-determined points during treatment for infective exacerbations or

as a screening test at clinic visits would be needed to clarify whether SIFT-MS is genuinely useful in monitoring treatment response.

Concentrations of exhaled VOCs, including acetone, butanol, methanol, ethanol, propanol, ammonia and isoprene from healthy controls were compared to previous studies to verify the accuracy of breath analytical methods used in this study. Measured concentrations fell into the reported ranges for all compounds except propanol (418, 462, 482, 483) which was higher in our study compared to a previously reported median [range] of 18 [0-135] ppbv (483) for reasons that are unclear but might be related to its presence in alcohol-based hand gels (484) used extensively in RBH clinical areas.

It is notable that, under all three conditions tested, accuracy of the diagnostic prediction model improved when all 12 VOCs were incorporated, as opposed to using only discriminatory VOCs. This suggests some individual measurements are underpowered (because of the large CoV with some compounds) but still contribute to the sensitivity of the binary regression model. Further prospective studies would be required to elucidate the influence of each individual VOC that did not reach statistical significance when comparing groups.

A further limitation of this work is that, although subjects fasted to reduce the potential influence of oral contamination on VOC concentration, it was not possible to stratify patients by concurrent medications (other than inhaled antibiotics) due to relatively small sample size and vast number of drug/dose combinations. It is possible that some medications, particularly those delivered directly to the respiratory tract such as mucolytics and corticosteroids, might influence VOC profile; this needs to be considered during future studies. Finally, it was not possible to formally measure breath exhalation rates in this work, although all subjects exhaled slowly and filled a Nalophan bag. It is possible, that, as with FeNO, VOC concentration demonstrates flow dependency (485) but, as the ultimate aim of this work was to develop a simple non-invasive tool that could be used in children, I felt that the most straightforward sampling approach should be tested in the first instance, though this is another limitation of this study.

6.4.1: Conclusions from Breath Study

There remains an urgent need for rapid, non-invasive tool with which to screen for and detect Pa infection in CF because eradication can be achieved by early, aggressive therapy. This was the largest study of well-phenotyped CF patients and healthy controls to date using standardised techniques for collection and analysis of exhaled breath samples. Despite this, although a VOC signature that differentiates between patients according to Pa status appears to be present, there is a significant signal-to-noise component in this cohort of patients. Whilst the findings are of interest when comparing well characterised groups, the technique is not sufficiently sensitive for screening or diagnosis on an individual case basis and significant improvements are needed before this can be applied to the population most in need, young, non-expectorating patients with early infection. The data do not support use of any individual VOC as non-invasive biomarker of Pa infection; whilst single VOCs may help our understanding of the action of Pa in the CF airway, they are unlikely to offer clinical utility. Post-hoc analysis demonstrates proof-of-concept that patterns of VOCs might be more useful as a screening tool for exacerbations or to monitor response to treatment and future work should place emphasis on validation of these findings in another cohort and establishing a more sensitive and specific fingerprint for Pa, perhaps through inclusion of additional VOCs or by applying a combination of analytical techniques (486).

Part II: Novel Treatment Approach for *Pseudomonas aeruginosa* Infection in CF

Chapter 7: Bacteriophage Therapy – Background

7.1: Historical Perspective

Bacteriophages, also known as phages (from the Greek meaning “to eat”), are viruses that specifically infect bacteria but never eukaryotic cells, playing a key role in maintaining microbial equilibrium in the environment (487). Alluded to by Hankin in 1896 following the observation that antibacterial activity in the River Ganges might be limiting the spread of cholera (488), they were formally described by William Twort and Felix d’Herelle in 1915 and 1917 (489), the latter using phage therapeutically in humans for the first time in 1919 to treat dysentery (490, 491). For a short time afterwards, phage therapy was heralded as a panacea for bacterial infection but, due to limited understanding at the time of phage biology, efficacy in clinical trials was variable (490-492) and, following the discovery of penicillin in 1928 (493), therapeutic use ceased in the West although continued to be widespread in Eastern Europe and the former Soviet Union (490, 494, 495).

Despite confirmation of the existence of bacteriophage in 1941 by transmission electron microscopy (TEM) which allowed direct visualisation for the first time (496), Western interest resurfaced only after antimicrobial resistance was identified as a major global health risk (203) and accessibility of historical phage research increased with the advent of Perestroika, subsequent dissolution of the Soviet Union and ending of the Cold War in 1989 (491). Despite the long history of phage therapy and it being available over-the-counter in some former Soviet republics (491, 497), it is not currently licensed for routine use in the West although is used for decontamination and preservation of food for human consumption (498-500). The potential impact of widespread phage therapy on the natural equilibrium that exists between microbial communities is cited as a concern and the perception that viruses are detrimental to health is likely also a barrier to their use (497). However, ethical approval has recently been granted for clinical trials (501, 502), several phage products are

now approved by the FDA (501, 503) and, anecdotally, during the course of this work a number of patients providing sputum or breath samples expressed interest in receiving phage for their chronic Pa infection, having had diminishing benefits with repeated and even prolonged courses of intravenous antibiotics. With this and the ongoing stagnation in development of new antibiotics for increasingly resistant organisms in mind, investigation of the safety and efficacy of bacteriophage as a novel therapeutic agent is important for the future of treating chronic Pa infection in CF.

7.2: Bacteriophage Biology

7.2.1: Classification and Morphology

In contrast to the eukaryotic cell, the viral genome is composed of either DNA or ribonucleic acid (RNA), but not both (504). Bacteriophages are the largest virus group with over 5500 identified, however taxonomy remains controversial (505). Most are DNA viruses without a viral envelope; 96% are tailed and the remainder are polyhedral, filamentous or pleomorphic (506). Bacteriophage heads are usually icosahedral in shape though octahedral forms have also been described (496). Morphology shows diversity that is not apparent in viruses that infect other organisms but can be simplified into five distinct classes (496, 507). This is shown in Figure 7.2.1.1.

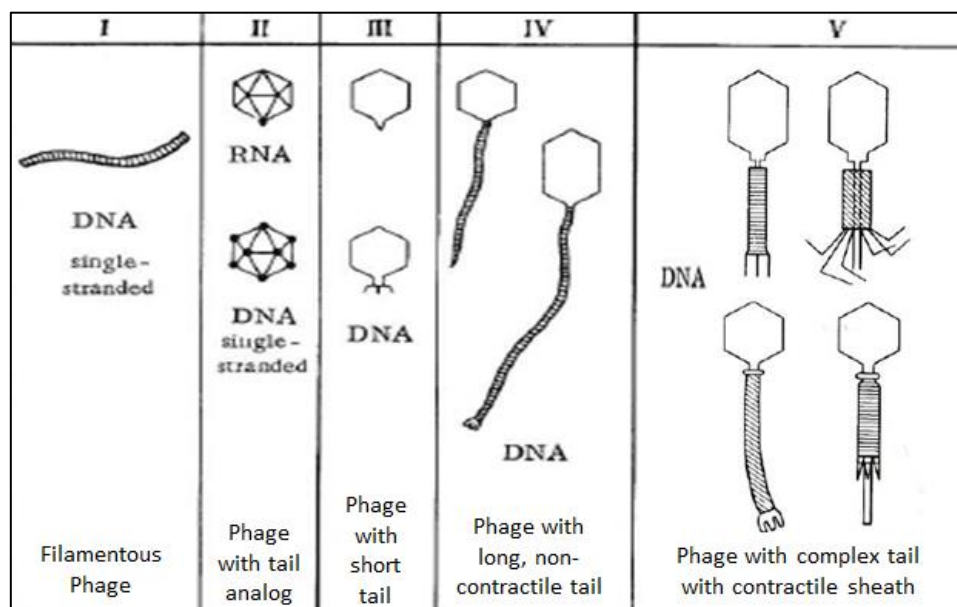


Figure 7.2.1.1: Schematic showing morphological classification of bacteriophage. Adapted from (496).

7.2.2.: Life Cycle

In common with all other viruses, bacteriophage requires a host cell to replicate. To infect the host, phage attach to specific receptors on the bacterial surface (adsorption) via base plates on their tails, which then contract, releasing lysozyme to digest peptidoglycan and puncture the cell membrane. Rapid ATP-driven transfer of the viral genome into the bacterial cell subsequently occurs and phage initiate either lytic or lysogenic replication (508, 509).

Lytic (virulent) phages take over the cell machinery of the bacterial host, using it to produce proteins and nucleic acids that are translated by host ribosomes into new viral components. As these are assembled into new bacteriophage particles, enzymes such as endolysin are produced that destroy the bacterial cell wall from the inside, allowing the replicated phage to be released (490, 510). The three phases of the lytic life cycle can thus be described as adsorption, maturation and lysis. The number of phage produced, termed burst size, varies (usually 20-100) and is dependent on several variables including density of the host cell population (511). The typical life cycle of lytic phage is 30-60 minutes and, as they rapidly destroy the bacterial host, they are considered most suitable for therapeutic use (490).

Lysogenic (temperate) phages infect bacterial cells in the same way as lytic phage but, instead of inducing rapid lysis, they can integrate their genome into that of the bacteria allowing the host to continue normal replication with transmission of the phage genome (or prophage) into each daughter cell. Lysogenic phage can become lytic or be excised from the host genome, either spontaneously or following induction (for example by radiation). There are concerns that excision might allow phage to pick up and transfer bacterial DNA to subsequent hosts (512) or increase bacterial virulence by modifying the phenotype (491, 513) . Lysogenic phages are therefore less useful therapeutically and a failure to differentiate them from lytic phages might have contributed to the variable efficacy seen in early clinical trials (490).

A schematic representation of the lytic and lysogenic bacteriophage life cycles is shown in Figure 7.2.2.1.

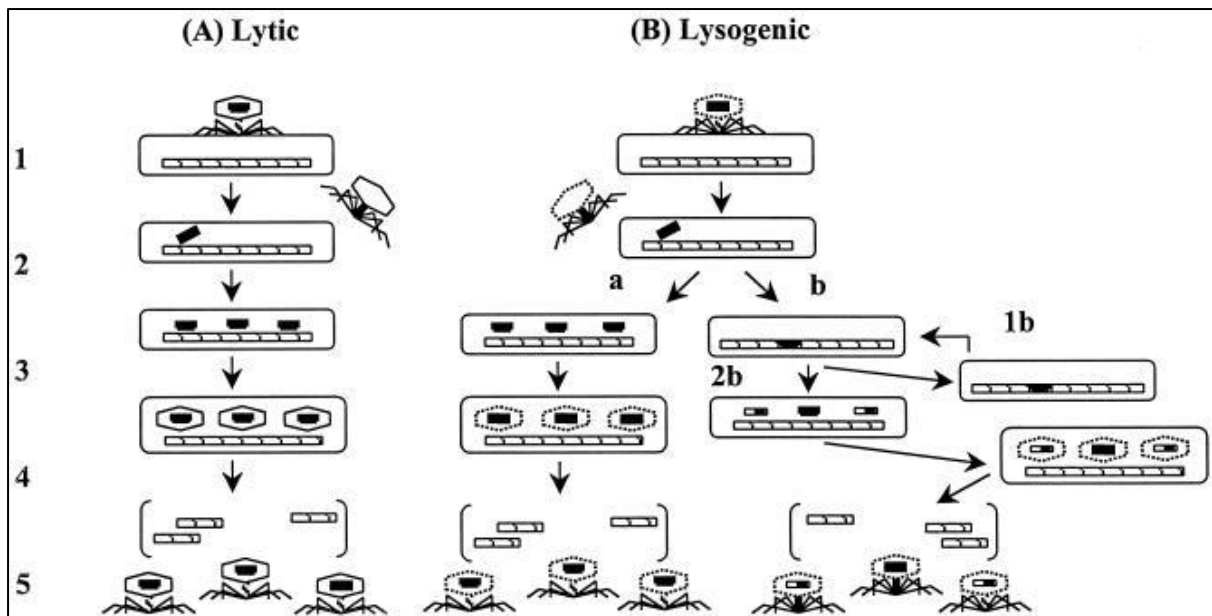


Figure 7.2.2.1: Schematic diagram showing replication cycles of lytic and lysogenic phage. Step 1 (attachment) and step 2 (injection of viral genome into the bacterial host cell) are the same in both cycles. In the lytic cycle (A), step 3 shows replication of phage DNA, stage 4 assembly of new phage and step 5 release of phage with bacterial cell lysis. Lysogenic phage (B) can either follow a lytic cycle (a) or integrate into the host chromosome (b). They can then replicate for many generations (1b) and/or undergo lysogenic induction (2b) where the phage genome is extracted from the bacterial genome, with or without fragments of bacterial DNA. Adapted from reference (490).

7.3: Clinical Applications

Following the first successful demonstration of phage therapy in humans in 1919, it was used intravenously to treat a variety of conditions including cholera, *Staphylococcal* bacteraemia, chronic orthopaedic infections and typhoid fever (491). Oral efficacy against colitis caused by *Shigella* or *Salmonella* has been reported and there is evidence that phage can translocate from gut to bloodstream in humans (514) and cross the blood-brain barrier in mice (515), lending credence to the concept that orally administered phage might combat systemic infection. Topical phage is also efficacious; cocktails targeting skin infections caused by organisms including *Staphylococcus* and *Streptococcus* are available without prescription in Georgia and are updated periodically to take into account emergent problematic strains (491). Although, by definition, phage require a bacterial host to survive, murine studies have demonstrated persistence in the blood, spleen and liver for up to ten

days following intravenous administration indicating that prophylactic therapy, historically used to prevent dysentery outbreaks in the former Soviet Union (497), might also be efficacious. A review of phage therapy for pulmonary infections, including Georgian data going back to the 1930s, has recently been published, making these studies accessible in English for the first time (516).

7.4: Bacteriophage and *Pseudomonas aeruginosa* Infection

Bacteriophage specific for Pa was first isolated in 1945 (517) and is a potential alternative to antibiotic therapy for an organism considered a “phenomenon of bacterial resistance” (518). Early animal studies demonstrated that topical application of phage could prevent destruction of skin grafts by Pa (519) and more recent work has shown that survival in mice following intraperitoneal injection of a lethal dose of Pa is prolonged by either simultaneous or delayed (up to six hours depending on the study) injection of bacteriophage (520-522). More relevant to CF infection are murine studies using bioluminescent Pa which demonstrate reduction in luminescence and disease severity (as assessed by histological analysis of lung tissue) in phage-treated mice compared with controls (523-525).

Phage are commonly used for Pa urinary tract and wound infections in Russia and Georgia (526) but accessible evidence is limited to an Australian case report of usage in refractory urine infection (527), a non-controlled study of Pa infection in burn wounds (528) and a small phase I/II placebo-controlled randomised trial demonstrating safety and efficacy following topical administration of bacteriophage for chronic antibiotic-resistant otitis (502). Although *in vitro* models suggest that phage can be deposited successfully in the human lung by nebulisation (529), to date there have been no studies of efficacy in lung infection undertaken in accordance with strict regulatory criteria although two small Georgian trials have demonstrated reduction in Pa load in the sputum of nine CF patients following treatment with aerosolised bacteriophage (530).

7.5: Advantages and Disadvantages of Phage Therapy

Phage therapy has a number of theoretical advantages over antibiotics. Efficacy against a wide variety of pathogens, including those that are multi-drug resistant (531) and in antibiotic-resistant biofilms (532-534), has been demonstrated. Lytic phages are bactericidal by definition, unlike antibiotics which can be bacteriostatic and allow resistance to evolve more readily (503, 535). Phage are highly specific for their target bacterial species (536) and thus less likely to either kill or induce resistance in non-targeted commensal bacteria contributing to the healthy human microbiome, both of which are issues with conventional antibiotics (503, 531, 535). Unlike antibiotics which require repeated dosing for maintenance of minimum inhibitory concentrations, lytic phage multiply in the presence of a host, increasing in concentration at the site of an infection and not elsewhere (537, 538). This makes toxicity less likely than with antibiotic therapy (and single dosing a possibility) but there are concerns that impure phage preparations contain bacterial endotoxin that could induce host immune responses, as might substances liberated following phage-induced lysis of pathogens (501, 503, 539), although it could be argued that this is also theoretically possible with bactericidal antibiotics. Furthermore, newer methods of phage preparation can reduce contamination with bacterial components (540). In common with antibiotics, phage can notionally be administered by several routes, in different formulations and be combined with one another or with other antimicrobials to increase their antibacterial spectrum (490, 497, 503, 514, 515, 531). Bacteriophage are widely distributed in nature so in theory development costs should be no more than for new antibiotics with the added benefit that their use might reduce evolving resistance and prolong effectiveness of current antimicrobials (503). It is suggested that bacterial resistance to phage might develop in the same way as it has done to antibiotics; this has not been the case in nature as phage have also evolved at a rapid rate to retain efficacy against their bacterial hosts (541). It is possible that using phage therapeutically might alter the equilibrium between bacterial and phage mutation frequency, though this seems unlikely from the collated evidence to date.

A potential drawback of phage therapy is that the narrow therapeutic range requires susceptibility of the pathogen to be established prior to commencing treatment (490, 503, 531) which can be time consuming and costly. This can be assuaged by formulating cocktails containing several strains of phage and using knowledge of local endemic bacterial strains to guide therapy (503, 531, 538). As previously discussed, concerns exist regarding transfer of bacterial virulence factors by phage with evidence that conversion of Pa from a planktonic to mucoid phenotype by induction of alginate production is associated with presence of lysogenic phage (542). Vigilance in selecting only lytic phages for *in vivo* therapy has been suggested as a strategy that would avoid such issues but the finding that lytic phages may be involved in selecting for mucoid strains of *Pseudomonas fluorescens*, which bears some similarities to Pa, is worrying (543). Comparison of the virome in CF and non-CF patients demonstrates higher abundance of *Staphylococcus* phage and less phage diversity in CF, likely reflecting adaptation due to infection, although a similar increase in Pa phage is not seen despite universal infection with Pa in CF patients in this study (544). This implies that, although concerns regarding changes in bacterial virulence are valid, mucoid transformation is likely due to various other mechanisms rather than phage presence alone and should not be seen as a contraindication to clinical use. Concerns that phage efficacy might be reduced due to interaction with the humoral immune system is also cited as a potential drawback (503, 545); clearance of phage in B-cell deficient mice is impaired compared to wild type mice (546) and constant “natural immunisation” to phage is likely in humans due to persistent environmental exposure (545). However, phage purification can reduce carriage of bacterial constituents likely to be culpable for inducing an immune response (540) and inherent immunogenicity of many phage to eukaryotic cells is minimal (545). Rapid removal of phage by the reticuloendothelial system is another concern but could be overcome by repeated dosing, phage PEGylation (547) or use of engineered mutants (540) which may also enhance efficacy (548, 549), though this approach would itself raise concerns over potential for evolution and mutation of both phage and bacteria *in vivo*. The need to delineate safety, pharmacokinetics and efficacy exists for all new therapies; given that phage are ubiquitous in

nature and human exposure goes back millennia, long-term safety is more assured and time to market, which may be critical given the epidemic of antibiotic resistance (208), is likely to be less than for newer synthetic compounds. The potential benefit of phage therapy outweighs the risks and therefore forms the basis for the second part of my experimental work in this thesis. Although it is clear that phage therapy *should* work, I aimed to assess whether it *does* work, both *in vitro* and *in vivo*, in preparation for possible clinical use.

7.6: Hypothesis and Aims

7.6.1: Hypothesis

Novel bacteriophage cocktails are safe and efficacious against a standard laboratory and clinical strains of *Pseudomonas aeruginosa* both *in vitro* and in a murine model of acute infection.

7.6.2: Aims and Objectives

- To characterise bacteriophage strains present in three novel bacteriophage cocktails and to investigate their interaction with Pa using transmission electron microscopy (TEM).
- To test *in vitro* efficacy of these three bacteriophage cocktails against i) clinical strains of Pa from CF patients and ii) a genetically modified bioluminescent form of the laboratory strain PAO1, in preparation for non-invasive monitoring of response to therapy *in vivo*.
- To establish if luminescence of a genetically modified strain of PAO1 i) is a proxy measure of bacterial density and ii) that changes in luminescence are proportional to the degree of phage-mediated bacterial killing *in vitro*.
- Provided *in vitro* efficacy is shown, to establish if phage cocktails are safe and efficacious when used *in vivo* in a murine model of acute Pa infection.
- If safety and efficacy are demonstrated *in vivo*, to determine if phage retains efficacy i) against Pa in sputum from CF patients and ii) following nebulisation, factors that are both relevant to future clinical trials in human subjects.

Chapter 8: General Materials and Methods

8.1: Pa Storage

Clinical and fluorescent strains of PAO1 were provided respectively by the microbiology laboratory at the Royal Brompton Hospital and Dr. Andrew Ulijasz, Imperial College London, on nutrient agar slopes which were stored for ongoing use at 4°C. Luminescent PAO1 was provided on agar slopes containing 10mg/L gentamicin. Towards the end of the life of original agar slopes, Microbank™ beads (Prolab Diagnostics, UK) were utilised for longer-term storage. These are prepared by inoculating Pa from the original agar slopes into vials of beads suspended in a cryopreservative with a sterile loop and leaving at room temperature. After ten minutes, the cryopreservative is removed using a sterile Microlance™ needle and syringe and the vials are stored at -20°C until required. To demonstrate the process is successful, one bead is introduced into sterile TSB and incubated overnight with agitation. New cultures are made periodically (6-9 monthly) to ensure ongoing viability of the microorganisms.

8.2: Pa Culture

Bacterial cultures were performed by introduction of Pa into 10mls of sterile TSB either i) from agar slopes using a plastic single-used sterile inoculation loop or ii) by transfer of a Microbank™ bead using a sterile 19G Microlance™ needle. TSB was then incubated overnight with agitation at 37°C

8.3: Semi-Solid Agar

Semi-solid agar was produced in-house by dissolving 3g TSB powder and 0.4g agar (both Sigma, UK) in 100mls deionised water and autoclaving at 121°C.

8.4: Standard Plaque Assays

Standard plaque assays were used to determine phage efficacy throughout experimental work in this thesis. These are produced by measuring optical density of overnight Pa culture in TSB using spectrophotometry (Spectronic, UK) at a wavelength of 620nm (OD₆₂₀) and adjusting this to 0.1 by

dilution with sterile TSB. 100µl of this broth is added to 3mls of semi-solid agar that has previously been microwaved for two minutes and maintained at 55°C in a water bath. The broth is then poured over a nutrient agar plate, creating a uniform carpet of bacteria. The plate is allowed to cool and solidify at room temperature. Potential antibacterials are pipetted onto the carpets prior to incubation overnight at 37°C to stimulate bacterial growth.

8.5: Phage Cocktails

Special Phage Services (AmpliPhi) isolated fifty-two phages against Pa from sewage and soil samples between June 2006 and 2008 using various protocols as previously described (550). They then tested these in triplicate against plaque assays of Pa strains to assess lytic activity. Ten bacteriophage strains were found to infect 77/80 (96%) of clinical Pa isolates with only three clinical isolates resistant to all phages. Four phages (Pa1, Pa24, Pa25 and Pa26) had the broadest lytic spectrum, two of which were in phage cocktail 1 (as supplied by Special Phage Services) which was used for the majority of *in vivo* experimental work in this thesis.

All phages were stable when stored at 4°C for a period of twelve months with a non-statistically significant reduction in concentration of 0.8 Log. At 25°C, average reduction was 3 Log after twelve months and at 37°C some phage had no viable particles remaining by three months. These characteristics were previously demonstrated by Special Phage Services prior to commencement of my experimental work in this thesis. Based on these findings, I therefore stored all phage used in this at 4°C and requested new stocks for use every nine months.

Chapter 9: Characterisation of Phage Cocktails

The experimental work in this chapter was undertaken to achieve the first aim of Part II, which was to visualise bacteriophage and their interaction with Pa.

9.1: Materials and Methods

9.1.1: Electron Microscopy

Electron microscopy (EM) uses a beam of electrons, as opposed to light, for magnification. In 1873, Ernst Abbe first published an equation demonstrating that the resolution of the conventional light microscope was limited by the wavelength and diffraction of light (551). Although it had been postulated over fifty years previously that electrons could be deflected by magnetic fields, it was not until the publication of the de Broglie hypothesis in 1924 that the wavelength of electrons was recognised as being many orders of magnitude less than photons (552). The first prototype electron microscope with a higher resolution than the light microscope (50nm vs. maximum of 200nm) was built in 1933 by Ernst Ruska, who was awarded the Nobel Prize in physics in 1986 (553). Modern electron microscopes have a quoted resolution of up to 50 picometres (554) although the model used during this work had a resolution limit of approximately 0.5nm.

9.1.2: Transmission Electron Microscopy (TEM)

TEM relies on the principles first utilised by Max Knoll and Ernst Ruska in the 1930s. An electron beam emitted by a cathode is transmitted in a vacuum through an ultrathin section of specimen and emerges carrying information that varies according to how much of the beam scatters and absorbs (555). This information is magnified via a series of lenses and, in our facility, is connected to a charge-coupled camera (CCD) which displays the image in real time on a monitor. All experiments in this section were undertaken using a Hitachi H7000 TEM (125kV, maximum magnification 600,000x and digital imaging to 1376 x 1032 pixels) attached to a 1000x1000 CCD. A schematic and photograph of the TEM are shown in Figure 9.1.1.1 and 9.1.1.2.

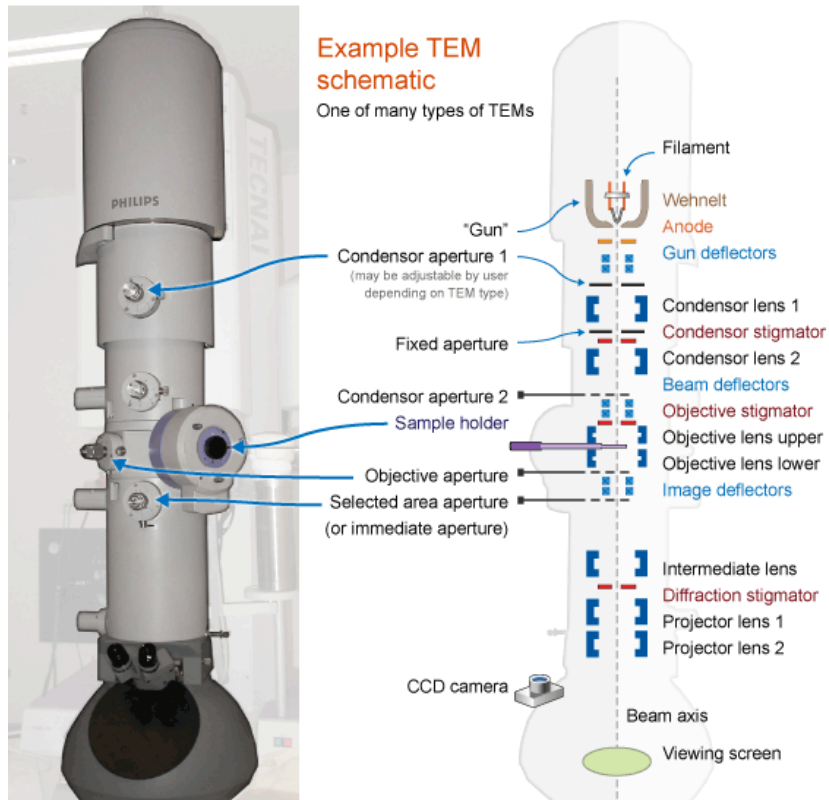


Figure 9.1.1.1 (above): Schematic diagram of a transmission electron microscope. Reproduced from <http://www.amrf.org.au/myscope/tem/introduction/>

Figure 9.1.1.2 (below): Photograph of transmission electron microscope at RBH used for bacteriophage visualisation. Images are transmitted to the screen on the right of the picture and adjustments to the magnification and focus are made from the panel and screen shown on the left of the picture.

9.1.3: Negative Staining of Bacteriophage

A negative staining technique was used for visualisation of phage and any Pa that might be present; this is more difficult than positive staining as it relies on some stain remaining around the edge of a virus so that details are clearly defined. There are a number of different protocols (556-559), all of which require a degree of persistence to ensure that just the right amount of stain is taken up. The protocol I used was kindly provided by Dr. Ann Dewar at the Royal Brompton Hospital and, as I had success after a few attempts of using it, others were not required.

10µl droplets of the suspension to be imaged were pipetted onto composite FormvarTM/carbon TEM grids (Agar Scientific, UK) held in EM grid-grade forceps and allowed to air dry for 30 seconds. The grid was placed in a 40µm nylon cell strainer (BD Falcon, USA) that fitted securely above a 50ml polypropylene conical tube (BD Falcon, UK) containing 25mls 10% neutral buffered formalin solution (Sigma, UK) in a fume cupboard for twenty minutes. The grids were then placed shiny side down into 500µl of uranyl acetate dehydrate (Agar Scientific, UK) in a shallow 12 well plate (Thermo Scientific, UK) for seven minutes. The grids were held in EM grid-grade forceps against Whatman filter paper (Sigma, UK) to allow excess uranyl acetate to be absorbed before 10µl of 2% phosphotungstic acid (PTA) adjusted to pH 7.2 with sodium hydroxide (VWR International Ltd, UK) was pipetted onto the dull side of the grid. This was allowed to stand for 1 minute before excess stain was wicked away from the grids using Whatman paper. The grids were allowed to air dry for one hour before being visualised by TEM. Several different suspensions were tested at different time points, in an attempt to try and determine the rate of phage-induced bacterial lysis, although as previously mentioned it is known that lytic phage typically have a life-cycle of between 30-60 minutes (490):

1. Phage cocktails alone (1-3)
2. Phage cocktail 1 + clinical Pa strain
3. Phage cocktail 1 + PAO1]
 - i. 0hrs
 - ii. 2hrs
 - iii. 4hrs
 - iv. 8hrs
 - v. 24hrs

For suspensions where phage and Pa were tested together, Pa was introduced from agar slopes into 10mls TSB (Oxoid, UK) using a single-use sterile plastic inoculation loop and agitated overnight at 37°C. The broth was centrifuged (ALC, Italy) at 4°C for ten minutes at 2000g (3500rpm, rotor radius 15cm) and the remaining fluid subsequently removed using a 10ml Costar™ serological pipette (Corning, USA). The resultant cell pellet was then resuspended in 10mls TSB; 100µl of this was mixed in an autoclaved Eppendorf with 100µl phage cocktail 1. At each time given time point, 10µl of this PAO1/phage suspension was pipetted onto the Formvar™/carbon grids, fixed and stained as previously described above, allowing bacteria/phage interaction at each time point to be assessed.

9.2: Results

All electron micrographs in this thesis were generated using Hitachi H7000 TEM (125kV, maximum magnification 600,000x and digital imaging to 1376 x 1032 pixels) attached to a 1000x1000 charge-coupled camera. Assistance in using the electron microscope was kindly provided by Dr. Amelia Shoemark, Royal Brompton Hospital.

9.2.1: Phage Cocktails Alone

Eleven different strains of anti-Pa phage were present in the cocktails provided. Only one (Pa37) was present in more than one cocktail. Cocktail 1 contained three strains (Pa24, Pa25 and Pa37), cocktail 2 four strains (Pa39, Pa67, Pa 77 and Pa119) and cocktail 3 five strains (Pa3, Pa6, Pa10, Pa32 and Pa37). On TEM, it was not possible to differentiate each of these phages from one another but some morphological differences were apparent. Figures 9.2.1.1 and 9.2.1.2 show examples of phages from cocktail 1, figures 9.2.1.3 and 9.2.1.4 show from cocktail 2 and figures 9.2.1.5 and 9.2.1.6 from cocktail 3.

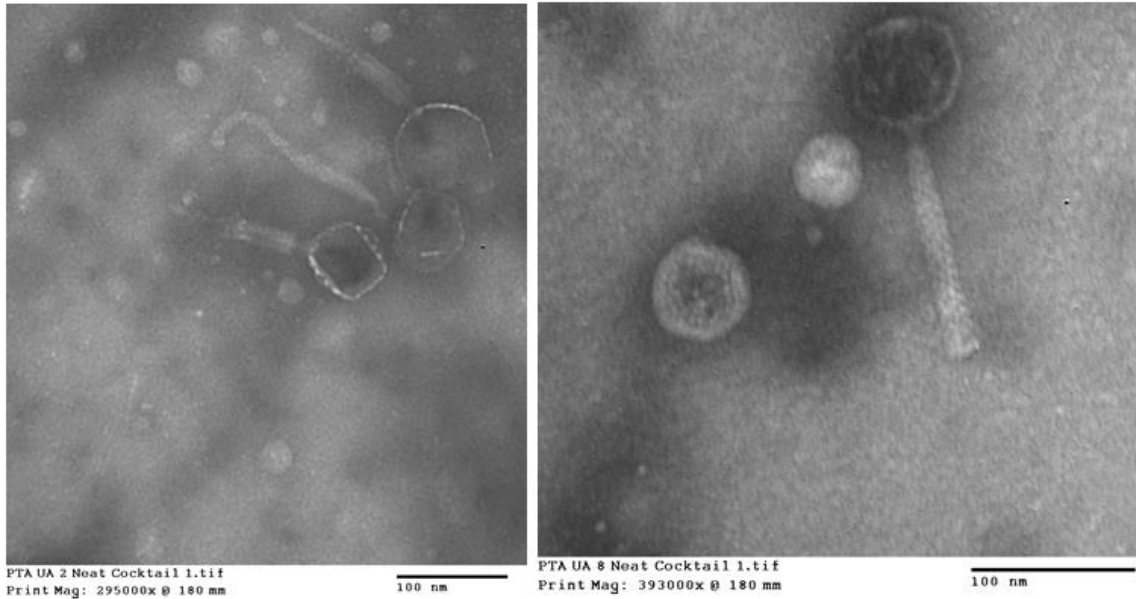


Figure 9.2.1.1: Morphological differences in heads and tails of phage seen on TEM of phage cocktail 1.

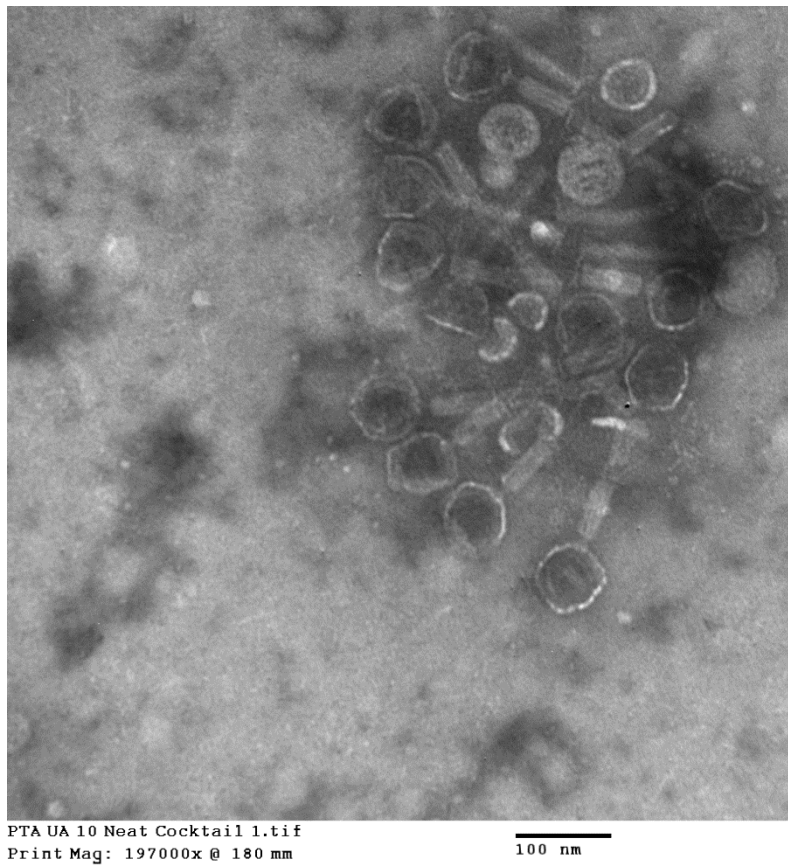


Figure 9.2.1.2: Multiple phage from cocktail 1.

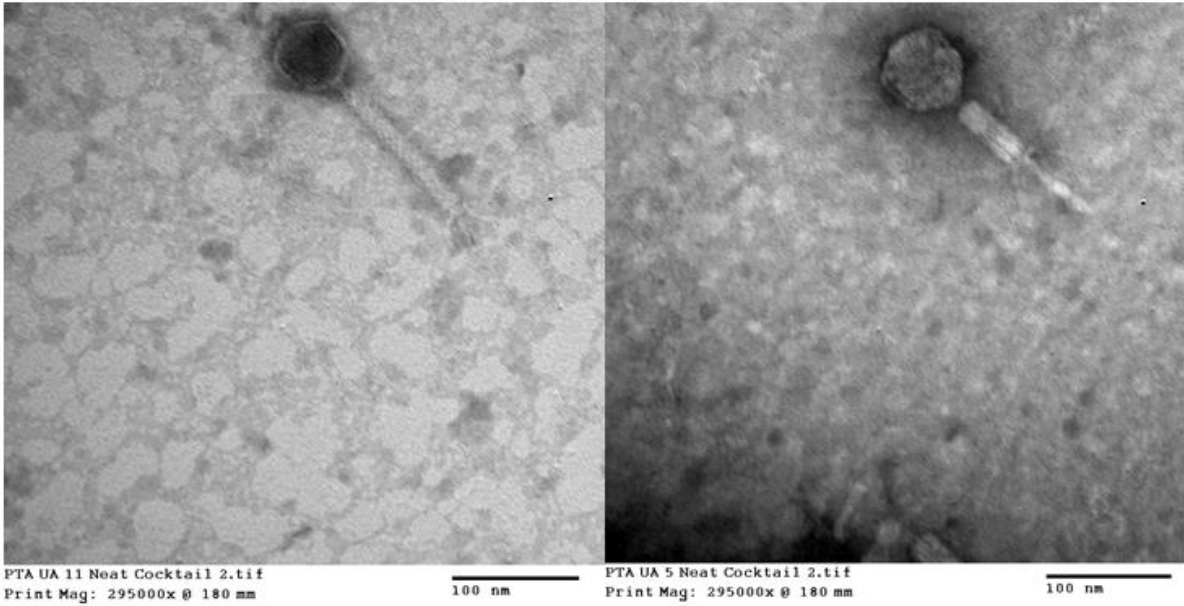


Figure 9.2.1.3: Morphological differences in head and tail seen on TEM of phage cocktail 2.

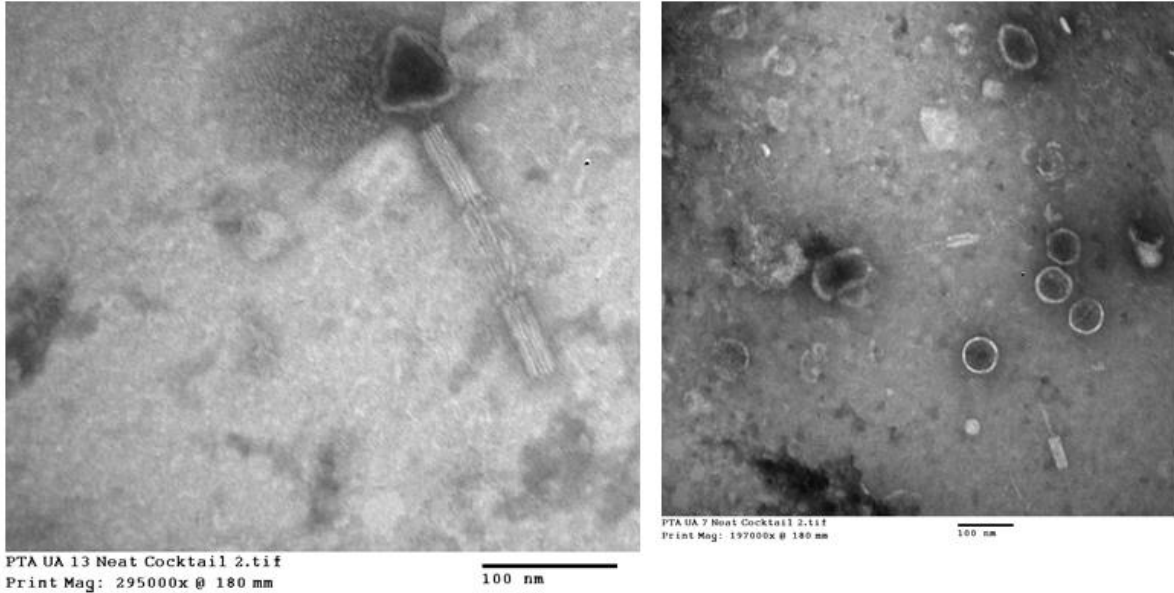


Figure 9.2.1.4: Differing morphology, triangular head (left image) and multiple phage particles (right image); projection of TEM appears topographical on the right with several phage particles visualised from above, demonstrating one of the difficulties encountered when imaging virus particles with TEM.

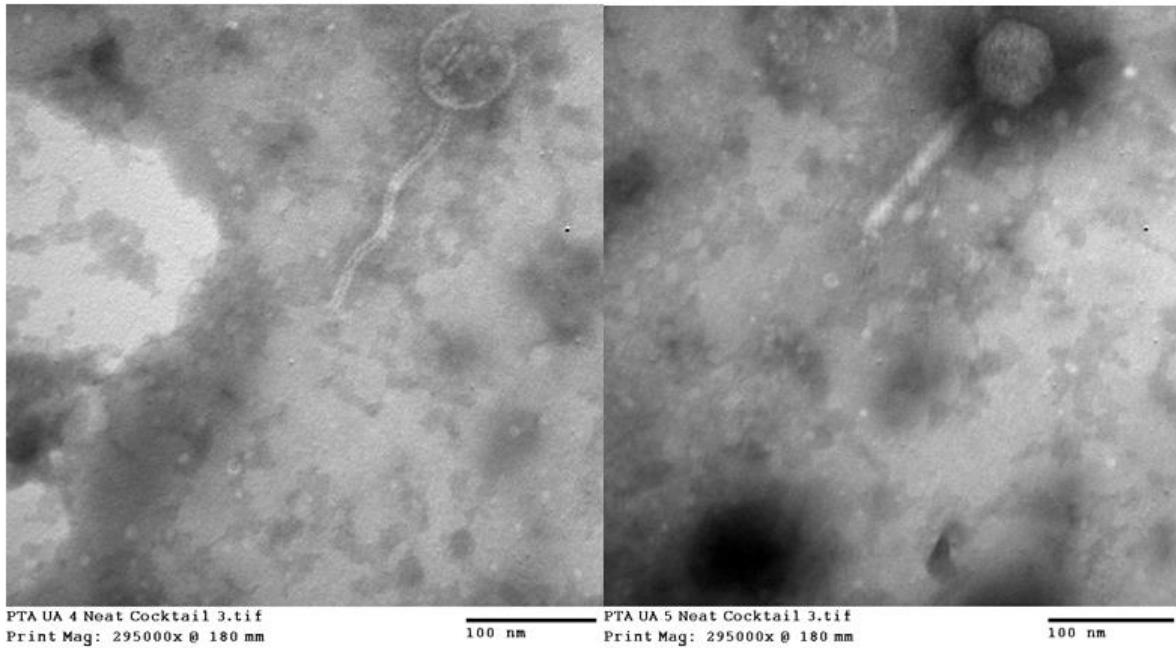


Figure 9.2.1.5: Morphological differences in head and tail seen on TEM of phage cocktail 3.

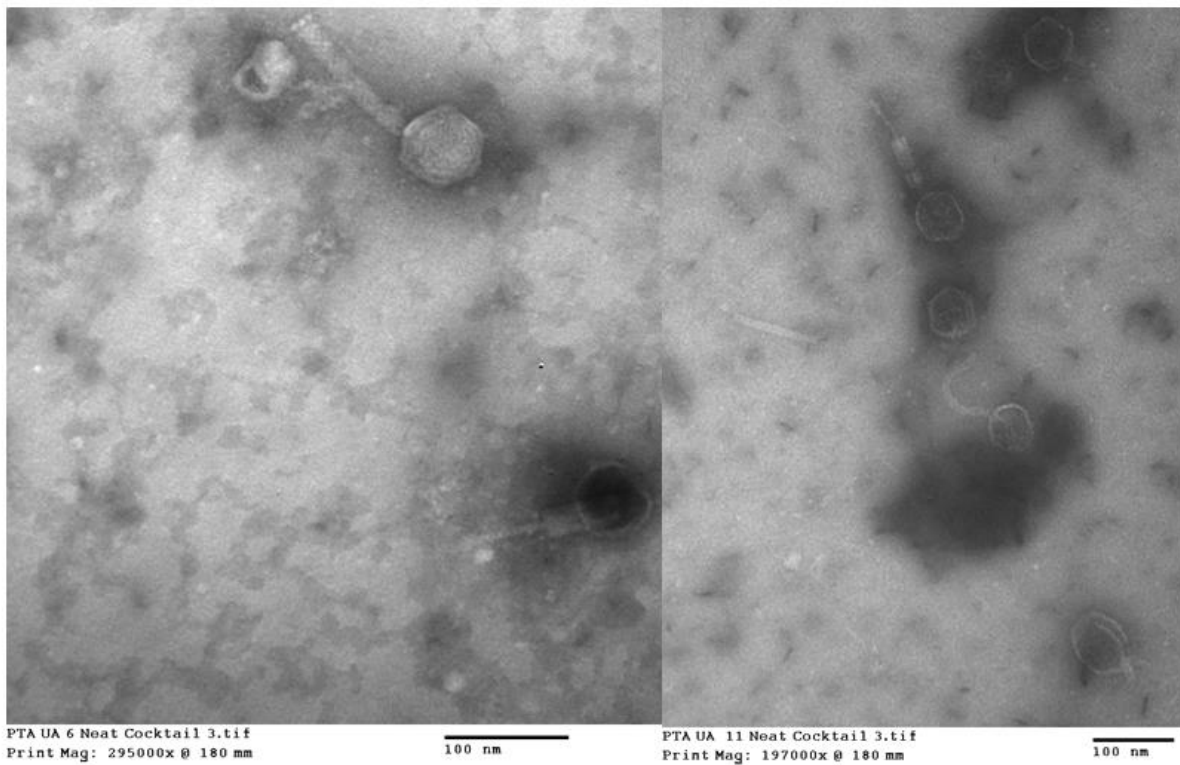


Figure 9.2.1.6: Differing morphology, dark head and contracted tail on bottom phage, lighter head and non-contractile tail in upper phage (left image) and projection of multiple phage, some seen from top down and others in the horizontal plane (right image).

9.2.2: Pa Alone

Overnight batch culture of PAO1 and the clinical strain selected for *in vivo* experiments typically had an optical density between 1.5 and 1.8. Visualisation using TEM at these optical densities was difficult due to large numbers of bacteria in each field. An optical density of 1 was therefore used in subsequent attempts, equating to a theoretical 1×10^7 CFU in the initial 10 μ l pipetted onto the EM grids. As multiple bacteria were visible at this concentration but could still be seen as distinct, separate entities, planned experiments with lower optical densities of bacteria were not required. Figure 9.2.2.1 shows images of the clinical Pa (laboratory number Pa12B-4973) and Figure 9.2.2.2 shows PAO1; an image of phage from cocktail 3 is depicted alongside to demonstrate the size difference.

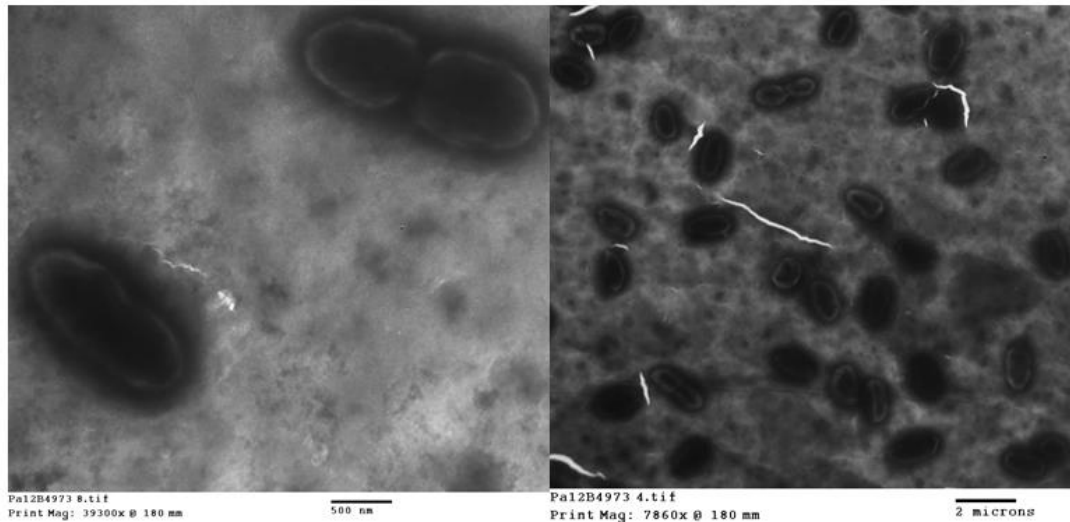


Figure 9.2.2.1: TEM of the clinical strain of Pa selected for use in vivo. Note the reduction in magnification compared to that which was used for phage particles.

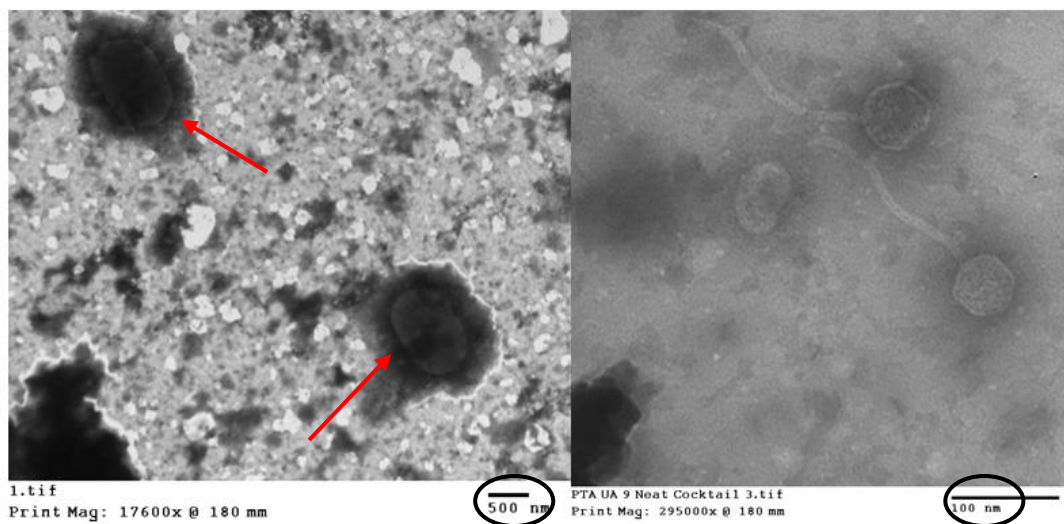
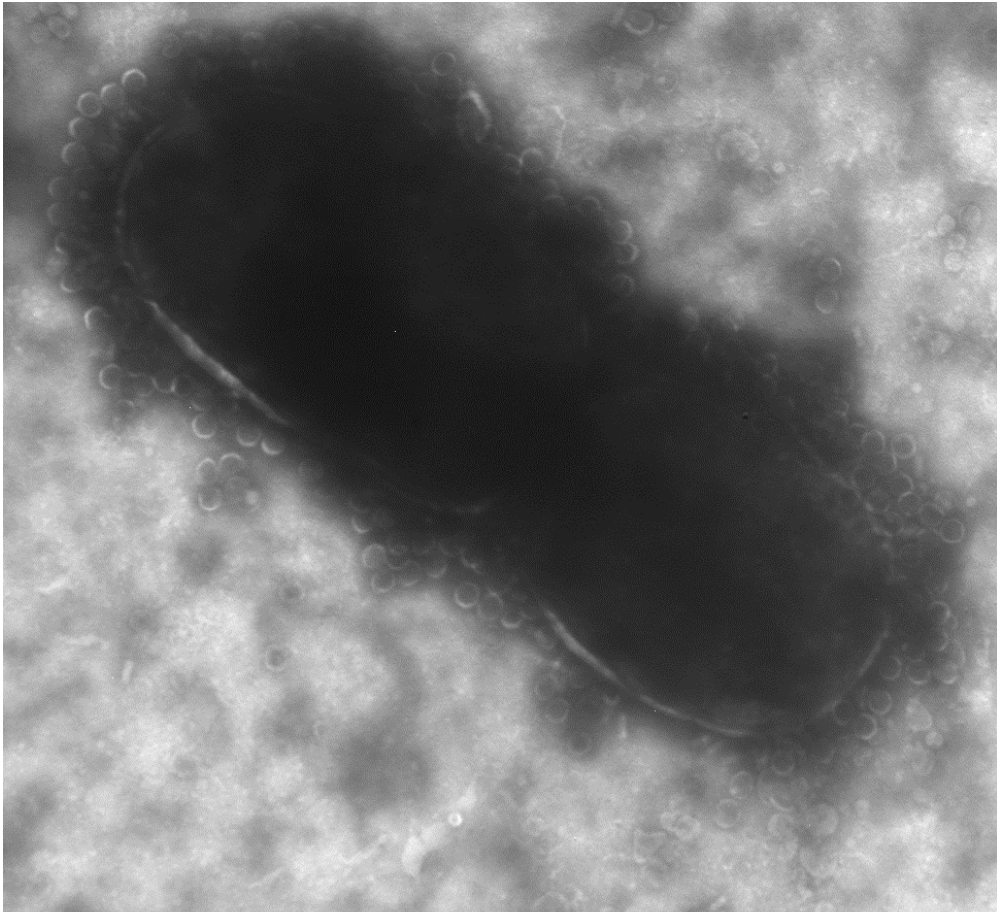


Figure 9.2.2.2: TEM of PAO1 (left image, denoted by red arrows) at lesser magnification than phage from cocktail 3 (right image). Note differences in scale in black circles.

9.2.3: Pa and Phage Cocktail 1

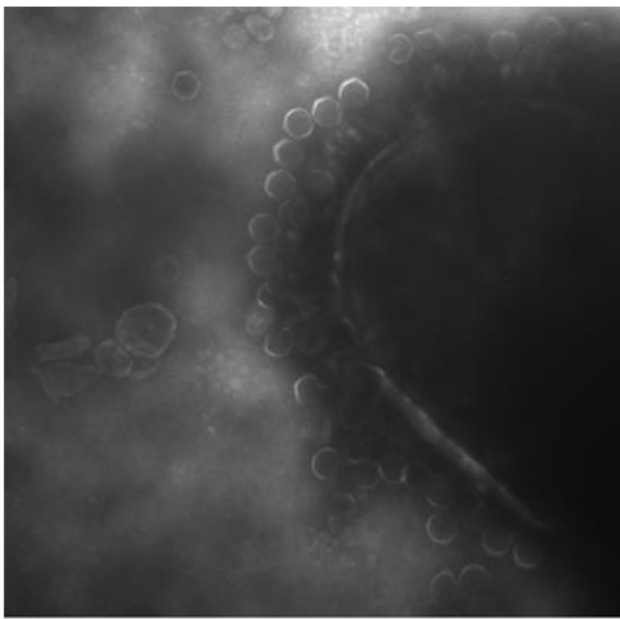
Several attempts were required to visualise PAO1 and phage together. Images taken at 0hrs and 2hrs showed phage congregating around PAO1 and, after both 2hrs and 4hrs, phage particles were visible within the bacterial cell wall. This is shown in Figure 9.2.3.1 – 9.2.3.6. At both 8hrs and 24hrs, it was not possible to visualise either intact phage or PAO1, suggesting that the process of bacterial cell lysis was complete, in keeping with the published literature (490).



6.tif
Print Mag: 58900x @ 180 mm

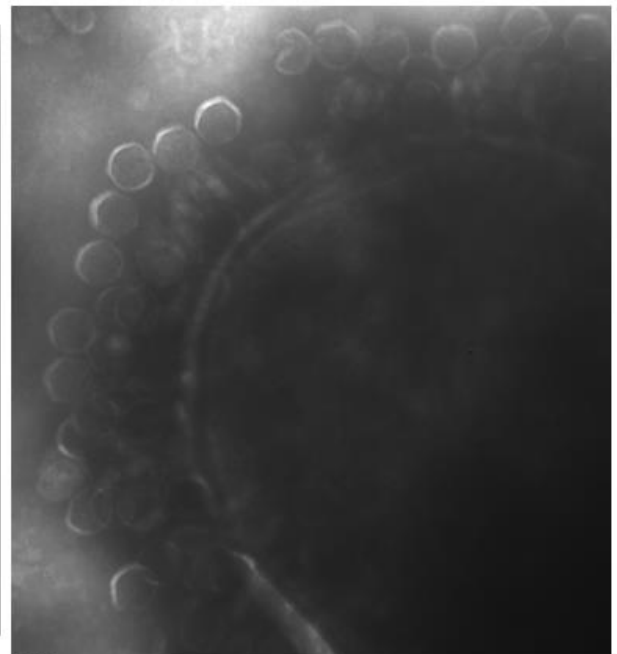
500 nm

Figure 9.2.3.1: TEM of PAO1 and phage cocktail 1, 2hrs after being mixed. Phage have congregated on the bacterial cell wall with possible loss of cell wall integrity and heads are predominantly black.



5.tif
Print Mag: 118000x @ 180 mm

100 nm



8.tif
Print Mag: 197000x @ 180 mm

100 nm

Figure 9.2.3.2: Higher magnification at 2hrs; phage particles visible within PAO1 in the right image.

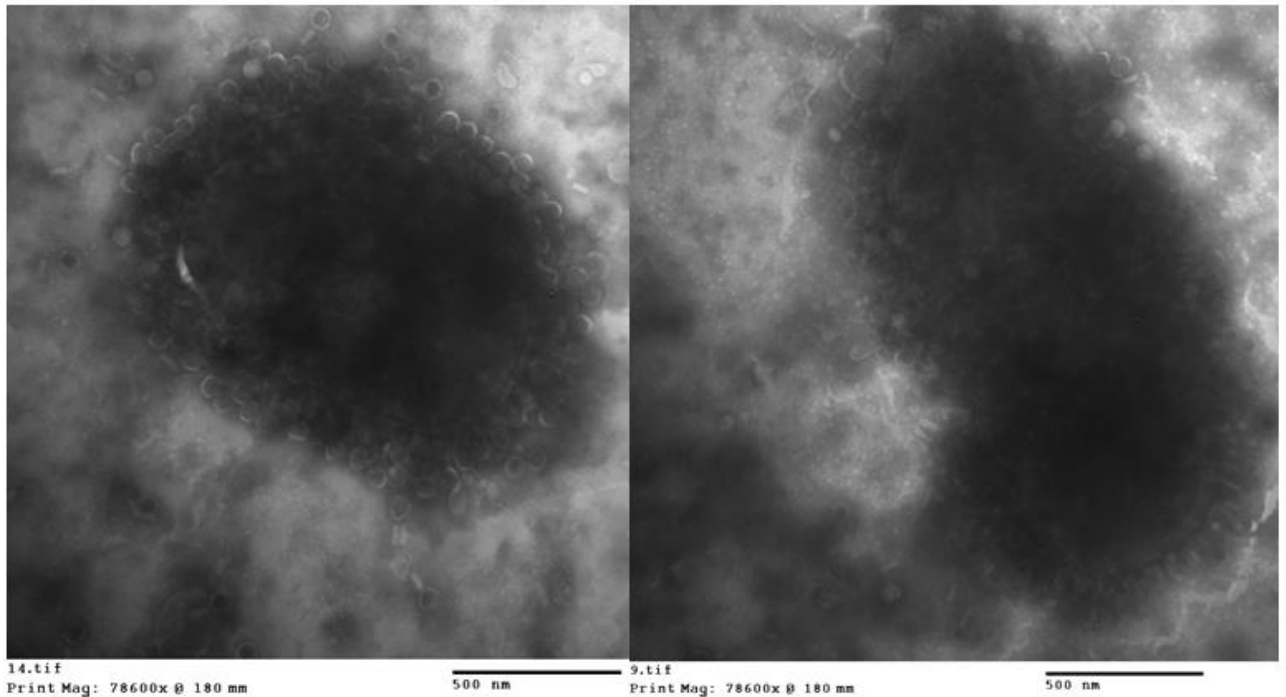


Figure 9.2.3.3: Further TEM of PAO1 and phage cocktail 1 2hrs after being added together. More phage particles visible within bacterial cell wall on right TEM.

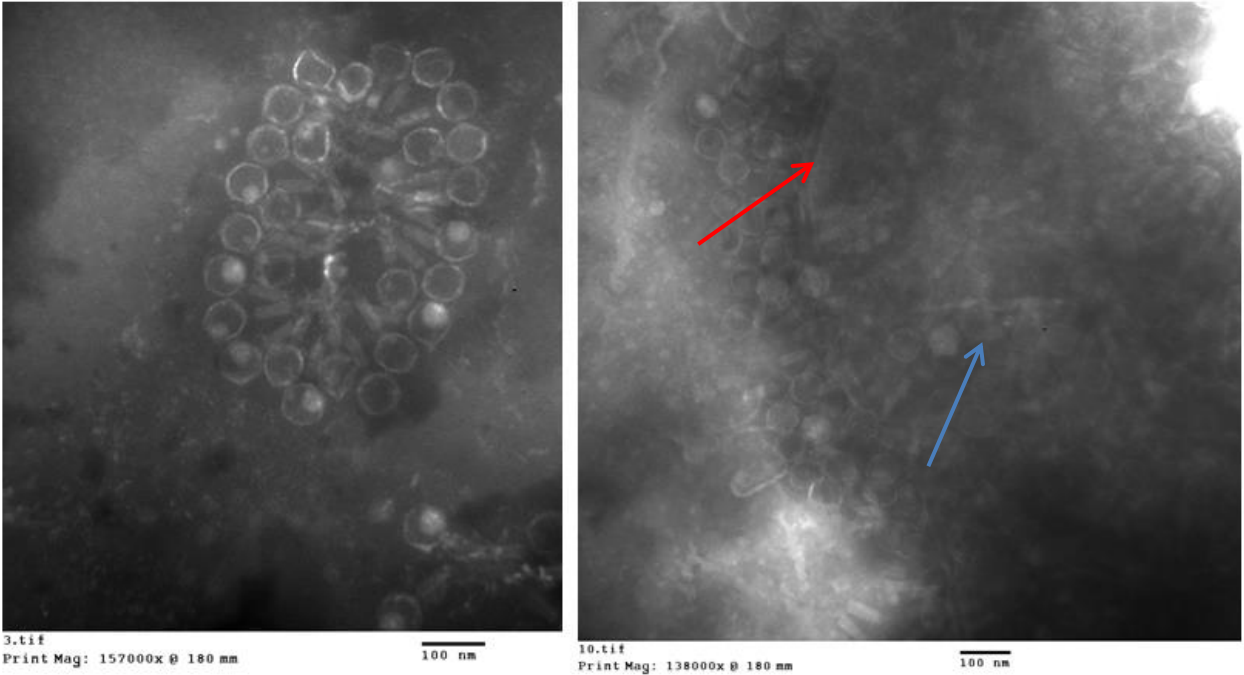


Figure 9.2.3.4: Higher magnification at 2hrs with phage, all with black heads, congregated around a bacterial cell that is now indistinct (left image); TEM at 4hrs with multiple phage visible inside and outside the bacterial cell wall. Red arrow points to bacterial cell wall and blue arrow shows phage particles within the cell.

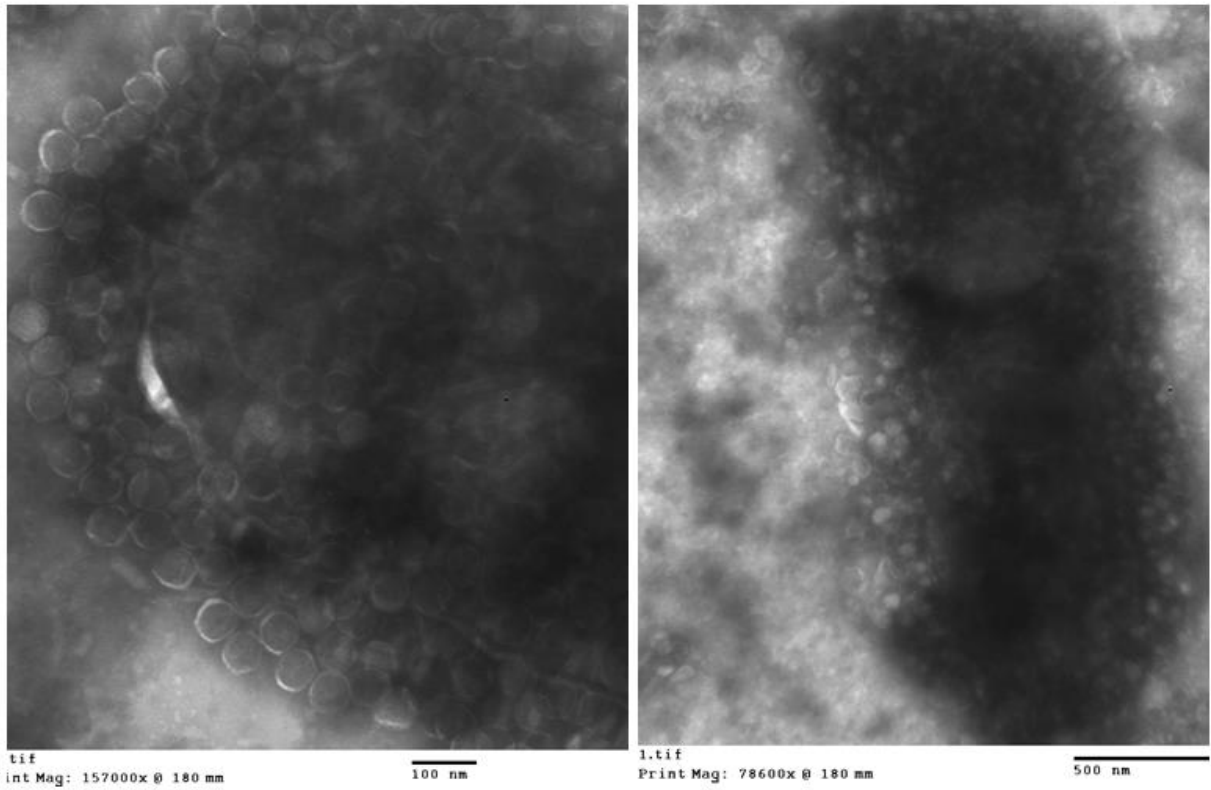


Figure 9.2.3.5: TEM of PAO1 and phage cocktail 1 hrs after being added together. Phage visible within cell walls; note most phage heads are black.

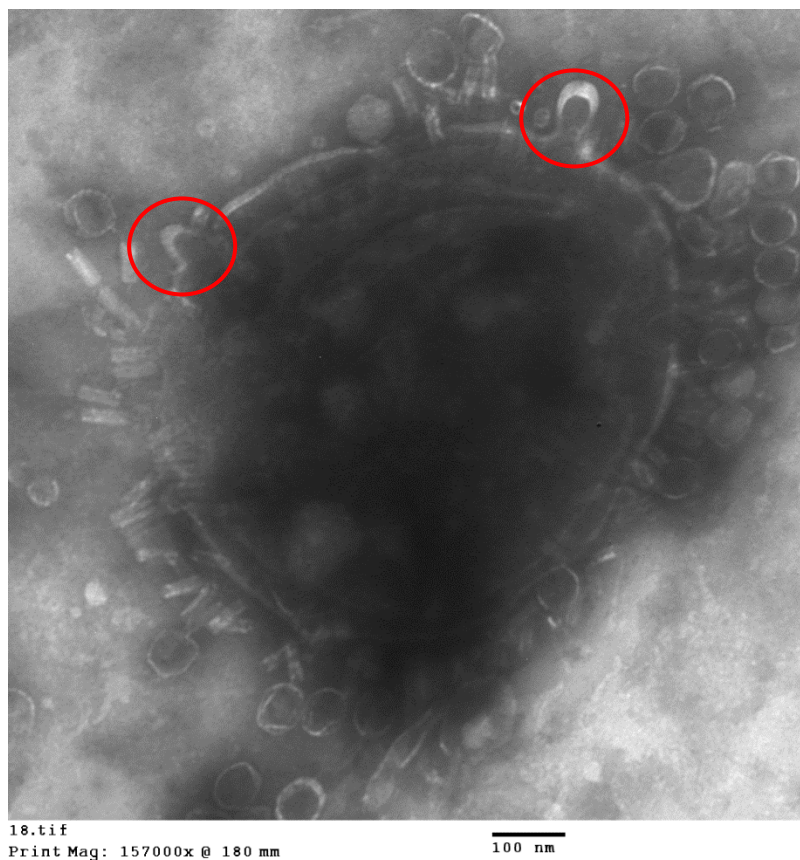


Figure 9.2.3.6: Pouching out of bacterial cell wall (circled in red), possibly representative of points at where cell lysis is beginning.

9.3: Discussion

The experiments in this chapter were undertaken in order to visualise the bacteriophage present in three novel cocktails and to investigate their interaction with Pa, and this aim was achieved.

Following the schematic phage classification in Figure 7.2.1.1, bacteriophages visualised by TEM in each of the three cocktails belonged to either class IV or V. Class IV phage with non-contractile tails are most widely distributed in nature. Tails are curved to varying degrees and striations on the tail are a characteristic feature; if these are not visualised, it is most likely due to inadequate resolution as opposed to the structures being absent (496). Most phage with non-contractile tails have polyhedral heads, usually an icosahedron or octahedron, an example of which is seen in Figure 9.2.1.1. The structure of the class IV bacteriophage endplate has significant variation but is often difficult to visualise, as seen in my images, due to the relatively small size in comparison to the head and tail. Furthermore, the endplate is delicate so integrity is easily compromised during sample preparation and, as TEM only images in one plane, it is often impossible to appreciate the spatial configuration of the endplate using this technique. By contrast, the endplate of class V phage almost universally gives off long, thin fibres, seen in Figures 9.2.1.3 and 9.2.1.4. The tails consist of an outer sheath and hollow inner rod; the sheath is stretched when class V phage are intact and the inner rod only becomes exposed when the sheath contracts. Most class V phage contain double-stranded high molecular weight DNA, necessary for transmitting the larger volumes of genetic information that are necessary for replication compared to phage with simpler tail structures. When this DNA is injected into host bacterial cells, the tails of class V phage contract and the virus is no longer active; class IV phage infect bacteria in a similar fashion but no change in tail structure is seen. Common to both class IV and V phage following infection of a bacterial host is a change in the appearance of the head as seen under TEM; the heads of phage particles containing DNA appear white when negatively stained whilst those where DNA has been transmitted to a bacterial host appear black. This is best seen in Figure 9.2.1.6, along with changes in contractile tail morphology. Only general morphological

changes could be detected using TEM rather than eleven distinct phages from the three cocktails being distinguishable; it is entirely possible given the nature of TEM that class III phage were present as phage heads without long tails being seen. These were assumed to be class IV or V particles seen from above, though class III phages infecting various species of Pa have been described (496).

A striking feature of TEM images of phage and Pa is the difference in size between the two, with far less magnification required to visualise bacterial cells. From TEM images it is clear that phage start to attack Pa almost immediately; tail attachment to the bacterial cell wall via the endplate occurs in a co-ordinated fashion in images taken after 2hrs, as shown in Figures 9.2.3.1 and 9.2.3.2, and in later images there is evidence of phage replication occurring within the bacterial cell wall. Imaging at both 8hrs and 24hrs after phage was added to Pa did not delineate any phage particles or Pa, suggesting that the process of cell lysis was complete. This was relevant to ongoing work as it showed a signal might be expected within a short time frame if these phage cocktails were efficacious *in vitro* and *in vivo* and that Pa might not be recovered if prolonged periods elapsed between infection and sample collection.

Chapter 10: *In vitro* Efficacy of Phage Cocktails

The experiments in this chapter were designed to test the hypothesis that bacteriophage cocktails were efficacious *in vitro* against i) clinical strains of Pa from CF patients and ii) a genetically modified bioluminescent form of the laboratory strain PAO1. This needed to be done prior to *in vivo* experiments to ensure that the proposal for non-invasively monitoring response in a murine model was feasible. If efficacy could not be demonstrated *in vitro*, then phage therapy would be unlikely to be effective *in vivo* and, even if I proved *in vitro* efficacy, if bioluminescence was not shown to be an accurate proxy measure of bacterial density then it would not be useful for monitoring the response to phage treatment in a murine model.

10.1: Materials and Methods

Standard plaques of non-mucoid Pa strains (n=3 for each strain so that repeatability of any treatment effect could be demonstrated) from five chronically infected, as defined by Leeds Criteria (440), adult CF patients were produced as described in Section 8.4. 10µl of each phage cocktail (1, 2 and 3, each containing 6.2×10^{10} phage forming units (PFU)/ml) was serially diluted with SM buffer (giving dilutions from neat to 10^{-6}) and pipetted onto the cooled bacterial carpet. 10µl of SM buffer was also pipetted onto an area of the plaques as a control. Plates were incubated overnight at 37°C after phage droplets had dried.

Plaque assay was also used to assess efficacy of each cocktail against PAO1, a well described laboratory reference strain (560, 561), that was transformed with a recombinant plasmid containing the *luxCDABE* gene cassette of *Photobacterium luminescens* (kindly provided by Dr. Shona Nelson, UWE, Bristol) in order to make it bioluminescent. The recombinant plasmid, pBBR1MCS-5 lite, was constructed by insertion of the 7kb *EcoRI* fragment from plasmid pLite27 (562) into the broad host range plasmid pBBR1MCS-5 (563) with the *luxCDABE* genes, under the control of the Ap lac promoter. All plasmid reconstruction was undertaken at UWE and I was sent the bioluminescent PAO1 on gentamicin agar slopes, ready for use.

Efficacy of each cocktail against the five clinical strains and bioluminescent PAO1 was assessed by visualisation and digital photography of the bacterial carpets following overnight incubation. Pa was determined to be susceptible at a given concentration of phage if inhibition of growth was demonstrated where 10µl of that concentration had been pipetted.

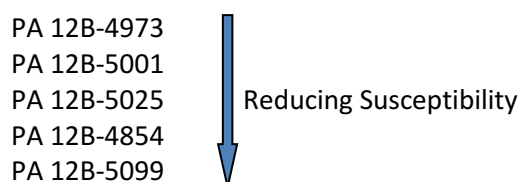
10.2: Results

Table 10.2.1 summarises efficacy of each phage cocktail against each strain of Pa. Clinical strains are numbered according to their Royal Brompton clinical microbiology lab number (with my own identifying number (1-5) in parentheses). Where there was incomplete inhibition of growth, this is stated in brackets and if there was no inhibition, this is recorded as none. Photographs of each plate were taken; examples of these are shown in Figure 10.2.1.

Pa Strain	Cocktail 1	Cocktail 2	Cocktail 3
PA12B-4854 [1]	10 ⁻²	None	None
PA12B-4973 [2]	All	All (less at 10 ⁻⁵ /10 ⁻⁶)	All
PA12B-5001 [3]	10 ⁻⁵ (less at 10 ⁻⁴ /10 ⁻⁵)	10 ⁻⁵	All
PA12B-5025 [4]	10 ⁻²	10 ⁻²	10 ⁻⁴
PA12B-5099 [5]	10 ⁻²	None	None
PAO1 pBBR1MCS5	All	All	All

Table 10.2.1: Dilutions at which bacteriophage cocktails were effective *in vitro* against five clinical [1-5] and one laboratory strain of Pa. Each cocktail was tested down to a dilution of 10⁻⁶; if Pa was sensitive at all dilutions, this is marked as “all” and if there was no inhibition of Pa growth, this is marked as “none”.

These results demonstrate that these bacteriophage cocktails are efficacious against clinical Pa strains isolated from CF patients *in vitro*, in keeping with previous studies (564, 565). Based on this, order of order of susceptibility of the clinical strains to phage cocktails was defined as:



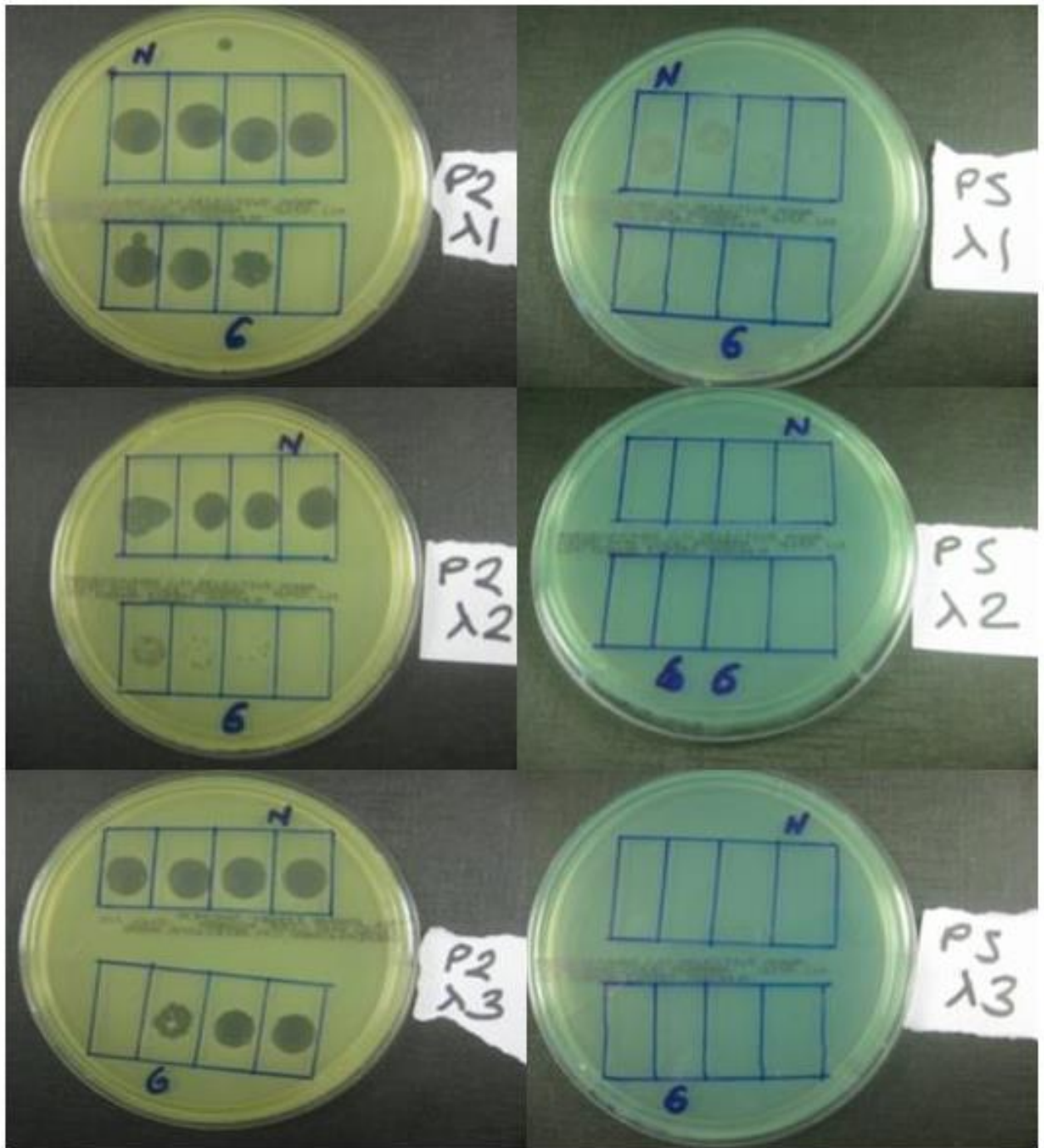


Figure 10.2.1: Photographs showing inhibition of Pa growth with bacteriophage cocktails; P2 = *Pseudomonas aeruginosa* 2 (PA12B-4973) and P5 = *Pseudomonas aeruginosa* 5 (PA12B-5099). λ_1 , λ_2 and λ_3 = Phage 1, 2 and 3.

Note different appearances of the two Pa strains (P2 is light green in the left column and P5 is darker green in the right column). Clear circles indicate where there has been inhibition of bacterial growth by phage. The left hand column shows that P2 is sensitive to λ_1 at phage concentrations from neat (N) down to 10^{-6} (the final box is a control where $10\mu\text{l}$ SM buffer is added), sensitive to λ_2 to dilutions down to 10^{-4} and to λ_3 to 10^{-6} . In the right hand column, there is less inhibition of growth; P5 is only sensitive down to a dilution of 10^{-2} with λ_1 and there is no inhibition of growth with λ_2 and λ_3 , as shown by the bacterial carpets having no clear circles in all boxes where $10\mu\text{l}$ of phage at each dilution was added.

10.3: Discussion

Phage cocktail 1 was most efficacious overall against clinical Pa strains. In order to maximise the likelihood of a signal being detected, this was selected to be used *in vivo*. Coincidentally, later work investigating the potential effects of bacteriophage cocktail alone on inflammatory response in the airway lung (Section 12.3.4) showed that cocktails 2 and 3 were far more immunogenic than cocktail 1. This was subsequently discussed with Amplphi who stated that they were aware of this and that both cocktails 2 and 3 were at a far less advanced stage of production than cocktail 1. The selection of cocktail 1 for *in vivo* work was therefore serendipitously further justified. PA12B-4973 (referred to from here on as "clinical strain") was most sensitive to phage cocktail 1, so was chosen as the *in vivo* strain for ongoing use. All three cocktails were equally efficacious against bioluminescent PAO1 pBBR1MCS5-lite (referred to as PAO1 from here on); with this established, it was necessary to clarify that luminescence was an accurate proxy measure of bacterial density *in vitro* prior to formulating a protocol for *in vivo* experiments using this strain.

It is relevant to note that antibiotic susceptibilities (as provided by RBH microbiology lab) indicated that these phage cocktails might be efficacious in situations where conventional antibiotics might not. Table 10.3.1 shows that PA12B-5025 was inherently resistant to 8/11 antibiotics tested *in vitro* but was **not** the least susceptible strain to phage, being sensitive at dilutions down to 10^{-2} for cocktails 1 and 2 and down to 10^{-4} for cocktail 3.

	PA12B-4973	PA12B-5001	PA12B-5025	PA12B-4854	PA12B-5099
Amikacin	S	S	R	S	S
Aztreonam	S	S	R	S	S
Ceftazidime	S	S	R	S	S
Chloramphenicol	S	S	S	R	S
Ciprofloxacin	S	S	S	I	S
Colistin	S	S	S	S	S
Co-trimoxazole	R	R	R	R	R
Meropenem	S	S	R	S	S
Piptazobactam	S	S	R	S	S
Timentin	S	S	R	S	S
Tobramycin	S	S	S	S	S

Table 10.3.1: *In vitro* antibiotic susceptibility of five clinical strains of Pa used for phage sensitivity assays.

Chapter 11: Preparation for Non-Invasive Monitoring of Response

The initial intention for *in vivo* studies of phage efficacy was to use optical imaging to take sequential images of mice at various time points after infection \pm phage treatment in order to determine the efficacy and pharmacokinetics of therapy without need for animals to be sacrificed at different time points. This was in order to adhere with the guiding principles underpinning humane use of animals in scientific research which aim to replace the use of animals, reduce the number of animals used and refine experiments such that suffering is minimised (3Rs). The experiments in this chapter were formulated to answer the question of whether non-invasive monitoring of response to phage therapy *in vivo* was a feasible approach.

11.1: Materials and Methods

11.1.1: Luminescence of Pa Alone

PAO1 was introduced from nutrient agar slopes containing 10mg/L gentamicin into 10mls TSB using a single-use plastic inoculation loop and agitated overnight at 37°C. Optical density of this broth was measured by spectrophotometry and adjusted by dilution to six optical densities (between 0.025 and 1) using sterile TSB. 500 μ l of each solution was pipetted into a 24 well Nunclon™ plate (Nunc A/S, Denmark) and luminescence measured using IVIS™ optical imaging system (Xenogen Biosciences, USA) using a camera coupled to LivingImage software (version 3.1, Xenogen). Data was exported to Excel 2010 (Microsoft, USA) and luminescence of TSB alone (background) subtracted from total luminescence to give a value for the luminescence attributable to bacteria. Six measurements were made at each optical density and then plotted using Prism 6.0 (GraphPad, USA).

11.1.2: Luminescence of Pa and Bacteriophage

Luminescence of PAO1 following bacteriophage treatment was assessed in two ways:

1. 500µl of a stock broth of PAO1 adjusted to an optical density of 1 by dilution using spectrophotometry was added to 12 wells of a 24 well Nunclon™ plate. Each bacteriophage cocktail was serially diluted from neat down to a concentration of 10^{-2} using sterile SM buffer and 50µl of each dilution was added to one of the wells containing PAO1. A control well of PAO1 was treated with 50µl of SM buffer alone. The plates were kept at 37°C and luminescence in each well was assessed as described in Section 11.1.1 at three time points (0, 6 and 24hrs after addition of bacteriophage cocktail). After 24hrs, 10µl of each broth was serially diluted, as per Miles and Misra protocol (566), and plated onto PSA to determine number of colony-forming units per millilitre (CFU/ml) of PAO1 remaining. PSA plates were incubated overnight at 37°C prior to performing colony counts. The experiment was later repeated but with plating performed 48hrs following addition of bacteriophage (to see whether this had any additional impact on bacterial killing).
2. 500µl of six different optical densities of PAO1 were added to 12 wells of a 24 well Nunclon™ plate and 50µl of neat bacteriophage cocktail was added (n=3 for each cocktail). Three control wells were inoculated with 50µl of SM buffer alone. Plates were kept at 37°C and luminescence measured at 0, 24 and 48hrs as previously described.

11.1.3: Fluorescent Pa and Response to Bacteriophage Cocktail

The methodology in Section 11.1.2 demonstrated that the luminescent strain of PAO1 was not suitable for non-invasive monitoring of response to phage therapy (see results in section 11.2.1). A fluorescent strain of PAO1 (561, 567) modified with a heme-based chromophore (kindly provided by Dr. Andrew Ulijasz, Imperial College London), was thus investigated to see whether it was a more suitable strain for non-invasive monitoring of response to phage therapy.

Efficacy of phage cocktail 1 against PAO1 expressing near-infrared fluorescent protein (iRFP) was established using standard plaque assay as described in Section 8.4. PAO1 expressing iRFP was then introduced from agar slope into 10mls TSB using a single-use plastic inoculation loop and incubated and agitated overnight at 37°C. This was centrifuged at 4°C for 10 minutes at 2000g and the resultant cell pellet resuspended in TSB. Optical density of this broth was adjusted by dilution with sterile TSB to 0.05, 0.1, 0.25, 0.5 and 1 using spectrophotometry. That fluorescence was a proxy measure of bacterial density was established with methodology as described previously in Section 11.1.1, although an Infinite Pro plate reader (Tecan, Switzerland) was used to measure fluorescence of 500µl of iRFP PAO1 (n=6 at each optical density) in a black µclear™ 96-well plate (Greiner Bio-One, Germany) rather than the IVIS/LivingImage setup. These results are shown in section 11.2.3.

To establish the effect of phage on fluorescence, 100µl of iRFP PAO1 at each of the five optical densities was added to a black µclear™ 96-well plate, in triplicate. 10µl of phage cocktail 1 was added to each well containing Pa and to three wells containing 100µl of TSB alone (controls, n=3). The plate was incubated without agitation at 37°C in an Infinite™ Pro plate reader (Tecan, Switzerland) which was configured to take absorbance (a proxy measure of bacterial density) and fluorescence readings automatically every 60 minutes which were exported using Magellan™ data analysis software (Tecan, Switzerland). Fluorescence filters were set at 690/9nm and 725/20nm for excitation and emission respectively and absorbance was measured at 600nm according to standard protocols (567, 568). This methodology was also used to measure fluorescence and absorbance of wild-type PAO1 (effectively a control experiment, as wild-type PAO1 should not fluoresce).

11.2: Results

11.2.1: Luminescence vs. Optical Density

A linear relationship between bacterial density and luminescence was demonstrated by the first part of the described methodology. Figure 11.2.1.1 shows an example of the images produced using IVIS and LivingImage in combination and Table 11.2.1.1 shows corrected luminescence readings (n=6 at each optical density) that were obtained by subtraction of the luminescence attributable to TSB alone from the total measured luminescence.

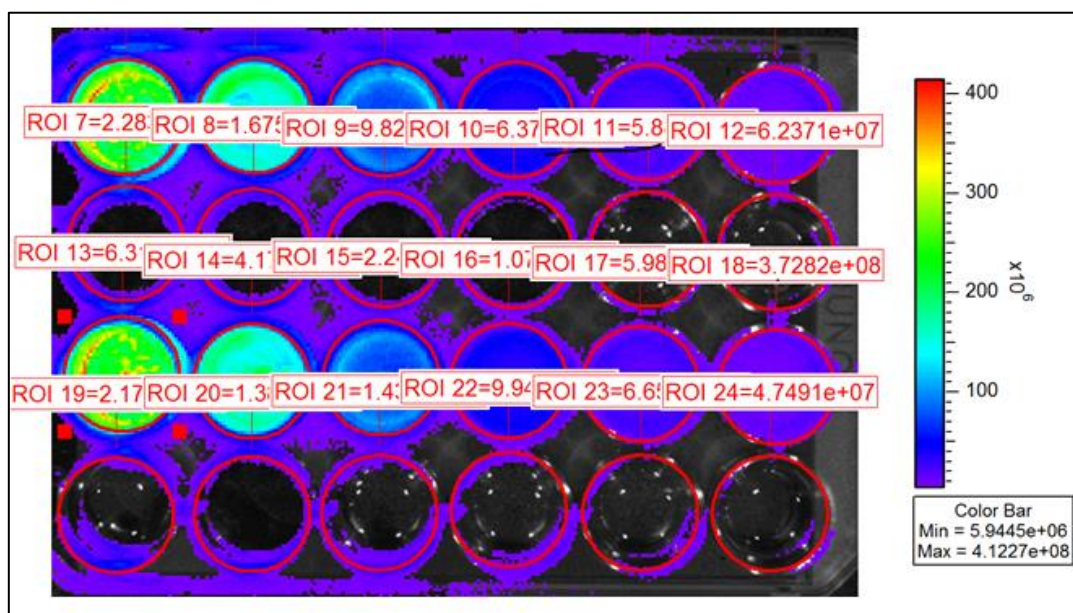


Figure 11.2.1.1: Example of IVIS LivingImage picture produced when photographing 24 well plates containing luminescent PAO1. Note decreasing luminescence from left to right in the top and third rows, reflecting a sequential drop in the optical density of PAO1 added to each well (from 1.0 down to 0.05 in both these rows). Rows 2 and 4 were kept empty in order to minimise the risk of contamination between wells.

0.025	0.05	0.1	0.2	0.4	1.0
3.23E+08	6.56E+08	1.1E+09	2.192E+09	3.323E+09	4.91E+09
3.26E+08	6.02E+08	1.1E+09	2.108E+09	3.622E+09	5.66E+09
3.19E+08	5.87E+08	1.11E+09	2.306E+09	4.302E+09	6.38E+09
3.29E+08	6.24E+08	1.02E+09	2.049E+09	3.573E+09	5.25E+09
3.21E+08	6.2E+08	1.05E+09	2.109E+09	3.44E+09	5.52E+09
3.25E+08	5.51E+08	1.03E+09	2.202E+09	4.13E+09	6.27E+09

Table 11.2.1.1: Luminescence readings at each optical density for PAO1 (n=6).

When luminescence was plotted against optical density, a linear relationship became apparent; this is shown in Figure 11.2.1.2; each point represents the mean reading (n=6) and the error bars are indicative of the range.

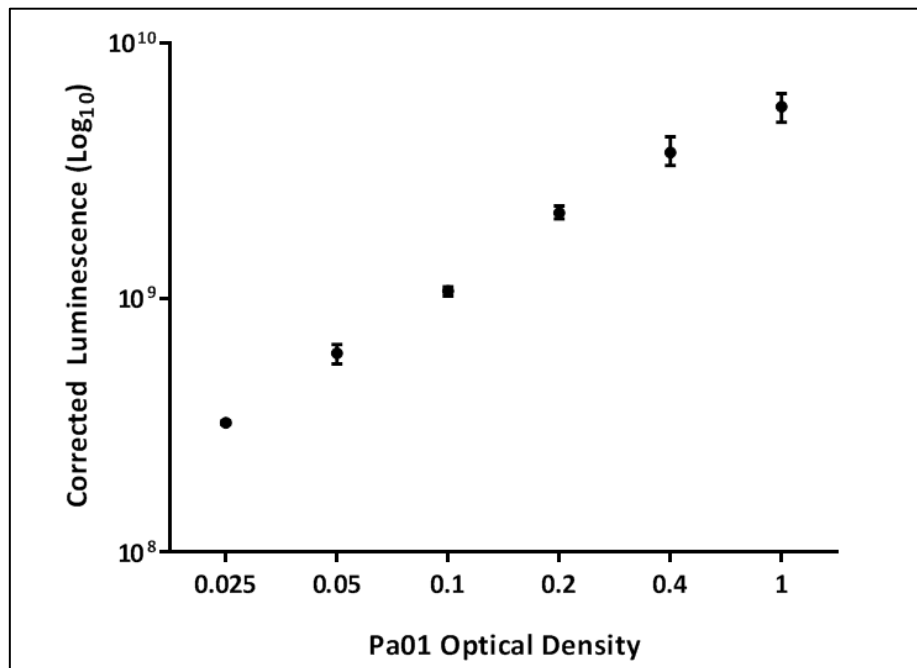


Figure 11.2.1.2: Linear relationship between luminescence and optical density for a genetically modified strain of PAO1.

11.2.2: Luminescence following Bacteriophage Treatment

As linearity of luminescence against optical density was established, it was necessary to determine how this was affected by bacteriophage therapy. In the first experiment, each cocktail was added at dilutions from neat to 10⁻² to 500µl of PAO1 at an optical density of 1 and luminescence measured at 0, 6 and 24hrs. At 0hrs, luminescence was of a similar magnitude, as would be expected, to that seen in the preceding section where linearity was established. After 6hrs, luminescence had declined with addition of each of the phage cocktails but was highest in wells where each neat bacteriophage cocktail had been added and typically lowest where phage cocktail at a 1 in 100 concentration was used. After 24hrs, the magnitude of luminescence had again declined but there was no consistent relationship between this and the concentration of bacteriophage that had been added to PAO1; for cocktails 1 and 2 the luminescence was lowest in wells where bacteriophage at 1 in 10 dilution had

been added whilst for cocktail 3 luminescence was lowest where neat bacteriophage was used. This is shown in Figures 11.2.2.1 and 11.2.2.2.

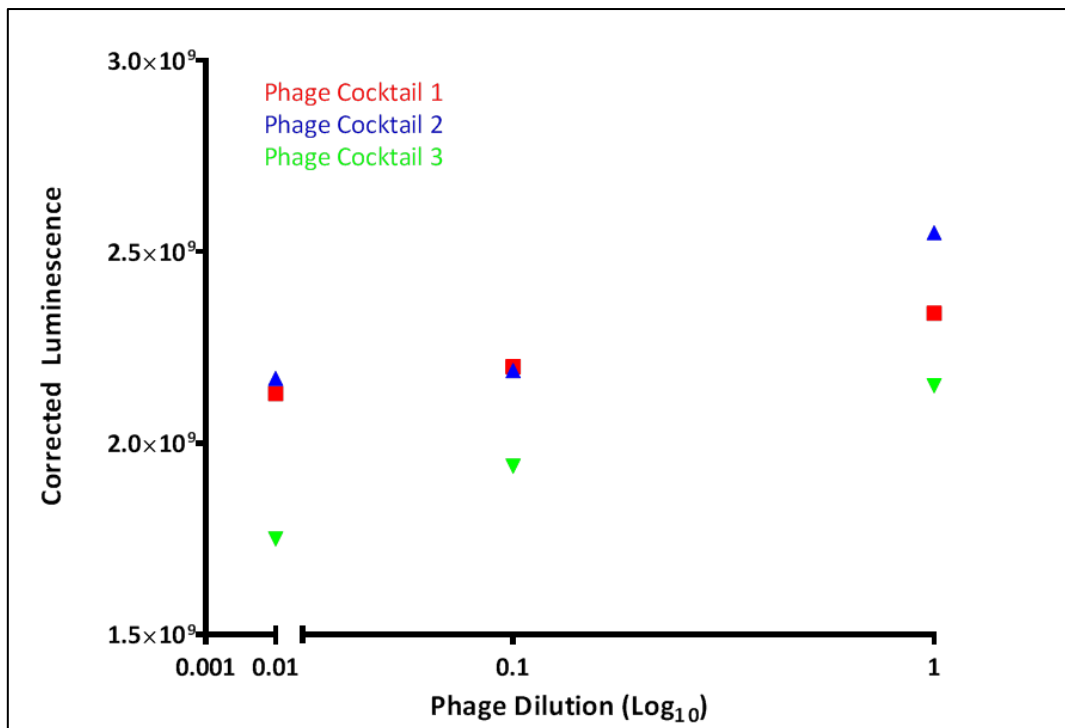


Figure 11.2.2.1: Graph showing luminescence of PAO1 (with an initial optical density of 1), 6hrs after treatment with three bacteriophage cocktails at three concentrations (Log_{10} dilutions).

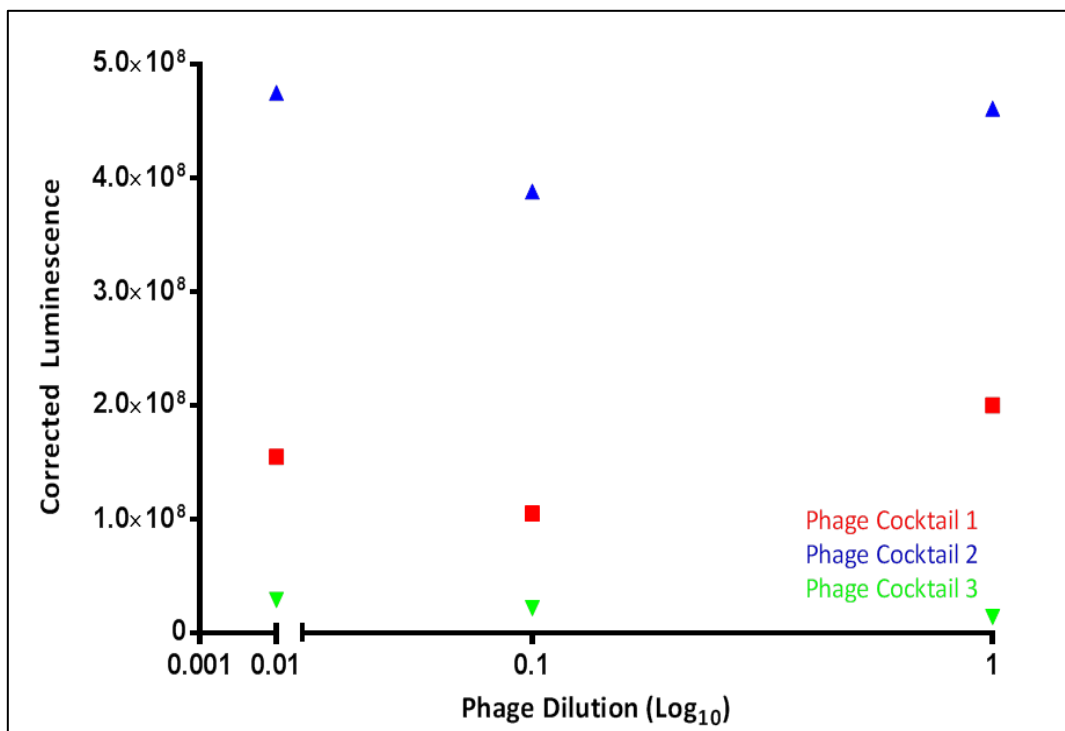


Figure 11.2.2.2: Graph showing luminescence of PAO1 (with an initial optical density of 1), 24hrs after treatment with three bacteriophage cocktails at three concentrations (Log_{10} dilutions).

When bacterial colonies were counted from the broths in the 24 well plates after the 24hr luminescence readings were taken, there was only a trend towards bacteriophage being more effective at higher concentrations (neat > 10^{-1} > 10^{-2}). The number of colonies recovered from each of the broths at each dilution was very similar; this was expected given earlier *in vitro* work that suggested PAO1 was highly sensitive to all three cocktails. However, this was not reflected in luminescence; after 24hrs there was a significant disparity between luminescence of the broths according to which phage had been used (Figure 11.2.2.2) which cannot be explained by significantly different numbers of bacteria being present in the wells. Colony counts are shown in Table 11.2.2.1; note that it was not possible to count colonies in wells that were not treated with bacteriophage, even at the lowest dilutions of 10^{-8} , again indicating sensitivity of PAO1 to all three phage cocktails. Luminescence of these control wells at 24hrs was slightly less than that seen at the optical density of 1 in the previous linearity experiment but significantly (and paradoxically) higher than that of wells treated with phage cocktails.

Broth Dilution	Neat	10^{-1}	10^{-2}	10^{-3}	10^{-4}	10^{-5}	10^{-6}	10^{-7}	10^{-8}
Phage 1 Strength									
Neat	+++	102	21	13	0	0	0	0	0
1 in 10 Dilution	+++	65	12	8	3	0	0	0	0
1 in 100 Dilution	+++	58	29	18	5	7	7	12	7

Broth Dilution	Neat	10^{-1}	10^{-2}	10^{-3}	10^{-4}	10^{-5}	10^{-6}	10^{-7}	10^{-8}
Phage 2 Strength									
Neat	+++	110	22	29	19	41	8	6	5
1 in 10 Dilution	+++	75	29	8	10	17	6	2	4
1 in 100 Dilution	+++	++	9	9	13	23	70	67	45

Broth Dilution	Neat	10^{-1}	10^{-2}	10^{-3}	10^{-4}	10^{-5}	10^{-6}	10^{-7}	10^{-8}
Phage 3 Strength									
Neat	+++	93	17	4	1	0	0	0	0
1 in 10 Dilution	+++	89	17	9	3	0	1	0	1
1 in 100 Dilution	+++	92	9	1	2	0	0	0	0

Broth Dilution	10^{-4}	10^{-5}	10^{-6}	10^{-7}	10^{-8}
LPA Broth (Control) No bacteriophage	+++ Green	+++ Green	+++ Light Green	+++ Light Green	+++ Light Green

Table 11.2.2.1: Colony counts after plating serially diluted PAO1 broths with an initial optical density of 1 onto PSA 24hrs after treatment with three bacteriophage cocktails at three concentrations. The bottom table demonstrates that it was not possible to count colonies, even at dilutions of 10^{-8} , where phage was not added to the broths.

In the second experiment, luminescence of differing optical densities of 500µl of PAO1 alone was measured at 0, 24 and 48hrs, and also at these time points following addition of 50µl of each neat bacteriophage cocktail. For the control broths where no bacteriophage was added, luminescence at 0hrs mirrored earlier linearity experiments (Figure 11.2.2.3) as would be expected. It was less at 24hrs than at 0hrs but remained higher at higher starting optical densities (Figure 11.2.2.4). At 48hrs luminescence declined further and there was a loss of the linear relationship seen previously such that broths with higher initial optical densities at time point 0 now had the lowest luminescence, although measurements were much more variable (Figure 11.2.2.5).

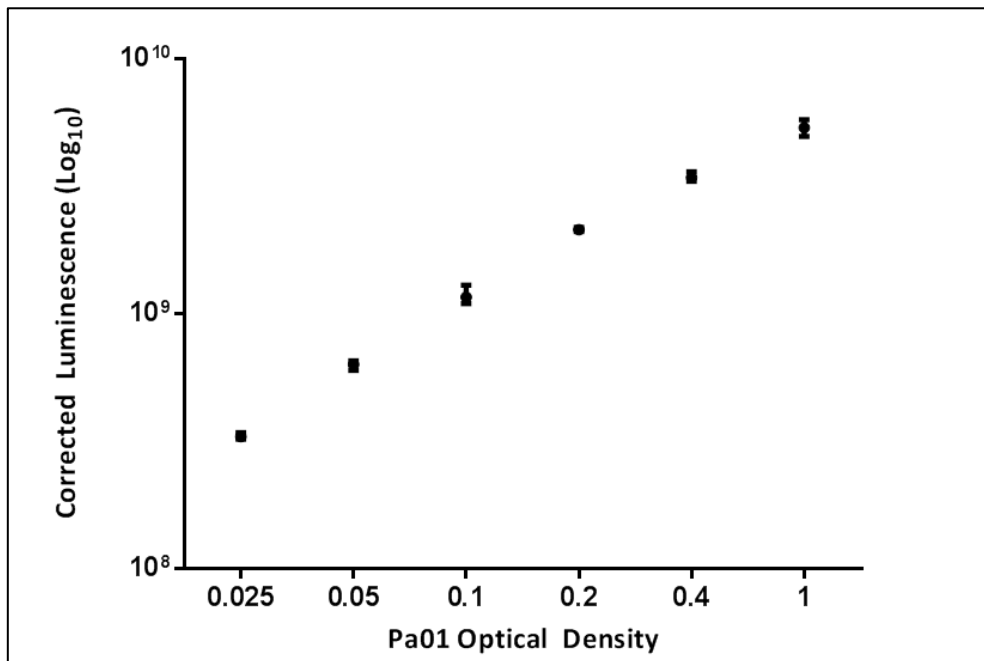


Figure 11.2.2.3: Graph showing luminescence of PAO1 at different optical densities prior to addition of 50µl of neat bacteriophage cocktails (n=3 at each optical density, time 0hrs).

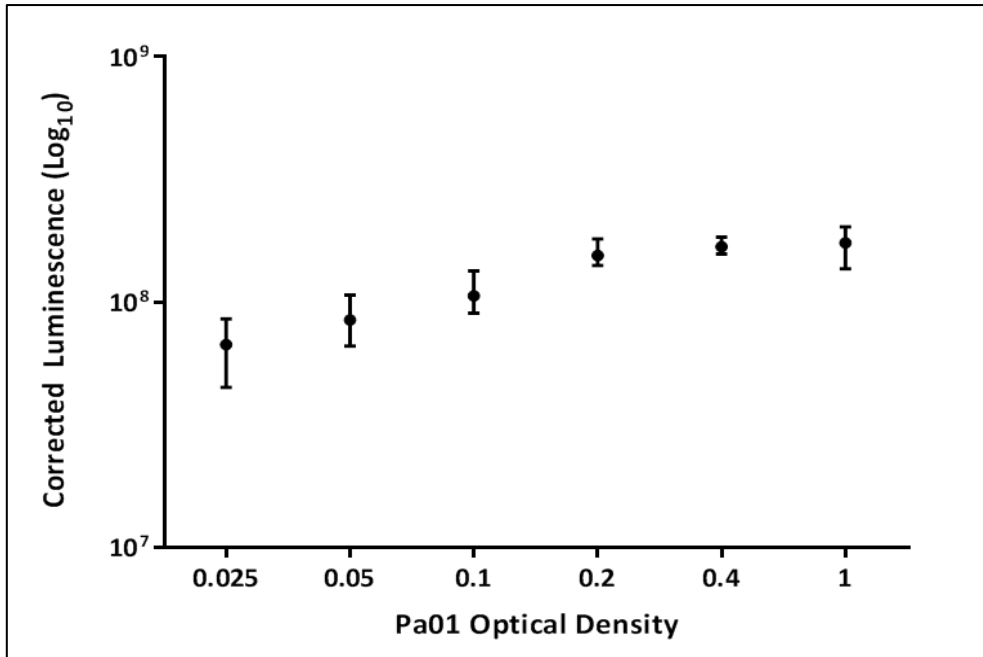


Figure 11.2.2.4: Graph showing luminescence of PAO1 at different optical densities (n=3) after 24hrs incubation at 37°C.

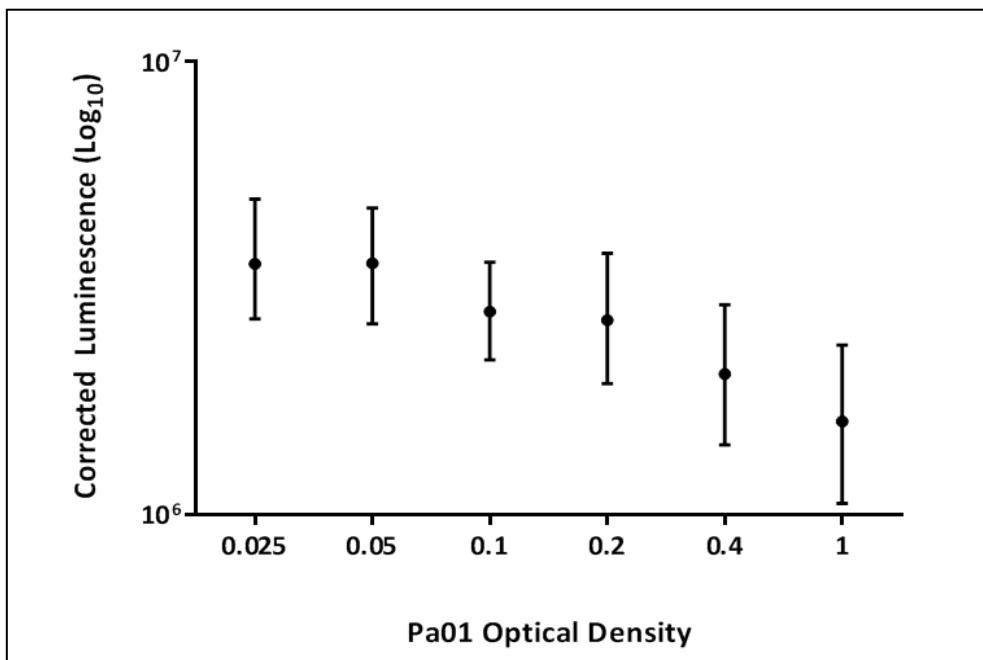


Figure 11.2.2.5: Graph showing luminescence of PAO1 at different optical densities (n=3) after 48hrs incubation at 37°C

Where PAO1 was treated with neat bacteriophage cocktail, differences in luminescence became apparent after 24hrs. These were not consistent between different cocktails. Luminescence trended towards being greater in the broths that had a higher initial optical density for those treated with cocktails 1 and 2, but was lower at higher starting optical densities for cocktail 3 (Figure 11.2.2.6).

More important was that the magnitude of luminescence was higher in the treated broths compared with the control broths after 24hrs, which was paradoxical given that phage-induced killing of PAO1 at this time point was demonstrated in the first part of this section.

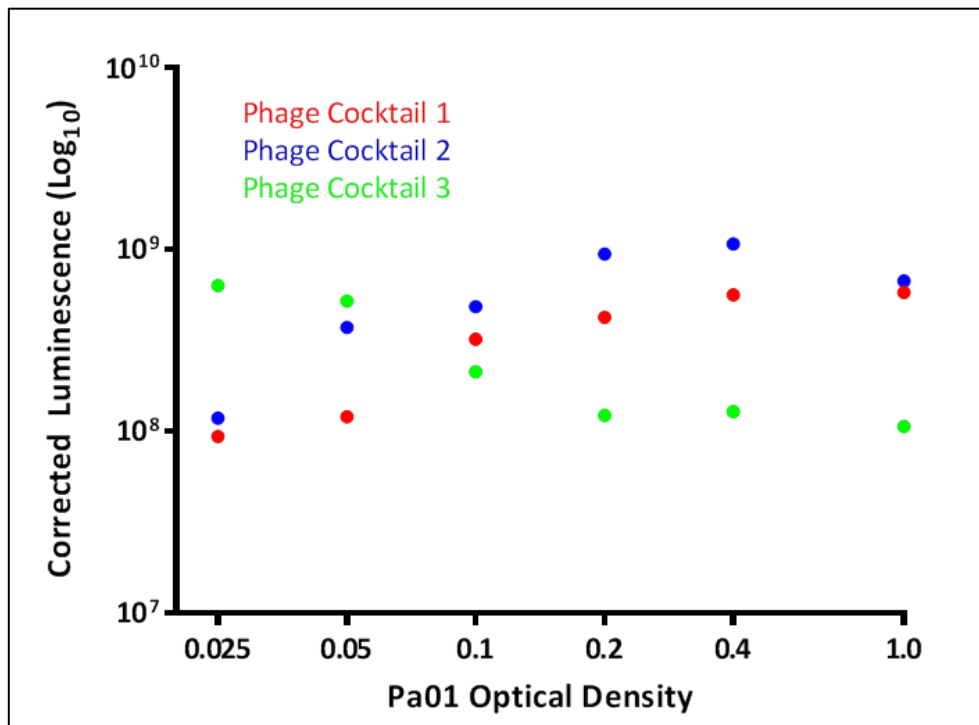


Figure 11.2.2.6: Graph showing luminescence of PAO1 at different optical densities 24hrs after addition of 50µl of three bacteriophage cocktails.

After 48hrs incubation at 37°C with bacteriophage cocktails, luminescence of PAO1 did not appear to be related to initial optical density of the original broths. Luminescence of broths treated with phage cocktails were significantly different between the 24 and 48hr time point ($p < 0.05$ using Wilcoxon matched-pairs signed rank test) although the pattern of luminescence compared to initial optical density had changed; luminescence of cocktail 3 tended to be greater in broths that had higher initial optical densities, having been lower after 24hrs though no obvious linear pattern was apparent across each of the optical densities (Figure 11.2.2.7). Importantly, the magnitude of luminescence at 48hrs was significantly **greater** in all treated broths when compared to the PAO1 control broths that were not inoculated with bacteriophage after 48hrs incubation at 37°C, despite the fact that the number of bacteria in the broths would have decreased with the addition of phage.

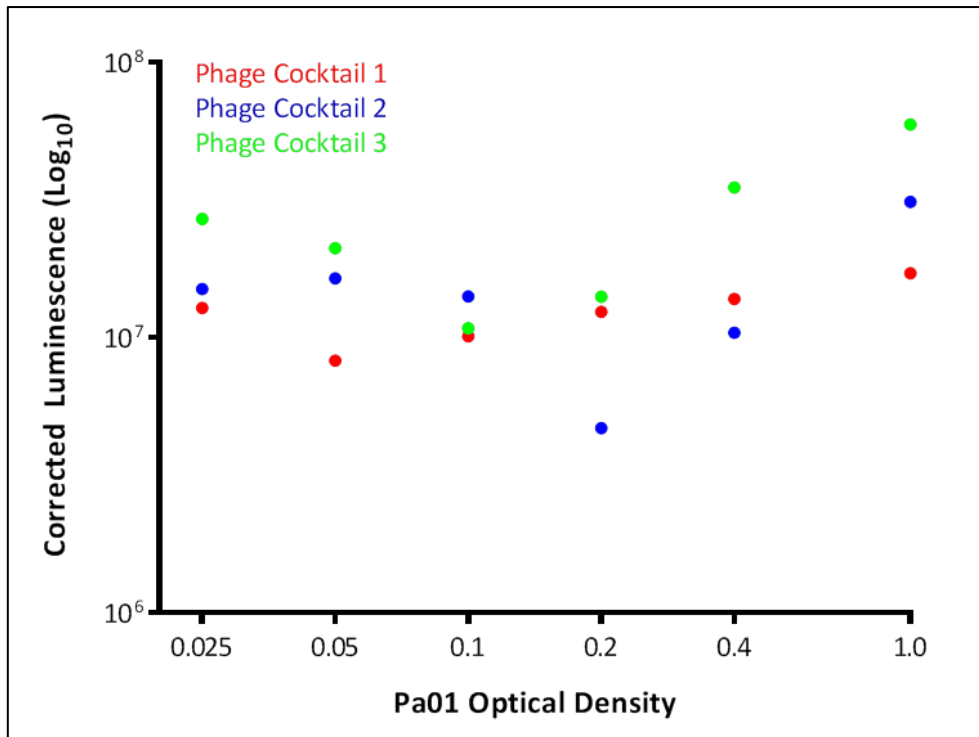


Figure 11.2.2.7: Graph showing luminescence of PA01 at different optical densities 48hrs after addition of 50µl of three bacteriophage cocktails.

11.2.3: Fluorescence vs. Optical Density

iRFP PA01 was sensitive to phage cocktail 1 on standard plaque assay, as shown in Figure 11.2.3.1. A relationship between bacterial density and fluorescence was demonstrated by the first part of the described methodology. Table 11.2.3.1 shows corrected fluorescence readings (obtained following subtraction of fluorescence attributable to TSB alone from total measured fluorescence, n=6 for each optical density) and Figure 11.2.3.2 demonstrates that this was relatively linear, with each point representing the mean reading (n=6 at each optical density) and the error bars indicating the range. This suggests that the iRFP PA01 would be a suitable infection with which to monitor response to bacteriophage, although when compared to the graph of luminescence against optical density (Figure 11.2.1.2) it is apparent that fluorescence measurements demonstrated more variability.



Figure 11.2.3.1 (left): Standard plaque assay for iRFP PAO1. Phage cocktail 1 was serially Log₁₀ diluted and 10µl pipetted onto the bacterial carpet. Inhibition of growth is demonstrated down to a phage dilution of 10⁻⁵ with no inhibition as lower dilutions or where 10µl SM buffer (C = control) was added.

0.05	0.1	0.25	0.5	1
468	705	2674	4771	5006
1075	890	504	4086	8647
257	74	1241	4908	6643
952	1192	1007	2371	6616
50	2166	2908	3666	7229
239	628	2328	3228	8544

Table 11.2.3.1: Fluorescence readings at each optical density for PAO1 (n=6).

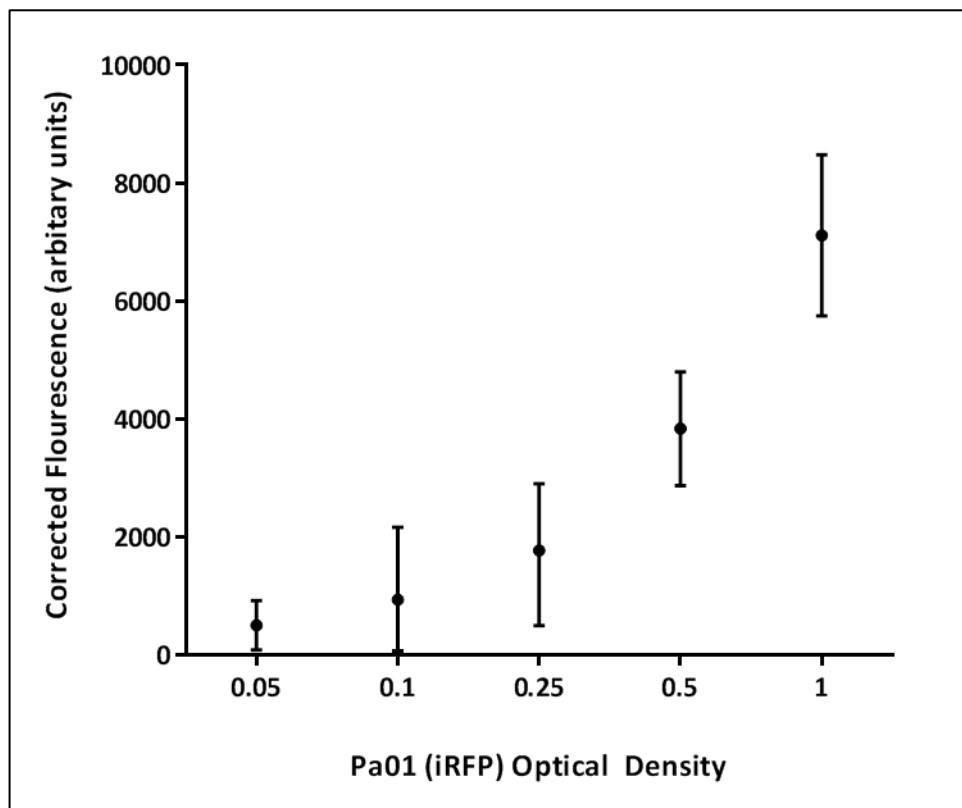


Figure 11.2.3.2: Linear relationship between fluorescence and optical density for a genetically modified strain of PAO1 (iRFP).

11.2.4: Fluorescence following Bacteriophage Treatment

Unlike the luminescent strain of PAO1, a clear reduction in fluorescence was demonstrated when iRFP PAO1 was treated with phage cocktail 1. This was most apparent for broths with a starting optical density of 0.05 and 0.1 which showed consistent increase in fluorescence over time, with no peak reached by the end of the experiment. iRFP PAO1 with a starting OD of 0.25 had a lower peak in fluorescence of approximately 10000 arbitrary units after 18hrs which was sustained through to the 48hr end point. The broths with starting OD of 0.5 and 1 peaked in fluorescence at around the same time but this then declined such that, by the end point differences in fluorescence between phage-treated and control wells (n=3 for each), was minimal. As expected, fluorescence of wild-type PAO1 wells was persistently low, regardless of the starting optical density, and did not change significantly over time.

Absorbance, considered an accurate proxy measure of bacterial density (like optical density), was measured sequentially over the course of the experiment. Absorbance of wild-type PAO1 that was treated with phage remained lower than untreated wild-type PAO1 wells until at least 30hrs; depending on the starting optical density, absorbance of phage-treated wells surpassed that of untreated wells after this point. For the iRFP PAO1, absorbance of phage-treated wells followed a similar pattern at starting optical densities of 0.05, 0.1 and 0.25, although the time point at which absorbance of the treated wells surpassed that of untreated wells was earlier, at around 15-18hrs after the start of the experiment. For iRFP at starting optical densities of 0.5 and 1.0, absorbance of phage-treated wells remained lower than that of untreated wells throughout. Graphs of fluorescence and absorbance for wild-type PAO1 and iRFP PAO1 with starting optical densities of 0.05 and 0.1 that were treated with either phage or with SM buffer (controls) are shown in Figure 11.2.4.1. Graphs of fluorescence and absorbance for starting iRFP PAO1 optical densities of 0.25, 0.5 and 1.0 are shown in Appendix A2.

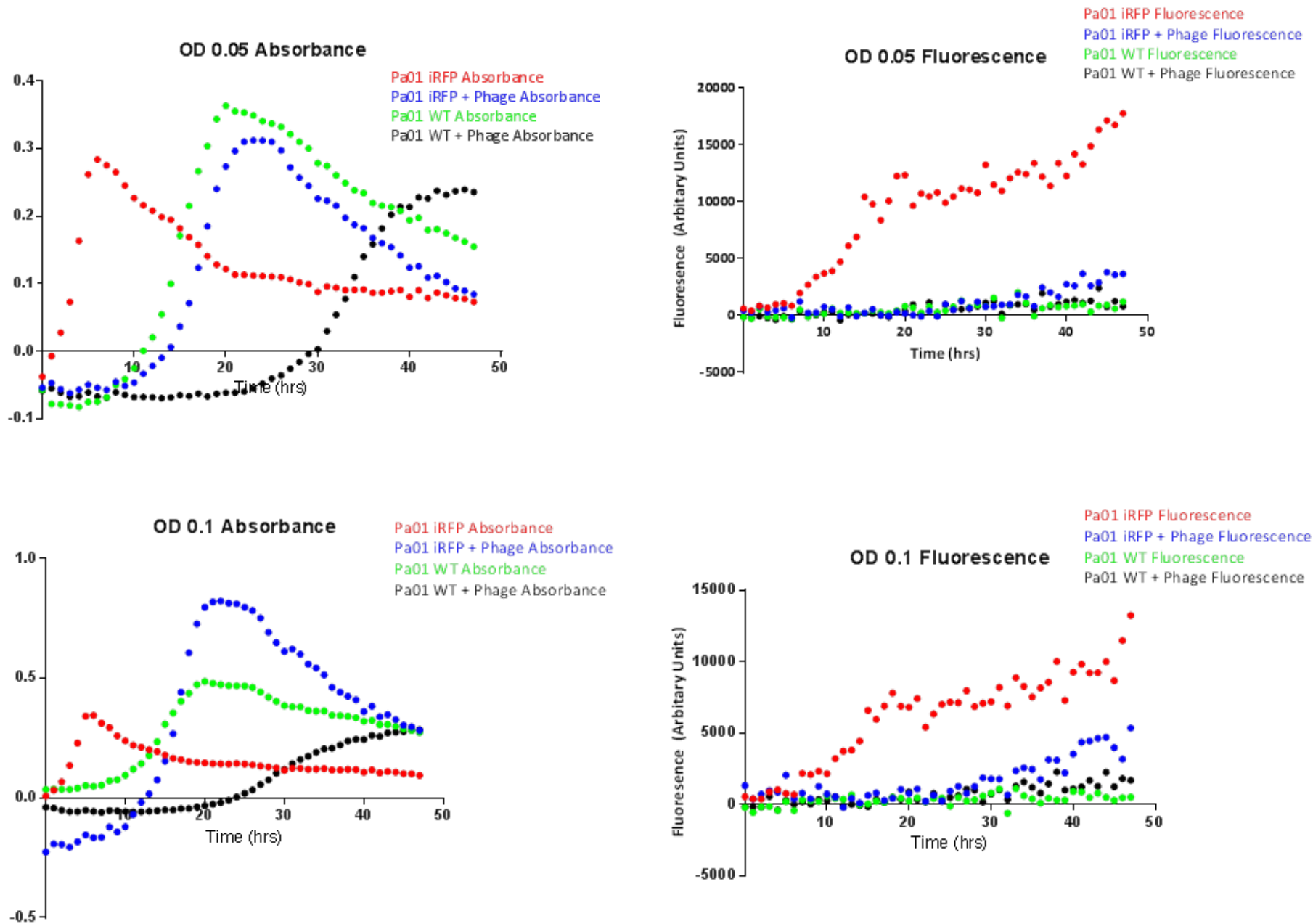


Figure 11.2.4.1: Graphs showing absorbance and fluorescence over time for wild type (WT) PAO1 and iRFP Pa01 with starting optical densities of 0.05 (top) and 0.1 (bottom) with and without treatment with phage cocktail. Note that fluorescence of iRFP is reduced over the entire 48hrs when phage is added (blue lines compared to red lines) at both starting optical densities, indicating impairment of growth by phage, but that absorbance is paradoxically not reduced; this suggests that absorbance is not an accurate proxy measure of bacterial density. As expected, there is no difference in fluorescence of WT Pa01 regardless of whether phage is added or not.

11.3: Discussion

The aim of this chapter was to determine whether non-invasive monitoring of response to phage therapy was a feasible approach. Ultimately, the experiments demonstrated that, whilst both luminescence and fluorescence of modified Pa strains were good proxy measures of bacterial density, for different reasons it was unlikely that efficacy of phage therapy *in vivo* could be accurately monitored by using these organisms.

All three phage cocktails demonstrated efficacy *in vitro* against a luminescent strain of PAO1 and cocktail 1 was also shown to be effective against fluorescent PAO1. Luminescence and fluorescence both increased in a linear fashion with increasing optical density, indicating that both readouts were accurate proxy measures of bacterial density. However, at both 6hrs and 24hrs, luminescence was paradoxically highest in wells where more bacteriophage had been added and therefore, by conjecture, more phage-induced killing was likely to have occurred. This assumption was shown to be incorrect by experiments demonstrating minimal difference in CFU/ml from wells treated with concentrations of bacteriophage cocktail that ranged from neat to 10^{-2} ; the reasons for this are not entirely clear although, given the dramatic decrease in CFU/ml in phage-treated wells compared to control wells, it is possible that a threshold effect was reached even when phage was diluted 100-fold and, in order to see a dose-related difference in phage-mediated killing, further phage dilution might have been necessary. As these phage cocktails contained 6.2×10^{10} PFU/ml, 50 μ l added to each well contained 3.1×10^9 PFU/ml; if 500 μ l of PAO1 with an optical density of 1 contain 5×10^8 CFU/ml, more than six phages were present for every PAO1 when neat cocktails were added. Given the lytic life cycle previously described and demonstrated, even at the lowest concentrations of 10^{-2} where 0.06 phage per PAO1 would initially have been present, it would only take one lytic life cycle with 20 PFU (burst size) released from an infected PAO1 for the ratio to tip back in favour of the bacteriophages. Lower phage dilutions were not tested as paradoxical results were also seen in later

experiments. These findings verified that the strain of luminescent PAO1 being used was not suitable for accurately monitoring response to phage non-invasively. These data are discussed further below.

Although differences in luminescence with the addition of differing concentrations of phage cocktail were minimal, differences were apparent between the cocktails. At both 6hrs and 24hrs, the luminescence was significantly higher in wells treated with cocktail 1 than in wells treated with cocktail three; this was a reproducible finding (data not shown). There was no clear explanation for this given that previous experiments did not demonstrate differences in sensitivity of this particular strain of modified PAO1 to the three cocktails and it raises questions as to the feasibility of using luminescence as a non-invasive marker of response. However, as PAO1 luminescence was lower at 6hrs and lower still at 24hrs than that seen for PAO1 broths with a starting optical density of 1 in the linearity experiments, it remained possible that non-invasive monitoring *in vivo* might be useful. It was necessary to elucidate i) whether this reduction was due to phage-induced killing and ii) whether a signal could still be seen at lower optical densities, given that *in vivo* infection was likely to be with a much more reduced inoculum of PAO1.

In the second experiment in this section, PAO1 luminescence had declined after 24hrs but remained highest at higher optical densities. After 48hrs, there was further reduction in luminescence which was most marked in wells where optical density had initially been highest; at this time point, the most luminescence was from wells with the lowest starting optical density. This might be explained by the bacterial growth curve shown in Figure 11.3.1; when bacteria are grown under favourable laboratory conditions (batch culture), they have five distinct phases of growth (569-573):

- I. Lag phase
- II. Exponential phase
- III. Stationary phase
- IV. Death phase
- V. Long-term stationary phase

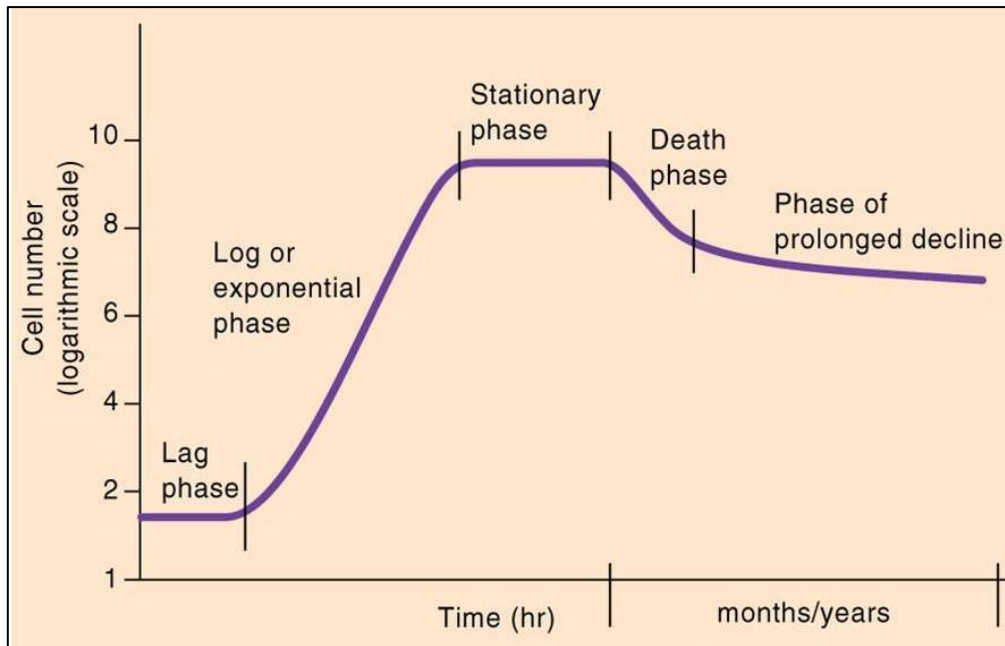


Figure 11.3.1: Bacterial growth curve. Slow initial growth, followed by rapid exponential growth, stationary phase, rapid death phase and then more prolonged phase of decline due to accumulation of toxins and depletion of nutrients.

Lag phase occurs as bacteria adjust to a growth medium, often with transient upregulation of genes involved in metabolism (569), which is followed by exponential growth. This occurs by binary fission that slows as nutrients become limited and bacteria enter a stationary phase of growth associated with metabolic and morphological changes (573). It has been shown that, independent of environmental conditions, bacteria grown in batch culture lose viability and go from the stationary phase to death phase, the mechanisms for which are not fully understood. However, as some bacteria in culture enter a long-term stationary phase, it is likely that depletion of nutrients and accumulation of toxins alone does not account for the death phase and that there are inherent mechanisms of pre-programmed bacterial apoptosis and quorum sensing that have evolved to ensure long-term survival of a species (570). Both these potential mechanisms may have contributed to the finding here that PAO1 at the highest initial optical densities (and luminescence) had lower luminescence after 48hrs; it is possible that these populations reached critical mass sooner and were therefore more likely to be metabolically inactive or dead.

Luminescence of PAO1 broths treated with each of the bacteriophage cocktails was higher at both 24hrs and 48hrs than luminescence of the untreated broths. This was unexpected because it was previously shown that significant phage-related killing occurred by the 24hr time point and, if luminescence truly is a proxy measure of bacterial density, as demonstrated by the initial linearity experiments, then it could reasonably have been expected to fall. A possible explanation for this anomaly is that the particular strain of PAO1 used in these experiments was labelled with a full complement of *lux* genes, imparting the ability for it to continually produce light whilst under the control of the constitutive promoter and negating the need for a luciferin as an exogenous substrate. Whilst this added to convenience of using this strain, an unwanted consequence may be that, following bacteriophage infection and osmotic lysis of the PAO1 cell wall prior to release of new phage particles, luciferase might also be released, thereby increasing measured luminescence despite fewer viable bacteria being present. There is no clear pattern of luminescence variation across the strains of phage cocktail and initial optical densities at the 24hr and 48hrs time points but it is likely that a combination of this mechanism and those relating to initial bacterial density and the previously described selective growth pressures in batch culture all played a role. These findings were replicated on a number of occasions and, as a consequence, it was concluded that this strain of luminescent PAO1 was not suitable to take forward for non-invasive *in vivo* monitoring, although, as it was sensitive to bacteriophage cocktails at all dilutions, it could be used for more conventional monitoring of response in a murine model.

As a consequence of the shortcomings of luminescent PAO1 *in vitro*, the fluorescent strain of PAO1 was investigated as a potential alternative for non-invasive monitoring. Absorbance readings for iRFP PAO1 in phage-treated wells rose more slowly than in untreated wells, but had a greater peak when starting optical densities were 0.05, 0.1 or 0.25 (but not 0.5 or 1), whilst fluorescence was consistently lower in phage-treated wells throughout the course of the experiment. Absorbance measurements using automated plate readers are at least as accurate as traditional methods of

spectrophotometry using cuvettes but may not increase linearly with increasing cell density (574), it is not possible to differentiate between viable and dead cells and the technique is only accurate when cell density is between $10^8 - 10^{10}$ CFU/ml (575). For these reasons the absorbance curves obtained are likely to be an inaccurate readout of true bacterial density. However, the curves for iRFP PAO1, with and without phage added, and for wild-type PAO1 are similar to the typical bacterial growth curve shown in Figure 11.3.1 and the slower rise in the phage-treated wells could be indicating inhibition of growth. This is seen more clearly in wells containing wild-type PAO1 treated with phage which have a very prolonged delay in increasing absorbance and therefore do not have a shape akin to the usual bacterial growth curve. The difference in the absorbance curves between wild-type PAO1 and iRFP PAO1 suggest that the transformation of PAO1 with the chromophore might alter bacterial growth properties and phage susceptibility, an important point to consider if using this organism as evidence of clinical applicability in human subjects.

The fluorescence curves obtained are understandably identical (showing minimal fluorescence) for both phage-treated and untreated wild-type PAO1. Fluorescence is consistently lower over the 48hr experimental period in wells containing iRFP that were treated with phage compared with control wells, regardless of the starting optical density of the broths. However, fluorescence does not appear to be a linear readout of bacterial density; peak fluorescence of PAO1 iRFP with a starting optical density of 0.05 is 17796 arbitrary units and is still increasing at the end of the experiment whilst peak fluorescence of PAO1 iRFP with a starting optical density of 1 was only 11796 after 15hrs and started to decline thereafter. Absorbance at these times was 0.073 for the broth with a starting optical density of 0.05 and 0.295 for the broth with a starting optical density of 1. At time zero for the broth with a starting optical density of 1, absorbance was 0.087, similar to that of the 0.05 broth at 48hrs, yet the fluorescence was only 6765 compared to 17796 arbitrary units. Hence, although the curves consistently demonstrate lower fluorescence in iRFP PAO1 wells that were treated with phage, the relationship between bacterial density and fluorescence appears far more complex and fluorescence alone would not allow any quantitative inference of bacterial load in a murine model of

infection. A further concern is that, although the iRFP integrated into the PAO1 genome is only expressed in metabolically active cells, there is a lag time between cells becoming inactive and the fluorescence dropping off. A reduction in iRFP should correlate with bacterial cells entering the stationary phase; however, this is only seen in untreated iRFP broths with a starting optical density of 1, where absorbance clearly correlates with fluorescence, everywhere else the fluorescence continues to increase despite the absorbance curves appearing to demonstrate cessation of logarithmic growth.

Despite these concerns, as there was clearly a reduction in fluorescence signal when iRFP was treated with phage, a preliminary *in vivo* experiment was attempted, with the same methodology as described in Section 12.2.2. 50µl of iRFP PAO1 at an optical density of 2 (incompatible with life based on dose-finding experiments in Section 12 but deliberately high in order to give the best chance of seeing a signal) was nasally instilled into two BALB/c mice under isoflurane anaesthesia; one mouse was treated simultaneously with 20µl bacteriophage cocktail 1 and the other with 20µl SM buffer. Pictures were taken using the LivingImage system 30 minutes and 60 minutes after the infection; no signal was seen at either time point. The experiment was not repeated due to i) concerns about animal welfare (high infectious dose and repeated inhalational anaesthesia) and ii) fluorescence alone being unlikely to provide sufficient information with regards to the safety and efficacy of phage treatment. A proof-of-concept experiment, conducted by Caroline Mullineaux-Sanders at Imperial College London, demonstrated that it is possible to visualise iRFP PAO1 in BALB/c mice using the LivingImage system. In this experiment, inoculum far in excess (6×10^9 CFU) of what was lethal in nasal infection dose-finding experiments (2×10^7 CFU, Section 12.2.2) was injected directly into lung tissue of already dead mice and, even then, only a small focus of fluorescence was visible. For these reasons, it was felt that monitoring of phage response using iRFP PAO1 was unlikely to be fruitful; attempts to establish surrogate readouts of efficacy were abandoned at this point and ongoing work focused on analysis of samples obtained by more conventional, invasive techniques.

Chapter 12: *In vivo* Efficacy of Phage Cocktail

12.1.1: Ethics Statement

All *in vivo* work was carried out in accordance with the Animals (Scientific Procedures) Act of 1986 following my completion of Modules 1-4 of the Imperial College/Central Biomedical Sciences Pre-Licence training course and the subsequent issue of a Personal Licence. Animals were housed in a specialist facility in accordance with European regulations. Food and drink were provided *ad libitum* and the work was prospectively approved by the United Kingdom Home Office.

12.2: Materials and Methods

12.2.1: Preparation of Pa for Murine Infection

For all *in vivo* work, PAO1 and the selected clinical strain of Pa (see Chapter 10) were inoculated into 10mls TSB as previously described and cultured overnight at 37°C with agitation. Broths were then centrifuged (ALC, Italy) at 2000g at 4°C for ten minutes and the resultant cell pellet resuspended in 10mls of phosphate buffered saline (PBS: Gibco, UK). Optical density of broths was measured by spectrophotometry and adjusted by dilution with sterile PBS. Serial dilution and plating of a broth with a starting optical density of 1 onto PSA confirmed that this was equivalent to approximately 1×10^9 CFU/ml.

Varying doses of inoculum were used for different *in vivo* experiments. All were prepared using optical density as a proxy measure of bacterial density with sterile PBS used for dilution. Spectrophotometry at OD₆₂₀ was used throughout.

12.2.2: Dose-Finding Methodology

Female adult BALB/c (Harlan, UK) mice were used for *in vivo* work. These were initially selected because they are an albino strain and therefore more suitable for non-invasive monitoring with optical imaging. In the dose-finding study, mice (n=3 /group) were anaesthetised by isoflurane inhalation and infected by nasal gavage (sniffing) of 50µl of either PAO1 or the clinical strain at ODs

of 1, 0.5, 0.1 and 0.05 (equivalent to 1×10^9 , 5×10^8 , 1×10^8 and 5×10^7 CFU/ml). After 24hrs, mice infected with the three highest inoculums of PAO1 were either deceased or very unwell and mice infected with anything greater than 5×10^7 CFU/ml of the clinical strain were deceased or showing signs of severe infection such as hunching, irregular respiration and paucity of movement. A maximum inoculum of 5×10^7 CFU/ml (OD 0.05) was thus selected for initial experimental use.

12.2.3: Murine Infection Protocol

Mice were infected by pipetting 50 μ l of PAO1 or the clinical strain intranasally following induction of anaesthesia by isoflurane inhalation. 20 μ l (12.4×10^8 PFU/ml = 1.24×10^9 PFU in 20 μ l) of phage cocktail or SM buffer (controls) was administered, the timing of which varied according to the experiment protocol. A number of different conditions were investigated:

- I. Infection with 5×10^7 CFU/ml (2.5×10^6 CFU) PAO1 or the clinical strain followed immediately by administration of 20 μ l of phage cocktail 1 or SM buffer. Bronchoalveolar lavage (BAL) performed after 48hrs.
- II. Infection with 1×10^8 CFU/ml (5×10^6 CFU) PAO1 followed immediately by administration of 20 μ l of phage cocktail 1 or SM buffer. BAL performed after 48hrs.
- III. Infection with 5×10^8 CFU/ml (2.5×10^7 CFU) PAO1 followed immediately by administration of 20 μ l of phage cocktail 1 or SM buffer. BAL performed after 24hrs.
- IV. Infection with 5×10^8 CFU/ml (2.5×10^7 CFU) PAO1 followed by administration 24hrs later of 20 μ l of phage cocktail 1 or SM buffer, under second isoflurane anaesthesia. BAL performed 24hrs after second anaesthetic.
- V. Administration of 20 μ l of phage cocktail 1 or SMB buffer followed by infection 48hrs later with 5×10^8 CFU/ml (2.5×10^7 CFU) PAO1, under second isoflurane anaesthesia. BAL performed 24hrs after second anaesthetic.
- VI. Administration of 20 μ l of phage cocktail (1, 2 or 3) or SM buffer. BAL performed after 48hrs.

Conditions I-III were not representative of the clinical situation as bacteriophage was administered at the time of Pa infection; however this strategy was used initially because I felt that it was most likely to yield a signal. Initiation of treatment post-infection, as in condition IV, is the probable scenario in a medical setting. Condition V, where phage was administered prophylactically, is a strategy that might also be useful clinically if i) phage persistence can be demonstrated without a Pa host being present and ii) phage itself does not cause an inflammatory response in the lung, which was assessed by condition VI.

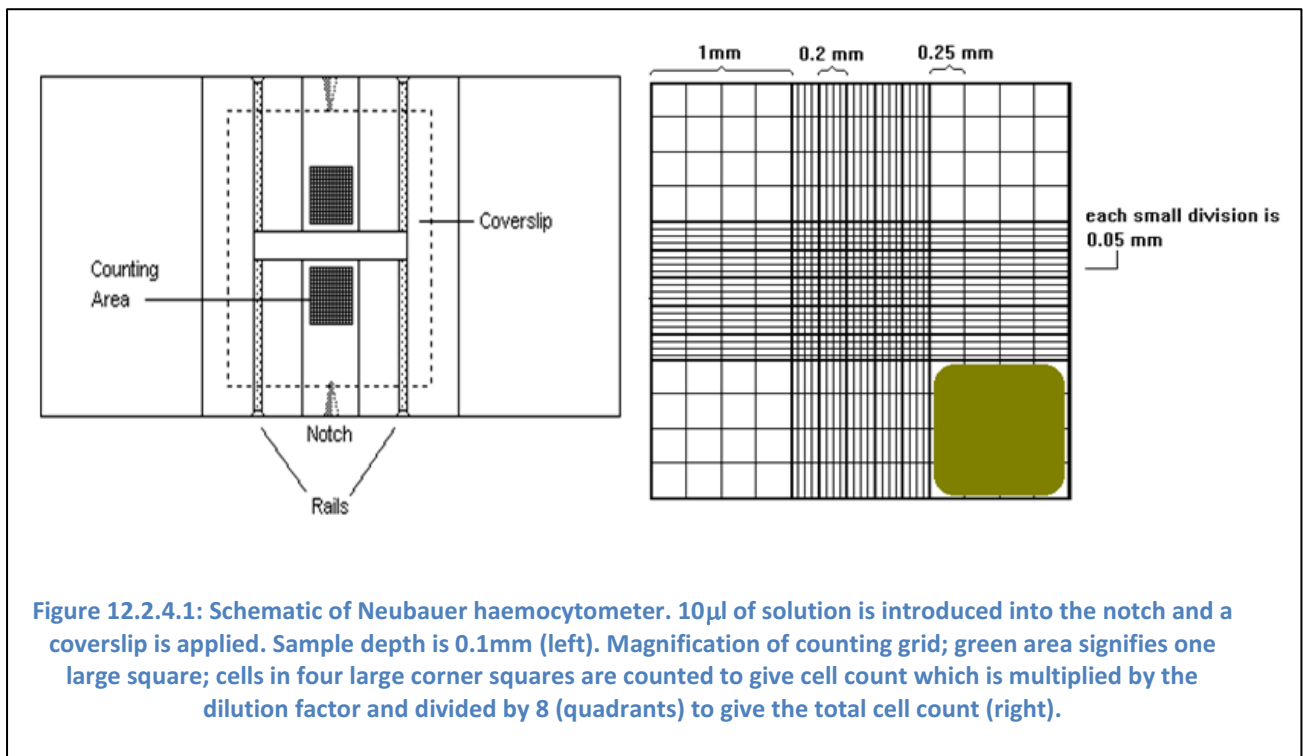
All conditions were assessed by analysis of BALF and non-quantitative splenic culture (a proxy measure of systemic spread of infection). BALF was obtained following induction of terminal general anaesthesia by administration of Hypnorm (Vetapharma, UK) and Hypnovel (Roche, UK) that had been mixed in a 1:1:2 ratio with water for injections and has been demonstrated to provide good surgical anaesthesia with a single injection (576). 400µl was administered intraperitoneally with a 25g Microlance™ needle (BD, Ireland) and 1ml Plastipak™ syringe (BD, Spain). When anaesthesia was achieved, midline abdominal incision was made and exsanguination induced by cutting the ascending aorta. Following cessation of circulation, the trachea was surgically exposed by blunt dissection and cannulated with 22g Abbocath™ (Hospira, UK). Bronchoalveolar lavage was performed with sequential instillation and aspiration of 500µl PBS (three cycles) from a 1ml syringe. BALF was collected into 1.5ml Eppendorf Tubes™ (Eppendorf, UK) and spleens were harvested into Eppendorf Tubes™ containing 500µl sterile PBS. All samples were transported on ice for processing.

12.2.4: Processing of Samples

100µl of BALF was serially Log₁₀ diluted and 5 x 10µl drops cultured overnight at 37°C on PSA plates as per Miles and Misra (566) prior to colony counting. Non-quantitative culture of homogenised explanted spleens was also performed by pipetting of 5 x 10µl droplets onto PSA.

The remaining BALF was centrifuged at 4°C for ten minutes at 2000g. 100µl aliquots of supernatant were removed using a pipette and stored at -80°C for later batched analysis of soluble inflammatory markers using a multiplex ELISA platform (MesoScale Discovery, United States). The remaining cell pellet was resuspended by adding 200µl PBS and put on a vortex mixer (Stuart™, UK) at 1000rpm. 20µl of this was then added to 40µl trypan blue (Sigma, UK) and 20µl PBS (1 in 4 dilution); inflammatory cells were quantified from 20µl of this suspension visualised under a light microscope (Leitz Labrolux, Germany) on a Neubauer haemocytometer. If more than 100 cells per field were visible, dilution of the suspension was increased until ≤ 100 cells/field were visible. Both viable (white) and dead cells (stained blue due to integrity of cell wall being compromised) were counted in each of the four large corners (Figure 12.2.4.1); cells touching only the upper and left edges of smaller squares were counted in order to prevent counting the same cell twice. The number of cells per ml was calculated using the following formula:

$$\text{Total Cells} \times 10^4/\text{ml} = (\text{Live Cells} + \text{Dead Cells}) \times \text{dilution factor}/8 \text{ (quadrants on haemocytometer)}$$



Differential cell count was performed following cytopsin (Shandon, UK) at 400rpm for five minutes on a further 100µl of the resuspended cell pellet. After air-drying for ten minutes, slides were fixed in methanol for five minutes before being allowed to dry. Staining was done with May-Grunwald-Giesma Quickstain (Sigma, UK); reagents were added to Coplin jars and slides dipped 5 times into reagent A, 20 times into reagent B, 5 times into reagent C and then into water to remove excess stain. Slides were dried overnight before coverslips were mounted using one drop of DPX (Sigma, UK) in a fume cupboard. After drying, slides were blinded by Dr. Michael Waller, Clinical Research Fellow, Imperial College London, before I counted 300 cells per slide using light microscopy; the proportion of neutrophils, eosinophils and lymphocytes was measured and absolute numbers calculated following unblinding of slides (using the total cell count done previously).

12.2.5: Cytokine Analysis

Batched supernatant samples were analysed for soluble inflammatory markers using a multiplex ELISA as previously discussed. The assay uses capture antibodies in 96-well plates to simultaneously detect multiple cytokines, namely interleukin (IL) 1b, IL-12p70, IL-6, IL-10, interferon gamma (IFN- γ), tumour necrosis factor alpha (TNF- α) and KC (keratinocyte chemoattractant), the murine analogue of IL-8 (577). These cytokines were part of a standard "Mouse Pro-inflammatory 7-Plex Ultra-Sensitive Kit" (Product Number K15012C-1) available from MesoScale Discovery. This was selected as all seven cytokines have key roles in inflammation and infection and preformed kits were more cost-effective than custom-made plates. I was keen to also measure macrophage inflammatory protein-2 (MIP-2), a cytokine that promotes neutrophil chemotaxis and degranulation. The additional expense of adding this could not be justified as KC is also a neutrophil chemoattractant that binds to the same CXCR2 chemokine receptor as MIP-2 and thus has a very similar function (578). Further information about the measured cytokines is given in the product insert (see Appendix A3).

100µl aliquots of frozen supernatant were thawed and 45µl added to 5µl of bovine serum albumin (BSA) which acts as a carrier protein to prevent loss of analyte to the labware. 25µl of this mixture

was required for analysis which was performed as per the manufacturer's protocol. Standard calibration curves (in duplicate for each plate) were prepared, also as per the standard operating procedure, full details of which are given in the MesoScale product guidelines that have been reproduced in Appendix A3.

12.2.6: Statistical Analysis

Based on modest group sizes and assuming non-Gaussian data distribution, Mann-Whitney t-test was performed where treated and control groups were being compared. Kruskal-Wallis test with Dunn's multiple comparisons test was used if more than two groups were being compared. If correlations were calculated, Spearman rank (non-parametric) was used. All statistical analyses were performed using Prism 6.0 (GraphPad, USA) or Excel 2010 (Microsoft, USA).

12.3: Results

12.3.1: Simultaneous Administration of Bacteriophage and Pa

Mice were infected with 2.5×10^6 bacteria of either PAO1 (n=16) or the clinical strain of Pa (n=12) and treated under the same anaesthetic with either phage cocktail 1 (n=14) or SM buffer (n=14). BALF culture demonstrated that all phage-treated mice and most control mice cleared Pa; 2/6 control mice infected with the clinical strain had persistent infection but with low bacterial load (20 and 40 CFU/ml) on quantitative culture. There was no statistically significant difference in colony counts between phage-treated and control animals at this low inoculum of either PAO1 or the clinical strain and no evidence of systemic spread, as indicated by positive splenic cultures, was seen.

Although there was no difference in bacterial load after 48hrs, inflammation assessed by total and differential cell counts was significantly reduced in phage-treated animals compared with controls. Total inflammatory cells were lower with both PAO1 and the clinical strain when phage had been administered, with a significant reduction in neutrophils with both strains and fewer macrophages being observed with the clinical strain. This is shown in Table 12.3.1.1 and Figures 12.3.1.1 and 12.3.1.2. An example of BALF fluid as seen under the light microscope is shown in Figure 12.3.1.3.

		n	Total Cells (x10 ⁴ /ml)	p	Neutrophils (x10 ⁴ /ml)	P	Macrophages (x10 ⁴ /ml)	p	Lymphocytes (x10 ⁴ /ml)	p
PAO1	Controls	8	288.8 [275.5 – 337.5]	<0.01	229 [190.1 – 285.9]	<0.01	76.6 [36.3 – 86.3]	0.32	5.624 [4.9 – 9.8]	0.78
	Phage-treated	8	205.5 [134.5 – 288.5]		138.2 [91.86 – 230.8]		56.05 [37.3 – 76.2]		6.3 [1.9 – 10.5]	
Clinical Strain	Controls	6	228 [173.3 – 346.5]	<0.01	174 [112.1 – 266.8]	<0.01	62.97 [39.0 – 71.2]	<0.05	6.8 [1.4 – 19.2]	0.57
	Phage-treated	6	112.4 [71 – 146.5]		73.17 [35.15 – 102.1]		37.9 [22.8 – 56.9]		4.1 [2.1 – 9.3]	

Table 12.3.1.1: Inflammatory cells and differential (median [range]) in BALF at 48hrs from mice infected with 2.5 x 10⁶ PAO1 or a clinical strain of Pa and simultaneously administered either bacteriophage or SM buffer (controls). A significant reduction in total cells and was seen with both bacterial strains where bacteriophage was given.

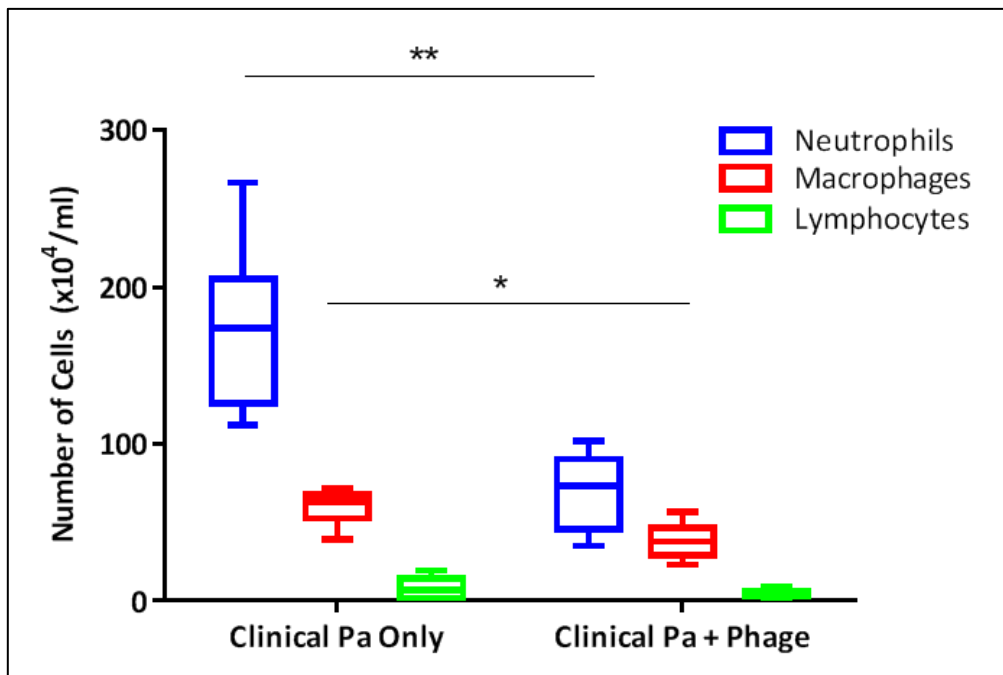


Figure 12.3.1.1: Differential cell counts (median/range) from BAL performed at 48hrs in mice inoculated with 2.5x10⁶ of a clinical strain of Pa and simultaneously treated with 20µl phage cocktail 1 (1.24 x 10⁹ PFU) or SM buffer. Note significant reduction in neutrophils (p < 0.01) and macrophages (p < 0.05).

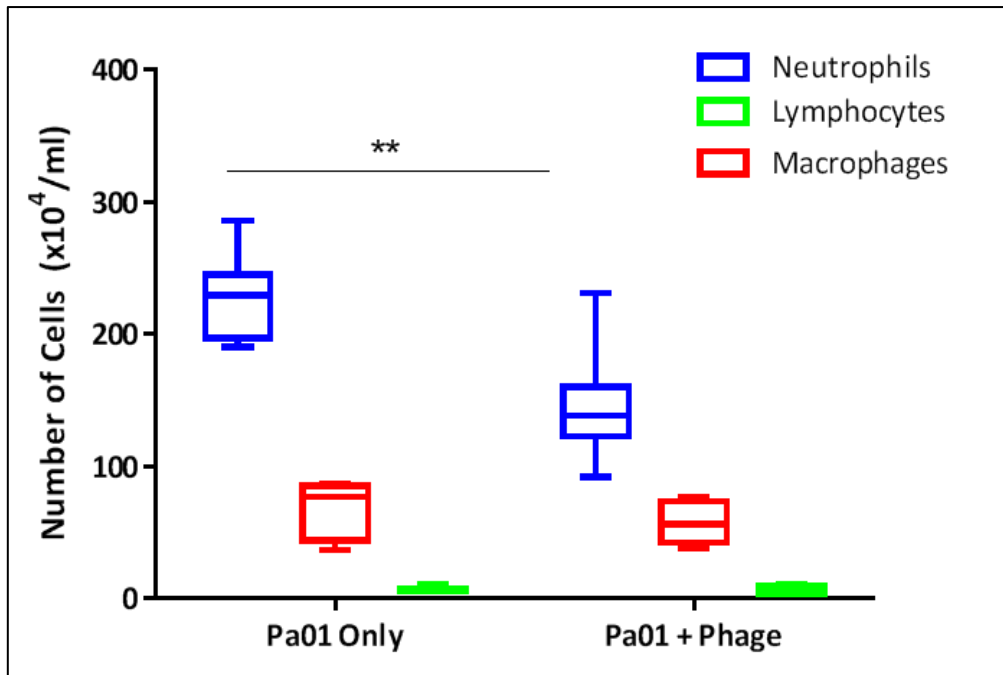


Figure 12.3.1.2: Differential cell counts (median/range) from BAL performed at 48hrs in mice inoculated with 2.5×10^6 of PAO1 and simultaneously treated with $20 \mu\text{l}$ phage cocktail 1 (1.24×10^9 PFU) or SM buffer. Note significant reduction in neutrophils ($p < 0.01$).

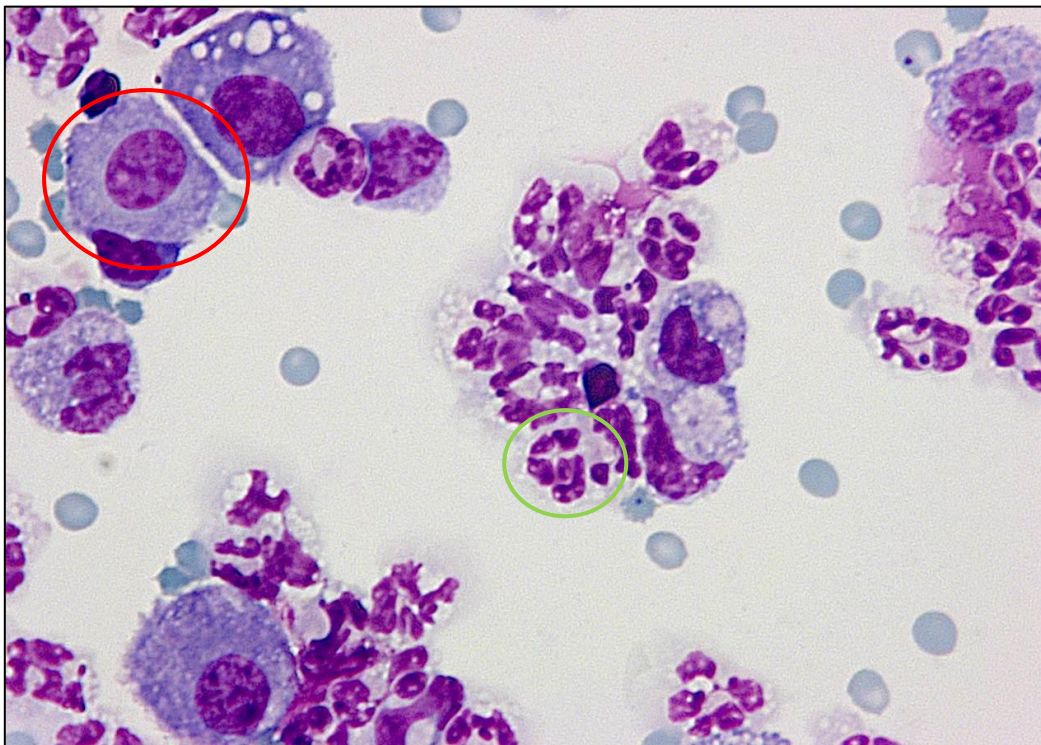


Figure 12.3.1.3: Example of mouse BALF under 40x light magnification. Macrophages with single large nucleus (circled in red) are predominant in uninfected BALF (see later experiments with phage or SM buffer alone) whilst smaller neutrophils with multi-lobular nucleus (circled in green) are the principle cell in BALF of mice infected with Pa.

Differences in inflammatory cell count persisted when the inoculum of PAO1 was increased to 5×10^6 CFU (condition II) but there remained no difference in bacterial load, with all phage treated and control mice (n=9 in each group) still able to clear the larger infectious dose after 48hrs. This is shown in Table 12.3.1.2 and Figure 12.3.1.4.

		n	Total Cells (x10 ⁴ /ml)	p	Neutrophils (x10 ⁴ /ml)	P	Macrophages (x10 ⁴ /ml)	p	Lymphocytes (x10 ⁴ /ml)	p
PAO1	Controls	9	243.0 [214.0-382.0]	<0.01	206.0 [160.1 – 331.6]	<0.01	54.8 [16.1 – 101.0]	0.05	11.5 [0.0 – 25.7]	0.94
	Phage-treated	9	151.0 [139.0 – 265.0]		122.1 [105.4 – 187.4]		31.6 [18.2 – 56.5]		8.5 [1.5 – 27.5]	

Table 12.3.1.2: Inflammatory cells and differential in BALF at 48hrs from mice infected with 5×10^6 PAO1 and simultaneously administered either bacteriophage or SM buffer (controls). A significant reduction in total cells was seen where bacteriophage was given although no difference in bacterial load was demonstrated.

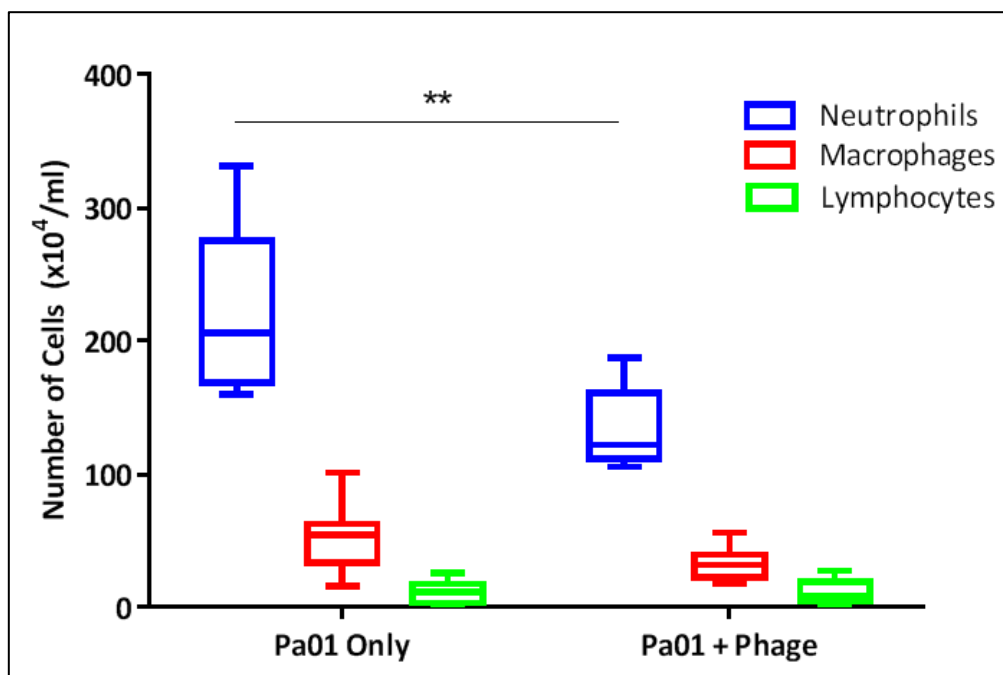


Figure 12.3.1.4: Differential cell counts (median/range) from BAL performed at 48hrs in mice inoculated with 5×10^6 of PAO1 and simultaneously treated with 20 μ l phage cocktail 1 (1.24×10^9 PFU) or SM buffer. Note significant reduction in neutrophils (p <0.01).

Levels of inflammatory cytokines were also lower in BALF supernatant. At the inoculum of 2.5×10^6 CFU this was only seen with the clinical strain and not with PAO1; this was thought to be attributable to differences in virulence, suggested by mice being less tolerant of higher inoculums of the clinical

strain in the initial dose finding study. However, when the infectious dose of PAO1 was increased to 5×10^6 CFU (condition II, results above), there was still no difference in cytokine levels (or bacterial load) despite the differential cell count being significantly different. Table 12.3.1.3 shows cytokine levels (median/range) for both strains at the initial 2.5×10^6 infectious dose and Figure 12.3.1.5 depicts the five cytokines that were significantly different between treated and control mice infected with the clinical strain. Table 12.3.1.4 shows cytokine levels in mice infected with 5×10^6 PAO1; higher doses of the clinical strain were not used in ongoing work as mice were either dead or extremely unwell within 24hrs of infection and had to be sacrificed for ethical reasons.

		n	IL-1 β	p	IL-6	p	IL-10	p	IL12-p70	p
PAO1	Controls	8	117.6 [83.7 – 181.5]	0.16	4136 [1078 – 8526]	0.08	23.1 [8.0 – 47.5]	0.49	146.4 [68.8 – 285]	0.49
	Phage-treated	8	151 [111.7 – 206.3]		1847 [527.6 – 2857]		17.4 [4.1 – 56.1]		173.8 [77.1 – 303.3]	
Clinical Strain	Controls	6	110.2 [92.2 – 161.1]	0.14	2451 [658 – 2989]	0.03	13.2 [4.9 – 40.9]	0.04	184.5 [121.7 – 257.7]	0.01
	Phage-treated	6	90.3 [39.5 – 130.7]		671.9 [247.5 – 1256]		5.2 [1.5 – 8.7]		90.9 [57.8 – 149.5]	

		n	TNF- α	p	IFN- γ	p	KC	p
PAO1	Controls	8	267.8 [107.6 – 902]	0.93	179.4 [75.1 – 236.8]	0.70	638.5 [254.9 – 1107]	0.43
	Phage-treated	8	337.9 [144.4 – 642]		173.3 [113.7 – 346.2]		741.9 [336.5 – 1385]	
Clinical Strain	Controls	6	303.6 [186.5 – 561.8]	0.03	147.0 [52.6 – 243.2]	0.87	590.2 [378.8 – 1272]	0.04
	Phage-treated	6	142.6 [82.7 – 247.2]		159.6 [73.0 – 311.3]		378.4 [261.1 – 469.1]	

Table 12.3.1.3: Levels of pro-inflammatory cytokines (median [range] in picograms (pg)/ml) in BALF at 48hrs from mice infected with 2.5×10^6 PAO1 or a clinical strain of Pa and simultaneously administered either bacteriophage or SM buffer (controls). A significant reduction in 5/7 measured cytokines is demonstrated in mice infected with the clinical strain, but no differences are seen in mice infected with PAO1 at this dose.

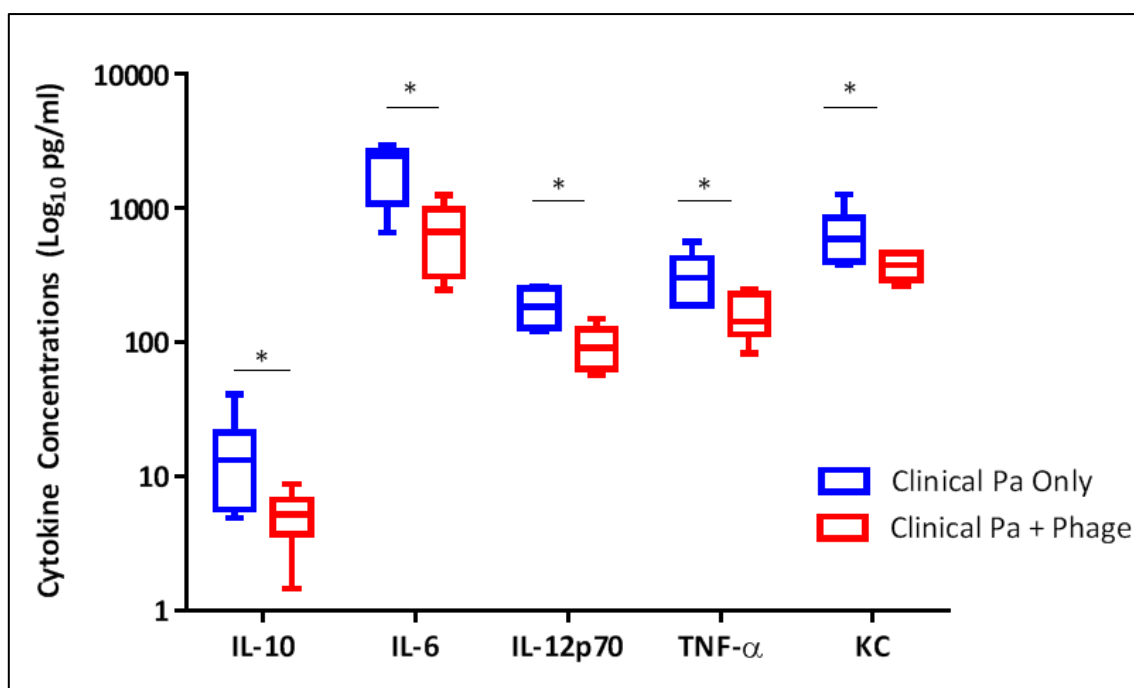


Figure 12.3.1.5: Pro-inflammatory cytokines (median/range) from BAL performed at 48hrs in mice inoculated with 2.5×10^6 of a clinical strain of Pa and simultaneously treated with $20 \mu\text{l}$ bacteriophage cocktail (containing 1.24×10^9 PFU) or SM buffer.

Cytokine	Controls (n=6)	Phage-Treated (n=6)	p
IL-1 β	153.3 [36.9 – 225.2]	195.2 [89.6 – 331.4]	0.33
IL-6	10913 [1065 – 20217]	6429 [1904 – 21720]	0.36
IL-10	62.9 [12.0 – 79.6]	37.4 [10.5 – 73.0]	0.19
IL-12p70	391.7 [125.0 – 568.8]	238.5 [154.2 – 553.4]	0.24
TNF- α	1343 [208.1 – 3610]	776.5 [278.5 – 3150]	0.19
IFN- γ	105.0 [21.2 – 204.3]	109.4 [47.1 – 363.4]	0.37
KC	1370 [221.1 – 2403]	887.4 [376 – 1806]	0.15

Table 12.3.1.4: Levels of pro-inflammatory cytokines (median [range] in pg/ml) in BALF at 48hrs from mice infected with 5×10^6 PAO1 and simultaneously administered either bacteriophage or SM buffer (controls).

As all mice were able to clear Pa infection regardless of whether they had been treated with the bacteriophage cocktail, condition III was implemented, whereby the inoculum of PAO1 was increased tenfold (to 2.5×10^7 CFU) and BAL carried out after 24hrs rather than 48hrs. The rationale behind this was threefold: i) increased inoculum would stress the murine immune system and be inherently more difficult for mice to clear naturally, ii) by performing BAL at 24hrs sicker mice could also be studied rather than needing to be sacrificed for ethical reasons and iii) TEM undertaken previously demonstrated that bacteriophage begin infecting Pa within hours, so any difference in bacterial load might reasonably be expected to be apparent early on, rather than necessarily 48hrs

post-treatment. Under these conditions, a signal for bacterial killing was detected; all control mice (n=6) had detectable Pa infection (median [range] 1305 [190-4700 CFU/ml) and no bacteria were cultured from any mice treated with bacteriophage (n=6), p <0.01. This is shown in Figure 12.3.1.6. There was no growth from splenic cultures of treated or control mice. Unlike the previous experiments, no difference in inflammatory cell counts was demonstrated, as shown in Table 12.3.1.5 and Figure 12.3.1.7 but two cytokines (IL-10 and IL-1b) were significantly different between the groups, shown in Figure 12.3.1.8. All cytokine measurements under this condition are summarised in Table 12.3.1.6.

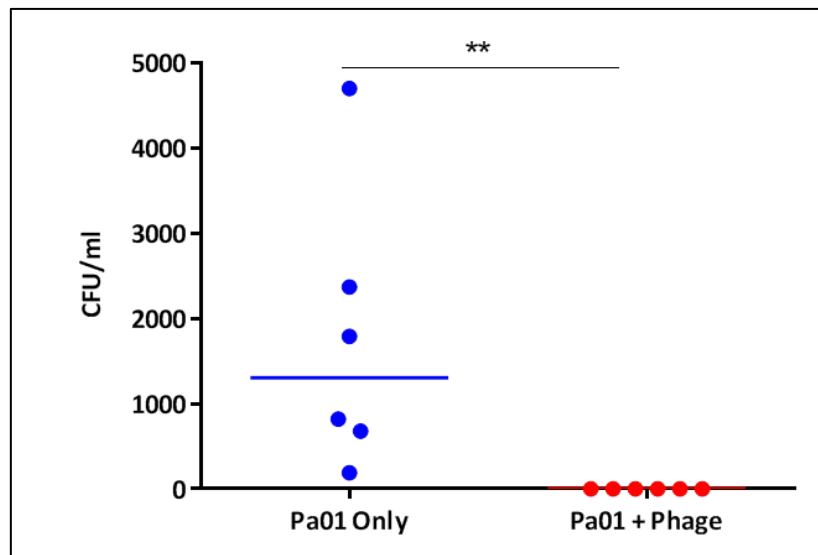


Figure 12.3.1.6: Colony counts/ml from BAL performed at 24hrs in mice inoculated with 2.5×10^7 of PAO1 and simultaneously treated with $20 \mu\text{l}$ bacteriophage cocktail (containing 1.24×10^9 PFU) or SM buffer.

		n	Total Cells ($\times 10^4/\text{ml}$)	p	Neutrophils ($\times 10^4/\text{ml}$)	p	Macrophages ($\times 10^4/\text{ml}$)	p	Lymphocytes ($\times 10^4/\text{ml}$)	P
PAO1	Controls	6	166 [129.5 – 345]	0.40	151.2 [121.2 – 317.4]	0.47	9.30 [6.00 – 23.52]	0.78	1.75 [0.0 – 6.90]	0.67
	Phage-treated	6	162.5 [129.5 – 191.5]		145.8 [114.9 – 164.4]		12.64 [2.72 – 16.30]		2.02 [0.56 – 4.08]	

Table 12.3.1.5: Inflammatory cells and differential in BALF at 24hrs from mice infected with 2.5×10^7 PAO1 and simultaneously administered either bacteriophage or SM buffer (controls). No differences in inflammatory cell count are observed.

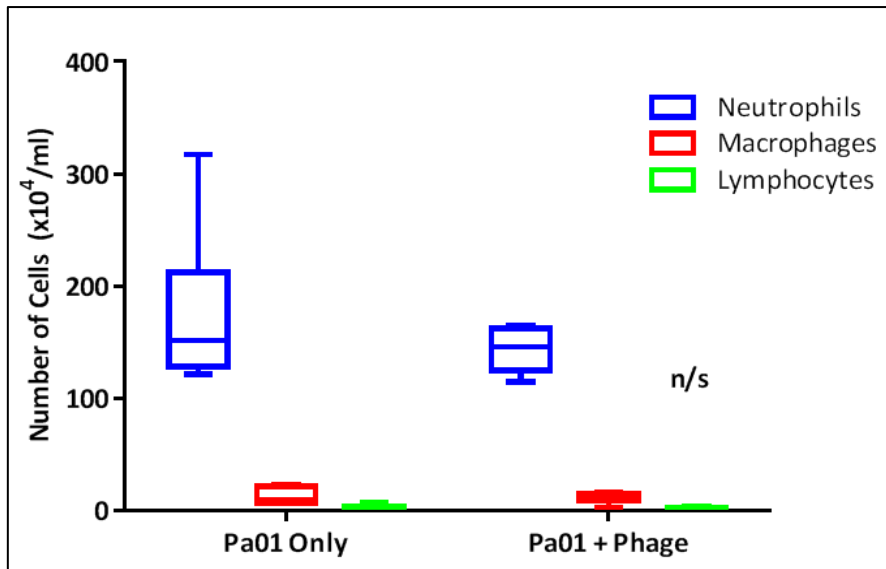


Figure 12.3.1.7: Differential cell counts (median/range) from BAL performed at 24hrs in mice inoculated with 2.5×10^7 of PAO1 and simultaneously treated with $20 \mu\text{l}$ phage cocktail 1 (1.24×10^9 PFU) or SM buffer.

Cytokine	Controls (n=6)	Phage-Treated (n=6)	p
IL-1 β	431 [313.3 – 536.3]	266.8 [194.9 – 364.6]	0.02
IL-6	9824 [6151 – 45226]	5755 [4116 – 13282]	0.06
IL-10	150.7 [114.5 – 321.7]	81.4 [40.0 – 113.6]	<0.01
IL-12p70	270.4 [169.7 – 374.7]	288.7 [118.4 – 321.8]	0.68
TNF- α	9822 [8643 – 10020]	9444 [6268 – 9791]	0.31
IFN- γ	142.5 [28.9 – 263.4]	212.3 [69.3 – 579.7]	0.39
KC	4109 [2116 – 5230]	4370 [3728 – 5155]	0.39

Table 12.3.1.6: Levels of pro-inflammatory cytokines (median [range] in pg/ml) in BALF at 24hrs from mice infected with 2.5×10^7 PAO1 and simultaneously administered either bacteriophage or SM buffer (controls). A significant reduction is seen in two cytokines and a strong trend toward reduction in IL-6 is shown.

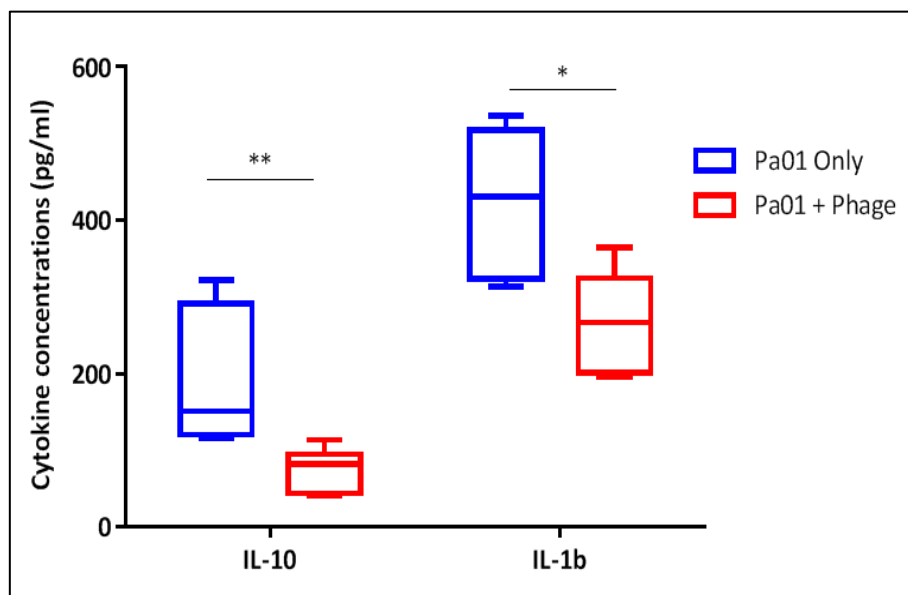


Figure 12.3.1.8: Significant difference in two pro-inflammatory cytokines (median/range) from BAL performed at 24hrs in mice inoculated with 2.5×10^7 of PAO1 and simultaneously treated with $20 \mu\text{l}$ phage cocktail 1 (1.24×10^9 PFU) or SM buffer.

12.3.2: Delayed Administration of Bacteriophage (Post Pa-Infection)

A signal for improved bacterial killing and reduced inflammatory response following treatment with anti-Pa bacteriophage was demonstrated in results section 12.3.1. However, as simultaneous administration of therapy does not mimic the clinical situation, condition IV set out to investigate the potential of bacteriophage treatment being administered after infection. Mice were intranasally infected with 2.5×10^7 CFU of PAO1 and treated with intranasal phage cocktail or SM buffer 24hrs post-infection, with BAL performed a further 24hrs later. This higher inoculum of PAO1 again produced a significant signal in regards to bacterial killing; all control mice (n=8) had positive BAL cultures (median [range] 5950 [40-194000] CFU/ml) whilst only one mouse in the treatment arm (n=7, due to technical difficulties with one BAL) had bacteria isolated from BALF (median [range] 0 [0-160] CFU/ml, $p < 0.01$). This is shown in Figure 12.3.2.1. There was growth of Pa from non-quantitative splenic culture in 25% (2/8) of the control mice, indicating systemic spread, but no growth from the spleens of any of the phage-treated mice. There was a reduction in IL-10 ($p < 0.05$) and KC ($p < 0.01$) but no differences in any of the other tested cytokines or inflammatory cell counts. This is shown in Table 12.3.2.1, Figure 12.3.2.2 and Table 12.3.2.2 and Figure 12.3.2.3.

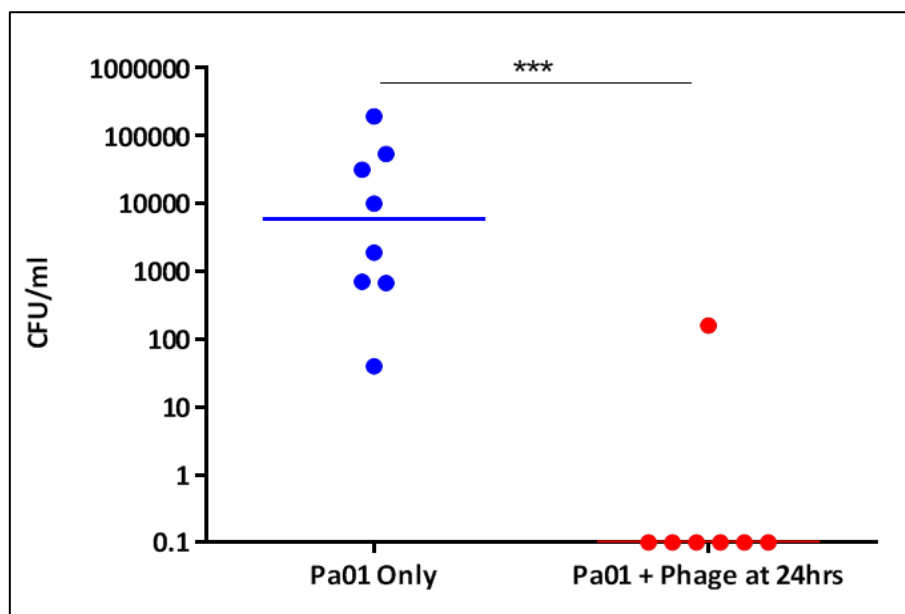


Figure 12.3.2.1: Colony counts/ml from BAL performed at 48hrs in mice inoculated with 2.5×10^7 of PAO1 and treated with $20 \mu\text{l}$ bacteriophage cocktail (containing 1.24×10^9 PFU) or SM buffer 24hrs post-infection.

		n	Total Cells (x10 ⁴ /ml)	p	Neutrophils (x10 ⁴ /ml)	p	Macrophages (x10 ⁴ /ml)	p	Lymphocytes (x10 ⁴ /ml)	P
PAO1	Controls	8	297.5 [230.5 – 447]	0.84	253.0 [202.8 – 390.4]	0.84	46.49 [20.24 – 57.48]	0.39	5.34 [1.85 – 7.50]	0.64
	Phage-treated	7	310.5 [224.0 – 391.0]		240.4 [185.9 – 337.6]		48.67 [33.68 – 67.28]		4.59 [0.78 – 8.76]	

Table 12.3.2.1: Inflammatory cells and differential in BALF at 48hrs from mice infected with 2.5x10⁷ PAO1 and administered either bacteriophage or SM buffer (controls) 24hrs post-infection. No differences in inflammatory cell count are observed.

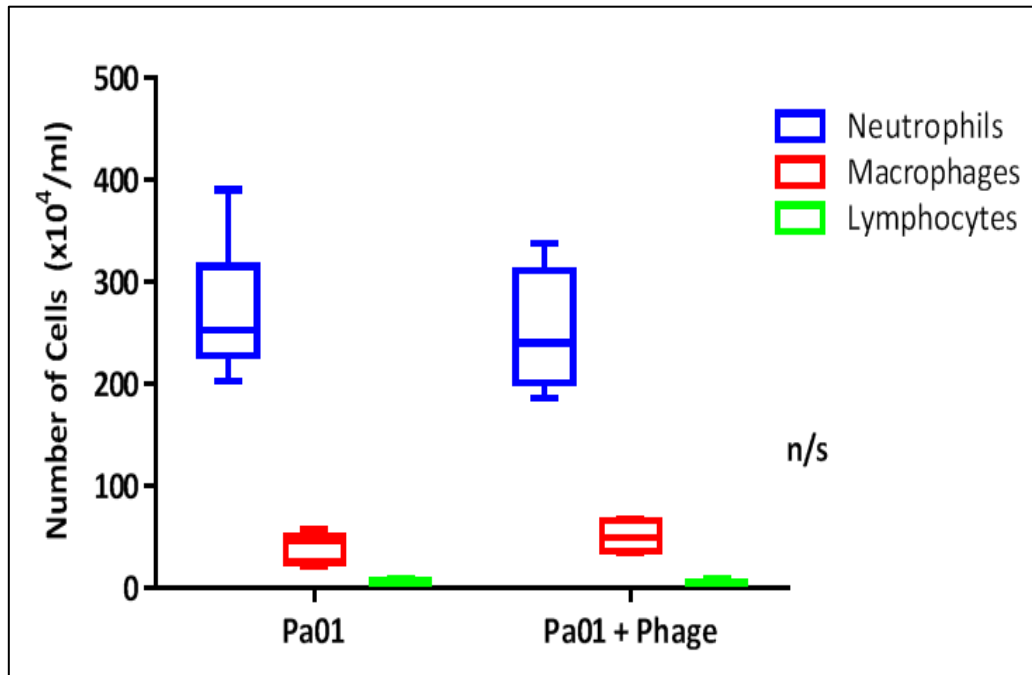


Figure 12.3.2.2: Differential cell counts (median/range) from BAL performed at 48hrs in mice inoculated with 2.5x10⁷ of PAO1 and treated with 20µl phage cocktail 1 (1.24 x 10⁹ PFU) or SM buffer 24hrs post-infection.

Cytokine	Controls (n=8)	Phage-Treated (n=7)	p
IL-1β	409.4 [165.2 – 631.0]	333.5 [60.0 – 387.5]	0.67
IL-6	18393 [4198 – 40792]	6590 [1147 – 10620]	0.28
IL-10	237.4 [132.7 – 290.0]	150.5 [69.0 – 231.5]	0.03
IL-12p70	97.5 [54.0 – 156.5]	64.5 [40.6 – 147.7]	0.45
TNF-α	4334 [1573 – 11426]	5256 [1835 – 6993]	0.68
IFN-γ	47.7 [30.4 – 228.8]	49.9 [22.2 – 77.3]	0.67
KC	2960 [2507 – 4239]	1512 [1024 – 2791]	<0.01

Table 12.3.2.2: Levels of pro-inflammatory cytokines (median [range] in pg/ml) in BALF at 48hrs from mice infected with 2.5x10⁷ PAO1 and administered either bacteriophage or SM buffer (controls) 24hrs post-infection. A significant difference is seen in two cytokines.

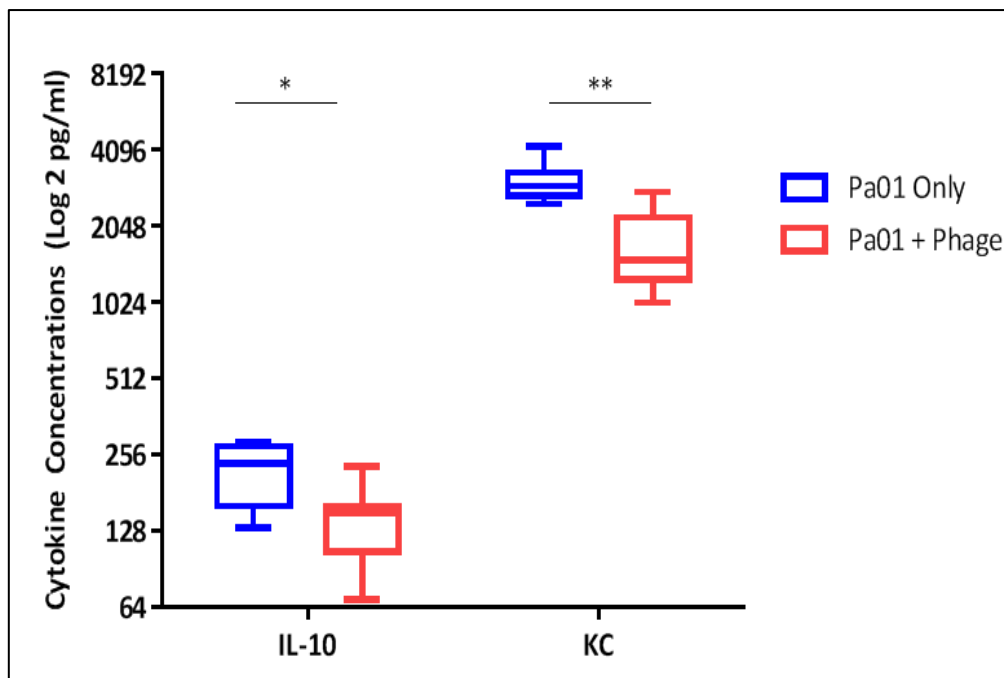


Figure 12.3.2.3: Significant difference in two pro-inflammatory cytokines (median/range) from BAL performed at 48hrs in mice inoculated with 2.5×10^7 of PAO1 and treated with $20 \mu\text{l}$ phage cocktail 1 (1.24×10^9 PFU) or SM buffer 24hrs post-infection.

12.3.3: Prophylactic Administration of Bacteriophage

Having demonstrated that bacteriophage cocktail is efficacious in improving bacterial clearance and also reduced some, but not all, measures of inflammation, the therapeutic potential of prophylactic therapy was investigated. The specific question was, if phage is given prophylactically, in the absence of any Pa, would it be able to survive long enough in the host to exert beneficial effects when Pa is introduced. This would be a beneficial approach in CF patients as it would allow pre-emptive therapy that may prevent infection from ever being established, perhaps at times of increased risk such as intercurrent viral infection or need for general anaesthesia. Such an approach using prophylactic nebulised gentamicin was demonstrated to be effective in a pilot study of children with CF (579) although a later study of cycled prophylactic therapy did not show benefit and raised concerns about disruption of the pulmonary microbiome (580). Emergence of resistant strains is another concern associated with long-term antibiotic prophylaxis (581) and for these reason an alternative approach using highly-specific bacteriophage is appealing.

20µl of bacteriophage or SM buffer was instilled intranasally 48hrs prior to inoculation with 2.5×10^7 CFU of PAO1 with BAL being performed 24hrs after the bacterial infection. Two control mice died post-infection, prior to BAL being performed. Of the surviving mice (n=5), all had persistent and high levels of bacteria in the BALF (median [range] CFU/ml) whilst the majority of phage-treated animals (n=7) had successfully cleared the infection and those which had not had only low levels of bacteria detected (median [range] 0 [0-20]), $p < 0.01$). This is shown in Figure 12.3.3.1. 80% (4/5) surviving control mice had positive splenic cultures, indicating systemic spread; this was not seen in any phage-treated mice. Figure 12.3.3.2 shows splenic cultures of treated and control mice on PSA.

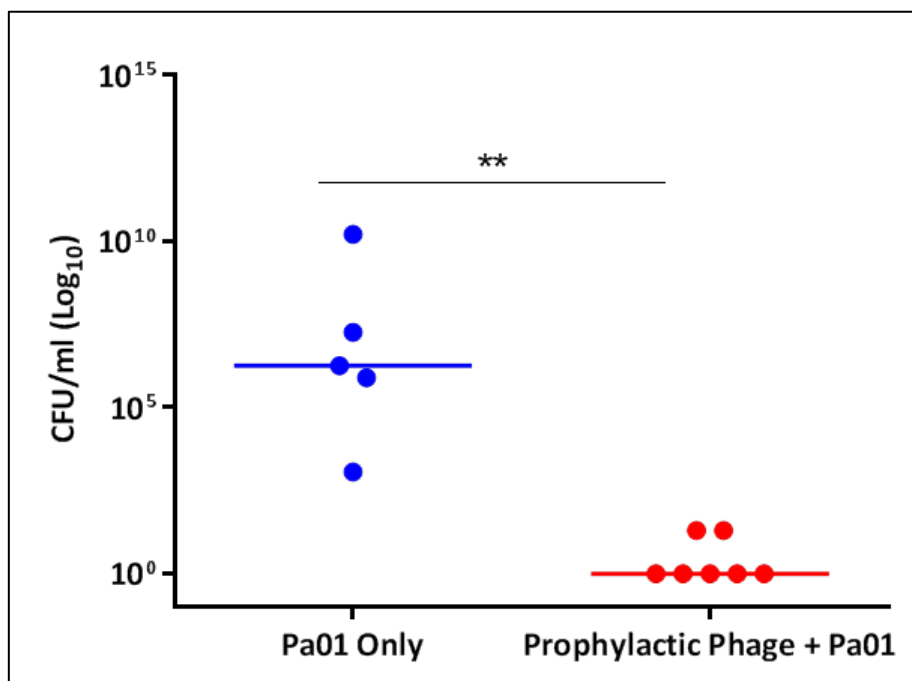
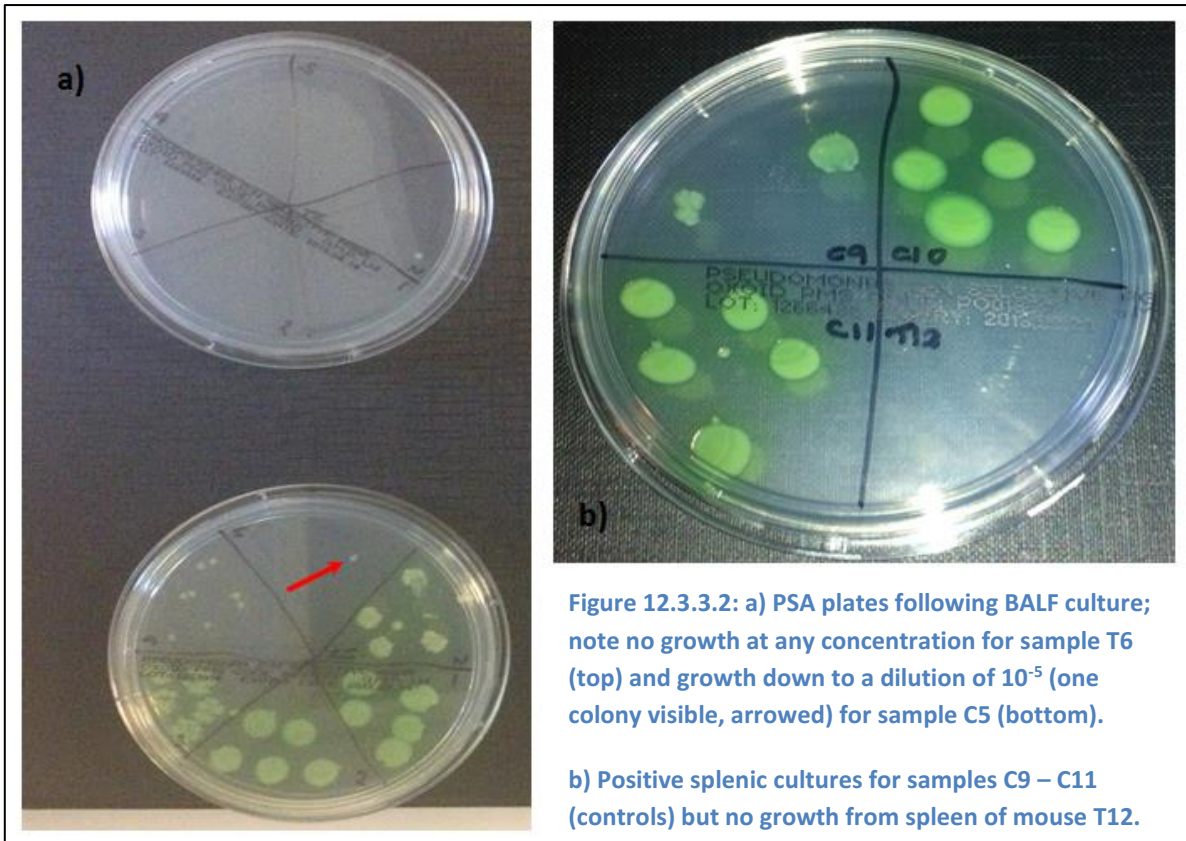


Figure 12.3.3.1: Colony counts/ml from BAL performed at 24hrs in mice inoculated with 2.5×10^7 of PAO1 following pre-treatment with 20µl bacteriophage cocktail (containing 1.24×10^9 PFU) or SM buffer 48hrs prior to infection (prophylactically).



In addition to prophylactic phage therapy having an effect on bacterial killing, there were also differences in total and differential cell counts and KC, all of which were significantly reduced in treated mice compared with controls. Other measured cytokines were similar between groups. This is shown in Table 12.3.3.1, Figure 12.3.3.3 and Table 12.3.3.2 and Figure 12.3.3.4.

		n	Total Cells ($\times 10^4/\text{ml}$)	p	Neutrophils ($\times 10^4/\text{ml}$)	p	Macrophages ($\times 10^4/\text{ml}$)	p	Lymphocytes ($\times 10^4/\text{ml}$)	P
PAO1	Controls	5	336.0 [309.0 – 425.5]	<0.01	272.2 [179.1 – 364.2]	<0.05	57.1 [52.1 – 146.8]	0.74	7.2 [5.65 – 10.08]	<0.05
	Phage-treated	7	192.0 [173.5 – 309]		142.5 [72.96 – 251.2]		59.0 [35.1 – 111.4]		2.0 [0.94 – 7.68]	

Table 12.3.3.1: Inflammatory cells and differential in BALF at 24hrs from mice infected with 2.5×10^7 PAO1 following administration of either bacteriophage or SM buffer (controls) 48hrs prior to infection (prophylactically). Note significant reduction in total cells, neutrophils and lymphocytes in treated mice.

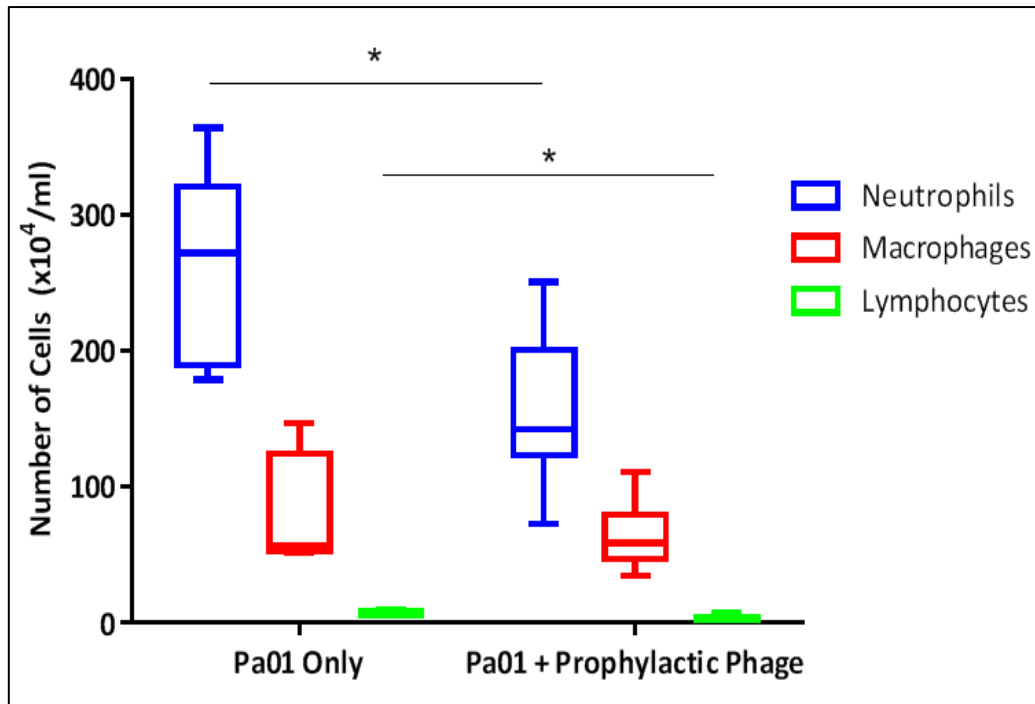


Figure 12.3.3.3: Differential cell counts (median/range) from BAL performed at 24hrs in mice inoculated with 2.5×10^7 of PAO1 following pre-treatment with $20 \mu\text{l}$ phage cocktail 1 (containing 1.24×10^9 PFU) or SM buffer 48hrs prior to infection (prophylactically).

Cytokine	Controls (n=5)	Phage-Treated (n=7)	p
IL-1 β	199.4 [151.0 – 1924]	134.0 [5.6 – 204.5]	0.10
IL-6	2044 [966.1 – 20364]	2023 [206.1 – 20638]	0.98
IL-10	82.8 [46.8 – 1150]	90.7 [6.4 – 462.8]	0.86
IL-12p70	229.6 [58.7 – 276.6]	320.9 [60.2 – 546.9]	0.26
TNF- α	6699 [646.2 – 9246]	1571 [9.0 – 3279]	0.27
IFN- γ	133.6 [9.0 – 453.9]	297.4 [2.9 – 1123]	0.50
KC	7775 [2685 – 14610]	1189 [43 – 2552]	<0.01

Table 12.3.3.2: Levels of pro-inflammatory cytokines (median [range] in pg/ml) in BALF at 24hrs from mice infected with 2.5×10^7 PAO1 and following pre-treatment with either bacteriophage or SM buffer (controls) 48hrs prior to infection (prophylactically). A significant reduction is seen in KC under these conditions.

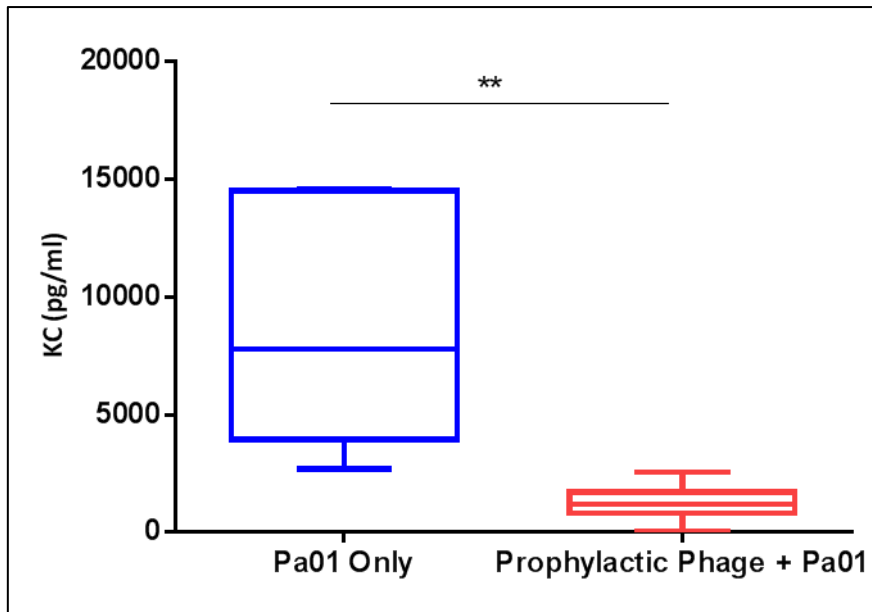


Figure 12.3.3.4: Significant reduction in KC (median/range) from BAL performed at 24hrs in mice inoculated with 2.5×10^7 of PAO1 following pre-treatment with $20 \mu\text{l}$ phage cocktail 1 (containing 1.24×10^9 PFU) or SM buffer 48hrs prior to infection (prophylactically).

12.3.4: Administration of Bacteriophage Cocktails Alone

The finding that bacteriophage administered prophylactically to mice had a significant effect on both bacterial killing and measures of inflammation raises the possibility that this may be a useful therapy to prevent Pa infection. However, two key questions must be answered prior to considering this: i) how long does bacteriophage persist in the lungs if there is no infection present and ii) does bacteriophage itself cause an inflammatory response that is being masked in these experiments by the overwhelming reaction to Pa infection. The first question has been answered to a degree in the literature (524) although not with the cocktails being used here. If prophylactic therapy is to be considered in the future, I would plan to instil phage cocktails alone into murine lungs and quantify PFU/ml in BAL at serial time points using methodology similar to that used by Ampliphi to quantify phage particles following nebulisation (as described in Appendix A5). The second question is more important because, although fears about safety of bacteriophage with regards to bacterial lysis leading to toxicity have been assuaged by previous experiments, it remains unclear whether the cocktails are completely benign when administered alone. Prophylactic therapy, which might be

initiated in the way that Flucloxacillin is for children diagnosed with CF in the neonatal period in the UK, would have to be shown to be safe and not pro-inflammatory. This is of particular importance when considering prophylactic phage therapy in CF because it is possible that defective CFTR primes the airways for excessive inflammation (15), even prior to bacterial infection (171, 582, 583), and thus anything that triggers an inflammatory response might be detrimental. A further issue is that, if phage does elicit an immune response in humans, efficacy will likely be reduced over time, as has been shown in trials of gene therapy using adenoviral vectors (584).

20µl of phage cocktail 1, 2 or 3 (treated, n=6 in each group) or SM buffer (controls, n=10) was administered intranasally to mice and BAL performed 48hrs later. There was a significant increase in total inflammatory cells and neutrophils in mice administered phage cocktail 2, an increase in neutrophils in mice administered phage cocktail 3 and a trend towards increased neutrophils in mice that received phage cocktail 1, although the latter did not reach statistical significance. No other differences were observed between groups. This is summarised in Table 12.3.4.1 and Figure 12.3.4.1. There was no bacterial growth from the BALF of any mice, as might be expected given that phage was administered without any Pa co-infection.

	n	Total Cells (x10 ⁴ /ml)	p	Neutrophils (x10 ⁴ /ml)	p	Macrophages (x10 ⁴ /ml)	p	Lymphocytes (x10 ⁴ /ml)	P
Phage Cocktail 1 Only	6	21.5 [8.5 – 32.5]	0.01	3.5 [0.15 – 10.8]	<0.01	14.7 [7.9 – 20.8]	0.05	1.3 [0.48 – 3.7]	0.16
Phage Cocktail 2 Only	6	78.5 [16.3 – 128.5]*		20.1 [0.22 – 75.2]**		29.4 [15.6 – 111.7]		4.3 [0.46 – 17.4]	
Phage Cocktail 3 Only	6	31.9 [25.8 – 56.8]		2.5 [1.5 – 18.6]*		22.4 [14.0 – 52.4]		1.5 [0.61 – 2.9]	
SM Buffer Only	10	17.0 [9.5 – 67.3]		0.27 [0.0 – 1.6]		19.6 [10.82 – 62.8]		0.61 [0.10 – 3.0]	

Table 12.3.4.1: Inflammatory cells and differential in BALF at 48hrs from mice inoculated with 20µl (1.24x10⁹ PFU) phage cocktail 1, 2 or 3 or SM buffer (controls). Values highlighted in red indicate groups where significant differences on post-hoc analysis were seen using Dunn’s multiple comparisons test.

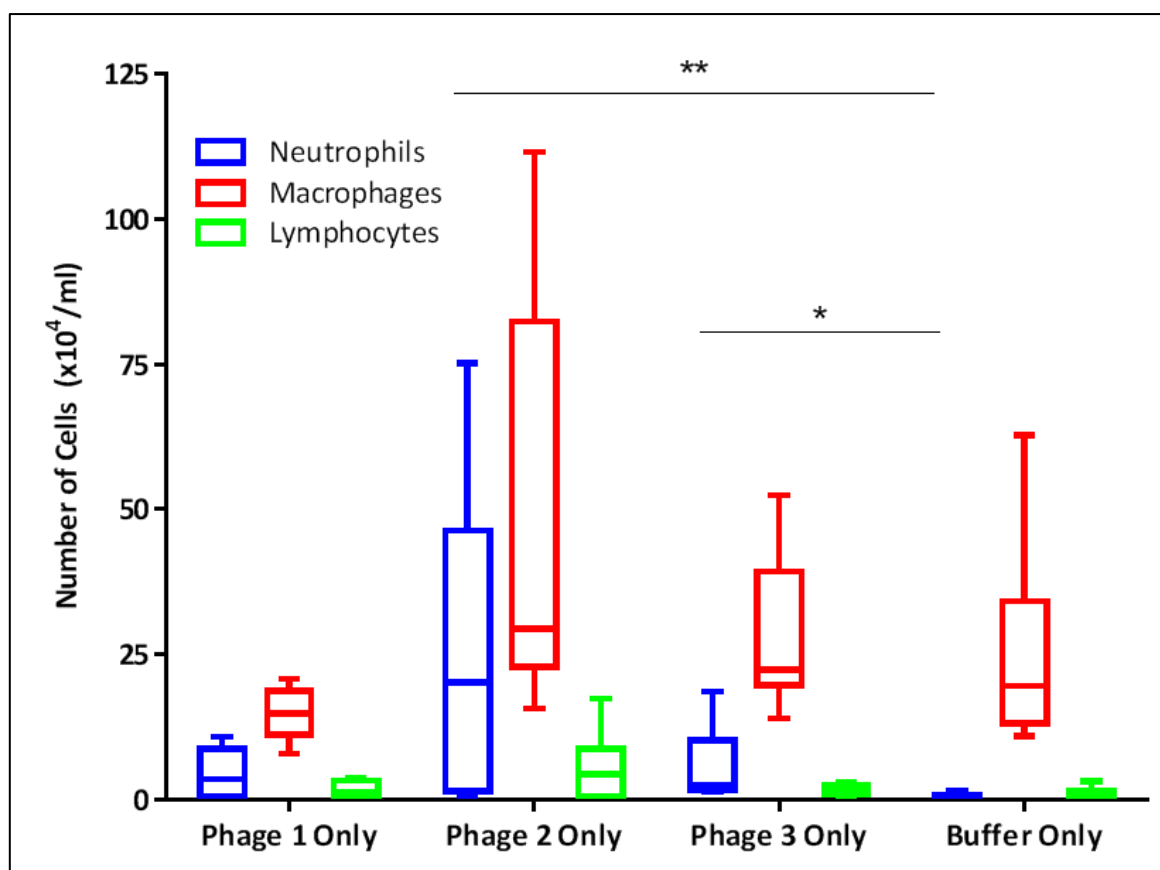


Figure 12.3.4.1: Differential cell counts (median/range) from BAL performed at 48hrs in mice inoculated with 20 μ l phage cocktail 1, 2 or 3 (1.24×10^9 PFU) or SM buffer (controls).

Cytokine	Controls (n=10)	Phage Cocktail 1 (n=6)	Phage Cocktail 2 (n=6)	Phage Cocktail 3 (n=6)	p
IL-1 β	2.5 [0.18 – 5.1]	4.0 [0.85 – 8.5]	5.8 [0.95 – 23.1]	5.1 [1.6 – 14.3]	0.24
IL-6	8.7 [0.0 – 29.7]	1.6 [0.0 – 25.3]	11.1 [1.7 – 75.3]	27.1 [0.0 – 40.8]	0.14
IL-10	1.2 [0.0 – 5.9]	0.0 [0.0 – 2.6]	1.6 [0.0 – 3.7]	0.07 [0.0 – 6.4]	0.64
IL-12p70	22.3 [0.0 – 102.8]	6.7 [0.0 – 42.5]	5.3 [0.0 – 44.8]	58.8 [47.9 – 102.8]	0.007
TNF- α	5.1 [2.0 – 11.4]	7.9 [0.5 – 16.5]	11.5 [3.5 – 27.4]	2.6 [0.0 – 15.7]	0.09
IFN- γ	0.0 [0.0 – 0.74]	0.02 [0.0 – 0.33]	1.1 [0.0 – 3.5]	0.15 [0.0 – 4.1]	0.07
KC	38.8 [6.2 – 63.5]	124.6 [52.3 – 225.0]*	99.4 [2.7 – 320.0]	90.6 [0.36 – 107.0]	0.07

Table 12.3.4.2: Levels of pro-inflammatory cytokines (median [range] in pg/ml) in BALF at 48hrs from mice inoculated with 20 μ l (1.24×10^9 PFU) phage cocktail 1, 2 or 3 or SM buffer (controls). Values highlighted in red indicate groups where significant differences on post-hoc analysis were seen using Dunn's multiple comparisons test. Note that TNF- α , IFN- γ and KC trend towards being significantly different; increasing numbers might have led to these values reaching significance.

12.3.5: Cytokine Comparisons

Although most conditions tested were not directly comparable due to methodological differences, results from conditions I and II using PAO1 were compared as the intranasal inoculum was doubled but the remainder of the experimental protocol was unchanged. 6/7 measured cytokines were

significantly higher in mice infected with the bigger infective dose but IFN- γ was higher in mice infected with the lower dose (2.5×10^6 CFU). No significant difference was seen in total inflammatory cell count across the two conditions. This is shown in Figure 12.3.5.1.

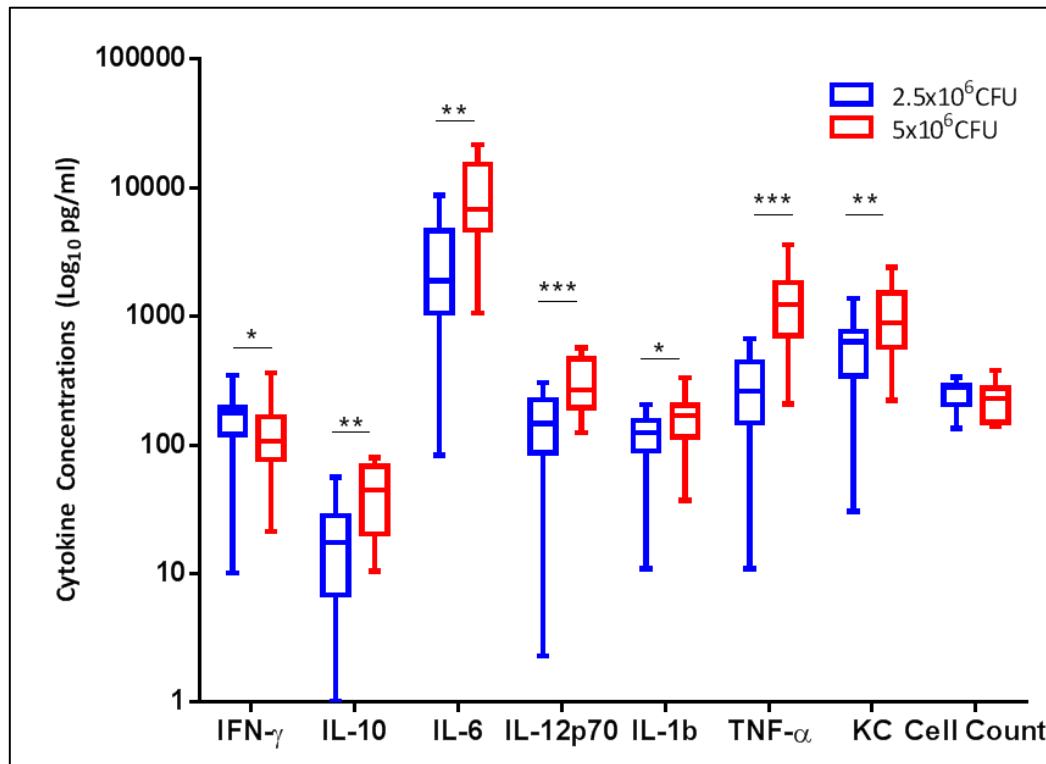


Figure 12.3.5.1: Pro-inflammatory cytokines (median/range) from BAL performed at 48hrs in mice inoculated with either 2.5×10^6 or 5×10^6 of PAO1 and simultaneously treated with $20 \mu\text{l}$ bacteriophage cocktail 1 (containing 1.24×10^9 PFU) or SM buffer.

12.3.6: Cytokine Correlations

To determine if cytokine levels were correlated with one another, and with total cell number and differential cell count, Spearman rank calculations were performed across all tested conditions. As multiple comparisons were performed, correlations were only deemed significant if p-values were reported as 0.000000. Spearman r values are shown in Table 12.3.6.1.

	IFN- γ	IL-10	IL-12p70	IL-1 β	IL-6	KC	TNF- α	Total Cells	Neutrophils	Macrophages	Lymphocytes
IFN- γ		0.519	0.827	0.510	0.484	0.526	0.538	0.438	0.434	0.300	0.365
IL-10	0.519		0.607	0.857	0.857	0.887	0.912	0.659	0.709	0.189	0.254
IL-12p70	0.827	0.607		0.625	0.631	0.611	0.647	0.426	0.430	0.172	0.381
IL-1 β	0.510	0.857	0.625		0.883	0.913	0.899	0.560	0.615	0.050	0.257
IL-6	0.484	0.857	0.631	0.883		0.830	0.851	0.641	0.691	0.123	0.327
KC	0.526	0.887	0.611	0.913	0.830		0.950	0.549	0.609	0.026	0.221
TNF- α	0.538	0.912	0.647	0.899	0.851	0.950		0.553	0.627	0.013	0.215
Total Cells	0.438	0.659	0.426	0.561	0.641	0.550	0.553		0.967	0.602	0.535
Neutrophils	0.434	0.709	0.430	0.615	0.691	0.609	0.627	0.967		0.434	0.448
Macrophages	0.300	0.189	0.172	0.050	0.123	0.026	0.013	0.602	0.434		0.522
Lymphocytes	0.365	0.254	0.381	0.256	0.327	0.221	0.215	0.535	0.448	0.522	

Table 12.3.6.1: Spearman r correlation co-efficients (measured cytokines and inflammatory cell counts). Cells highlighted in red had a calculated p value of 0.000000 and are felt to show significant correlation.

12.4: Discussion

Efficacy of bacteriophage cocktail 1 against both a clinical strain of Pa and the laboratory strain PAO1 has been demonstrated in this section. At lower infective doses, no difference in bacterial burden was demonstrated as most mice cleared infection regardless of whether they received phage therapy although there was a reduction in inflammatory cells with phage treatment. At higher infective doses with BAL performed earlier (24hrs vs. 48hrs), the objective of achieving persistent infection was achieved, but only in control mice; all mice treated with phage retained the ability to clear the lungs of infection though no difference was seen in inflammatory cell count. A similar pattern of findings was seen in mice that received phage 24hrs post- or 48hrs pre-infection (prophylactically). Efficacy when given prophylactically casts doubts on conventional wisdom that phage are rapidly removed by the host reticuloendothelial system if no bacterial host is present (585) and parallels studies indicating that phage, although cleared from the circulation, may remain viable in the spleen for several weeks post-administration (586). Across each condition, a variety of differences in soluble inflammatory cytokines present in BALF was demonstrated, although there was no clear pattern, which could be attributed to biological variation between animals under each tested condition. A relative weakness of this work is that the mice varied in age across the different conditions tested as the experimental procedures were time-consuming and impossible for a single investigator to complete them in a short time period; ideally, I would have liked to have analysed samples from multiple mice sacrificed at different time points to better understand the kinetics of the inflammatory processes. Concerns that osmotic lysis of Pa by phage might lead to toxicity, secondary to release of bacterial endotoxins, *in vivo* were allayed as mice administered higher inoculums had minimal bacterial growth from BALF if also treated with phage and remained healthy, as assessed by physical examination, at the time of sacrifice. In addition, there was no evidence of a vast inflammatory surge in BALF, as might be expected with endotoxin release. However, there are concerns that phage therapy may initiate a systemic inflammatory response as demonstrated by increased neutrophils and KC in BALF of mice treated with all three phage cocktails alone compared

to SM buffer alone. The response was less than that elicited by Pa infection but casts doubt on the potential for using these particular cocktails in cases where infection is not already established unless further purification to reduce the amount of bacterial endotoxin in the cocktails can be achieved. A recent Belgian study demonstrated that it is possible to prepare a cocktail appropriate for clinical use in human trials on a small scale within a laboratory (587) but historically there have been challenges with purification that have held back large-scale manufacture of phage products (539, 588). A weakness of my work is that lung histology was not undertaken; in future toxicity experiments that will need to be undertaken prior to a clinical trial, it would be useful to assess this in addition to BALF inflammatory cell counts to ensure that phage administration itself does not induce microscopic damage to the lung parenchyma.

Previous studies looking at anti-Pa phage efficacy *in vivo* have demonstrated reduction in bioluminescence (523, 589), soluble inflammatory markers and survival (523, 524) if treatment is administered prophylactically. Phage therapy has been shown to improve survival if given within two hours of infection although this effect wanes with longer delays in treatment (523, 524); in one of these studies, this might be attributed to a higher infective dose (524) but in the other (523) the dose was only 1×10^7 CFU of luminescent bacteria in 50 μ l of PBS (less than half the higher inoculum in this study) so it is likely that there were strain-specific differences in virulence. Another study demonstrated phage efficacy in a murine model when it was administered 24hrs post-infection but this was to treat *Burkholderia cepacia* complex (Bcc) rather than Pa infection (590). There are a number of novel findings in this section; lung histology has been compared in phage-treated and control animals (523, 524) but no previously published work has studied the effect of phage therapy on BALF differential cell counts or utilised such an extensive cytokine panel. Most previous work has survival following a lethal dose of Pa infection as the primary outcome measure whereas this study was focused on infection and inflammatory outcomes which are likely more relevant to a clinical setting. No previous studies have investigated change in cell counts in BALF samples. This is relevant

as persistent neutrophilic inflammation has been associated with lung injury (143) and, even during periods of stability, CF patients with chronic Pa infection have higher inflammatory indices than subjects without CF (591). Reduction in bacterial load demonstrated in previous studies does not necessarily equate to attenuation of inflammatory damage. An important unanswered concern was whether phage therapy itself induces a host inflammatory response either directly or secondary to phage-induced Pa lysis (leading to release of toxins such as LPS) or reduces the response by hastening bacterial clearance and the experiments performed here go some way towards answering that. In addition to BALF data showing reduced neutrophils and bacterial load under certain conditions, regular physical examination of mice receiving phage therapy did not reveal evidence of toxicity and, indeed, a survival benefit of treatment was demonstrated under several experiments that used a higher inoculum of PAO1.

In keeping with the observation that BALB/c mice are inherently resistant to Pa infection (592), most mice in this study were able to clear a low dose of intranasally administered Pa with no evidence of systemic spread, even in the absence of phage treatment. However, mice demonstrated neutrophilic inflammation (localised to BALF) at 48hrs in response to both strains of Pa which reduced markedly with simultaneous administration of bacteriophage. This is significant because, although there might be dissociation between infection and inflammation in CF (171, 583), the role of neutrophils in mediating tissue injury is clear (593-597) and treatments that reduce their number may be of benefit (597, 598). In addition, reduced levels of TNF- α , IL-6, IL-10, IL-12p70 and KC were observed in mice infected with the clinical Pa strain and treated with phage. TNF- α plays a vital role in the acute phase response; it promotes recruitment of neutrophils to sites of infection (599, 600) and, along with bacterial endotoxin (601), is one of the physiological stimuli for IL-6 production. The correlation ($r^2 = 0.72$) between these two measures is therefore to be expected. IL-12p70, the biologically active form of IL-12, is important in Th1 immune responses to bacteria and viruses (602) and KC is a major neutrophil chemoattractant (603). Given these roles for TNF- α , IL-6, IL12p-70 and KC and the fact

that there were fewer BALF neutrophils in phage-treated mice, the reduction in these four cytokines is not unexpected. When given to mice infected with small doses of a clinical strain of Pa, bacteriophage appears to complement the inherent resistance of these mice to Pa, perhaps hastening clearance (not demonstrated here as BALF culture was done at 48hrs but implied by later results where BALF was cultured earlier) and thereby diminishing the inflammatory response. That there was no significant reduction in cytokine levels in phage-treated mice given a low dose of PAO1 likely reflects a difference in virulence between the two Pa species reflected by: i) differences being apparent in phage-treated mice when the inoculum of PAO1 was increased and ii) mice being unable to survive higher inoculums of the clinical strain. It is worth noting that, although neutrophils were reduced in BALF performed at 48hrs in mice given a low inoculum of PAO1 and simultaneously treated with phage, this was not seen when higher PAO1 inoculums were administered, which was surprising. However, as BAL was performed earlier, 24hrs after the higher infective dose, with persistence of bacteria demonstrated only in the control mice, it could be inferred that the inflammatory response to infection in the phage-treated mice was likely to be more short-lived and that, had it been possible to perform BAL serially, a difference in inflammatory cell counts might have manifested at later time points due to ongoing bacteraemia in lungs of control mice. That some cytokines were lower in treated mice despite no difference in inflammatory cells lends credence to this theory, particularly as IL-10 was one of the cytokines reduced in phage-treated animals.

A reduction in IL-10 was demonstrated in phage-treated mice infected with a low dose of the clinical strain Pa which seems counter-intuitive as IL-10 is known to inhibit production of pro-inflammatory cytokines (including IL-1 β , IL-6, IL-12 and TNF- α) by T-cells, thereby down-regulating the acute immune response (604), and there is close correlation of IL-10 with IL-1 β , IL-6 and TNF- α (r^2 0.73 – 0.79) but not with IL-12p70 (r^2 = 0.368) in this study. IL-10 was also reduced in phage-treated mice when the inoculum was increased and when phage was administered 24hrs post-infection, with no difference seen when phage was administered prophylactically, making it, along with KC, one of only two cytokines that was reduced across more than one of the conditions being tested. Recent

evidence suggests that IL-10 responses are related to the strength of a preceding pro-inflammatory response (604), which is subsequently down-regulated by IL-10 to prevent ongoing inflammation; high levels are associated with protracted infection and blockade of IL-10 may in fact promote clearance of bacteria (605). If this is the case, and there remains no consensus in the literature due to the complexity of the IL-10 response (604), then reduced IL-1 β , IL-6 and TNF- α in experiments with the clinical strain, reduced IL-1 β and a trend towards reduced IL-6 ($p = 0.06$) when the inoculum of PAO1 was increased with simultaneous dosing of phage and a trend towards reduced IL-1 β and IL-6 with later dosing of phage, could account for reduced “anti-inflammatory” IL-10; with less initial inflammation in phage-treated mice, less IL-10 was produced. Further support for such a theory is the fact that IL-10, of all the measured cytokines in this study, correlated most strongly with absolute neutrophil count across each of the tested conditions ($r^2 = 0.50$). However, from my data, it is not possible to distinguish if IL-10 and neutrophil levels have any direct influence on one another or whether levels of IL-10 simply change *pari-passu* with changes in neutrophil count that are driven by other pro-inflammatory cytokines.

Persistent infection was established in all conditions where PAO1 inoculum was increased tenfold (to 2.5×10^7 CFU/ml) and no bacteriophage was given. Efficacy of bacterial killing when phage was given simultaneously, after bacterial infection (mimicking a clinical “treatment” scenario) or beforehand (as “prophylaxis”) was demonstrated by a significant reduction in bacterial load and, in some conditions, attenuation of the inflammatory response, suggesting potential clinical utility.

There are some discrepant results that are difficult to explain, notably the finding that prophylactic phage therapy significantly reduced inflammatory cell count following infection with high dose PAO1 but simultaneous therapy did not, with bacterial killing demonstrated under both conditions. As previous work suggests that PFU declines by half a log per day in the absence of a bacterial host (524) it might be reasoned that prophylactic therapy would be less effective, particularly as TEM images indicate that phage would be efficacious almost immediately after administration. Whilst the

results from most conditions could not be compared directly due to differences in methodology, the two experiments where PAO1 infection was established at an inoculum of 2.5×10^6 CFU and 5×10^6 CFU were undertaken using identical methodology aside from the dose of infection. No differences were seen in inflammatory cell counts (although phage treatment ameliorated inflammation in both conditions) whilst levels of 6/7 cytokines were significantly higher in mice given the larger infectious dose. It is simplistic to think that a double dose of inoculum would lead to a linear change in results but, given the trend towards higher cytokine levels in these mice, it is surprising that no difference in inflammatory cells was seen. A further result that cannot be explained is that TNF- α was higher in mice given the lower infectious dose.

A chronic infection model with mucoid Pa strains or biofilm modes of growth was not established in this study. In general, CFTR-knockout mice do not recapitulate the lung disease characteristics of CF (606) and methods such as instillation of Pa embedded in agar beads to prevent mechanical clearance have therefore been used in attempts to establish and mimic chronic infection in murine models (607-610). Whilst this approach might be useful for studying host responses, I decided against using a similar strategy to test bacteriophage as a topically applied therapy as phage penetration might have been adversely affected by the presence of the agar which would cast doubt on any data obtained; in the future, it may be possible to study such mechanisms in alternative animal models such as the ENaC over-expressing mouse (150) or the CF pig. However, as it is entirely possible that biofilms might shield Pa from instilled bacteriophage, as they do antibiotics (611, 612), the lack of a chronic infection model is a relative weakness of my work. Counter to this concern is evidence implicating bacteriophage in physiological cell death within Pa biofilms (613) and for certain strains of bacteriophage possessing enzymes that degrade bacterial exopolysaccharide in biofilm matrices (614, 615). Phage has been shown to be effective against Pa biofilms *in vitro* (616-618) and, as bacteriophage is considered benign (although my data suggest that, in their current form, the cocktails I tested are pro-inflammatory), there should theoretically be no disadvantage to

using high doses if this improves efficacy; experiments to establish the dose:response relationship need to be undertaken to confirm this. High antibiotic doses are more likely to cause toxicity and, whilst low antibiotic concentrations have been shown to inhibit biofilm formation (619, 620), other studies suggest that antibiotic concentrations for treating biofilms, particularly older biofilms (621), are likely to be higher than for treating planktonic growths (622). Concerns about antibiotic toxicity are compounded by the fact that sub-therapeutic concentrations may in fact encourage biofilm formation (623) making phage, either as monotherapy or an adjunct, even more appealing.

Bacteriophages are widely reported as being harmless to eukaryotic cells (586, 624) although an inflammatory response, most marked with cocktails 2 and 3, was demonstrated in this work. This was attributed to the cocktails being in prototype development phase and not yet meeting Good Manufacturing Practice (GMP) criteria. Phage cocktail 1 was least immunogenic, likely due to containing the lowest level of lipopolysaccharide (found in the outer membrane of gram negative organisms used in phage manufacture); Ampliphi state that phage-induced inflammation should not remain an issue when cocktails are synthesised for clinical use but repeat testing in a murine model should be carried out when these purified cocktails become available. That a host immune response was seen raises the concern that repeated dosing of phage might be ineffective, as demonstrated previously in trials of gene therapy using viral vectors (281, 625). However, although anti-phage antibodies have previously been reported in the literature (626), the effect of phage might be too rapid for immunity to develop (590). If a clinical trial is approved, therapy would be guided using knowledge of local epidemic strains to selected appropriate phages and it might be possible to choose phages with different Pa antigenicity for repeat dosing in order to reduce the risk of inactivation by the adaptive human immune response. I would have liked to investigate the effects of repeated infection and dosing of phage in a murine model, primarily to see whether efficacy was maintained with repeated phage therapy, but the implications of this in regard to animal welfare cannot be justified until a GMP product is available and it was not approved by our project licence.

12.5: Conclusions from *in vivo* Work

A number of infection protocols, as outlined in Section 12.2.3 were investigated in the acute murine model. The key results in BALF from phage-treated mice compared to controls are summarised in

Table 12.5.1:

Condition	Phage Administration	CFU/ml	Inflammatory Cells	Cytokines
Low Dose PAO1	Simultaneous	No growth	Reduced	No difference
Low Dose Clinical Strain	Simultaneous	No growth	Reduced	Reduced (IL-6, IL-10, IL12p70, TNF- α and KC)
High Dose PAO1	Simultaneous	Reduced	No difference	Reduced (IL-10 and IL-1b)
High Dose PAO1	Delayed	Reduced	No difference	Reduced (IL-10 and KC)
High Dose PAO1	Prophylactic	Reduced	Reduced	Reduced (KC)

Table 12.5.1: Key results from BALF in phage-treated mice when compared to control mice under five different infection conditions.

From a translational perspective, the *in vivo* work has three key findings. Firstly, no evidence of murine toxicity due to rapid lysis of Pa by bacteriophage was seen, suggesting that this approach would be safe in a human trial. Secondly, a beneficial effect of phage treatment once infection was established provides support for bacteriophage as a therapy. Thirdly, and perhaps most encouragingly, administration prior to infection was efficacious, both aiding clearance and reducing inflammation. Recent studies have demonstrated proof-of-concept for prophylactic phage therapy in humans, particularly for gastrointestinal infections (490, 491). This is an attractive treatment strategy for periods when patients might be at high-risk, for example during outbreaks of epidemic Pa strains, or, if concerns regarding immunogenicity of phage cocktails are resolved, even as a routine therapy in all CF patients to try and prevent Pa infection from becoming established in the first place.

Chapter 13: *In vitro* Efficacy of Phage Cocktails Following Nebulisation

As bacteriophages are living organisms, stability following nebulisation (the preferred route if being administered in patients with CF due to the benefits of local delivery to the site of infection) cannot be assumed. For this reason, efficacy of bacteriophage cocktails *in vitro* was assessed following nebulisation through different commercially-available nebulisation systems.

13.1: Materials and Methods

Three different nebulisation systems were investigated:

- I. LC Plus (Pari, UK): a standard jet nebuliser that has been widely used for many years. As the technology is old, nebulisation times are longer than more modern systems and large volumes of sample might be required to counteract sample waste during nebulisation.
- II. AeroEclipse II (Trundell, UK): Actuated delivery jet nebuliser that is more efficient at drug delivery than the LC Plus because the drug is only delivered during inspiration. A trade-off is that delivery times are longer than the LC Plus.
- III. eFlow™ Rapid (Pari, UK): Vibrating mesh nebuliser that delivers drug quicker than conventional nebulisation systems and is more compact due to no need for a separate air compressor, although the cost (approximately £600) is a drawback. Due to the vibrating mesh mechanism, another concern is that bacteriophage might be damaged during passage through the nebuliser.

Four individual phages were assessed through each of these systems; these were different from cocktails used in earlier experiments as selection was optimised by Ampliphi over the course of my work to cover local strains. This was achieved after I collected over 200 clinical isolates from the Royal Brompton Hospital and sent them to Ampliphi for sensitivity testing on standard plaque assays, as described in Section 8.4, in late 2012 and early 2013. Preliminary attempts to collect bacteriophage downstream following nebulisation through the LC Plus and AeroEclipse II were

made. These included using cooled tubing that would theoretically allow rapid condensation of the nebulised mist back into a liquid form; this was unsuccessful as only small amounts of phage solution could be recovered - although droplets were visible in the tubing, they were not readily collectable. Attempts to collect all the nebulised mist into a bag downstream from the nebuliser were also unfeasible as the rate of airflow from the compressors (approximately 8 litres/minute) meant that a 120 litre bag was required for a fifteen minute nebulisation time. Whilst Douglas bags with a capacity of 100 litres are readily available, the practicalities of then trying to condense such a large volume back into a collectable amount of liquid were impossible to overcome. A compromise was to simply sample the phage solution at regular intervals from the nebulisation chambers of the LC Plus and AeroEclipse II; as these are recirculating systems, it was thought to be reasonable to presume that any liquid taken from the nebulisation chamber after connection to the air compressor would have passed through the system at least once and hence, if efficacy was demonstrated, this would by proxy prove that the phage was able to survive nebulisation. For the eFlow, downstream collection was easier to achieve as it does not require large volumes of compressed air to function.

For the LC Plus and AeroEclipse II, 5mls of each phage was added to the nebulisation chamber which was connected to the air compressor and nebulised for five minutes into a biological safety cabinet. After five minutes, the compressor was switched off and 0.5mls of the phage solution remaining in the nebulisation chamber was pipetted into an Eppendorf. The process was repeated with sampling of 0.5mls of phage solution after 10 and 15 minutes nebulisation time; mist was barely visible after the latter time point. This process was repeated six times for each phage. Nebulisers were washed with hot soapy water and left to air dry between each different phage being tested. Control samples (n=6) were also collected. This was achieved by putting 2.5mls of phage 1-4 into the nebulisation chamber, without running the air compressor, and collecting 0.5ml aliquots into Eppendorfs after 15 minutes. This is summarised in Figure 13.1.1 and an example of the nebulisation set-up using air compressors is shown in Figure 13.1.2.

Pari LC/AE II - protocol

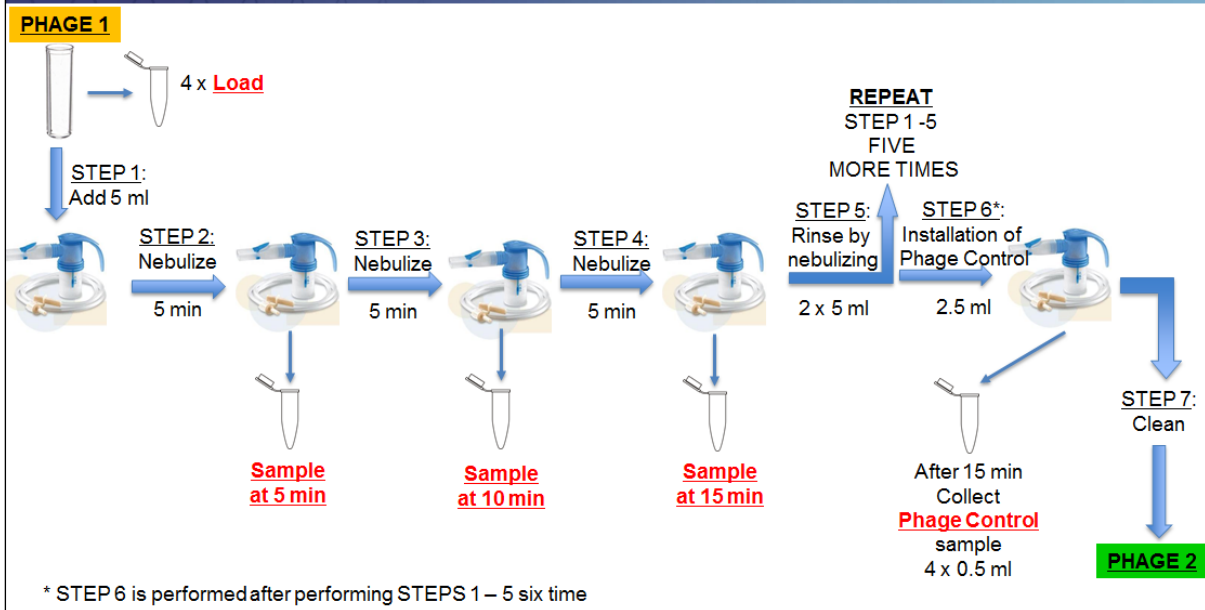


Figure 13.1.1: Flowchart showing nebuliser testing protocol for Pari LC Plus and Aeroeclipse II.



Figure 13.1.2: Experimental nebuliser set-up. Six compressors running in parallel, attached to AeroEclipse II nebulisers within biological safety cabinet. Compressors were stopped after 5, 10 and 15 minutes and 0.5ml aliquots of phage removed from the nebulisation chambers. These aliquots were subsequently analysed to establish remaining phage titres/ml and efficacy against PAO1.

For the eFlow rapid, 5mls of phage was added to the nebulisation chamber and the outflow to the nebuliser was capped off using a black rubber bung from a 50ml Plastipak™ syringe (BD, Spain). The nebuliser was run until dry; this was confirmed by the automatic eFlow sensor that beeps when the nebulisation chamber is empty. The mouthpiece was tipped carefully so that the nebulised solution pooled into the rubber bung that was used to cap off the nebuliser and 0.5ml aliquots of phage were pipetted from this into Eppendorfs. This process was repeated six times for each phage (1-4) with the eFlow cleaned in between, in line with the manufacturers' recommendations. Control samples were obtained by placing 2.5mls of each phage into the nebulisation chamber but not switching it on and removing 0.5ml aliquots of phage after ten minutes (the maximum time required for nebulisation of the cocktails). A summary of this protocol is shown in Figure 13.1.3.

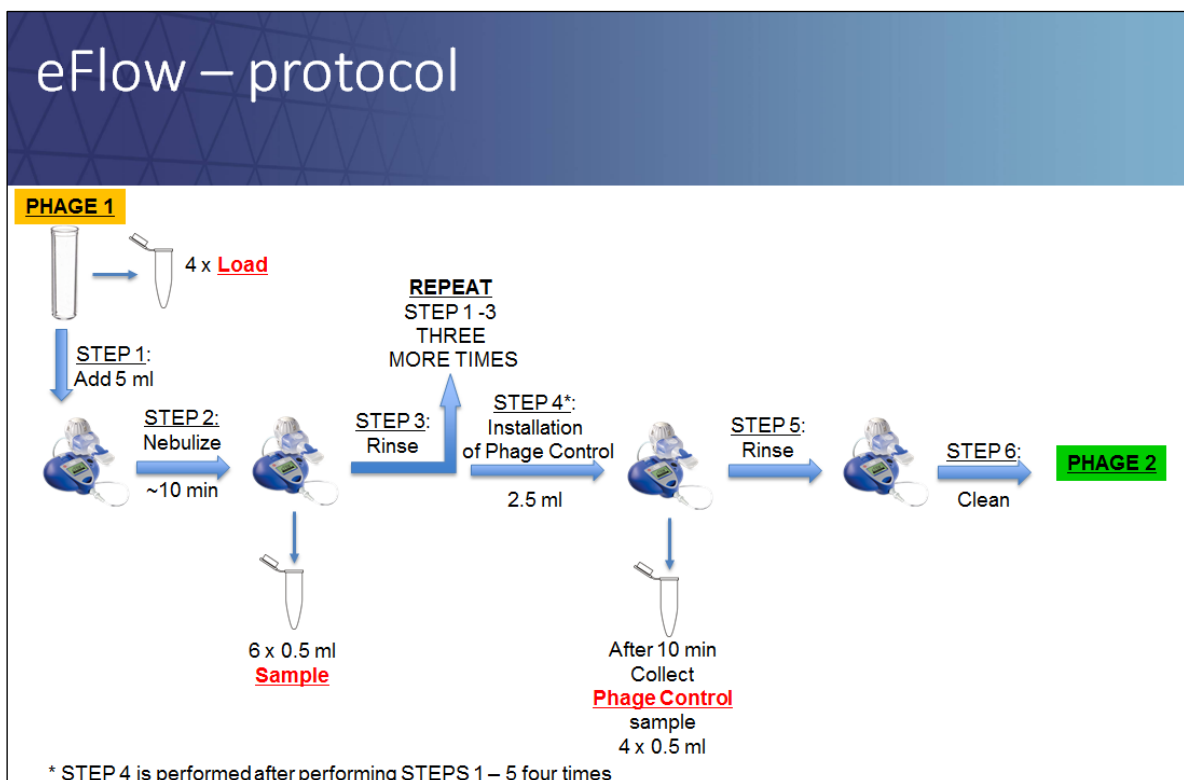


Figure 13.1.3: Flowchart showing nebuliser testing protocol for eFlow rapid.

Blinded negative control samples (0.5ml aliquots of normal saline, n=4) and positive control samples (0.5ml aliquots of phage 1-4, n=4 for each phage) were also prepared. Each sample from the entire experiment (n=278) was given a unique identification number and shipped to Amplphi at a constant

temperature of between 2-8°C for blinded analysis. Absolute quantification of phage in each of the 278 samples was performed by assessing efficacy against two strains of Pa; the standard operating protocol (SOP) for this experiment can be found in the Appendix A5. Results were subsequently sent back to me for unblinding and statistical analysis.

In addition, I performed my own assessment of phage efficacy for each condition (phage 1-4, with each nebuliser plus controls) prior to receiving data from Ampliphi. Bacterial carpets of PAO1 were prepared as described in Section 8.4 and allowed to cool. Serial dilutions (from neat to 10⁻⁶ using SM buffer) of each phage taken either i) 15 minutes after nebulisation commenced for Pari LC and AeroEclipse II or ii) when nebulisation was complete for eFlow were made. 10µl of each dilution was pipetted onto the bacterial carpets with 10µl SM buffer also pipetted into one section as a negative control. The plates were incubated overnight at 37°C and photographed the next day.

13.2: Results

Continued efficacy of phage 1-4 following nebulisation was demonstrated under each of the conditions tested. These results are summarised in Table 13.2.1

	Storage	Control	LC Plus	AeroEclipse II	E-Flow
Phage 1	Partly Neat	Partly Neat	Not sensitive	Partly Neat	Partly Neat
Phage 2	-3	-3	-2	-3	-4
Phage 3	Neat	Neat	Neat	Neat	-2
Phage 4	-1	-1	Neat (-1)	Neat (-2)	Neat (-1)

Table 13.2.1: Dilutions down to which bacteriophage cocktail efficacy was demonstrated following passage through three different nebuliser systems. If numbers are shown in brackets, partial efficacy was seen to these dilutions. Note that no difference was seen in efficacy for phage applied directly from storage and control samples taken after 10 or 15 minutes in nebuliser chambers.

Although no significant loss of effectiveness was seen, it was notable that, when bacteriophage were nebulised via eFlow, enhanced efficacy, particularly with phage 2 and 3, was noted, as shown in Figures 13.2.1 (a and b). PAO1 was not especially sensitive to phage 1, regardless of whether it had gone through the nebuliser or not.

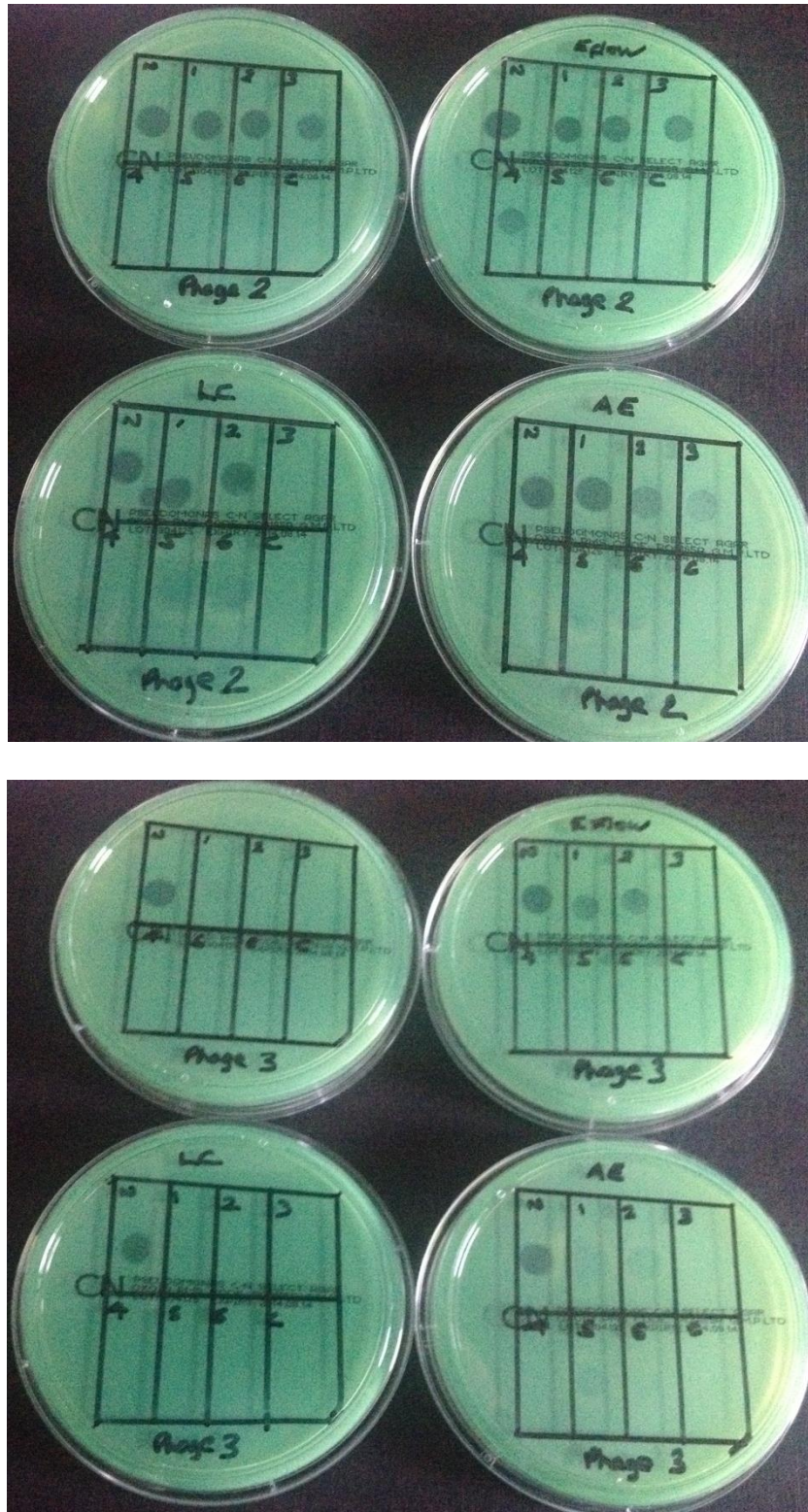


Figure 13.2.1: (a, top): Sensitivity of PAO1 to phage 2 to a dilution of 10^{-3} when phage applied from stores or from being kept in chambers of LC Plus, AeroEclipse II or eFlow but not being nebulised (top left plate), with sensitivity after nebulisation of 10^{-4} with eFlow, 10^{-2} for LC Plus and 10^{-3} for AeroEclipse II. A similar pattern is seen (b, below) with phage 3 where sensitivity of PAO1 is maintained at dilutions of 10^{-1} whether it is from stores (top left plate) or nebulised via LC Plus or AeroEclipse II, but increased to 10^{-3} when nebulised through eFlow (top right plate).

Whilst no obvious loss of bacteriophage effectiveness was evident, a reduction in absolute phage titres under some conditions was demonstrated using the Ampliphi SOP. LCP caused significant decrease in titres of phage 1, 2 and 4 within five minutes of starting nebulisation and phage 3 within 15 minutes (all $p < 0.05$). This is summarised in Table 13.2.2 and Figure 13.2.2 which summarises changes in titres of phage 3 over time compared to controls.

	LCP Phage 1	AE Phage 1	eFlow Phage 1	LCP Phage 2	AE Phage 2	eFlow Phage 2
Start Titre (PFU/ml)	4.3×10^7	1.29×10^8	1.86×10^8	4.94×10^8	3.91×10^8	4.91×10^8
End Titre (PFU/ml)	2.17×10^6	5.38×10^7	3.41×10^8	1.03×10^8	9.78×10^7	2.37×10^8
Log Difference	-1.9	-0.50	0.30	-0.70	-0.73	-0.34

	LCP Phage 3	AE Phage 3	eFlow Phage 3	LCP Phage 4	AE Phage 4	eFlow Phage 4
Start Titre (PFU/ml)	5.16×10^6	9.87×10^6	2.13×10^6	1.32×10^8	3.79×10^8	1.14×10^8
End Titre (PFU/ml)	1.81×10^6	1.05×10^7	2.655×10^8	3.34×10^6	8.20×10^8	8.01×10^8
Log Difference	-0.46	0.03	1.1	-2.37	0.02	0.01

Table 13.2.2: Change in phage titres after 15 mins nebulisation (LCP/AE) or at end of nebulisation (eFlow).

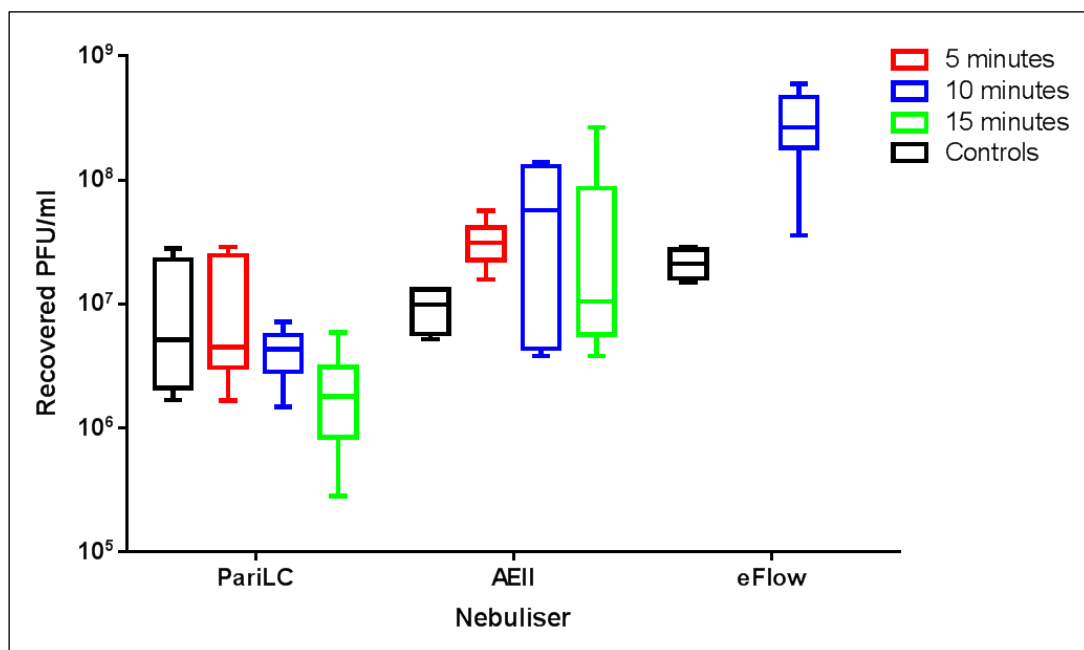


Figure 13.2.2: Box-and-whiskers plot (Tukey) showing change in Phage 3 titres over time with nebulisation. Note, only 10 minute data available for eFlow as nebuliser was run until dry.

13.3: Discussion

I have demonstrated here that phage 1-4 remained efficacious following passage through three different nebulisation systems, which was reassuring in terms of planning for a future clinical trial in human subjects. This was slightly surprising given that difficulties in delivering plasmid DNA vectors for gene therapy have been encountered due to degradation caused by hydrodynamic shearing forces (627), a phenomenon first observed when bacteriophage DNA was passed through a hypodermic needle (628). Shearing forces are thought to be particularly significant with jet nebulisers such as the LC Plus and AeroEclipse II which use compressed air to atomise liquid medications into respirable mists and less of a concern with vibrating mesh nebulisers, which are also more efficient (629). However, recent studies and our own experience at the Royal Brompton during planning for the CF gene therapy trial, showed that the most effective and efficient drug delivery was with the AeroEclipse II in breath-actuated mode (283, 630). This nebulises only during inspiration when the Bernoulli effect of expanding gas from the compressor is enhanced by negative pressure pulling down a central column in the nebuliser (629) so that suspension is not lost during expiration, as it is with the LC Plus. A recent study using a compressor-driven Porta-neb (Respironics, UK) connected to an Anderson cascade impactor also demonstrated phage efficacy post-nebulisation with 25% deposition in secondary bronchi and alveoli (corresponding to stages four and seven of the seven-stage cascade impactor (631)). A further study showed that 12% of phage particles nebulised via AeroEclipse II were contained within particles small enough to reach the lower respiratory tract ($<4.7\mu\text{m}$), although only 1% were viable when given through an Omron nebuliser (632).

My results indicate that the vibrating mesh eFlow is the best nebuliser to take forward into a clinical trial, as there was no decrease in efficacy of any of the nebulised phage cocktails and, in fact, it seemed that for phage 2 and 3, efficacy increased compared to bacteriophage that had not been nebulised. The reasons for this are unclear but, as the findings were replicated on two different cocktails on three occasions, they are unlikely to be artefactual. It is conceivable that passage via the

eFlow has a concentrating effect on the phage that enhances their activity. This theory is given credence by the finding that absolute PFU/ml (determined using the Ampliphi protocol) showed an increase per millilitre for three out of the four phage following eFlow nebulisation, although it is discrepant that there was an apparent reduction in phage 2 titres despite increased effectiveness on bacterial carpet assays (Figure 13.2.1). This has been discussed with Ampliphi who stated that a difference of ± 0.5 log falls within the acceptable variability of the methodology for this experiment; the 0.34 log reduction in phage 2 titres is therefore within this accepted level and the apparent drop in titres was deemed non-significant. Ideally, I would have liked Ampliphi to repeat this part of the study but, by the time I noted these results, it was not possible. It was felt that too much time had elapsed since the initial analysis of nebulised phage for comparisons to the re-tested samples to be meaningfully interpreted and I acknowledge this as a weakness of this study.

Furthermore, if the eFlow was concentrating phage, similar improvement in efficacy might have been expected for phage 4, assuming other components of phage suspensions other than the constituent viruses were similar, and this was not seen. Phage 1 was less effective against PAO1 than the other three tested phages and thus enhancement of effect by eFlow was less likely to be expected; the fact that phage 1 became ineffective against PAO1 following nebulisation via LCP further suggests that this is the least favourable system to take forward into a clinical trial. It is worth noting that the AeroEclipse II has an advantage over eFlow in terms of cost and, as it was used in continuous rather than breath-actuated mode in these experiments, efficiency might have been under-estimated by these experiments. For these reasons, I would conclude that, although the data suggests that the eFlow is the best candidate to take forward into a clinical trial of nebulised bacteriophage, the AeroEclipse II has merits and is worthy of ongoing consideration.

Chapter 14: Efficacy of Phage Cocktails against CF Sputum

Although demonstrating *in vivo* benefit in a murine model and *in vitro* efficacy of phage following nebulisation is important, extrapolation into assumed benefit in CF patients is over-simplistic. Airway mucus, which is a heterogeneous mix of cells, cell debris and secreted polypeptides (633) within larger molecules called mucins, tends to be more viscous in CF due to impaired mucociliary clearance (634). Therefore, although direct delivery of bacteriophage cocktail to the lungs via nebulisation would be the preferred route of administration in CF patients with Pa infection (as high concentrations are delivered directly to the site of infection, systemic side effects are minimised and factors affecting efficacy such as gastrointestinal absorption are partly circumvented), it is likely that chronic airway inflammation and impaired ciliary function would make delivery far less efficient than that seen with nasal instillation in a non-CF murine model where preceding airway infection and inflammation would be negligible. Positron emission tomography (PET) studies have demonstrated that deposition of nebulised therapy distal to airway obstruction is reduced in CF (635) and, as infection typically starts in the smaller airways, this may limit efficacy. It has previously been demonstrated that CF sputum is a barrier to large nanospheres of the type that might be used to delivery gene therapy to the lungs (636), although this was less of an issue with smaller particles more similar in size to bacteriophages. In this section, the hypothesis that CF sputum could present a barrier to bacteriophage efficacy is investigated.

14.1: Materials and Methods

Sputum from adult patients (n=40) with CF was collected after obtaining informed consent (consent form, Appendix A1). As in the SIFT-MS pilot study in Part I (Section 4.1), all subjects were inpatients on Foulis Ward at the Royal Brompton Hospital and were chronically infected with Pa, as defined by Leeds Criteria (440, 637), with a Pa-positive sputum culture in the preceding two weeks. Patients provided samples following morning or early-afternoon physiotherapy. Retrospective analysis of

treatments that subjects were having at the time was undertaken at the end of the study but patients were initially selected at random.

Sputum samples were divided into three (n=34) or four aliquots (n=6). One aliquot was sent to our microbiology laboratory for microscopy, culture and sensitivity testing (M,C+s) and any Pa isolated was stored on agar slopes (Oxoid, UK) for later sensitivity to phage testing by standard plaque assay as previously described (Section 8.4). The remaining aliquots were divided by approximate weight and volume by visual inspection although it was not feasible to do this precisely without artificially affecting sputum rheology; as the aim of this section was to determine if untreated sputum presents a barrier to bacteriophage, it was not possible to ensure that each aliquot was of exactly equal weight and volume. Initially, (n=34, 2 aliquots), 100µl of phage cocktail or SMB was pipetted directly onto the sputum samples which were then incubated and agitated at 37°C for 48hrs. Samples were then serially diluted and cultured onto PSA overnight as previously described before colony counts were performed. An RhDNase subgroup (n=6, 3 aliquots) was later added as I noted in the initial experiments that phage was particularly efficacious against sputa from two patients not on this medication, raising the possibility RhDNase might be inhibiting activity. The third aliquot in this subgroup was treated with 100µl of phage cocktail and 2.5mg (2.5mls) of RhDNase; to ensure that any differences seen were not due to dilution, 2.5mls of SMB was added to the phage only and SMB only aliquots in this arm of the study. These samples were incubated and cultured in the same way as the other 34 sputa before colony counts were again performed. To confirm whether RhDNase affected phage efficacy, standard bacterial carpets of PAO1 were produced (as described in Section 8.4) and treated with 10µl of phage alone, RhDNase alone and phage + RhDNase in dilutions ranging from neat to 10⁻⁶.

14.2: Results

Our microbiology laboratory isolated 51 strains of Pa from the 40 patient sputa. 31 isolates were non-muroid and 20 muroid. A summary of what was isolated is shown in Table 14.2.1:

Isolate	n
Pa + PaM (\pm other bacteria)	13
Pa only	7 (2 with two strains)
Pa + other bugs	9
PaM only	4
PaM + other bugs	3
No growth from sputum	4

Table 14.2.1: Organisms isolated from sputa of inpatients (n=40) on Foulis Ward.

18/31 (58.1%) non-muroid and 11/20 (55%) muroid Pa were sensitive to phage cocktail to some degree on standard plaque assay. Strains from 14 patients were not sensitive on plaque assay and in 4 patients there was no growth from the sputum sample provided. Therefore, 22/36 (61.1%) of the CF patients had at least one strain of Pa in their sputum that was sensitive to phage cocktail on plaque assay. The lowest dilution to which bacterial growth in serially diluted samples treated either with SMB or phage was seen in these “sensitive” sputa is summarised in Table 14.2.2 (overleaf).

Concerns that RhdNase might inhibit phage activity were allayed on bacterial carpet experiments which showed no reduction in efficacy. This is shown in Figure 14.2.1:

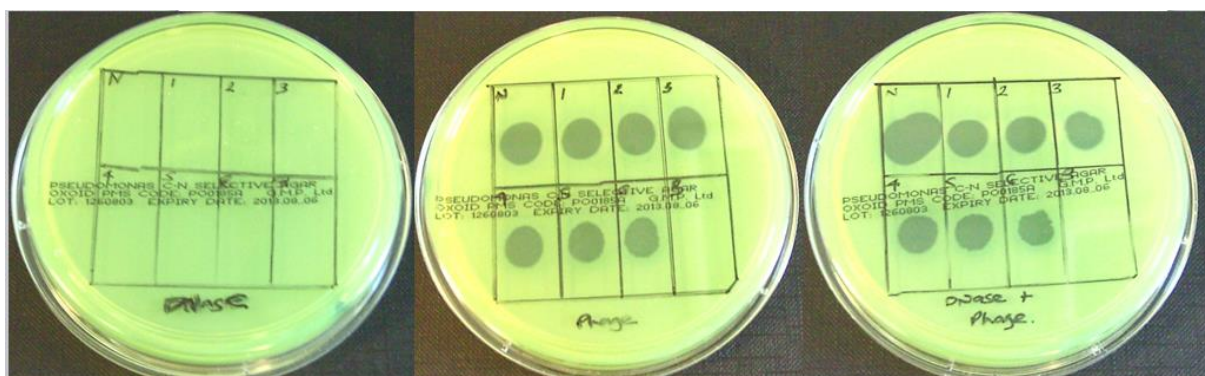


Figure 14.2.1: Ongoing efficacy of phage cocktail 1 against PAO1 when given with RhdNase. Note no effect on bacterial growth by addition of serial dilutions of RhdNase alone to PAO1 bacterial carpet (far left). These photographs suggest that RhdNase will not directly impair phage activity by damaging viral DNA.

Patient Number	Buffer Dilution down to which CFU (number) visible	Phage Dilution down to which CFU (number) visible	Sensitivity on Plaque Assay (Phage Dilution)
1	10 ⁻⁶ (1)	10 ⁻⁶ (3)	a) Non-mucoid 10 ⁻⁶ b) Mucoïd 10 ⁻³
2	10 ⁻⁴ (3)	10 ⁻² (14)	Mucoïd 10 ⁻³
3	10 ⁻⁷ (1)	10 ⁻³ (2)	a) Non-mucoïd 10 ⁻⁴ b) Mucoïd 10 ⁻⁴
4	10 ⁻⁶ (2)	10 ⁻⁷ (1)	Non-mucoïd 10 ⁻⁶
5	10 ⁻⁶ (4)	10 ⁻² (8)	Non-mucoïd 10 ⁻²
6	Neat (+++), 10 ⁻¹ (1)	Neat (+++), 10 ⁻¹ (0)	Mucoïd 10 ⁻⁶
7	10 ⁻⁴ (3)	10 ⁻⁴ (1)	a) Non-mucoïd 10 ⁻² b) Mucoïd not sensitive
8	10 ⁻⁷ (18), 10 ⁻⁶ (89)	10 ⁻⁷ (2), 10 ⁻⁶ (26)	Non-mucoïd 10 ⁻²
9	10 ⁻⁵ (31)	10 ⁻⁶ (36)	Non-mucoïd 10 ⁻⁶
10	10 ⁻⁷ (1)	10 ⁻⁵ (28)	a) Non-mucoïd 10 ⁻⁶ b) Mucoïd 10 ⁻⁶
11	10 ⁻⁷ (1), 10 ⁻⁶ (8)	10 ⁻⁷ (0), 10 ⁻⁶ (12)	a) Non-mucoïd 1 10 ⁻⁵ b) Non-mucoïd 2 10 ⁻³
12	10 ⁻⁶ (2), 10 ⁻⁵ (21)	10 ⁻⁶ (1), 10 ⁻⁵ (5)	a) Non-mucoïd 10 ⁻² b) Mucoïd 10 ⁻²
13	10 ⁻⁶ (7)	10 ⁻⁵ (12)	a) Non-mucoïd 10 ⁻⁵
14	10 ⁻⁷ (+++)	10 ⁻⁷ (+++)	a) Non-mucoïd neat b) Mucoïd not sensitive
15	10 ⁻⁷ (1), 10 ⁻⁶ (5)	10 ⁻⁷ (0), 10 ⁻⁶ (3)	Mucoïd 10 ⁻⁵
16	10 ⁻⁷ (5), 10 ⁻⁶ (51)	10 ⁻⁷ (2), 10 ⁻⁶ (3)	a) Non-mucoïd 10 ⁻² b) Mucoïd 10 ⁻¹
17	10 ⁻⁷ (2), 10 ⁻⁶ (8), 10 ⁻⁵ (2)	10 ⁻⁷ (2), 10 ⁻⁶ (11), 10 ⁻⁵ (26)	Mucoïd 10 ⁻⁶

Table 14.2.2: Sensitivity of CF Sputa (n=17) Treated with SM Buffer or Bacteriophage Cocktail and of Pa Strains Isolated from these Sputa on Plaque Assay (to Phage Cocktail at Dilutions from Neat to 10⁻⁶).

Dilutions down to which colonies are visible are shown, with absolute numbers of CFU in brackets. The lines in red highlight where there is no difference between CFU whether sputa are treated with phage or buffer, despite the Pa strains isolated from the sputa being sensitive on plaque assay.

As there were both mucoïd and non-mucoïd strains that were sensitive on plaque assay but that did not appear to be sensitive in sputum (patients 4, 9, 11, 18 and 20 grew only non-mucoïd strains), the question of whether sputum is a barrier to phage efficacy does not appear to be related to whether or not strains are mucoïd or non-mucoïd.

Similarly, the lowest dilution to which bacterial growth was seen in the subgroup of “sensitive” sputa that had an additional aliquot which was treated with RhDNase is shown in table 14.2.3:

Patient Number	Buffer Only	Phage Only	Phage + RhDNase	Plaque Assay
18	10 ⁻⁵ (3)	10 ⁻⁵ (3)	10 ⁻³ (19)	a) Non-mucoid 10 ⁻³
19	10 ⁻⁷ (+++)	10 ⁻⁷ (1)	10 ⁻⁵ (1)	a) Non-mucoid 10 ⁻¹ b) Mucoid not sensitive
20	10 ⁻³ (+++)	10 ⁻³ (+++)	10 ⁻² (+++)	a) Non-mucoid 1 10 ⁻² b) Non-mucoid 2 n/s
21	10 ⁻⁷ (3)	10 ⁻⁶ (5)	10 ⁻⁵ (7)	a) Non-mucoid 10 ⁻³ b) Mucoid 10 ⁻³
22	10 ⁻⁷ (1)	10 ⁻⁶ (4)	10 ⁻⁵ (13)	a) Non-mucoid n/s b) Mucoid 10 ⁻¹

Table 14.2.3: Sensitivity of CF Sputa (n=5) Treated with SM Buffer Alone, Bacteriophage Cocktail Alone or Bacteriophage Cocktail + RhDNase and of Pa Strains Isolated from these Sputa on Plaque Assay (to Phage Cocktail at Dilutions from Neat to 10⁻⁶)

The red text in both tables indicates where there was no difference in CFU in sputa treated with SMB or phage, despite at least one of the strains isolated from the sputa being sensitive to phage on plaque assay. Therefore, 10/22 (45.5%) of patients with sputum that contained at least one sensitive strain of Pa did not show a decrease in CFU following direct phage application. Even accounting for the fact that three of these patients had two strains isolated in the sputa, of which one was not sensitive and might therefore account for the perceived lack of efficacy, this means that sputum appeared to be a barrier to phage efficacy in 7/22 patients (31.2%) who should theoretically have demonstrated a reduction in CFU isolated from their sputa after topical administration of phage (based on their Pa strains being shown to be sensitive on plaque assay).

14.3: Discussion

Just over half of all Pa samples isolated from this cohort of CF patients (n=40) were sensitive to bacteriophage cocktail on standard plaque assay, with 22/40 patients (55.0%) having at least one sensitive strain in their sputa. However, seven of these patients did not demonstrate a reduction in CFU following direct administration of phage cocktail to sputa, suggesting that sputum itself may be a barrier to efficacy and that, if our cohort is reflective of the wider CF population, only 37.5% of CF patients may see a benefit from this phage cocktail.

A subgroup of samples (n=6) had an additional aliquot that was treated with RhDNase and striking differences were seen in efficacy. Contrary to concerns that RhDNase may be inhibiting phage activity, all five of the sputa in this subgroup that contained a Pa strain that was sensitive to phage on plaque assay had a further reduction in bacterial growth (to varying degrees) when RhDNase was used in conjunction with the phage cocktail. The most prominent example of this is shown in Figure 14.3.1. Confirmatory experiments where phage cocktail was mixed with RhDNase and agitated for 48hrs prior to being applied to a standard plaque of PAO1 again demonstrated that RhDNase had no inhibitory effect on phage activity (Figure 14.2.1). As RhDNase reduces sputum viscosity in CF (241) and regular use has been shown to improve mucus clearance and improve lung function (242, 244), it is likely that concomitant use in this experiment potentiated bacteriophage activity by reducing the protective barrier provided by cellular and other debris in sputum.



Figure 14.3.1: Photograph showing difference in phage efficacy when used in conjunction with RhDNase. Top left plate (buffer) shows growth from all five 10µl drops added at dilutions down to 10^{-7} compared to growth from only one of the 10µl drops (circled in red) added at a dilution of 10^{-5} in the top right plate (phage + RhDNase). In the bottom plate (phage only), growth is seen from three of the drops at a dilution of 10^{-6} , suggesting that use of RhDNase in conjunction with phage cocktails might help to improve bacterial killing by a one log factor.

A French study has previously concluded that the microenvironment in the CF lung **does not** impair phage activity, based on the observation that bacteriophage counts increased (and therefore, by proxy, must have been infecting bacteria) in 41/48 (86%) Pa sputum samples from CF patients onto which a cocktail containing ten phage was applied (638). An alternative explanation for my observation that Pa strains that were sensitive on plaque assay were resistant when phage was directly applied to sputum is that identification of strains in the microbiology laboratory may not accurately reflect the composition of bacteria within the sputum due to significant phenotypic variability, which is a particular feature of Pa (639). Although there are an average of four Pa morphotypes in CF sputa and, in some cases, each of these morphotypes have different antibiotic susceptibilities (640), in this study a maximum of only two morphotypes were isolated from sputum, implying that other strains of Pa might have been present within the sputa that were not susceptible to bacteriophage. Sputum samples only represent a “snapshot” in time of the bacterial milieu in the CF airway (641) and recent studies suggest pulmonary exacerbations in CF occur due to changes in community structure rather than an increase in bacterial density with diversification of Pa communities particularly implicated (154). As all sputa in this study were taken from exacerbating patients, isolation of only 51 strains of Pa from 40 CF sputa in this study is likely to represent significantly less than 50% of the true number of strains that were present in the sputum samples.

The discrepancy I have observed between bacteriophage killing of pure Pa isolates and those in sputum needs to be further clarified if phage therapy with this cocktail is to be taken forward as a clinical trial will focus on CF patients infected with susceptible strains as identified by our microbiology laboratory. It is unclear how many sputum samples would need to be collected prior to confirming that a patient is eligible for inclusion into a clinical trial because the susceptibility of pre-treatment samples to phage therapy might change over time, reflecting geographical variability within the airways or temporal changes in the microbiome. For this reason, several sputum samples would need to be tested for phage susceptibility over a given time period and, given the likelihood that multiple morphotypes of Pa might be present within sputum samples, a large number of

colonies per morphotype identified (as opposed to the current practice of selecting a single isolate of a single morphotype during processing of mixed culture plates for antibiotic susceptibility testing) would need to be plated. This would help determine if there is variability in phage susceptibility not only between but also within different Pa morphotypes. A standard operating protocol for this work has already been drafted in preparation for ongoing study. I have undertaken preliminary experiments (data not shown) which strongly suggest that individual colonies of Pa that appear morphotypically similar on streak culture plates obtained from the clinical microbiology lab at RBH do indeed differ in i) visual appearances when prepared as bacterial carpets (as described in Section 8.4) and ii) in their susceptibility to phage cocktail. This highlights that, whilst correlation between bacteriophage activity *in vitro* and subsequent success *in vivo* has previously been described in a murine model (642), a personalised approach based on more extensive culturing and sensitivity testing should be considered. Whilst this is costly and time-consuming, in the context of a proof-of-concept clinical trial it is imperative as it gives the best chance of demonstrating efficacy and reduces the likelihood of inconclusive results which have previously been seen in clinical trials of bacteriophage therapy (Section 7.1).

Summary and Future Directions

Despite advances in diagnosis and treatment of CF over the past three decades, which have led to significant improvement in life expectancy, it remains a life-limiting condition with no currently available definitive curative therapy. The primary cause of morbidity and mortality is respiratory failure, secondary to successive infections with various microorganisms, the most prevalent of which is *Pseudomonas aeruginosa* (Pa). The two primary aims of my PhD were to determine i) whether recent advances in mass spectrometry could enable improved detection and thereby more rapid treatment of Pa infection and ii) whether bacteriophage therapy is a viable alternative to conventional anti-Pa therapy. The latter is particularly important in light of increasing antibiotic resistance, treatment failures despite therapy with apparently appropriate antibiotics and no extra benefit being gained from administration of higher dose or prolonged antibiotic regimes, as demonstrated by the EPIC trial in over 300 children with recently acquired Pa infection (643)

SIFT-MS and Pa: Key Findings and Future Directions

During initial familiarisation with SIFT-MS and throughout the experimental work of this thesis, there were intermittent problems with the technology resulting in periods when the machine could not be used. This led to a series of unplanned experiments where I had to confirm the ability of our instrument to detect VOCs of interest. Whilst this delayed starting recruitment for the exhaled breath study, which was the foremost objective of this part of the thesis, the data ultimately produced are more robust as a consequence.

A pilot sputum study was planned so that I could become acquainted with using SIFT-MS; I did not expect that the results of this would differ significantly from previously published work, particularly in relation to HCN, which, at the outset of my PhD, was the VOC which I felt had most biomarker potential. As a consequence, bacterial culture experiments were performed and SIFT-MS data compared with a validated, semi-quantitative method of HCN detection in order to see if there

was correlation between the two techniques. Though this was confirmed, it highlighted a further concern; headspace HCN at high (non-physiological) concentrations “flood” the SIFT-MS instrument, making subsequent analyses inaccurate. That this was a flaw with the technology, and not confined to HCN alone, was confirmed by analysis of laboratory-grade butanol, which also caused signal carryover when high levels were detected. However, as measured levels were far in excess of what is likely to present in exhaled human breath, even in patients with Pa infection, and having shown that both HCN and butanol were accurately quantified with our instrument, I felt that breath studies could begin despite this weakness of the SIFT-MS instrument being identified.

Twelve VOCs of interest were selected for further study on the basis of previously published literature and results of my pilot study. Repeatability and reproducibility were investigated and it was noted that the co-efficient of variation for some of these VOCs was extremely high (median of up to 85.4% for hydrogen sulphide); this meant that small differences in certain individual VOCs were unlikely to be detected, regardless of sample size. This is another relative drawback of the current technology, reflected in my final exhaled breath data by improved sensitivity and specificity of diagnostic prediction models when additional VOCs are included, when individually these VOCs do not differ significantly between groups. For these reasons, before summarising the key findings and future directions of exhaled breath analysis in CF, it is important to highlight that my data strongly suggest that SIFT-MS currently remains a research tool rather than one that can be used in a clinical setting to guide patient management.

My key findings from studying exhaled breath were that differences exist in individual VOCs between groups of i) healthy subjects and patients with CF (which may provide insight into disease mechanisms but is not of diagnostic utility) and ii) CF patients with and without infection. No one VOC was shown to be a reliable biomarker of infection and combination of VOCs into a “fingerprint” is more likely to identify patients with and without Pa infection. In its current form, SIFT-MS is not sufficiently sensitive to differentiate between individual patients; the translational objective of this

part of my PhD, to establish a non-invasive technique with which to screen for Pa infection, was therefore not achieved. With improvements in instrument sensitivity (such that VOC can be reliably detected in the parts-per-trillion range) and the addition of other VOCs to the breath fingerprint, discrimination might improve, making the test clinically applicable; a precedent for this is the ^{13}C urea breath test for detection of *Helicobacter pylori* infection.

A novel finding from my SIFT-MS work, although not part of the initial hypotheses, was that isoprene in exhaled breath of CF patients with doctor-defined infective exacerbations was significantly higher than in CF patients who were in a period of clinical stability. Isoprene has previously been associated with oxidative stress, providing a plausible biological mechanism for this finding. This needs validation in a second cohort of patients; if reproducible, I would propose a prospective study in which isoprene be measured at defined points of infective exacerbations (admission, day seven and day fourteen) to see whether it correlates with treatment response. More importantly, if it can be shown that isoprene increases before clinical deterioration, it has potential as a screening tool for outpatient visits. As I found no association with $\text{FEV}_{1\text{L}}$, the information would be a useful adjunct to that provided by spirometry and has the potential to guide clinical decisions such that full-blown exacerbations might be prevented. A weakness of this work is that flow rates for breath collection into Nalophan bags could not be accurately standardised; in any validation cohort it would be useful to investigate if exhalation rates have any effect on measured concentrations of different VOCs.

Non-Invasive Detection of Pa: Future Directions

Whilst undertaking my PhD, the Royal Brompton Hospital was awarded funding by the CF Trust to establish the Pa Strategic Research Centre (SRC), a group of collaborators focused on several areas of Pa research. One project will take forward further non-invasive and metabolic profiling methods of detection. Whilst I have demonstrated proof-of-concept for a signal that differentiates according to Pa status, given concerns about the ability of current SIFT-MS instruments to discriminate between individuals rather than groups, other mass spectrometry techniques have been suggested to take

this work forward. A research proposal has been submitted i) to identify novel Pa biomarkers (such as cell membrane or quorum sensing molecules) from patient microbiological samples using rapid evaporation ionisation mass spectrometry (REIMS) and ii) to analyse liquid samples such as EBC, saliva and urine from CF patients with and without Pa infection using desorption electrospray ionisation (DESI). A new protocol for breath analysis, where exhaled breath is mixed with a solvent aerosol that has undergone high-voltage ionisation prior to analysis with mass spectrometry, is also proposed. This technique is similar to electrospray ionisation that has made direct analysis of solutions possible. The benefit of this proposal is that a purpose-built atmospheric pressure ionisation source will be built in the Respiratory Biomedical Research Unit; it will therefore be possible to analyse patient samples directly (online), rather than having to transport breath samples to another site. Although stability of exhaled breath in Nalophan bags has been demonstrated, having the technology and patients on the same hospital site should allow a much larger volume of data to be collected, with measurements from patients theoretically possible on each day of an admission to hospital or every outpatient visit. This work will be developed for her PhD by Emmanuelle Bardin.

Although our SIFT-MS is not currently being taken forward for ongoing Pa work, it has been used to differentiate between benign and malignant oesophageal tumours with 90% accuracy via VOC analysis of exhaled breath (644). Oesophageal cancer is usually diagnosed at an advanced stage; survival is therefore poor (15% over five years (645)). Currently, diagnosis relies on fiberoptic endoscopy which is both invasive and expensive; economic modelling suggests that, if SIFT-MS screening becomes a clinical tool, savings to the NHS could be around £145 million. A second, larger cohort of patients is currently being recruited from University College London Hospital, Royal Marsden Hospital and Guy's and St. Thomas' Hospital to see whether these findings are reproducible.

Finally, it has recently been reported that German shepherd dogs can be trained to identify VOCs in urine that are associated with prostate cancer, with sensitivity and specificity of up to 100% and 98% respectively (646). Other reports suggest that canine recognition of smell can be used to detect lung and breast cancer (647), basal cell carcinoma (648) and monitor blood sugar levels in Type I diabetes (649). On the basis of these findings, we are thus exploring the potential for dogs to be trained to detect Pa through collaboration with the charity Medical Detection Dogs. If this is feasible, a study comparing sensitivity and specificity of sniffer dog detection with that of other technologies such as electronic nose and mass spectrometry and electronic nose is planned.

Bacteriophage Therapy: Key Findings and Future Directions

Initially, *in vitro* efficacy of bacteriophage cocktails against a laboratory and five clinical strains of Pa was demonstrated using standard plaque assays. As there is a drive towards minimising use of animals and because it would facilitate non-invasive monitoring of response to treatment at serial time points, *in vitro* assays to determine whether killing of luminescent and fluorescent Pa by bacteriophage correlated with bacterial density were performed; these showed that luminescence following phage therapy did not reflect bacterial density (probably due to release of luciferase following bacterial lysis) and could not therefore be used as a proxy measure for phage efficacy. Whilst fluorescence was shown to correlate with bacterial density *in vitro*, it was not sufficiently sensitive to be measured accurately when introduced into a murine model at non-lethal levels. Consequently, conventional monitoring of phage cocktail efficacy was performed; in a murine acute infection model, Pa was administered intranasally and mice were treated i) simultaneously, ii) subsequently or iii) prophylactically with bacteriophage with quantification of inflammatory cells and cytokines in bronchoalveolar lavage fluid at various time points. The key findings were:

- Bacteriophage cocktail enables clearance of high-dose Pa infection from the murine lung whether given simultaneously, prophylactically or 24hrs post-infection.

- Inflammatory cell counts (predominantly neutrophils) in response to Pa infection are reduced when bacteriophage cocktail is administered simultaneously or prophylactically. This was not seen in all conditions tested however; this may have been due to a threshold effect caused by high inoculums of Pa being administered or because BAL was performed at earlier time points in some experiments.
- Soluble inflammatory markers in response to Pa infection are reduced under certain conditions when bacteriophage cocktail is administered. There was some variability in the pattern of cytokines; this could be attributed to biological differences (it was not possible to standardise age of mice being used for example) or to experimental protocols being different. It is possible that, as I aimed to minimise the number of mice being used, some measurements were underpowered, as indicated by several tested conditions approaching, but not quite reaching, statistical significance.

As prophylactic bacteriophage was efficacious, I set out to determine if bacteriophage cocktails alone induced an inflammatory response; a significant increase in neutrophils was noted with administration of phage cocktails 2 and 3, which were in the prototype stage and did not meet GMP standards at the time these experiments were performed. There was a non-significant increase in neutrophils following administration of cocktail 1. These studies will clearly need to be repeated with the final, GMP-compliant bacteriophage cocktail formulations, prior to administration in human subjects. The effect of repeated dosing, both in terms of detecting cumulative phage-induced inflammation or decreased efficacy due to formation of memory T-cells or specific anti-phage antibodies also needs to be investigated.

With efficacy of bacteriophage demonstrated *in vivo*, it was important to determine whether i) nebulisation was an appropriate route of administration for bacteriophage cocktails and ii) whether sputum was a barrier to bacteriophage delivery. Nebulisation of bacteriophage is the most attractive potential route of delivery in any future clinical trial as it theoretically deposits medication directly

into sites of infection. Concerns about nebulisation inactivating bacteriophage due to shearing of DNA were allayed by showing that phage collected downstream through three different nebuliser systems remained efficacious against PAO1, although there were reductions in absolute phage titres that varied according to the phage strain and nebuliser used. A new nebulisation system favoured by AmpliPhi, the Philips Micro, has since been tested by Helena Lund-Palau, visiting medical student from Barcelona; results of this are awaited. For a future clinical trial, it might be necessary beforehand to demonstrate if bacteriophage should be co-administered with other medications, for example RhDNase, with which some synergy was demonstrated *in vitro*, or be given sequentially following airway clearance in order to improve deposition. Techniques to model medication deposition are available and these can be modified to mimic the environment in the CF lung. However, given that there are accepted protocols for medication administration, (RhDNase is given an hour before physiotherapy with nebulised antibiotics post-physiotherapy in an attempt to maximize dose and deposition for example), these studies, whilst of scientific interest, should not delay the start of any clinical trial. I would envisage that bacteriophage, like antibiotics, would be nebulised after physiotherapy to ensure optimal deposition.

Frequency of dosing also needs to be established; further work is needed to establish how long bacteriophage survive in the absence of a bacterial host (if prophylactic therapy is to be considered in the future). In theory, bacteriophage should multiply wherever sensitive strains of Pa are present and there is a therefore a rationale for repeated daily dosing; however, unlike antibiotics, concentrations should not decrease in the presence of bacteria so it is unclear how often to give treatment. Any future clinical trial should therefore have several arms using different dosing regimens. However, each subject in these trials will likely have i) different milieu of Pa within the lungs and ii) heterogeneous lung disease, such that deposition of nebulised bacteriophage will vary, making direct comparisons difficult. In the first instance, I would aim to recruit patients for a pilot study. Safety needs to be established initially (likely with a dose escalation protocol) and, if this is demonstrated, primary outcome measures of reduction in sputum bacterial load and improvement

in FEV₁ would be assessed. Despite my initial concerns that patients would be reluctant to participate in a trial using a nebulised virus, I had overwhelmingly positive responses from subjects who provided sputum samples in this study; over 75% immediately stated that they would like to try bacteriophage therapy when I showed them the findings of my *in vitro* and *in vivo* experiments. Other hurdles (including regulatory approvals) need to be cleared before a clinical trial can start, the most significant of which is concerns about the practicalities of manufacturing large quantities of bacteriophage to GMP standards. A new Amplphi facility in Slovenia has been approved and is currently producing anti-Staphylococcal bacteriophage for another trial programme; the aim is for this to switch to full-scale production of anti-Pseudomonal phage in the future.

With regards to the issue of whether sputum is a barrier to phage, I found that, despite strains of Pa being sensitive to bacteriophage cocktail *in vitro* on bacterial carpets, this was not always the case when sputum containing the same strain of Pa was treated directly with bacteriophage, although I did demonstrate a possible synergistic effect through co-treating sputum with RhDNase. The discord between sensitivity of bacterial isolates and Pa in sputum needs further investigation. This has already been commenced by Valerie Khoo, undergraduate medical student at Imperial College London; preliminary data suggests that, although multiple single Pa colonies isolated from CF sputum might be identical in appearance, their susceptibility to bacteriophage cocktail differs significantly. This suggests multiple different strains of Pa are present within each sputum sample, most of which are not being isolated by the clinical microbiology laboratory as they have no reason to plate out multiple single colonies that are identical on visual inspection for the purposes of antibiotic sensitivity testing. For this reason, future work needs to focus upon identifying just how much Pa diversity there is within sputum samples (ideally using high-throughput molecular techniques) and how this diversity changes in individual patients over time. This information could then be used to tailor phage cocktail therapy for individual patients, thereby maximising any potential clinical improvement (which may still occur even if only some strains of Pa are sensitive) and reduction in sputum bacterial load. I would also plan future work to focus upon possible

synergistic effects of antibiotics and bacteriophage; this can be performed relatively easily *in vitro* using antibiotic discs from our microbiology laboratory, with and without bacteriophage cocktail. Demonstrating synergy *in vivo* would be more difficult; as safety and efficacy of both bacteriophage and antibiotics has been demonstrated independently, it would be difficult to justify using animal testing particularly as, in reality, all CF patients receiving bacteriophage for Pa infection in the future are already likely to be on first-line nebulised antibiotics.

A significant relative weakness of my *in vivo* work is that efficacy was only demonstrated in an acute model of murine infection. Wild-type mice have the advantage of being small, with a short generation time, making them cheap and meaning that relatively large numbers can be used for parallel experiments. However, these mice do not recapitulate CF lung disease and, as demonstrated by early experiments with low infectious doses of Pa, have an inherent ability to clear Pa infection. I would ideally have liked to test bacteriophage efficacy in a chronic murine infection model that can be established through instillation of Pa-laden agarose beads (650) which act as an artificial biofilm to prevent mechanical clearance. There was insufficient time to establish this model and, as agarose beads themselves are not identical to Pa alginate, which is more elastic (651), the effect of this on bacteriophage efficacy would have been unclear. An even better model for CF lung disease would have been the β -ENaC over-expressing mouse or the CF ferret or pig but these were not readily available. Larger animals are more expensive and labour-intensive (requiring meconium ileus surgery in the neonatal period for example) than mice and using these would have been beyond the scope of my PhD. Although I only demonstrated efficacy in previously healthy wild-type mice with no barrier to bacteriophage deposition, unlike the likely situation in airways of CF patients with chronic Pa infection, proposals for a clinical trial in human patients has been favourably received by the Medicines and Healthcare products Regulatory Agency (MHRA), although a formal preclinical animal toxicology programme will be required.

Conclusions

During the course of this PhD, I have demonstrated proof-of-concept that a signal exists by which CF patients with and without Pa infection can be differentiated. I have also shown that bacteriophage not only allows rapid clearance of Pa infection but, also reduces inflammation within the murine lung. Both strands of this work therefore have potential to improve patient outcomes, although a significant amount of further work is necessary before either approach can be used routinely in a clinical setting.

References

1. Chang AB, Grimwood K, Maguire G, King PT, Morris PS, Torzillo PJ. Management of bronchiectasis and chronic suppurative lung disease in indigenous children and adults from rural and remote Australian communities. *The Medical journal of Australia*. 2008;189(7):386-93.
2. Li AM, Sonnappa S, Lex C, Wong E, Zacharasiewicz A, Bush A, et al. Non-CF bronchiectasis: does knowing the aetiology lead to changes in management? *The European respiratory journal : official journal of the European Society for Clinical Respiratory Physiology*. 2005;26(1):8-14.
3. Stockley RA, Bayley D, Hill SL, Hill AT, Crooks S, Campbell EJ. Assessment of airway neutrophils by sputum colour: correlation with airways inflammation. *Thorax*. 2001;56(5):366-72.
4. BTS statement on criteria for specialist referral, admission, discharge and follow-up for adults with respiratory disease. *Thorax*. 2008;63 Suppl 1:i1-i16.
5. Langton Hower SC. Is limited computed tomography the future for imaging the lungs of children with cystic fibrosis? *Archives of disease in childhood*. 2006;91(5):377-8.
6. Cooper P, MacLean J. High-resolution computed tomography (HRCT) should not be considered as a routine assessment method in cystic fibrosis lung disease. *Paediatric respiratory reviews*. 2006;7(3):197-201.
7. Tiddens HA. Chest computed tomography scans should be considered as a routine investigation in cystic fibrosis. *Paediatric respiratory reviews*. 2006;7(3):202-8.
8. Aziz ZA, Davies JC, Alton EW, Wells AU, Geddes DM, Hansell DM. Computed tomography and cystic fibrosis: promises and problems. *Thorax*. 2007;62(2):181-6.
9. O'Connell OJ, McWilliams S, McGarrigle A, O'Connor OJ, Shanahan F, Mullane D, et al. Radiologic imaging in cystic fibrosis: cumulative effective dose and changing trends over 2 decades. *Chest*. 2012;141(6):1575-83.
10. Gaillard EA, Carty H, Heaf D, Smyth RL. Reversible bronchial dilatation in children: comparison of serial high-resolution computer tomography scans of the lungs. *European journal of radiology*. 2003;47(3):215-20.
11. Mott LS, Park J, Murray CP, Gangell CL, de Klerk NH, Robinson PJ, et al. Progression of early structural lung disease in young children with cystic fibrosis assessed using CT. *Thorax*. 2012;67(6):509-16.
12. Smyth A, Elborn JS. Exacerbations in cystic fibrosis: 3--Management. *Thorax*. 2008;63(2):180-4.
13. Justicia JL, Sole A, Quintana-Gallego E, Gartner S, de Gracia J, Prados C, et al. Management of pulmonary exacerbations in cystic fibrosis: still an unmet medical need in clinical practice. *Expert review of respiratory medicine*. 2015;9(2):183-94.
14. Pillarisetti N, Williamson E, Linnane B, Skoric B, Robertson CF, Robinson P, et al. Infection, Inflammation, and Lung Function Decline in Infants with Cystic Fibrosis. *American journal of respiratory and critical care medicine*. 2011;184(1):75-81.
15. Rao S, Grigg J. New insights into pulmonary inflammation in cystic fibrosis. *Arch Dis Child*. 2006;91(9):786-8.
16. Cohen-Cymberek M, Shoseyov D, Kerem E. Managing Cystic Fibrosis Strategies That Increase Life Expectancy and Improve Quality of Life. *American journal of respiratory and critical care medicine*. 2011;183(11):1463-71.
17. Sanders DB, Hoffman LR, Emerson J, Gibson RL, Rosenfeld M, Redding GJ, et al. Return of FEV1 After Pulmonary Exacerbation in Children With Cystic Fibrosis. *Pediatr Pulmonol*. 2010;45(2):127-34.
18. Waters V, Stanojevic S, Atenafu EG, Lu A, Yau Y, Tullis E, et al. Effect of pulmonary exacerbations on long-term lung function decline in cystic fibrosis. *Eur Respir J*. 2012;40(1):61-6.
19. de Boer K, Vandemheen KL, Tullis E, Doucette S, Fergusson D, Freitag A, et al. Exacerbation frequency and clinical outcomes in adult patients with cystic fibrosis. *Thorax*. 2011;66(8):680-5.

20. Andersen DH. Cystic fibrosis of the pancreas and its relation to celiac disease: A clinical and pathologic study. *Am J Dis Child*. 1938;56(2):344-99.
21. Quinton PM. Physiological basis of cystic fibrosis: a historical perspective. *Physiological reviews*. 1999;79(1 Suppl):S3-S22.
22. Collins FS. Cystic fibrosis: molecular biology and therapeutic implications. *Science*. 1992;256(5058):774-9.
23. Wildhagen MF, ten Kate LP, Habbema JD. Screening for cystic fibrosis and its evaluation. *British medical bulletin*. 1998;54(4):857-75.
24. Dodge JA, Morison S, Lewis PA, Coles EC, Geddes D, Russell G, et al. Incidence, population, and survival of cystic fibrosis in the UK, 1968-95. UK Cystic Fibrosis Survey Management Committee. *Archives of disease in childhood*. 1997;77(6):493-6.
25. 2014 Registry Annual Data Report [Internet]. 2014.
26. Castellani C, Southern KW, Brownlee K, Dankert Roelse J, Duff A, Farrell M, et al. European best practice guidelines for cystic fibrosis neonatal screening. *J Cyst Fibros*. 2009;8(3):153-73.
27. Riordan JR, Rommens JM, Kerem B, Alon N, Rozmahel R, Grzelczak Z, et al. Identification of the cystic fibrosis gene: cloning and characterization of complementary DNA. *Science*. 1989;245(4922):1066-73.
28. Kerem B, Rommens JM, Buchanan JA, Markiewicz D, Cox TK, Chakravarti A, et al. Identification of the cystic fibrosis gene: genetic analysis. *Science*. 1989;245(4922):1073-80.
29. Rommens JM, Iannuzzi MC, Kerem B, Drumm ML, Melmer G, Dean M, et al. Identification of the cystic fibrosis gene: chromosome walking and jumping. *Science*. 1989;245(4922):1059-65.
30. White R, Woodward S, Leppert M, O'Connell P, Hoff M, Herbst J, et al. A closely linked genetic marker for cystic fibrosis. *Nature*. 1985;318(6044):382-4.
31. Tsui LC, Buchwald M, Barker D, Braman JC, Knowlton R, Schumm JW, et al. Cystic fibrosis locus defined by a genetically linked polymorphic DNA marker. *Science*. 1985;230(4729):1054-7.
32. Clinical and Functional Translation of CFTR (CFTR2) [Internet]. 2012 [cited 2012]. Available from: <http://www.cftr2.org/>.
33. Cheng SH, Gregory RJ, Marshall J, Paul S, Souza DW, White GA, et al. Defective intracellular transport and processing of CFTR is the molecular basis of most cystic fibrosis. *Cell*. 1990;63(4):827-34.
34. Gregory RJ, Cheng SH, Rich DP, Marshall J, Paul S, Hehir K, et al. Expression and characterization of the cystic fibrosis transmembrane conductance regulator. *Nature*. 1990;347(6291):382-6.
35. Rich DP, Anderson MP, Gregory RJ, Cheng SH, Paul S, Jefferson DM, et al. Expression of cystic fibrosis transmembrane conductance regulator corrects defective chloride channel regulation in cystic fibrosis airway epithelial cells. *Nature*. 1990;347(6291):358-63.
36. Tsui LC. Population Analysis of the Major Mutation in Cystic-Fibrosis. *Human Genetics*. 1990;85(4):391-2.
37. Dean M, Hamon Y, Chimini G. The human ATP-binding cassette (ABC) transporter superfamily. *Journal of Lipid Research*. 2001;42(7):1007-17.
38. Sheppard DN, Welsh MJ. Structure and function of the CFTR chloride channel. *Physiological reviews*. 1999;79(1 Suppl):S23-45.
39. Baker JM, Hudson RP, Kanelis V, Choy WY, Thibodeau PH, Thomas PJ, et al. CFTR regulatory region interacts with NBD1 predominantly via multiple transient helices. *Nat Struct Mol Biol*. 2007;14(8):738-45.
40. Cheng SH, Rich DP, Marshall J, Gregory RJ, Welsh MJ, Smith AE. Phosphorylation of the R domain by cAMP-dependent protein kinase regulates the CFTR chloride channel. *Cell*. 1991;66(5):1027-36.
41. Sheppard DN, Rich DP, Ostedgaard LS, Gregory RJ, Smith AE, Welsh MJ. Mutations in CFTR associated with mild-disease-form Cl⁻ channels with altered pore properties. *Nature*. 1993;362(6416):160-4.

42. Ostedgaard LS, Baldursson O, Vermeer DW, Welsh MJ, Robertson AD. A functional R domain from cystic fibrosis transmembrane conductance regulator is predominantly unstructured in solution. *Proc Natl Acad Sci U S A*. 2000;97(10):5657-62.
43. Mehta A. CFTR: More than just a chloride channel. *Pediatr Pulm*. 2005;39(4):292-8.
44. Hug MJ, Tamada T, Bridges RJ. CFTR and bicarbonate secretion by [correction of to] epithelial cells. *News in physiological sciences : an international journal of physiology produced jointly by the International Union of Physiological Sciences and the American Physiological Society*. 2003;18:38-42.
45. Tang L, Fatehi M, Linsdell P. Mechanism of direct bicarbonate transport by the CFTR anion channel. *Journal of cystic fibrosis : official journal of the European Cystic Fibrosis Society*. 2009;8(2):115-21.
46. Reddy MM, Light MJ, Quinton PM. Activation of the epithelial Na⁺ channel (ENaC) requires CFTR Cl⁻ channel function. *Nature*. 1999;402(6759):301-4.
47. Stutts MJ, Canessa CM, Olsen JC, Hamrick M, Cohn JA, Rossier BC, et al. CFTR as a cAMP-dependent regulator of sodium channels. *Science*. 1995;269(5225):847-50.
48. Schwiebert EM, Egan ME, Hwang TH, Fulmer SB, Allen SS, Cutting GR, et al. Cftr Regulates Outwardly Rectifying Chloride Channels through an Autocrine Mechanism Involving Atp. *Cell*. 1995;81(7):1063-73.
49. Gibson LE, Cooke RE. A test for concentration of electrolytes in sweat in cystic fibrosis of the pancreas utilizing pilocarpine by iontophoresis. *Pediatrics*. 1959;23(3):545-9.
50. Bush A, Wallis C. Time to think again: cystic fibrosis is not an "all or none" disease. *Pediatr Pulmonol*. 2000;30(2):139-44.
51. Bronsveld I, Mekus F, Bijman J, Ballmann M, de Jonge HR, Laabs U, et al. Chloride conductance and genetic background modulate the cystic fibrosis phenotype of Delta F508 homozygous twins and siblings. *J Clin Invest*. 2001;108(11):1705-15.
52. Davies JC, Griesenbach U, Alton E. Modifier genes in cystic fibrosis. *Pediatr Pulmonol*. 2005;39(5):383-91.
53. Hamosh A, Corey M. Correlation between Genotype and Phenotype in Patients with Cystic-Fibrosis. *New Engl J Med*. 1993;329(18):1308-13.
54. Castellani C, Cuppens H, Macek M, Jr., Cassiman JJ, Kerem E, Durie P, et al. Consensus on the use and interpretation of cystic fibrosis mutation analysis in clinical practice. *Journal of cystic fibrosis : official journal of the European Cystic Fibrosis Society*. 2008;7(3):179-96.
55. Zielenski J. Genotype and phenotype in cystic fibrosis. *Respiration; international review of thoracic diseases*. 2000;67(2):117-33.
56. Mahadeva R, Westerbeek RC, Perry DJ, Lovegrove JU, Whitehouse DB, Carroll NR, et al. Alpha1-antitrypsin deficiency alleles and the Taq-I G-->A allele in cystic fibrosis lung disease. *Eur Respir J*. 1998;11(4):873-9.
57. Garred P, Pressler T, Madsen HO, Frederiksen B, Svejgaard A, Hoiby N, et al. Association of mannose-binding lectin gene heterogeneity with severity of lung disease and survival in cystic fibrosis. *J Clin Invest*. 1999;104(4):431-7.
58. de Gracia J, Mata F, Alvarez A, Casals T, Gatner S, Vendrell M, et al. Genotype-phenotype correlation for pulmonary function in cystic fibrosis. *Thorax*. 2005;60(7):558-63.
59. Abman SH, Ogle JW, Butler-Simon N, Rumack CM, Accurso FJ. Role of respiratory syncytial virus in early hospitalizations for respiratory distress of young infants with cystic fibrosis. *The Journal of pediatrics*. 1988;113(5):826-30.
60. Ratjen F, Doring G. Cystic fibrosis. *Lancet*. 2003;361(9358):681-9.
61. Welsh MJ, Smith AE. Molecular mechanisms of CFTR chloride channel dysfunction in cystic fibrosis. *Cell*. 1993;73(7):1251-4.
62. Bobadilla JL, Macek M, Jr., Fine JP, Farrell PM. Cystic fibrosis: a worldwide analysis of CFTR mutations--correlation with incidence data and application to screening. *Human mutation*. 2002;19(6):575-606.

63. Mendell JT, Dietz HC. When the message goes awry: Disease-producing mutations that influence mRNA content and performance. *Cell*. 2001;107(4):411-4.
64. Schloesser M, Arleth S, Lenz U, Bertele RM, Reiss J. A Cystic-Fibrosis Patient with the Nonsense Mutation G542x and the Splice Site Mutation 1717-1. *J Med Genet*. 1991;28(12):878-80.
65. Lerer I, Sagi M, Cutting GR, Abeliovich D. Cystic-Fibrosis Mutations Delta-F508 and G542x in Jewish Patients. *J Med Genet*. 1992;29(2):131-3.
66. Shoshani T, Augarten A, Gazit E, Bashan N, Yahav Y, Rivlin Y, et al. Association of a nonsense mutation (W1282X), the most common mutation in the Ashkenazi Jewish cystic fibrosis patients in Israel, with presentation of severe disease. *American journal of human genetics*. 1992;50(1):222-8.
67. Cheng SH, Gregory RJ, Marshall J, Paul S, Souza DW, White GA, et al. Defective Intracellular-Transport and Processing of Cftr Is the Molecular-Basis of Most Cystic-Fibrosis. *Cell*. 1990;63(4):827-34.
68. Kalin N, Claass A, Sommer M, Puchelle E, Tummeler B. DeltaF508 CFTR protein expression in tissues from patients with cystic fibrosis. *J Clin Invest*. 1999;103(10):1379-89.
69. Bertrand CA, Frizzell RA. The role of regulated CFTR trafficking in epithelial secretion. *American journal of physiology Cell physiology*. 2003;285(1):C1-18.
70. Vij N, Fang S, Zeitlin PL. Selective inhibition of endoplasmic reticulum-associated degradation rescues DeltaF508-cystic fibrosis transmembrane regulator and suppresses interleukin-8 levels: therapeutic implications. *The Journal of biological chemistry*. 2006;281(25):17369-78.
71. Kopito RR. Biosynthesis and degradation of CFTR. *Physiological reviews*. 1999;79(1 Suppl):S167-73.
72. Estivill X, Bancells C, Ramos C. Geographic distribution and regional origin of 272 cystic fibrosis mutations in European populations. *The Biomed CF Mutation Analysis Consortium. Human mutation*. 1997;10(2):135-54.
73. Bompadre SG, Sohma Y, Li M, Hwang TC. G551D and G1349D, two CF-associated mutations in the signature sequences of CFTR, exhibit distinct gating defects. *The Journal of general physiology*. 2007;129(4):285-98.
74. Illek B, Zhang L, Lewis NC, Moss RB, Dong JY, Fischer H. Defective function of the cystic fibrosis-causing missense mutation G551D is recovered by genistein. *The American journal of physiology*. 1999;277(4 Pt 1):C833-9.
75. Ramsey BW, Davies J, McElvaney NG, Tullis E, Bell SC, Drevinek P, et al. A CFTR potentiator in patients with cystic fibrosis and the G551D mutation. *The New England journal of medicine*. 2011;365(18):1663-72.
76. Sermet-Gaudelus I. Ivacaftor treatment in patients with cystic fibrosis and the G551D-CFTR mutation. *European respiratory review : an official journal of the European Respiratory Society*. 2013;22(127):66-71.
77. Ahmed N, Corey M, Forstner G, Zielenski J, Tsui LC, Ellis L, et al. Molecular consequences of cystic fibrosis transmembrane regulator (CFTR) gene mutations in the exocrine pancreas. *Gut*. 2003;52(8):1159-64.
78. Peckham D, Conway SP, Morton A, Jones A, Webb K. Delayed diagnosis of cystic fibrosis associated with R117H on a background of 7T polythymidine tract at intron 8. *Journal of Cystic Fibrosis*. 2006;5(1):63-5.
79. Thauvin-Robinet C, Munck A, Huet F, Genin E, Bellis G, Gautier E, et al. The very low penetrance of cystic fibrosis for the R117H mutation: a reappraisal for genetic counselling and newborn screening. *J Med Genet*. 2009;46(11):752-8.
80. Gervais R, Dumur V, Rigot JM, Lafitte JJ, Roussel P, Claustres M, et al. High frequency of the R117H cystic fibrosis mutation in patients with congenital absence of the vas deferens. *The New England journal of medicine*. 1993;328(6):446-7.
81. Guggino WB, Stanton BA. New insights into cystic fibrosis: molecular switches that regulate CFTR. *Nature reviews Molecular cell biology*. 2006;7(6):426-36.

82. Sheppard DN, Ostedgaard LS, Winter MC, Welsh MJ. Mechanism of Dysfunction of 2 Nucleotide-Binding Domain Mutations in Cystic-Fibrosis Transmembrane Conductance Regulator That Are Associated with Pancreatic Sufficiency. *Embo J*. 1995;14(5):876-83.
83. Haardt M, Benharouga M, Lechardeur D, Kartner N, Lukacs GL. C-terminal truncations destabilize the cystic fibrosis transmembrane conductance regulator without impairing its biogenesis. A novel class of mutation. *The Journal of biological chemistry*. 1999;274(31):21873-7.
84. Flume PA, Liou TG, Borowitz DS, Li H, Yen K, Ordonez CL, et al. Ivacaftor in subjects with cystic fibrosis who are homozygous for the F508del-CFTR mutation. *Chest*. 2012;142(3):718-24.
85. Boyle MP, De Boeck K. A new era in the treatment of cystic fibrosis: correction of the underlying CFTR defect. *The Lancet Respiratory medicine*. 2013;1(2):158-63.
86. Boucher RC. New concepts of the pathogenesis of cystic fibrosis lung disease. *Eur Respir J*. 2004;23(1):146-58.
87. Wang X, Kim J, McWilliams R, Cutting GR. Increased prevalence of chronic rhinosinusitis in carriers of a cystic fibrosis mutation. *Archives of otolaryngology--head & neck surgery*. 2005;131(3):237-40.
88. Chang EH. New insights into the pathogenesis of cystic fibrosis sinusitis. *Int Forum Allergy Rh*. 2014;4(2):132-7.
89. Roby BB, McNamara J, Finkelstein M, Sidman J. Sinus surgery in Cystic Fibrosis patients: Comparison of sinus and lower airway cultures. *Int J Pediatr Otorhi*. 2008;72(9):1365-9.
90. Chang EH, Pezzulo AA, Meyerholz DK, Potash AE, Wallen TJ, Reznikov LR, et al. Sinus hypoplasia precedes sinus infection in a porcine model of cystic fibrosis. *Laryngoscope*. 2012;122(9):1898-905.
91. Robertson JM, Friedman EM, Rubin BK. Nasal and sinus disease in cystic fibrosis. *Paediatric respiratory reviews*. 2008;9(3):213-9.
92. King VV. Upper respiratory disease, sinusitis, and polyposis. *Clinical reviews in allergy*. 1991;9(1-2):143-57.
93. Gysin C, Althman GA, Papsin BC. Sinonasal disease in cystic fibrosis: clinical characteristics, diagnosis, and management. *Pediatr Pulmonol*. 2000;30(6):481-9.
94. Muhlebach MS, Miller MB, Moore C, Wedd JP, Drake AF, Leigh MW. Are lower airway or throat cultures predictive of sinus bacteriology in cystic fibrosis? *Pediatr Pulm*. 2006;41(5):445-51.
95. Ciofu O, Johansen HK, Aanaes K, Wassermann T, Alhede M, von Buchwald C, et al. P. aeruginosa in the paranasal sinuses and transplanted lungs have similar adaptive mutations as isolates from chronically infected CF lungs. *Journal of Cystic Fibrosis*. 2013;12(6):729-36.
96. Leung MK, Rachakonda L, Weill D, Hwang PH. Effects of sinus surgery on lung transplantation outcomes in cystic fibrosis. *American journal of rhinology*. 2008;22(2):192-6.
97. Agrons GA, Corse WR, Markowitz RI, Suarez ES, Perry DR. Gastrointestinal manifestations of cystic fibrosis: radiologic-pathologic correlation. *Radiographics : a review publication of the Radiological Society of North America, Inc*. 1996;16(4):871-93.
98. Scotet V, De Braekeleer M, Audrezet MP, Quere I, Mercier B, Dugueperoux I, et al. Prenatal detection of cystic fibrosis by ultrasonography: a retrospective study of more than 346 000 pregnancies. *J Med Genet*. 2002;39(6):443-8.
99. Noblett HR. Treatment of uncomplicated meconium ileus by Gastrografin enema: a preliminary report. *Journal of pediatric surgery*. 1969;4(2):190-7.
100. Del Pin CA, Czyrko C, Ziegler MM, Scanlin TF, Bishop HC. Management and survival of meconium ileus. A 30-year review. *Annals of surgery*. 1992;215(2):179-85.
101. Wouthuyzen-Bakker M, Bodewes FAJA, Verkade HJ. Persistent fat malabsorption in cystic fibrosis; lessons from patients and mice. *Journal of Cystic Fibrosis*. 2011;10(3):150-8.
102. Morton JR, Ansari N, Glanville AR, Meagher AP, Lord RV. Distal intestinal obstruction syndrome (DIOS) in patients with cystic fibrosis after lung transplantation. *Journal of gastrointestinal surgery : official journal of the Society for Surgery of the Alimentary Tract*. 2009;13(8):1448-53.

103. Mousa HM, Woodley FW. Gastroesophageal reflux in cystic fibrosis: current understandings of mechanisms and management. *Current gastroenterology reports*. 2012;14(3):226-35.
104. Orenstein SR, Orenstein DM. Gastroesophageal reflux and respiratory disease in children. *The Journal of pediatrics*. 1988;112(6):847-58.
105. Heine RG, Button BM, Olinsky A, Phelan PD, Catto-Smith AG. Gastro-oesophageal reflux in infants under 6 months with cystic fibrosis. *Arch Dis Child*. 1998;78(1):44-8.
106. Blondeau K, Pauwels A, Dupont L, Mertens V, Proesmans M, Orel R, et al. Characteristics of gastroesophageal reflux and potential risk of gastric content aspiration in children with cystic fibrosis. *Journal of pediatric gastroenterology and nutrition*. 2010;50(2):161-6.
107. Sabati AA, Kempainen RR, Milla CE, Ireland M, Schwarzenberg SJ, Dunitz JM, et al. Characteristics of gastroesophageal reflux in adults with cystic fibrosis. *Journal of Cystic Fibrosis*. 2010;9(5):365-70.
108. Phillips GE, Pike SE, Rosenthal M, Bush A. Holding the baby: head downwards positioning for physiotherapy does not cause gastro-oesophageal reflux. *Eur Respir J*. 1998;12(4):954-7.
109. Walkowiak J, Lisowska A, Blaszczynski M. The changing face of the exocrine pancreas in cystic fibrosis: pancreatic sufficiency, pancreatitis and genotype. *Eur J Gastroen Hepat*. 2008;20(3):157-60.
110. Marshall BC, Butler SM, Stoddard M, Moran AM, Liou TG, Morgan WJ. Epidemiology of cystic fibrosis-related diabetes. *The Journal of pediatrics*. 2005;146(5):681-7.
111. Wickens-Mitchell KL, Gilchrist FJ, McKenna D, Raffeeq P, Lenney W. The screening and diagnosis of cystic fibrosis-related diabetes in the United Kingdom. *Journal of cystic fibrosis : official journal of the European Cystic Fibrosis Society*. 2014;13(5):589-92.
112. Moran A, Doherty L, Wang X, Thomas W. Abnormal glucose metabolism in cystic fibrosis. *The Journal of pediatrics*. 1998;133(1):10-7.
113. Elder DA, Wooldridge JL, Dolan LM, D'Alessio DA. Glucose tolerance, insulin secretion, and insulin sensitivity in children and adolescents with cystic fibrosis and no prior history of diabetes. *The Journal of pediatrics*. 2007;151(6):653-8.
114. Moran A, Dunitz J, Nathan B, Saeed A, Holme B, Thomas W. Cystic fibrosis-related diabetes: current trends in prevalence, incidence, and mortality. *Diabetes care*. 2009;32(9):1626-31.
115. Moran A, Becker D, Casella SJ, Gottlieb PA, Kirkman MS, Marshall BC, et al. Epidemiology, pathophysiology, and prognostic implications of cystic fibrosis-related diabetes: a technical review. *Diabetes care*. 2010;33(12):2677-83.
116. LaRusch J, Jung J, General IJ, Lewis MD, Park HW, Brand RE, et al. Mechanisms of CFTR Functional Variants That Impair Regulated Bicarbonate Permeation and Increase Risk for Pancreatitis but Not for Cystic Fibrosis. *PLoS genetics*. 2014;10(7):e1004376.
117. Eggermont E. Gastrointestinal manifestations in cystic fibrosis. *Eur J Gastroenterol Hepatol*. 1996;8(8):731-8.
118. Robertson MB, Choe KA, Joseph PM. Review of the abdominal manifestations of cystic fibrosis in the adult patient. *Radiographics : a review publication of the Radiological Society of North America, Inc*. 2006;26(3):679-90.
119. Hernandez-Jimenez F, Fischman D, Cheriya P. Colon Cancer in Cystic Fibrosis patients: Is this a growing problem? *Journal of Cystic Fibrosis*. 2008;7(5):343-6.
120. FitzSimmons SC, Burkhart GA, Borowitz D, Grand RJ, Hammerstrom T, Durie PR, et al. High-dose pancreatic-enzyme supplements and fibrosing colonopathy in children with cystic fibrosis. *The New England journal of medicine*. 1997;336(18):1283-9.
121. Wilschanski M, Durie PR. Patterns of GI disease in adulthood associated with mutations in the CFTR gene. *Gut*. 2007;56(8):1153-63.
122. Aris RM, Merkel PA, Bachrach LK, Borowitz DS, Boyle MP, Elkin SL, et al. Guide to bone health and disease in cystic fibrosis. *The Journal of clinical endocrinology and metabolism*. 2005;90(3):1888-96.

123. Bronckers A, Kalogeraki L, Jorna HJN, Wilke M, Bervoets TJ, Lyaruu DM, et al. The cystic fibrosis transmembrane conductance regulator (CFTR) is expressed in maturation stage ameloblasts, odontoblasts and bone cells. *Bone*. 2010;46(4):1188-96.
124. Velard F, Delion M, Le Henaff C, Guillaume C, Gangloff S, Jacquot J, et al. Cystic fibrosis and bone disease: defective osteoblast maturation with the F508del mutation in cystic fibrosis transmembrane conductance regulator. *Am J Respir Crit Care Med*. 2014;189(6):746-8.
125. Conwell LS, Chang AB. Bisphosphonates for osteoporosis in people with cystic fibrosis. *The Cochrane database of systematic reviews*. 2009(4):CD002010.
126. Ernst MM, Johnson MC, Stark LJ. Developmental and psychosocial issues in cystic fibrosis. *Child and adolescent psychiatric clinics of North America*. 2010;19(2):263-83, viii.
127. Popli K, Stewart J. Infertility and its management in men with cystic fibrosis: review of literature and clinical practices in the UK. *Human fertility*. 2007;10(4):217-21.
128. Edenborough FP. Women with cystic fibrosis and their potential for reproduction. *Thorax*. 2001;56(8):649-55.
129. Registry UC. Annual Data Report 2012: Summary. 2013.
130. Fokkens WJ, Scheeren RA. Upper airway defence mechanisms. *Paediatric respiratory reviews*. 2000;1(4):336-41.
131. Knight DA, Holgate ST. The airway epithelium: Structural and functional properties in health and disease. *Respirology*. 2003;8(4):432-46.
132. Tarran R. Regulation of airway surface liquid volume and mucus transport by active ion transport. *Proceedings of the American Thoracic Society*. 2004;1(1):42-6.
133. Knowles MR, Boucher RC. Mucus clearance as a primary innate defense mechanism for mammalian airways. *J Clin Invest*. 2002;109(5):571-7.
134. Wine JJ. The genesis of cystic fibrosis lung disease. *J Clin Invest*. 1999;103(3):309-12.
135. Mehta H, Nazzal K, Sadikot RT. Cigarette smoking and innate immunity. *Inflamm Res*. 2008;57(11):497-503.
136. Tarran R, Button B, Boucher RC. Regulation of normal and cystic fibrosis airway surface liquid volume by phasic shear stress. *Annu Rev Physiol*. 2006;68:543-61.
137. Chilvers MA, O'Callaghan C. Local mucociliary defence mechanisms. *Paediatric respiratory reviews*. 2000;1(1):27-34.
138. Brooks SM. Perspective on the human cough reflex. *Cough*. 2011;7:10.
139. Whittsett JA, Alenghat T. Respiratory epithelial cells orchestrate pulmonary innate immunity. *Nat Immunol*. 2015;16(1):27-35.
140. Korfhagen TR, Kitzmiller J, Chen G, Sridharan A, Haitchi HM, Hegde RS, et al. SAM-pointed domain ETS factor mediates epithelial cell-intrinsic innate immune signaling during airway mucous metaplasia. *Proc Natl Acad Sci U S A*. 2012;109(41):16630-5.
141. Gordon SB, Read RC. Macrophage defences against respiratory tract infections. *British medical bulletin*. 2002;61:45-61.
142. Conese M, Copreni E, Di Gioia S, De Rinaldis P, Fumarulo R. Neutrophil recruitment and airway epithelial cell involvement in chronic cystic fibrosis lung disease. *Journal of cystic fibrosis : official journal of the European Cystic Fibrosis Society*. 2003;2(3):129-35.
143. Craig A, Mai J, Cai S, Jeyaseelan S. Neutrophil recruitment to the lungs during bacterial pneumonia. *Infection and immunity*. 2009;77(2):568-75.
144. Curtis JL. Cell-mediated adaptive immune defense of the lungs. *Proceedings of the American Thoracic Society*. 2005;2(5):412-6.
145. Corthay A. How do Regulatory T Cells Work? *Scand J Immunol*. 2009;70(4):326-36.
146. Sakaguchi S, Wing K, Onishi Y, Prieto-Martin P, Yamaguchi T. Regulatory T cells: how do they suppress immune responses? *Int Immunol*. 2009;21(10):1105-11.
147. Knowles MR, Robinson JM, Wood RE, Pue CA, Mentz WM, Wager GC, et al. Ion composition of airway surface liquid of patients with cystic fibrosis as compared with normal and disease-control subjects. *J Clin Invest*. 1997;100(10):2588-95.

148. Matsui H, Grubb BR, Tarran R, Randell SH, Gatzky JT, Davis CW, et al. Evidence for periciliary liquid layer depletion, not abnormal ion composition, in the pathogenesis of cystic fibrosis airways disease. *Cell*. 1998;95(7):1005-15.
149. Regnis JA, Robinson M, Bailey DL, Cook P, Hooper P, Chan HK, et al. Mucociliary clearance in patients with cystic fibrosis and in normal subjects. *Am J Respir Crit Care Med*. 1994;150(1):66-71.
150. Mall M, Grubb BR, Harkema JR, O'Neal WK, Boucher RC. Increased airway epithelial Na⁺ absorption produces cystic fibrosis-like lung disease in mice. *Nat Med*. 2004;10(5):487-93.
151. Konstan MW, Berger M. Current understanding of the inflammatory process in cystic fibrosis: onset and etiology. *Pediatr Pulmonol*. 1997;24(2):137-42; discussion 59-61.
152. Robinson M, Bye PT. Mucociliary clearance in cystic fibrosis. *Pediatr Pulmonol*. 2002;33(4):293-306.
153. Tarran R, Button B, Picher M, Paradiso AM, Ribeiro CM, Lazarowski ER, et al. Normal and cystic fibrosis airway surface liquid homeostasis. The effects of phasic shear stress and viral infections. *The Journal of biological chemistry*. 2005;280(42):35751-9.
154. Carmody LA, Zhao J, Schloss PD, Petrosino JF, Murray S, Young VB, et al. Changes in cystic fibrosis airway microbiota at pulmonary exacerbation. *Annals of the American Thoracic Society*. 2013;10(3):179-87.
155. Wat D. Impact of respiratory viral infections on cystic fibrosis. *Postgraduate medical journal*. 2003;79(930):201-3.
156. Armstrong D, Grimwood K, Carlin JB, Carzino R, Hull J, Olinsky A, et al. Severe viral respiratory infections in infants with cystic fibrosis. *Pediatr Pulmonol*. 1998;26(6):371-9.
157. Paes BA, Mitchell I, Banerji A, Lanctot KL, Langley JM. A decade of respiratory syncytial virus epidemiology and prophylaxis: translating evidence into everyday clinical practice. *Canadian respiratory journal : journal of the Canadian Thoracic Society*. 2011;18(2):e10-9.
158. Wang SZ, Xu H, Wraith A, Bowden JJ, Alpers JH, Forsyth KD. Neutrophils induce damage to respiratory epithelial cells infected with respiratory syncytial virus. *Eur Respir J*. 1998;12(3):612-8.
159. Chen JH, Stoltz DA, Karp PH, Ernst SE, Pezzulo AA, Moninger TO, et al. Loss of Anion Transport without Increased Sodium Absorption Characterizes Newborn Porcine Cystic Fibrosis Airway Epithelia. *Cell*. 2010;143(6):911-23.
160. Fisher JT, Tyler SR, Zhang Y, Lee BJ, Liu X, Sun X, et al. Bioelectric characterization of epithelia from neonatal CFTR knockout ferrets. *American journal of respiratory cell and molecular biology*. 2013;49(5):837-44.
161. Tuggle KL, Birket SE, Cui X, Hong J, Warren J, Reid L, et al. Characterization of defects in ion transport and tissue development in cystic fibrosis transmembrane conductance regulator (CFTR)-knockout rats. *PLoS one*. 2014;9(3):e91253.
162. Keiser NW, Birket SE, Evans IA, Tyler SR, Croke AK, Sun X, et al. Defective Innate Immunity and Hyper-Inflammation in Newborn CFTR-Knockout Ferret Lungs. *American journal of respiratory cell and molecular biology*. 2014.
163. Griesenbach U, Soussi S, Larsen MB, Casamayor I, Dewar A, Regamey N, et al. Quantification of Periciliary Fluid Height in Human Airway Biopsies Is Feasible, but Not Suitable as a Biomarker. *American journal of respiratory cell and molecular biology*. 2011;44(3):309-15.
164. Zabner J, Smith JJ, Karp PH, Widdicombe JH, Welsh MJ. Loss of CFTR chloride channels alters salt absorption by cystic fibrosis airway epithelia in vitro. *Mol Cell*. 1998;2(3):397-403.
165. Smith JJ, Travis SM, Greenberg EP, Welsh MJ. Cystic fibrosis airway epithelia fail to kill bacteria because of abnormal airway surface fluid (vol 85, pg 229, 1996). *Cell*. 1996;87(2):U25-U.
166. Hull J, Skinner W, Robertson C, Phelan P. Elemental content of airway surface liquid from infants with cystic fibrosis. *Am J Respir Crit Care Med*. 1998;157(1):10-4.
167. Zheng S, De BP, Choudhary S, Comhair SA, Goggans T, Slee R, et al. Impaired innate host defense causes susceptibility to respiratory virus infections in cystic fibrosis. *Immunity*. 2003;18(5):619-30.

168. Bruscia EM, Zhang PX, Ferreira E, Caputo C, Emerson JW, Tuck D, et al. Macrophages directly contribute to the exaggerated inflammatory response in cystic fibrosis transmembrane conductance regulator-/- mice. *American journal of respiratory cell and molecular biology*. 2009;40(3):295-304.
169. Gehrig S, Duerr J, Weitnauer M, Wagner CJ, Graeber SY, Schatterny J, et al. Lack of Neutrophil Elastase Reduces Inflammation, Mucus Hypersecretion, and Emphysema, but Not Mucus Obstruction, in Mice with Cystic Fibrosis-like Lung Disease. *Am J Resp Crit Care*. 2014;189(9):1082-92.
170. Bonfield TL, Hodges CA, Cotton CU, Drumm ML. Absence of the cystic fibrosis transmembrane regulator (Cftr) from myeloid-derived cells slows resolution of inflammation and infection. *J Leukoc Biol*. 2012;92(5):1111-22.
171. Khan TZ, Wagener JS, Bost T, Martinez J, Accurso FJ, Riches DW. Early pulmonary inflammation in infants with cystic fibrosis. *Am J Respir Crit Care Med*. 1995;151(4):1075-82.
172. Pillarisetti N, Williamson E, Linnane B, Skoric B, Robertson CF, Robinson P, et al. Infection, inflammation, and lung function decline in infants with cystic fibrosis. *Am J Respir Crit Care Med*. 2011;184(1):75-81.
173. Stoltz DA, Meyerholz DK, Pezzulo AA, Ramachandran S, Rogan MP, Davis GJ, et al. Cystic fibrosis pigs develop lung disease and exhibit defective bacterial eradication at birth. *Science translational medicine*. 2010;2(29):29ra31.
174. Pezzulo AA, Tang XX, Hoegger MJ, Alaiwa MH, Ramachandran S, Moninger TO, et al. Reduced airway surface pH impairs bacterial killing in the porcine cystic fibrosis lung. *Nature*. 2012;487(7405):109-13.
175. Abou Alaiwa MH, Reznikov LR, Gansemer ND, Sheets KA, Horswill AR, Stoltz DA, et al. pH modulates the activity and synergism of the airway surface liquid antimicrobials beta-defensin-3 and LL-37. *P Natl Acad Sci USA*. 2014;111(52):18703-8.
176. Quinton PM. Cystic fibrosis: impaired bicarbonate secretion and mucoviscidosis. *Lancet*. 2008;372(9636):415-7.
177. Gustafsson JK, Ermund A, Ambort D, Johansson ME, Nilsson HE, Thorell K, et al. Bicarbonate and functional CFTR channel are required for proper mucin secretion and link cystic fibrosis with its mucus phenotype. *The Journal of experimental medicine*. 2012;209(7):1263-72.
178. Abou Alaiwa MH, Beer AM, Pezzulo AA, Launspach JL, Horan RA, Stoltz DA, et al. Neonates with cystic fibrosis have a reduced nasal liquid pH; A small pilot study. *Journal of Cystic Fibrosis*. 2014;13(4):373-7.
179. McShane D, Davies JC, Davies MG, Bush A, Geddes DM, Alton EW. Airway surface pH in subjects with cystic fibrosis. *Eur Respir J*. 2003;21(1):37-42.
180. Lyczak JB, Cannon CL, Pier GB. Lung infections associated with cystic fibrosis. *Clinical microbiology reviews*. 2002;15(2):194-222.
181. Van Ewijk BE, Wolfs TF, Aerts PC, Van Kessel KP, Fleer A, Kimpen JL, et al. RSV mediates *Pseudomonas aeruginosa* binding to cystic fibrosis and normal epithelial cells. *Pediatr Res*. 2007;61(4):398-403.
182. Hoiby N. Recent advances in the treatment of *Pseudomonas aeruginosa* infections in cystic fibrosis. *BMC medicine*. 2011;9:32.
183. Foundation CF. Cystic Fibrosis Foundation Patient Registry 2013 Annual Data Report to the Center Directors. Bethesda, Maryland. 2013.
184. Hilty M, Burke C, Pedro H, Cardenas P, Bush A, Bossley C, et al. Disordered microbial communities in asthmatic airways. *PloS one*. 2010;5(1):e8578.
185. Zemanick ET, Wagner BD, Harris JK, Wagener JS, Accurso FJ, Sagel SD. Pulmonary exacerbations in cystic fibrosis with negative bacterial cultures. *Pediatr Pulmonol*. 2010;45(6):569-77.
186. Dickson RP, Erb-Downward JR, Huffnagle GB. The role of the bacterial microbiome in lung disease. *Expert review of respiratory medicine*. 2013;7(3):245-57.

187. Bruzzese E, Raia V, Spagnuolo MI, Volpicelli M, De Marco G, Maiuri L, et al. Effect of Lactobacillus GG supplementation on pulmonary exacerbations in patients with cystic fibrosis: a pilot study. *Clinical nutrition*. 2007;26(3):322-8.
188. Emerson J, Rosenfeld M, McNamara S, Ramsey B, Gibson RL. Pseudomonas aeruginosa and other predictors of mortality and morbidity in young children with cystic fibrosis. *Pediatr Pulmonol*. 2002;34(2):91-100.
189. Valerius NH, Koch C, Hoiby N. Prevention of chronic Pseudomonas aeruginosa colonisation in cystic fibrosis by early treatment. *Lancet*. 1991;338(8769):725-6.
190. Tramper-Stranders GA, van der Ent CK, Wolfs TF. Detection of Pseudomonas aeruginosa in patients with cystic fibrosis. *Journal of cystic fibrosis : official journal of the European Cystic Fibrosis Society*. 2005;4 Suppl 2:37-43.
191. Hilliard TN, Sukhani S, Francis J, Madden N, Rosenthal M, Balfour-Lynn I, et al. Bronchoscopy following diagnosis with cystic fibrosis. *Arch Dis Child*. 2007;92(10):898-9.
192. Gutierrez JP, Grimwood K, Armstrong DS, Carlin JB, Carzino R, Olinsky A, et al. Interlobar differences in bronchoalveolar lavage fluid from children with cystic fibrosis. *Eur Respir J*. 2001;17(2):281-6.
193. Gilchrist FJ, Salamat S, Clayton S, Peach J, Alexander J, Lenney W. Bronchoalveolar lavage in children with cystic fibrosis: how many lobes should be sampled? *Arch Dis Child*. 2011;96(3):215-7.
194. Ratjen F, Walter H, Haug M, Meisner C, Grasemann H, Doring G. Diagnostic value of serum antibodies in early Pseudomonas aeruginosa infection in cystic fibrosis patients. *Pediatr Pulmonol*. 2007;42(3):249-55.
195. Jensen PO, Givskov M, Bjarnsholt T, Moser C. The immune system vs. Pseudomonas aeruginosa biofilms. *FEMS immunology and medical microbiology*. 2010;59(3):292-305.
196. Stewart PS, Costerton JW. Antibiotic resistance of bacteria in biofilms. *Lancet*. 2001;358(9276):135-8.
197. Davies JC, Bilton D. Bugs, biofilms, and resistance in cystic fibrosis. *Respir Care*. 2009;54(5):628-40.
198. O'Toole GA, Kolter R. Flagellar and twitching motility are necessary for Pseudomonas aeruginosa biofilm development. *Mol Microbiol*. 1998;30(2):295-304.
199. Singh PK, Schaefer AL, Parsek MR, Moninger TO, Welsh MJ, Greenberg EP. Quorum-sensing signals indicate that cystic fibrosis lungs are infected with bacterial biofilms. *Nature*. 2000;407(6805):762-4.
200. Donlan RM, Costerton JW. Biofilms: survival mechanisms of clinically relevant microorganisms. *Clinical microbiology reviews*. 2002;15(2):167-93.
201. Lewis K. Persister cells. *Annual review of microbiology*. 2010;64:357-72.
202. Wagner VE, Iglewski BH. P. aeruginosa Biofilms in CF Infection. *Clinical reviews in allergy & immunology*. 2008;35(3):124-34.
203. Organisation WH. Antimicrobial Resistance2013. Available from: <http://www.who.int/mediacentre/factsheets/fs194/en/>.
204. Poole K. Multidrug efflux pumps and antimicrobial resistance in Pseudomonas aeruginosa and related organisms. *J Mol Microbiol Biotechnol*. 2001;3(2):255-64.
205. Ratjen F, Brockhaus F, Angyalosi G. Aminoglycoside therapy against Pseudomonas aeruginosa in cystic fibrosis: a review. *Journal of cystic fibrosis : official journal of the European Cystic Fibrosis Society*. 2009;8(6):361-9.
206. Gaspar MC, Couet W, Olivier JC, Pais AA, Sousa JJ. Pseudomonas aeruginosa infection in cystic fibrosis lung disease and new perspectives of treatment: a review. *European journal of clinical microbiology & infectious diseases : official publication of the European Society of Clinical Microbiology*. 2013;32(10):1231-52.
207. Ishida H, Ishida Y, Kurosaka Y, Otani T, Sato K, Kobayashi H. In vitro and in vivo activities of levofloxacin against biofilm-producing Pseudomonas aeruginosa. *Antimicrobial agents and chemotherapy*. 1998;42(7):1641-5.

208. Spellberg B, Guidos R, Gilbert D, Bradley J, Boucher HW, Scheld WM, et al. The epidemic of antibiotic-resistant infections: a call to action for the medical community from the Infectious Diseases Society of America. *Clinical infectious diseases : an official publication of the Infectious Diseases Society of America*. 2008;46(2):155-64.
209. Lister PD, Wolter DJ, Hanson ND. Antibacterial-resistant *Pseudomonas aeruginosa*: clinical impact and complex regulation of chromosomally encoded resistance mechanisms. *Clinical microbiology reviews*. 2009;22(4):582-610.
210. Livermore DM. Multiple mechanisms of antimicrobial resistance in *Pseudomonas aeruginosa*: our worst nightmare? *Clinical infectious diseases : an official publication of the Infectious Diseases Society of America*. 2002;34(5):634-40.
211. Cohen TS, Prince A. Cystic fibrosis: a mucosal immunodeficiency syndrome. *Nat Med*. 2012;18(4):509-19.
212. Sallenave JM. Phagocytic and signaling innate immune receptors: are they dysregulated in cystic fibrosis in the fight against *Pseudomonas aeruginosa*? *The international journal of biochemistry & cell biology*. 2014;52:103-7.
213. Lavoie EG, Wangdi T, Kazmierczak BI. Innate immune responses to *Pseudomonas aeruginosa* infection. *Microbes and infection / Institut Pasteur*. 2011;13(14-15):1133-45.
214. Luan X, Campanucci VA, Nair M, Yilmaz O, Belev G, Machen TE, et al. *Pseudomonas aeruginosa* triggers CFTR-mediated airway surface liquid secretion in swine trachea. *Proc Natl Acad Sci U S A*. 2014;111(35):12930-5.
215. Van de Weert-van Leeuwen PB, Van Meegen MA, Speirs JJ, Pals DJ, Rooijackers SH, Van der Ent CK, et al. Optimal complement-mediated phagocytosis of *Pseudomonas aeruginosa* by monocytes is cystic fibrosis transmembrane conductance regulator-dependent. *American journal of respiratory cell and molecular biology*. 2013;49(3):463-70.
216. Mueller-Ortiz SL, Drouin SM, Wetsel RA. The alternative activation pathway and complement component C3 are critical for a protective immune response against *Pseudomonas aeruginosa* in a murine model of pneumonia. *Infection and immunity*. 2004;72(5):2899-906.
217. Park JE, Yung R, Stefanowicz D, Shumansky K, Akhbar L, Durie PR, et al. Cystic fibrosis modifier genes related to *Pseudomonas aeruginosa* infection. *Genes and immunity*. 2011;12(5):370-7.
218. Descamps D, Le Gars M, Balloy V, Barbier D, Maschalidi S, Tohme M, et al. Toll-like receptor 5 (TLR5), IL-1beta secretion, and asparagine endopeptidase are critical factors for alveolar macrophage phagocytosis and bacterial killing. *Proc Natl Acad Sci U S A*. 2012;109(5):1619-24.
219. Gribar SC, Richardson WM, Sodhi CP, Hackam DJ. No longer an innocent bystander: epithelial toll-like receptor signaling in the development of mucosal inflammation. *Molecular medicine*. 2008;14(9-10):645-59.
220. Hemmi H, Takeuchi O, Kawai T, Kaisho T, Sato S, Sanjo H, et al. A Toll-like receptor recognizes bacterial DNA. *Nature*. 2000;408(6813):740-5.
221. Noulin N, Quesniaux VFJ, Schnyder-Candrian S, Schnyder B, Maillat I, Robert T, et al. Both hemopoietic and resident cells are required for MyD88-dependent pulmonary inflammatory response to inhaled endotoxin. *Journal of immunology*. 2005;175(10):6861-9.
222. Hajjar AM, Harowicz H, Liggitt HD, Fink PJ, Wilson CB, Skerrett SJ. An essential role for non-bone marrow-derived cells in control of *Pseudomonas aeruginosa* pneumonia. *American journal of respiratory cell and molecular biology*. 2005;33(5):470-5.
223. Blohmke CJ, Park J, Hirschfeld AF, Victor RE, Schneiderman J, Stefanowicz D, et al. TLR5 as an Anti-Inflammatory Target and Modifier Gene in Cystic Fibrosis. *Journal of immunology*. 2010;185(12):7731-8.
224. Deschaght P, Van Daele S, De Baets F, Vanechoutte M. PCR and the detection of *Pseudomonas aeruginosa* in respiratory samples of CF patients. A literature review. *Journal of cystic fibrosis : official journal of the European Cystic Fibrosis Society*. 2011;10(5):293-7.

225. Delhaes L, Monchy S, Frealle E, Hubans C, Salleron J, Leroy S, et al. The airway microbiota in cystic fibrosis: a complex fungal and bacterial community--implications for therapeutic management. *PloS one*. 2012;7(4):e36313.
226. Lynch SV, Bruce KD. The cystic fibrosis airway microbiome. *Cold Spring Harbor perspectives in medicine*. 2013;3(3):a009738.
227. Pedersen SS, Espersen F, Hoiby N. Diagnosis of chronic *Pseudomonas aeruginosa* infection in cystic fibrosis by enzyme-linked immunosorbent assay. *Journal of clinical microbiology*. 1987;25(10):1830-6.
228. Fomsgaard A, Dinesen B, Shand GH, Pressler T, Hoiby N. Antilipopolysaccharide antibodies and differential diagnosis of chronic *Pseudomonas aeruginosa* lung infection in cystic fibrosis. *Journal of clinical microbiology*. 1989;27(6):1222-9.
229. Pressler T, Frederiksen B, Skov M, Garred P, Koch C, Hoiby N. Early rise of anti-pseudomonas antibodies and a mucoid phenotype of *pseudomonas aeruginosa* are risk factors for development of chronic lung infection--a case control study. *Journal of cystic fibrosis : official journal of the European Cystic Fibrosis Society*. 2006;5(1):9-15.
230. Al-Saleh S, Dell SD, Grasemann H, Yau YC, Waters V, Martin S, et al. Sputum induction in routine clinical care of children with cystic fibrosis. *The Journal of pediatrics*. 2010;157(6):1006-11 e1.
231. Suri R, Marshall LJ, Wallis C, Metcalfe C, Shute JK, Bush A. Safety and use of sputum induction in children with cystic fibrosis. *Pediatr Pulm*. 2003;35(4):309-13.
232. Cheng K, Smyth RL, Govan JR, Doherty C, Winstanley C, Denning N, et al. Spread of beta-lactam-resistant *Pseudomonas aeruginosa* in a cystic fibrosis clinic. *Lancet*. 1996;348(9028):639-42.
233. Tubbs D, Lenney W, Alcock P, Campbell CA, Gray J, Pantin C. *Pseudomonas aeruginosa* in cystic fibrosis: cross-infection and the need for segregation. *Respir Med*. 2001;95(2):147-52.
234. Griffiths AL, Jansen K, Carlin JB, Grimwood K, Carzino R, Robinson PJ, et al. Effects of segregation on an epidemic *Pseudomonas aeruginosa* strain in a cystic fibrosis clinic. *Am J Respir Crit Care Med*. 2005;171(9):1020-5.
235. Ashish A, Shaw M, Winstanley C, Humphreys L, Walshaw MJ. Halting the spread of epidemic *pseudomonas aeruginosa* in an adult cystic fibrosis centre: a prospective cohort study. *JRSM short reports*. 2013;4(1):1.
236. Jones AM, Dodd ME, Morris J, Doherty C, Govan JR, Webb AK. Clinical outcome for cystic fibrosis patients infected with transmissible *pseudomonas aeruginosa*: an 8-year prospective study. *Chest*. 2010;137(6):1405-9.
237. Flume PA, Robinson KA, O'Sullivan BP, Finder JD, Vender RL, Willey-Courand DB, et al. Cystic fibrosis pulmonary guidelines: airway clearance therapies. *Respir Care*. 2009;54(4):522-37.
238. Volsko TA. Cystic fibrosis and the respiratory therapist: a 50-year perspective. *Respir Care*. 2009;54(5):587-94.
239. Bradley JM, Moran FM, Elborn JS. Evidence for physical therapies (airway clearance and physical training) in cystic fibrosis: an overview of five Cochrane systematic reviews. *Respir Med*. 2006;100(2):191-201.
240. McIlwaine MP, Alarie N, Davidson GF, Lands LC, Ratjen F, Milner R, et al. Long-term multicentre randomised controlled study of high frequency chest wall oscillation versus positive expiratory pressure mask in cystic fibrosis. *Thorax*. 2013;68(8):746-51.
241. Shak S, Capon DJ, Hellmiss R, Marsters SA, Baker CL. Recombinant human DNase I reduces the viscosity of cystic fibrosis sputum. *Proc Natl Acad Sci U S A*. 1990;87(23):9188-92.
242. Jones AP, Wallis C. Dornase alfa for cystic fibrosis. *The Cochrane database of systematic reviews*. 2010(3):CD001127.
243. Fuchs HJ, Borowitz DS, Christiansen DH, Morris EM, Nash ML, Ramsey BW, et al. Effect of aerosolized recombinant human DNase on exacerbations of respiratory symptoms and on pulmonary function in patients with cystic fibrosis. *The Pulmozyme Study Group. The New England journal of medicine*. 1994;331(10):637-42.

244. Griese M, App EM, Duroux A, Burkert A, Schams A. Recombinant human DNase (rhDNase) influences phospholipid composition, surface activity, rheology and consecutively clearance indices of cystic fibrosis sputum. *Pulmonary pharmacology & therapeutics*. 1997;10(1):21-7.
245. Williams HD, Behrends V, Bundy JG, Ryall B, Zlosnik JE. Hypertonic Saline Therapy in Cystic Fibrosis: Do Population Shifts Caused by the Osmotic Sensitivity of Infecting Bacteria Explain the Effectiveness of this Treatment? *Frontiers in microbiology*. 2010;1:120.
246. Elkins MR, Bye PT. Inhaled hypertonic saline as a therapy for cystic fibrosis. *Current opinion in pulmonary medicine*. 2006;12(6):445-52.
247. Wark P, McDonald VM. Nebulised hypertonic saline for cystic fibrosis. *The Cochrane database of systematic reviews*. 2009(2):CD001506.
248. Bilton D, Robinson P, Cooper P, Gallagher CG, Kolbe J, Fox H, et al. Inhaled dry powder mannitol in cystic fibrosis: an efficacy and safety study. *Eur Respir J*. 2011;38(5):1071-80.
249. Jaques A, Daviskas E, Turton JA, McKay K, Cooper P, Stirling RG, et al. Inhaled mannitol improves lung function in cystic fibrosis. *Chest*. 2008;133(6):1388-96.
250. Lands LC, Stanojevic S. Oral non-steroidal anti-inflammatory drug therapy for lung disease in cystic fibrosis. *The Cochrane database of systematic reviews*. 2013;6:CD001505.
251. Ross KR, Chmiel JF, Konstan MW. The role of inhaled corticosteroids in the management of cystic fibrosis. *Paediatric drugs*. 2009;11(2):101-13.
252. Balfour-Lynn IM, Elborn JS. "CF asthma": what is it and what do we do about it? *Thorax*. 2002;57(8):742-8.
253. Balfour-Lynn IM, Lees B, Hall P, Phillips G, Khan M, Flather M, et al. Multicenter randomized controlled trial of withdrawal of inhaled corticosteroids in cystic fibrosis. *Am J Respir Crit Care Med*. 2006;173(12):1356-62.
254. Cox G. Glucocorticoid treatment inhibits apoptosis in human neutrophils. Separation of survival and activation outcomes. *Journal of immunology*. 1995;154(9):4719-25.
255. Andrejak C, Nielsen R, Thomsen VO, Duhaut P, Sorensen HT, Thomsen RW. Chronic respiratory disease, inhaled corticosteroids and risk of non-tuberculous mycobacteriosis. *Thorax*. 2013;68(3):256-62.
256. Martin M, Shaw D. Effect of inhaled corticosteroids on the microbiology of the respiratory tract. *Respirology*. 2013;18(2):201-2.
257. Binder AM, Adjemian J, Olivier KN, Prevots DR. Epidemiology of nontuberculous mycobacterial infections and associated chronic macrolide use among persons with cystic fibrosis. *Am J Respir Crit Care Med*. 2013;188(7):807-12.
258. Wong C, Jayaram L, Karalus N, Eaton T, Tong C, Hockey H, et al. Azithromycin for prevention of exacerbations in non-cystic fibrosis bronchiectasis (EMBRACE): a randomised, double-blind, placebo-controlled trial. *Lancet*. 2012;380(9842):660-7.
259. Yousef AA, Jaffe A. The Role of Azithromycin in Patients with Cystic Fibrosis. *Paediatric respiratory reviews*. 2010;11(2):108-14.
260. Hoffmann N, Lee B, Hentzer M, Rasmussen TB, Song Z, Johansen HK, et al. Azithromycin blocks quorum sensing and alginate polymer formation and increases the sensitivity to serum and stationary-growth-phase killing of *Pseudomonas aeruginosa* and attenuates chronic *P. aeruginosa* lung infection in *Cftr(-/-)* mice. *Antimicrobial agents and chemotherapy*. 2007;51(10):3677-87.
261. Happoldt C, Caceres S, Malcolm KC, Taylor-Cousar JL, Saavedra MT, Nick JA, et al. Azithromycin Upregulates Adaptive Resistance Genes in *P. Aeruginosa* Biofilm Aggregates and Alters in Vitro Resistance to Antibiotics. *Pediatr Pulm*. 2014;49:320-.
262. Griese M, Kappler M, Eismann C, Ballmann M, Junge S, Rietschel E, et al. Inhalation treatment with glutathione in patients with cystic fibrosis. A randomized clinical trial. *Am J Respir Crit Care Med*. 2013;188(1):83-9.
263. Tirouvanziam R, Conrad CK, Bottiglieri T, Herzenberg LA, Moss RB, Herzenberg LA. High-dose oral N-acetylcysteine, a glutathione prodrug, modulates inflammation in cystic fibrosis. *Proc Natl Acad Sci U S A*. 2006;103(12):4628-33.

264. Clinical Guidelines: Care of Children with Cystic Fibrosis. Royal Brompton Hospital: Royal Brompton Hospital; 2014. Available from: www.rbht/nhs/uk/childrencf.
265. Smyth AR, Walters S. Prophylactic anti-staphylococcal antibiotics for cystic fibrosis. The Cochrane database of systematic reviews. 2014;11:CD001912.
266. Lillquist YP, Cho E, Davidson AG. Economic effects of an eradication protocol for first appearance of *Pseudomonas aeruginosa* in cystic fibrosis patients: 1995 vs. 2009. *Journal of cystic fibrosis : official journal of the European Cystic Fibrosis Society*. 2011;10(3):175-80.
267. Langton Hewer SC, Smyth AR. Antibiotic strategies for eradicating *Pseudomonas aeruginosa* in people with cystic fibrosis. The Cochrane database of systematic reviews. 2014;11:CD004197.
268. Retsch-Bogart GZ, Quittner AL, Gibson RL, Oermann CM, McCoy KS, Montgomery AB, et al. Efficacy and safety of inhaled aztreonam lysine for airway *Pseudomonas* in cystic fibrosis. *Chest*. 2009;135(5):1223-32.
269. Strandvik B, Hjelte L, Malmborg AS, Widen B. Home intravenous antibiotic treatment of patients with cystic fibrosis. *Acta paediatrica*. 1992;81(4):340-4.
270. Derichs N. Targeting a genetic defect: cystic fibrosis transmembrane conductance regulator modulators in cystic fibrosis. *European respiratory review : an official journal of the European Respiratory Society*. 2013;22(127):58-65.
271. Rowe SM, Heltshe SL, Gonska T, Donaldson SH, Borowitz D, Gelfond D, et al. Clinical mechanism of the cystic fibrosis transmembrane conductance regulator potentiator ivacaftor in G551D-mediated cystic fibrosis. *Am J Respir Crit Care Med*. 2014;190(2):175-84.
272. Nunley DR, Grgurich W, Iacono AT, Yousem S, Ohori NP, Keenan RJ, et al. Allograft colonization and infections with *Pseudomonas* in cystic fibrosis lung transplant recipients. *Chest*. 1998;113(5):1235-43.
273. Hofer M, Benden C, Inci I, Schmid C, Irani S, Speich R, et al. True survival benefit of lung transplantation for cystic fibrosis patients: the Zurich experience. *The Journal of heart and lung transplantation : the official publication of the International Society for Heart Transplantation*. 2009;28(4):334-9.
274. Inci I, Stanimirov O, Benden C, Kestenholz P, Hofer M, Boehler A, et al. Lung transplantation for cystic fibrosis: a single center experience of 100 consecutive cases. *European journal of cardio-thoracic surgery : official journal of the European Association for Cardio-thoracic Surgery*. 2012;41(2):435-40.
275. Aurora P, Spencer H, Moreno-Galdo A. Lung transplantation in children with cystic fibrosis: a view from Europe. *Am J Respir Crit Care Med*. 2008;177(9):935-6.
276. Walter S, Gudowius P, Bosshammer J, Romling U, Weissbrodt H, Schurmann W, et al. Epidemiology of chronic *Pseudomonas aeruginosa* infections in the airways of lung transplant recipients with cystic fibrosis. *Thorax*. 1997;52(4):318-21.
277. Kenny SL, Shaw TD, Downey DG, Moore JE, Rendall JC, Elborn JS. Eradication of *Pseudomonas aeruginosa* in adults with cystic fibrosis. *BMJ open respiratory research*. 2014;1(1):e000021.
278. Mayer-Hamblett N, Kronmal RA, Gibson RL, Rosenfeld M, Retsch-Bogart G, Treggiari MM, et al. Initial *Pseudomonas aeruginosa* treatment failure is associated with exacerbations in cystic fibrosis. *Pediatr Pulm*. 2012;47(2):125-34.
279. Alton EW, Middleton PG, Caplen NJ, Smith SN, Steel DM, Munkonge FM, et al. Non-invasive liposome-mediated gene delivery can correct the ion transport defect in cystic fibrosis mutant mice. *Nature genetics*. 1993;5(2):135-42.
280. Sanders N, Rudolph C, Braeckmans K, De Smedt SC, Demeester J. Extracellular barriers in respiratory gene therapy. *Advanced drug delivery reviews*. 2009;61(2):115-27.
281. Thomas CE, Ehrhardt A, Kay MA. Progress and problems with the use of viral vectors for gene therapy. *Nat Rev Genet*. 2003;4(5):346-58.

282. Alton EW, Stern M, Farley R, Jaffe A, Chadwick SL, Phillips J, et al. Cationic lipid-mediated CFTR gene transfer to the lungs and nose of patients with cystic fibrosis: a double-blind placebo-controlled trial. *Lancet*. 1999;353(9157):947-54.
283. Alton EW, Armstrong DK, Ashby D, Bayfield KJ, Bilton D, Bloomfield EV, et al. Repeated nebulisation of non-viral CFTR gene therapy in patients with cystic fibrosis: a randomised, double-blind, placebo-controlled, phase 2b trial. *The Lancet Respiratory Medicine*. 2015.
284. Wilschanski M, Miller LL, Shoseyov D, Blau H, Rivlin J, Aviram M, et al. Chronic ataluren (PTC124) treatment of nonsense mutation cystic fibrosis. *Eur Respir J*. 2011;38(1):59-69.
285. Clancy JP, Rowe SM, Accurso FJ, Aitken ML, Amin RS, Ashlock MA, et al. Results of a phase IIa study of VX-809, an investigational CFTR corrector compound, in subjects with cystic fibrosis homozygous for the F508del-CFTR mutation. *Thorax*. 2012;67(1):12-8.
286. Wainwright CE, Elborn JS, Ramsey BW, Marigowda G, Huang X, Cipolli M, et al. Lumacaftor-Ivacaftor in Patients with Cystic Fibrosis Homozygous for Phe508del CFTR. *The New England Journal of Medicine*. 2015.
287. Woods DE, Straus DC, Johanson WG, Jr., Berry VK, Bass JA. Role of pili in adherence of *Pseudomonas aeruginosa* to mammalian buccal epithelial cells. *Infection and Immunity*. 1980;29(3):1146-51.
288. Liedberg H, Lundberg T. Silver coating of urinary catheters prevents adherence and growth of *Pseudomonas aeruginosa*. *Urological Research*. 1989;17(6):357-8.
289. Azghani AO, Williams I, Holiday DB, Johnson AR. A beta-linked mannan inhibits adherence of *Pseudomonas aeruginosa* to human lung epithelial cells. *Glycobiology*. 1995;5(1):39-44.
290. Girod S, Galabert C, Lecuire A, Zahm JM, Puchelle E. Phospholipid composition and surface-active properties of tracheobronchial secretions from patients with cystic fibrosis and chronic obstructive pulmonary diseases. *Pediatr Pulmonol*. 1992;13(1):22-7.
291. Hurley MN, Camara M, Smyth AR. Novel approaches to the treatment of *Pseudomonas aeruginosa* infections in cystic fibrosis. *Eur Respir J*. 2012;40(4):1014-23.
292. Bjarnsholt T, Jensen PO, Rasmussen TB, Christophersen L, Calum H, Hentzer M, et al. Garlic blocks quorum sensing and promotes rapid clearing of pulmonary *Pseudomonas aeruginosa* infections. *Microbiology*. 2005;151(Pt 12):3873-80.
293. Alkawash MA, Soothill JS, Schiller NL. Alginate lyase enhances antibiotic killing of mucoid *Pseudomonas aeruginosa* in biofilms. *APMIS : Acta Pathologica, Microbiologica, et Immunologica Scandinavica*. 2006;114(2):131-8.
294. Lappala JW, Griswold KE. Alginate lyase exhibits catalysis-independent biofilm dispersion and antibiotic synergy. *Antimicrobial Agents and Chemotherapy*. 2013;57(1):137-45.
295. Salta M, Wharton JA, Dennington SP, Stoodley P, Stokes KR. Anti-biofilm performance of three natural products against initial bacterial attachment. *International Journal of Molecular Sciences*. 2013;14(11):21757-80.
296. Khan S, Tondervik A, Sletta H, Klinkenberg G, Emanuel C, Onsoyen E, et al. Overcoming drug resistance with alginate oligosaccharides able to potentiate the action of selected antibiotics. *Antimicrobial Agents and Chemotherapy*. 2012;56(10):5134-41.
297. Yoon SS, Coakley R, Lau GW, Lyman SV, Gaston B, Karabulut AC, et al. Anaerobic killing of mucoid *Pseudomonas aeruginosa* by acidified nitrite derivatives under cystic fibrosis airway conditions. *J Clin Invest*. 2006;116(2):436-46.
298. Zemke A, Lashua L, Gladwin M, Bomberger J. Sodium nitrite disrupts biotic biofilm formation by *Pseudomonas aeruginosa* on polarized human airway epithelial cells. *Nitric Oxide-Biol Ch*. 2013;31:S13-S4.
299. Major TA, Panmanee W, Mortensen JE, Gray LD, Hoglen N, Hassett DJ. Sodium nitrite-mediated killing of the major cystic fibrosis pathogens *Pseudomonas aeruginosa*, *Staphylococcus aureus*, and *Burkholderia cepacia* under anaerobic planktonic and biofilm conditions. *Antimicrobial Agents and Chemotherapy*. 2010;54(11):4671-7.

300. Banin E, Vasil ML, Greenberg EP. Iron and *Pseudomonas aeruginosa* biofilm formation. *Proc Natl Acad Sci U S A*. 2005;102(31):11076-81.
301. Musk DJ, Banko DA, Hergenrother PJ. Iron salts perturb biofilm formation and disrupt existing biofilms of *Pseudomonas aeruginosa*. *Chemistry & biology*. 2005;12(7):789-96.
302. Musk DJ, Jr., Hergenrother PJ. Chelated iron sources are inhibitors of *Pseudomonas aeruginosa* biofilms and distribute efficiently in an in vitro model of drug delivery to the human lung. *Journal of applied microbiology*. 2008;105(2):380-8.
303. Walker TS, Tomlin KL, Worthen GS, Poch KR, Lieber JG, Saavedra MT, et al. Enhanced *Pseudomonas aeruginosa* biofilm development mediated by human neutrophils. *Infection and immunity*. 2005;73(6):3693-701.
304. Parks QM, Young RL, Poch KR, Malcolm KC, Vasil ML, Nick JA. Neutrophil enhancement of *Pseudomonas aeruginosa* biofilm development: human F-actin and DNA as targets for therapy. *Journal of medical microbiology*. 2009;58(Pt 4):492-502.
305. McElvaney NG, Doujaiji B, Moan MJ, Burnham MR, Wu MC, Crystal RG. Pharmacokinetics of recombinant secretory leukoprotease inhibitor aerosolized to normals and individuals with cystic fibrosis. *The American review of respiratory disease*. 1993;148(4 Pt 1):1056-60.
306. McElvaney NG, Hubbard RC, Birrer P, Chernick MS, Caplan DB, Frank MM, et al. Aerosol Alpha-1-Antitrypsin Treatment for Cystic-Fibrosis. *Lancet*. 1991;337(8738):392-4.
307. Martin SL, Downey D, Bilton D, Keogan MT, Edgar J, Elborn JS, et al. Safety and efficacy of recombinant alpha(1)-antitrypsin therapy in cystic fibrosis. *Pediatr Pulm*. 2006;41(2):177-83.
308. Mahadeva R, Stewart S, Bilton D, Lomas DA. Alpha-1 antitrypsin deficiency alleles and severe cystic fibrosis lung disease. *Thorax*. 1998;53(12):1022-4.
309. Mosmann TR, Coffman RL. TH1 and TH2 cells: different patterns of lymphokine secretion lead to different functional properties. *Annual review of immunology*. 1989;7:145-73.
310. Johansen HK, Hougen HP, Rygaard J, Hoiby N. Interferon-gamma (IFN-gamma) treatment decreases the inflammatory response in chronic *Pseudomonas aeruginosa* pneumonia in rats. *Clinical and experimental immunology*. 1996;103(2):212-8.
311. Moss RB, Mayer-Hamblett N, Wagener J, Daines C, Hale K, Ahrens R, et al. Randomized, double-blind, placebo-controlled, dose-escalating study of aerosolized interferon gamma-1b in patients with mild to moderate cystic fibrosis lung disease. *Pediatr Pulmonol*. 2005;39(3):209-18.
312. Assani K, Tazi MF, Amer AO, Kopp BT. IFN-gamma stimulates autophagy-mediated clearance of *Burkholderia cenocepacia* in human cystic fibrosis macrophages. *PloS one*. 2014;9(5):e96681.
313. Mayer ML, Blohmke CJ, Falsafi R, Fjell CD, Madera L, Turvey SE, et al. Rescue of dysfunctional autophagy attenuates hyperinflammatory responses from cystic fibrosis cells. *Journal of immunology*. 2013;190(3):1227-38.
314. Knolle MD, Wilkinson A, Gorgono D, Grady D, Cox C, Barker H, et al., editors. Interferon Gamma Adjuvant Therapy For Pulmonary NTM Disease In Patients With Cystic Fibrosis. B38 UPDATE IN ADULT CYSTIC FIBROSIS; 2014: American Thoracic Society.
315. Ford-Hutchinson AW, Bray MA, Doig MV, Shipley ME, Smith MJ. Leukotriene B, a potent chemokinetic and aggregating substance released from polymorphonuclear leukocytes. *Nature*. 1980;286(5770):264-5.
316. Konstan MW, Doring G, Heltshe SL, Lands LC, Hilliard KA, Koker P, et al. A randomized double blind, placebo controlled phase 2 trial of BIIL 284 BS (an LTB4 receptor antagonist) for the treatment of lung disease in children and adults with cystic fibrosis. *Journal of cystic fibrosis : official journal of the European Cystic Fibrosis Society*. 2014;13(2):148-55.
317. Doring G, Bragonzi A, Paroni M, Akturk FF, Cigana C, Schmidt A, et al. BIIL 284 reduces neutrophil numbers but increases *P. aeruginosa* bacteremia and inflammation in mouse lungs. *Journal of cystic fibrosis : official journal of the European Cystic Fibrosis Society*. 2014;13(2):156-63.
318. Eigen H, Rosenstein BJ, FitzSimmons S, Schidlow DV. A multicenter study of alternate-day prednisone therapy in patients with cystic fibrosis. Cystic Fibrosis Foundation Prednisone Trial Group. *The Journal of pediatrics*. 1995;126(4):515-23.

319. Bush A, Davies J. Non! to non-steroidal anti-inflammatory therapy for inflammatory lung disease in cystic fibrosis (at least at the moment). *The Journal of pediatrics*. 2007;151(3):228-30.
320. Coakley RD, Grubb BR, Paradiso AM, Gatzky JT, Johnson LG, Kreda SM, et al. Abnormal surface liquid pH regulation by cultured cystic fibrosis bronchial epithelium. *Proc Natl Acad Sci U S A*. 2003;100(26):16083-8.
321. Garland AL, Walton WG, Coakley RD, Tan CD, Gilmore RC, Hobbs CA, et al. Molecular basis for pH-dependent mucosal dehydration in cystic fibrosis airways. *Proc Natl Acad Sci U S A*. 2013;110(40):15973-8.
322. Burns JL, Griffith A. Ph-Dependent Differential *Pseudomonas Aeruginosa* Killing in Cf Sputum Incubated in Hypertonic Saline Solutions. *Pediatr Pulm*. 2014;49:351-.
323. Langford DT, Hiller J. Prospective, controlled study of a polyvalent *pseudomonas* vaccine in cystic fibrosis--three year results. *Arch Dis Child*. 1984;59(12):1131-4.
324. Doring G, Meisner C, Stern M, Flagella Vaccine Trial Study G. A double-blind randomized placebo-controlled phase III study of a *Pseudomonas aeruginosa* flagella vaccine in cystic fibrosis patients. *Proc Natl Acad Sci U S A*. 2007;104(26):11020-5.
325. Hoiby N, Pedersen SS, Jensen ET, Pressler T, Shand GH, Kharazmi A, et al. Immunology of *Pseudomonas aeruginosa* infection in cystic fibrosis. *Acta Universitatis Carolinae Medica*. 1990;36(1-4):16-21.
326. Mansouri E, Gabelsberger J, Knapp B, Hundt E, Lenz U, Hungerer KD, et al. Safety and immunogenicity of a *Pseudomonas aeruginosa* hybrid outer membrane protein F-I vaccine in human volunteers. *Infection and immunity*. 1999;67(3):1461-70.
327. Ding B, von Specht BU, Li Y. OprF/I-vaccinated sera inhibit binding of human interferon-gamma to *Pseudomonas aeruginosa*. *Vaccine*. 2010;28(25):4119-22.
328. Hemachandra S, Kamboj K, Copfer J, Pier G, Green LL, Schreiber JR. Human monoclonal antibodies against *Pseudomonas aeruginosa* lipopolysaccharide derived from transgenic mice containing megabase human immunoglobulin loci are opsonic and protective against fatal *pseudomonas* sepsis. *Infection and immunity*. 2001;69(4):2223-9.
329. Pier GB, Boyer D, Preston M, Coleman FT, Llosa N, Mueschenborn-Koglin S, et al. Human monoclonal antibodies to *Pseudomonas aeruginosa* alginate that protect against infection by both mucoid and nonmucoid strains. *Journal of immunology*. 2004;173(9):5671-8.
330. DiGiandomenico A, Warrener P, Hamilton M, Guillard S, Ravn P, Minter R, et al. Identification of broadly protective human antibodies to *Pseudomonas aeruginosa* exopolysaccharide Psl by phenotypic screening. *The Journal of experimental medicine*. 2012;209(7):1273-87.
331. Milla CE, Chmiel JF, Accurso FJ, VanDevanter DR, Konstan MW, Yarranton G, et al. Anti-PcrV antibody in cystic fibrosis: a novel approach targeting *Pseudomonas aeruginosa* airway infection. *Pediatr Pulmonol*. 2014;49(7):650-8.
332. SugitaKonishi Y, Shibata K, Yun SS, HaraKudo Y, Yamaguchi K, Kumagai S. Immune functions of immunoglobulin Y isolated from egg yolk of hens immunized with various infectious bacteria. *Biosci Biotech Bioch*. 1996;60(5):886-8.
333. Nilsson E, Kollberg H, Johannesson M, Wejaker PE, Carlander D, Larsson A. More than 10 years' continuous oral treatment with specific immunoglobulin Y for the prevention of *Pseudomonas aeruginosa* infections: A case report. *J Med Food*. 2007;10(2):375-8.
334. Puschmann T. A history of medical education from the most remote to the most recent times. London: H.K Lewis; 1891. 613 p.
335. Kesselmeier J, Staudt M. Biogenic Volatile Organic Compounds (VOC): An Overview on Emission, Physiology and Ecology. *Journal of Atmospheric Chemistry*. 1999;33(1):23-88.
336. Penuelas J, Asensio D, Tholl D, Wenke K, Rosenkranz M, Piechulla B, et al. Biogenic volatile emissions from the soil. *Plant, cell & environment*. 2014.
337. Mendell MJ. Indoor residential chemical emissions as risk factors for-respiratory and allergic effects in children: a review. *Indoor Air*. 2007;17(4):259-77.

338. Dweik RA, Amann A. Exhaled breath analysis: the new frontier in medical testing. *J Breath Res.* 2008;2(3).
339. Pauling L, Robinson AB, Teranishi R, Cary P. Quantitative analysis of urine vapor and breath by gas-liquid partition chromatography. *Proc Natl Acad Sci U S A.* 1971;68(10):2374-6.
340. Narasimhan LR, Goodman W, Patel CK. Correlation of breath ammonia with blood urea nitrogen and creatinine during hemodialysis. *Proc Natl Acad Sci U S A.* 2001;98(8):4617-21.
341. Sehnert SS, Jiang L, Burdick JF, Risby TH. Breath biomarkers for detection of human liver diseases: preliminary study. *Biomarkers : biochemical indicators of exposure, response, and susceptibility to chemicals.* 2002;7(2):174-87.
342. Kaji H, Hisamura M, Saito N, Murao M. Gas chromatographic determination of volatile sulfur compounds in the expired alveolar air in hepatopathic subjects. *Journal of chromatography.* 1978;145(3):464-8.
343. Fens N, Zwinderman AH, van der Schee MP, de Nijs SB, Dijkers E, Roldaan AC, et al. Exhaled breath profiling enables discrimination of chronic obstructive pulmonary disease and asthma. *Am J Respir Crit Care Med.* 2009;180(11):1076-82.
344. Ibrahim B, Basanta M, Cadden P, Singh D, Douce D, Woodcock A, et al. Non-invasive phenotyping using exhaled volatile organic compounds in asthma. *Thorax.* 2011;66(9):804-9.
345. Rowland M, Lambert I, Gormally S, Daly LE, Thomas JE, Hetherington C, et al. Carbon 13-labeled urea breath test for the diagnosis of *Helicobacter pylori* infection in children. *The Journal of pediatrics.* 1997;131(6):815-20.
346. Wodehouse T, Kharitonov SA, Mackay IS, Barnes PJ, Wilson R, Cole PJ. Nasal nitric oxide measurements for the screening of primary ciliary dyskinesia. *Eur Respir J.* 2003;21(1):43-7.
347. Karadag B, James AJ, Gultekin E, Wilson NM, Bush A. Nasal and lower airway level of nitric oxide in children with primary ciliary dyskinesia. *Eur Respir J.* 1999;13(6):1402-5.
348. Dweik RA, Boggs PB, Erzurum SC, Irvin CG, Leigh MW, Lundberg JO, et al. An official ATS clinical practice guideline: interpretation of exhaled nitric oxide levels (FENO) for clinical applications. *Am J Respir Crit Care Med.* 2011;184(5):602-15.
349. Thomas SR, Kharitonov SA, Scott SF, Hodson ME, Barnes PJ. Nasal and exhaled nitric oxide is reduced in adult patients with cystic fibrosis and does not correlate with cystic fibrosis genotype. *Chest.* 2000;117(4):1085-9.
350. Zhou M, Liu Y, Duan Y. Breath biomarkers in diagnosis of pulmonary diseases. *Clinica chimica acta; international journal of clinical chemistry.* 2012;413(21-22):1770-80.
351. Wu L, Wang R. Carbon monoxide: endogenous production, physiological functions, and pharmacological applications. *Pharmacological reviews.* 2005;57(4):585-630.
352. Paredi P, Shah PL, Montuschi P, Sullivan P, Hodson ME, Kharitonov SA, et al. Increased carbon monoxide in exhaled air of patients with cystic fibrosis. *Thorax.* 1999;54(10):917-20.
353. Antuni JD, Kharitonov SA, Hughes D, Hodson ME, Barnes PJ. Increase in exhaled carbon monoxide during exacerbations of cystic fibrosis. *Thorax.* 2000;55(2):138-42.
354. McGrath LT, Mallon P, Dowey L, Silke B, McClean E, McDonnell M, et al. Oxidative stress during acute respiratory exacerbations in cystic fibrosis. *Thorax.* 1999;54(6):518-23.
355. Paredi P, Kharitonov SA, Leak D, Shah PL, Cramer D, Hodson ME, et al. Exhaled ethane is elevated in cystic fibrosis and correlates with carbon monoxide levels and airway obstruction. *Am J Respir Crit Care Med.* 2000;161(4 Pt 1):1247-51.
356. McGrath LT, Patrick R, Mallon P, Dowey L, Silke B, Norwood W, et al. Breath isoprene during acute respiratory exacerbation in cystic fibrosis. *Eur Respir J.* 2000;16(6):1065-9.
357. Olsson MJ, Lundstrom JN, Kimball BA, Gordon AR, Karshikoff B, Hosseini N, et al. The scent of disease: human body odor contains an early chemosensory cue of sickness. *Psychological science.* 2014;25(3):817-23.
358. Mazmanian SK, Round JL, Kasper DL. A microbial symbiosis factor prevents intestinal inflammatory disease. *Nature.* 2008;453(7195):620-5.

359. Blainey PC, Milla CE, Cornfield DN, Quake SR. Quantitative analysis of the human airway microbial ecology reveals a pervasive signature for cystic fibrosis. *Science translational medicine*. 2012;4(153):153ra30.
360. Harris JK, De Groote MA, Sagel SD, Zemanick ET, Kapsner R, Penvari C, et al. Molecular identification of bacteria in bronchoalveolar lavage fluid from children with cystic fibrosis. *Proc Natl Acad Sci U S A*. 2007;104(51):20529-33.
361. Cox CD, Parker J. Use of 2-aminoacetophenone production in identification of *Pseudomonas aeruginosa*. *Journal of clinical microbiology*. 1979;9(4):479-84.
362. Scott-Thomas AJ, Syhre M, Pattermore PK, Epton M, Laing R, Pearson J, et al. 2-Aminoacetophenone as a potential breath biomarker for *Pseudomonas aeruginosa* in the cystic fibrosis lung. *BMC pulmonary medicine*. 2010;10:56.
363. Lermusieau G, Bulens M, Collin S. Use of GC-olfactometry to identify the hop aromatic compounds in beer. *Journal of agricultural and food chemistry*. 2001;49(8):3867-74.
364. Scott-Thomas A, Pearson J, Chambers S. Potential sources of 2-aminoacetophenone to confound the *Pseudomonas aeruginosa* breath test, including analysis of a food challenge study. *J Breath Res*. 2011;5(4):046002.
365. Blumer C, Haas D. Mechanism, regulation, and ecological role of bacterial cyanide biosynthesis. *Archives of microbiology*. 2000;173(3):170-7.
366. Castric PA. Hydrogen-Cyanide Production by *Pseudomonas-Aeruginosa* at Reduced Oxygen Levels. *Can J Microbiol*. 1983;29(10):1344-9.
367. Broderick KE, Chan A, Balasubramanian M, Feala J, Reed SL, Panda M, et al. Cyanide produced by human isolates of *Pseudomonas aeruginosa* contributes to lethality in *Drosophila melanogaster*. *J Infect Dis*. 2008;197(3):457-64.
368. Sethi S, Nanda R, Chakraborty T. Clinical application of volatile organic compound analysis for detecting infectious diseases. *Clinical microbiology reviews*. 2013;26(3):462-75.
369. Zlosnik JE, Tavankar GR, Bundy JG, Mossialos D, O'Toole R, Williams HD. Investigation of the physiological relationship between the cyanide-insensitive oxidase and cyanide production in *Pseudomonas aeruginosa*. *Microbiology*. 2006;152(Pt 5):1407-15.
370. Anderson RD, Roddam LF, Bettiol S, Sanderson K, Reid DW. Biosignificance of bacterial cyanogenesis in the CF lung. *Journal of cystic fibrosis : official journal of the European Cystic Fibrosis Society*. 2010;9(3):158-64.
371. Stelmazynska T. Formation of HCN by human phagocytosing neutrophils--1. Chlorination of *Staphylococcus epidermidis* as a source of HCN. *The International journal of biochemistry*. 1985;17(3):373-9.
372. Stelmazynska T. Formation of HCN and its chlorination to ClCN by stimulated human neutrophils--2. Oxidation of thiocyanate as a source of HCN. *The International journal of biochemistry*. 1986;18(12):1107-14.
373. Stutz MD, Gangell CL, Berry LJ, Garratt LW, Sheil B, Sly PD, et al. Cyanide in bronchoalveolar lavage is not diagnostic for *Pseudomonas aeruginosa* in children with cystic fibrosis. *Eur Respir J*. 2011;37(3):553-8.
374. Sanderson K, Wescombe L, Kirov SM, Champion A, Reid DW. Bacterial cyanogenesis occurs in the cystic fibrosis lung. *Eur Respir J*. 2008;32(2):329-33.
375. Ryall B, Davies JC, Wilson R, Shoemark A, Williams HD. *Pseudomonas aeruginosa*, cyanide accumulation and lung function in CF and non-CF bronchiectasis patients. *Eur Respir J*. 2008;32(3):740-7.
376. Barnes PJ. Mechanisms in COPD: differences from asthma. *Chest*. 2000;117(2 Suppl):10S-4S.
377. Jatakanon A, Uasuf C, Maziak W, Lim S, Chung KF, Barnes PJ. Neutrophilic inflammation in severe persistent asthma. *Am J Respir Crit Care Med*. 1999;160(5 Pt 1):1532-9.
378. Enderby B, Smith D, Carroll W, Lenney W. Hydrogen Cyanide as a Biomarker for *Pseudomonas Aeruginosa* in the Breath of Children With Cystic Fibrosis. *Pediatr Pulm*. 2009;44(2):142-7.

379. Dummer J. Analysis of Volatile Biomarkers of Airway Inflammation in Breath: Otago; 2011.
380. Carroll W, Lenney W, Wang TS, Spanel P, Alcock A, Smith D. Detection of volatile compounds emitted by *Pseudomonas aeruginosa* using selected ion flow tube mass spectrometry. *Pediatr Pulm.* 2005;39(5):452-6.
381. Shestivska V, Spanel P, Dryahina K, Sovova K, Smith D, Musilek M, et al. Variability in the concentrations of volatile metabolites emitted by genotypically different strains of *Pseudomonas aeruginosa*. *Journal of applied microbiology.* 2012;113(3):701-13.
382. Gilchrist FJ, Alcock A, Belcher J, Brady M, Jones A, Smith D, et al. Variation in hydrogen cyanide production between different strains of *Pseudomonas aeruginosa*. *Eur Respir J.* 2011;38(2):409-14.
383. Shestivska V, Nemec A, Drevinek P, Sovova K, Dryahina K, Spanel P. Quantification of methyl thiocyanate in the headspace of *Pseudomonas aeruginosa* cultures and in the breath of cystic fibrosis patients by selected ion flow tube mass spectrometry. *Rapid communications in mass spectrometry : RCM.* 2011;25(17):2459-67.
384. Gilchrist FJ, Razavi C, Webb AK, Jones AM, Spanel P, Smith D, et al. An investigation of suitable bag materials for the collection and storage of breath samples containing hydrogen cyanide. *J Breath Res.* 2012;6(3):036004.
385. Gilchrist FJ, Bright-Thomas RJ, Jones AM, Smith D, Spanel P, Webb AK, et al. Hydrogen cyanide concentrations in the breath of adult cystic fibrosis patients with and without *Pseudomonas aeruginosa* infection. *J Breath Res.* 2013;7(2).
386. Lundquist P, Rosling H, Sorbo B. The origin of hydrogen cyanide in breath. *Archives of toxicology.* 1988;61(4):270-4.
387. Wang T, Pysanenko A, Dryahina K, Spanel P, Smith D. Analysis of breath, exhaled via the mouth and nose, and the air in the oral cavity. *J Breath Res.* 2008;2(3):037013.
388. Robertson JM, Friedman EM, Rubin BK. Nasal and sinus disease in cystic fibrosis. *Paediatric respiratory reviews.* 2008;9(3):213-9.
389. Dummer J, Storer M, Sturney S, Scott-Thomas A, Chambers S, Swanney M, et al. Quantification of hydrogen cyanide (HCN) in breath using selected ion flow tube mass spectrometry-HCN is not a biomarker of *Pseudomonas* in chronic suppurative lung disease. *J Breath Res.* 2013;7(1).
390. Labows JN, McGinley KJ, Webster GF, Leyden JJ. Headspace analysis of volatile metabolites of *Pseudomonas aeruginosa* and related species by gas chromatography-mass spectrometry. *Journal of clinical microbiology.* 1980;12(4):521-6.
391. Allardyce RA, Langford VS, Hill AL, Murdoch DR. Detection of volatile metabolites produced by bacterial growth in blood culture media by selected ion flow tube mass spectrometry (SIFT-MS). *Journal of microbiological methods.* 2006;65(2):361-5.
392. Awano S, Ansai T, Takata Y, Soh I, Yoshida A, Hamasaki T, et al. Relationship between volatile sulfur compounds in mouth air and systemic disease. *J Breath Res.* 2008;2(1).
393. Harvey-Woodworth CN. Dimethylsulphidemia: the significance of dimethyl sulphide in extra-oral, blood borne halitosis. *British dental journal.* 2013;214(7):E20.
394. Filipiak W, Sponring A, Baur MM, Filipiak A, Ager C, Wiesenhofer H, et al. Molecular analysis of volatile metabolites released specifically by *Staphylococcus aureus* and *Pseudomonas aeruginosa*. *BMC microbiology.* 2012;12:113.
395. Kamboures MA, Blake DR, Cooper DM, Newcomb RL, Barker M, Larson JK, et al. Breath sulfides and pulmonary function in cystic fibrosis. *Proc Natl Acad Sci U S A.* 2005;102(44):15762-7.
396. Barker M, Hengst M, Schmid J, Buers HJ, Mittermaier B, Klemp D, et al. Volatile organic compounds in the exhaled breath of young patients with cystic fibrosis. *Eur Respir J.* 2006;27(5):929-36.
397. Bean HD, Dimandja JM, Hill JE. Bacterial volatile discovery using solid phase microextraction and comprehensive two-dimensional gas chromatography-time-of-flight mass spectrometry. *Journal of chromatography B, Analytical technologies in the biomedical and life sciences.* 2012;901:41-6.

398. Tangerman A, Winkel EG. Intra- and extra-oral halitosis: finding of a new form of extra-oral blood-borne halitosis caused by dimethyl sulphide. *Journal of clinical periodontology*. 2007;34(9):748-55.
399. Tangerman A, Winkel EG. Extra-oral halitosis: an overview. *J Breath Res*. 2010;4(1):017003.
400. Bos LD, Sterk PJ, Schultz MJ. Volatile metabolites of pathogens: a systematic review. *PLoS pathogens*. 2013;9(5):e1003311.
401. van de Kant KDG, van der Sande LJTM, Jobsis Q, van Schayck OCP, Dompeling E. Clinical use of exhaled volatile organic compounds in pulmonary diseases: a systematic review. *Resp Res*. 2012;13.
402. Schulz S, Dickschat JS. Bacterial volatiles: the smell of small organisms. *Natural product reports*. 2007;24(4):814-42.
403. Robroeks CM, van Berkel JJ, Dallinga JW, Jobsis Q, Zimmermann LJ, Hendriks HJ, et al. Metabolomics of volatile organic compounds in cystic fibrosis patients and controls. *Pediatr Res*. 2010;68(1):75-80.
404. Savelev SU, Perry JD, Bourke SJ, Jary H, Taylor R, Fisher AJ, et al. Volatile biomarkers of *Pseudomonas aeruginosa* in cystic fibrosis and noncystic fibrosis bronchiectasis. *Letters in applied microbiology*. 2011;52(6):610-3.
405. Allardyce RA, Hill AL, Murdoch DR. The rapid evaluation of bacterial growth and antibiotic susceptibility in blood cultures by selected ion flow tube mass spectrometry. *Diagnostic microbiology and infectious disease*. 2006;55(4):255-61.
406. Scotter JM, Allardyce RA, Langford VS, Hill A, Murdoch DR. The rapid evaluation of bacterial growth in blood cultures by selected ion flow tube-mass spectrometry (SIFT-MS) and comparison with the BacT/ALERT automated blood culture system. *Journal of microbiological methods*. 2006;65(3):628-31.
407. Storer MK, Hibbard-Melles K, Davis B, Scotter J. Detection of volatile compounds produced by microbial growth in urine by selected ion flow tube mass spectrometry (SIFT-MS). *Journal of microbiological methods*. 2011;87(1):111-3.
408. Zhu J, Bean HD, Kuo YM, Hill JE. Fast detection of volatile organic compounds from bacterial cultures by secondary electrospray ionization-mass spectrometry. *Journal of clinical microbiology*. 2010;48(12):4426-31.
409. Thorn RM, Reynolds DM, Greenman J. Multivariate analysis of bacterial volatile compound profiles for discrimination between selected species and strains in vitro. *Journal of microbiological methods*. 2011;84(2):258-64.
410. Zechman JM, Aldinger S, Labows JN. Characterization of Pathogenic Bacteria by Automated Headspace Concentration Gas-Chromatography. *Journal of chromatography*. 1986;377:49-57.
411. Hoffman E SV. *Mass Spectrometry: Principles and Applications*. 3rd ed: Wiley-Interscience; 2007 November 6th 2007. 502 p.
412. Phillips M, Greenberg J. Ion-trap detection of volatile organic compounds in alveolar breath. *Clinical chemistry*. 1992;38(1):60-5.
413. Smith D, Spanel P. Selected ion flow tube mass spectrometry (SIFT-MS) for on-line trace gas analysis. *Mass spectrometry reviews*. 2005;24(5):661-700.
414. Smith D, Spanel P, Enderby B, Lenney W, Turner C, Davies SJ. Isoprene levels in the exhaled breath of 200 healthy pupils within the age range 7-18 years studied using SIFT-MS. *Journal of breath research*. 2009;4(1):017101.
415. Smith D, Turner C, Spanel P. Volatile metabolites in the exhaled breath of healthy volunteers: their levels and distributions. *J Breath Res*. 2007;1(1):014004.
416. Spanel P, Dryahina K, Smith D. Acetone, ammonia and hydrogen cyanide in exhaled breath of several volunteers aged 4-83 years. *J Breath Res*. 2007;1(1):011001.
417. Spanel P, Dryahina K, Smith D. The concentration distributions of some metabolites in the exhaled breath of young adults. *J Breath Res*. 2007;1(2):026001.

418. Diskin AM, Spanel P, Smith D. Time variation of ammonia, acetone, isoprene and ethanol in breath: a quantitative SIFT-MS study over 30 days. *Physiological measurement*. 2003;24(1):107-19.
419. Enderby B, Lenney W, Brady M, Emmett C, Spanel P, Smith D. Concentrations of some metabolites in the breath of healthy children aged 7-18 years measured using selected ion flow tube mass spectrometry (SIFT-MS). *J Breath Res*. 2009;3(3):036001.
420. Fens N, van der Schee MP, Brinkman P, Sterk PJ. Exhaled breath analysis by electronic nose in airways disease. Established issues and key questions. *Clinical and experimental allergy : journal of the British Society for Allergy and Clinical Immunology*. 2013;43(7):705-15.
421. Lindinger W, Hansel A, Jordan A. On-line monitoring of volatile organic compounds at pptv levels by means of proton-transfer-reaction mass spectrometry (PTR-MS) - Medical applications, food control and environmental research. *Int J Mass Spectrom*. 1998;173(3):191-241.
422. Rabis T, Sommerwerck U, Anhen O, Darwiche K, Freitag L, Teschler H, et al. Detection of infectious agents in the airways by ion mobility spectrometry of exhaled breath. *Int J Ion Mobil Spec*. 2011;14(4):187-95.
423. Mutlu GM, Garey KW, Robbins RA, Danziger LH, Rubinstein I. Collection and analysis of exhaled breath condensate in humans. *Am J Respir Crit Care Med*. 2001;164(5):731-7.
424. Hunt J. Exhaled breath condensate: an overview. *Immunology and allergy clinics of North America*. 2007;27(4):587-96; v.
425. Cunningham S, McColm JR, Ho LP, Greening AP, Marshall TG. Measurement of inflammatory markers in the breath condensate of children with cystic fibrosis. *Eur Respir J*. 2000;15(5):955-7.
426. Robroeks CM, Jobsis Q, Damoiseaux JG, Heijmans PH, Rosias PP, Hendriks HJ, et al. Cytokines in exhaled breath condensate of children with asthma and cystic fibrosis. *Annals of allergy, asthma & immunology : official publication of the American College of Allergy, Asthma, & Immunology*. 2006;96(2):349-55.
427. Miekisch W, Schubert JK, Noeldge-Schomburg GF. Diagnostic potential of breath analysis--focus on volatile organic compounds. *Clinica chimica acta; international journal of clinical chemistry*. 2004;347(1-2):25-39.
428. Phillips M. Breath tests in medicine. *Scientific American*. 1992;267(1):74-9.
429. Miekisch W, Kischkel S, Sawacki A, Liebau T, Mieth M, Schubert JK. Impact of sampling procedures on the results of breath analysis. *J Breath Res*. 2008;2(2):026007.
430. Thekedar B, Oeh U, Szymczak W, Hoeschen C, Paretzke HG. Influences of mixed expiratory sampling parameters on exhaled volatile organic compound concentrations. *J Breath Res*. 2011;5(1).
431. Eriksen S. Studying the Composition of Human Breath. *New Scientist*. 1964;381:608-11.
432. Steeghs MM, Cristescu SM, Harren FJ. The suitability of Tedlar bags for breath sampling in medical diagnostic research. *Physiological measurement*. 2007;28(1):73-84.
433. Mochalski P, Wzorek B, Sliwka I, Amann A. Suitability of different polymer bags for storage of volatile sulphur compounds relevant to breath analysis. *Journal of chromatography B, Analytical technologies in the biomedical and life sciences*. 2009;877(3):189-96.
434. Lindstrom AB, Pleil JD. A review of the USEPA's single breath canister (SBC) method for exhaled volatile organic biomarkers. *Biomarkers : biochemical indicators of exposure, response, and susceptibility to chemicals*. 2002;7(3):189-208.
435. Sin DW, Wong YC, Sham WC, Wang D. Development of an analytical technique and stability evaluation of 143 C3-C12 volatile organic compounds in Summa canisters by gas chromatography-mass spectrometry. *The Analyst*. 2001;126(3):310-21.
436. Doring G, Hoiby N, Consensus Study G. Early intervention and prevention of lung disease in cystic fibrosis: a European consensus. *Journal of cystic fibrosis : official journal of the European Cystic Fibrosis Society*. 2004;3(2):67-91.
437. Marchetti F, Giglio L, Candusso M, Faraguna D, Assael BM. Early antibiotic treatment of *Pseudomonas aeruginosa* colonisation in cystic fibrosis: a critical review of the literature. *European journal of clinical pharmacology*. 2004;60(2):67-74.

438. Hoiby N, Frederiksen B, Pressler T. Eradication of early *Pseudomonas aeruginosa* infection. *Journal of cystic fibrosis : official journal of the European Cystic Fibrosis Society*. 2005;4 Suppl 2:49-54.
439. Goeminne PC, Vandendriessche T, Van Eldere J, Nicolai BM, Hertog ML, Dupont LJ. Detection of *Pseudomonas aeruginosa* in sputum headspace through volatile organic compound analysis. *Respir Res*. 2012;13:87.
440. Lee TW, Brownlee KG, Conway SP, Denton M, Littlewood JM. Evaluation of a new definition for chronic *Pseudomonas aeruginosa* infection in cystic fibrosis patients. *Journal of cystic fibrosis : official journal of the European Cystic Fibrosis Society*. 2003;2(1):29-34.
441. Kumar S, Huang J, Abbassi-Ghadi N, Spanel P, Smith D, Hanna GB. Selected ion flow tube mass spectrometry analysis of exhaled breath for volatile organic compound profiling of esophago-gastric cancer. *Analytical chemistry*. 2013;85(12):6121-8.
442. Ordonez CL, Henig NR, Mayer-Hamblett N, Accurso FJ, Burns JL, Chmiel JF, et al. Inflammatory and microbiologic markers in induced sputum after intravenous antibiotics in cystic fibrosis. *American journal of respiratory and critical care medicine*. 2003;168(12):1471-5.
443. Goss CH, Burns JL. Exacerbations in cystic fibrosis. 1: Epidemiology and pathogenesis. *Thorax*. 2007;62(4):360-7.
444. Castric KF, Castric PA. Method for Rapid Detection of Cyanogenic Bacteria. *Appl Environ Microbiol*. 1983;45(2):701-2.
445. Takos A, Lai D, Mikkelsen L, Abou Hachem M, Shelton D, Motawia MS, et al. Genetic Screening Identifies Cyanogenesis-Deficient Mutants of *Lotus japonicus* and Reveals Enzymatic Specificity in Hydroxynitrile Glucoside Metabolism. *Plant Cell*. 2010;22(5):1605-19.
446. Wiehlmann L, Wagner G, Cramer N, Siebert B, Gudowius P, Morales G, et al. Population structure of *Pseudomonas aeruginosa*. *Proceedings of the National Academy of Sciences of the United States of America*. 2007;104(19):8101-6.
447. Bikov A, Paschalaki K, Logan-Sinclair R, Horvath I, Kharitonov SA, Barnes PJ, et al. Standardised exhaled breath collection for the measurement of exhaled volatile organic compounds by proton transfer reaction mass spectrometry. *BMC pulmonary medicine*. 2013;13(1):43.
448. Conway S. Segregation is good for patients with cystic fibrosis. *Journal of the Royal Society of Medicine*. 2008;101 Suppl 1:S31-5.
449. Spanel P, Wang T, Smith D. Quantification of hydrogen cyanide in humid air by selected ion flow tube mass spectrometry. *Rapid communications in mass spectrometry : RCM*. 2004;18(16):1869-73.
450. Smith D, Wang T, Spanel P. Analysis of ketones by selected ion flow tube mass spectrometry. *Rapid communications in mass spectrometry : RCM*. 2003;17(23):2655-60.
451. Hicks LC, Huang J, Kumar S, Powles ST, Orchard TR, Hanna GB, et al. Analysis of Exhaled Breath Volatile Organic Compounds in Inflammatory Bowel Disease: A Pilot Study. *J Crohns Colitis*. 2015;9(9):731-7.
452. Kumar S, Huang J, Abbassi-Ghadi N, Mackenzie HA, Veselkov KA, Hoare JM, et al. Mass Spectrometric Analysis of Exhaled Breath for the Identification of Volatile Organic Compound Biomarkers in Esophageal and Gastric Adenocarcinoma. *Ann Surg*. 2015;262(6):981-90.
453. Taylor-Robinson D, Whitehead M, Diderichsen F, Olesen HV, Pressler T, Smyth RL, et al. Understanding the natural progression in %FEV1 decline in patients with cystic fibrosis: a longitudinal study. *Thorax*. 2012;67(10):860-6.
454. Kerem E, Corey M, Gold R, Levison H. Pulmonary function and clinical course in patients with cystic fibrosis after pulmonary colonization with *Pseudomonas aeruginosa*. *The Journal of pediatrics*. 1990;116(5):714-9.
455. Gilchrist FJ, Sims H, Alcock A, Belcher J, Jones AM, Smith D, et al. Quantification of hydrogen cyanide and 2-aminoacetophenone in the headspace of *Pseudomonas aeruginosa* cultured under biofilm and planktonic conditions. *Anal Methods-Uk*. 2012;4(11):3661-5.

456. Vangnai AS, Arp DJ, Sayavedra-Soto LA. Two distinct alcohol dehydrogenases participate in butane metabolism by *Pseudomonas butanovora*. *J Bacteriol.* 2002;184(7):1916-24.
457. Vangnai AS, Sayavedra-Soto LA, Arp DJ. Roles for the two 1-butanol dehydrogenases of *Pseudomonas butanovora* in butane and 1-butanol metabolism. *J Bacteriol.* 2002;184(16):4343-50.
458. Arp DJ. Butane metabolism by butane-grown '*Pseudomonas butanovora*'. *Microbiology.* 1999;145 (Pt 5):1173-80.
459. Hazardous Substances Databank [Internet]. National Library of Medicine. 1994. Available from: http://www.epa.gov/chemfact/s_butano.txt.
460. Kubo I, Muroi H, Kubo A. Structural functions of antimicrobial long-chain alcohols and phenols. *Bioorg Med Chem.* 1995;3(7):873-80.
461. Agency HP. Phenol: Toxicology Overview. 2007.
462. Hryniuk A, Ross BM. A preliminary investigation of exhaled breath from patients with celiac disease using selected ion flow tube mass spectrometry. *Journal of gastrointestinal and liver diseases : JGLD.* 2010;19(1):15-20.
463. Brambilla DJ, Matsumoto AM, Araujo AB, McKinlay JB. The effect of diurnal variation on clinical measurement of serum testosterone and other sex hormone levels in men. *The Journal of clinical endocrinology and metabolism.* 2009;94(3):907-13.
464. Levi F, Schibler U. Circadian rhythms: mechanisms and therapeutic implications. *Annual review of pharmacology and toxicology.* 2007;47:593-628.
465. Kerkhof GA. Inter-individual differences in the human circadian system: a review. *Biological psychology.* 1985;20(2):83-112.
466. Horvath I, Hunt J, Barnes PJ, Alving K, Antczak A, Balint B, et al. Exhaled breath condensate: methodological recommendations and unresolved questions. *Eur Respir J.* 2005;26(3):523-48.
467. Cathcart MP, Love S, Hughes KJ. The application of exhaled breath gas and exhaled breath condensate analysis in the investigation of the lower respiratory tract in veterinary medicine: A review. *Vet J.* 2012;191(3):282-91.
468. Logan BK, Distefano S. Ethanol content of various foods and soft drinks and their potential for interference with a breath-alcohol test. *J Anal Toxicol.* 1998;22(3):181-3.
469. Hu W. Breath ethanol and acetone as indicators of serum glucose levels: An initial report. *Ethnic Dis.* 2005;15(3):32-4.
470. Kabadi UM, Eisenstein AB, Konda J. Elevated Plasma Ammonia Level in Hepatic Cirrhosis - Role of Glucagon. *Gastroenterology.* 1985;88(3):750-6.
471. Spanel P, Smith D. Progress in SIFT-MS: breath analysis and other applications. *Mass spectrometry reviews.* 2011;30(2):236-67.
472. Smith D, Spanel P, Enderby B, Lenney W, Turner C, Davies SJ. Isoprene levels in the exhaled breath of 200 healthy pupils within the age range 7-18 years studied using SIFT-MS. *J Breath Res.* 2010;4(1):017101.
473. Rosenfeld M, Emerson J, Accurso F, Armstrong D, Castile R, Grimwood K, et al. Diagnostic accuracy of oropharyngeal cultures in infants and young children with cystic fibrosis. *Pediatr Pulmonol.* 1999;28(5):321-8.
474. Jung A, Kleinau I, Schonian G, Bauernfeind A, Chen C, Griesse M, et al. Sequential genotyping of *Pseudomonas aeruginosa* from upper and lower airways of cystic fibrosis patients. *Eur Respir J.* 2002;20(6):1457-63.
475. de Carvalho Costa Cardinali L, Rocha GA, Rocha AM, de Moura SB, de Figueiredo Soares T, Esteves AM, et al. Evaluation of [¹³C]urea breath test and *Helicobacter pylori* stool antigen test for diagnosis of *H. pylori* infection in children from a developing country. *Journal of clinical microbiology.* 2003;41(7):3334-5.
476. Prince BJ, Milligan DB, McEwan MJ. Application of selected ion flow tube mass spectrometry to real-time atmospheric monitoring. *Rapid communications in mass spectrometry : RCM.* 2010;24(12):1763-9.

477. Carroll W, Lenney W, Wang T, Spanel P, Alcock A, Smith D. Detection of volatile compounds emitted by *Pseudomonas aeruginosa* using selected ion flow tube mass spectrometry. *Pediatr Pulmonol*. 2005;39(5):452-6.
478. Linnane SJ, Keatings VM, Costello CM, Moynihan JB, O'Connor CM, Fitzgerald MX, et al. Total sputum nitrate plus nitrite is raised during acute pulmonary infection in cystic fibrosis. *Am J Resp Crit Care*. 1998;158(1):207-12.
479. Nielsen DR, Leonard E, Yoon SH, Tseng HC, Yuan C, Prather KL. Engineering alternative butanol production platforms in heterologous bacteria. *Metabolic engineering*. 2009;11(4-5):262-73.
480. Chen W, Metsala M, Vaittinen O, Halonen L. Hydrogen cyanide in the headspace of oral fluid and in mouth-exhaled breath. *J Breath Res*. 2014;8(2):027108.
481. Smith D, Spanel P, Gilchrist FJ, Lenney W. Hydrogen cyanide, a volatile biomarker of *Pseudomonas aeruginosa* infection. *J Breath Res*. 2013;7(4):044001.
482. Turner C, Spanel P, Smith D. A longitudinal study of ammonia, acetone and propanol in the exhaled breath of 30 subjects using selected ion flow tube mass spectrometry, SIFT-MS. *Physiological measurement*. 2006;27(4):321-37.
483. Turner C, Spanel P, Smith D. A longitudinal study of breath isoprene in healthy volunteers using selected ion flow tube mass spectrometry (SIFT-MS). *Physiological measurement*. 2006;27(1):13-22.
484. Kramer A, Rudolph P, Kampf G, Pittet D. Limited efficacy of alcohol-based hand gels. *Lancet*. 2002;359(9316):1489-90.
485. Buchvald F, Bisgaard H. FeNO measured at fixed exhalation flow rate during controlled tidal breathing in children from the age of 2 yr. *Am J Resp Crit Care*. 2001;163(3):699-704.
486. Montuschi P, Paris D, Melck D, Lucidi V, Ciabattini G, Raia V, et al. NMR spectroscopy metabolomic profiling of exhaled breath condensate in patients with stable and unstable cystic fibrosis. *Thorax*. 2012;67(3):222-8.
487. Clokie MR, Millard AD, Letarov AV, Heaphy S. Phages in nature. *Bacteriophage*. 2011;1(1):31-45.
488. Hankin EH. L'action bactericide des eaux de la Jumna et du Gange sur le vibrion du cholera. *Ann Inst Pasteur*. 1896;10:511-23.
489. Duckworth DH. "Who discovered bacteriophage?". *Bacteriological reviews*. 1976;40(4):793-802.
490. Sulakvelidze A, Alavidze Z, Morris JG, Jr. Bacteriophage therapy. *Antimicrobial agents and chemotherapy*. 2001;45(3):649-59.
491. Abedon ST, Kuhl SJ, Blasdel BG, Kutter EM. Phage treatment of human infections. *Bacteriophage*. 2011;1(2):66-85.
492. Lobocka M, Szybalski WT. *Advances in Virus Research*. Bacteriophages, part A. Preface. *Advances in virus research*. 2012;82:xiii-xv.
493. Fleming A. On the Antibacterial Action of Cultures of a *Penicillium*, with Special Reference to their Use in the Isolation of *B. influenzae*. *British Journal of Experimental Pathology*. 1929;10(3):226-36.
494. Kutateladze M, Adamia R. Phage therapy experience at the Eliava Institute. *Medecine et maladies infectieuses*. 2008;38(8):426-30.
495. Fruciano DE, Bourne S. Phage as an antimicrobial agent: d'Herelle's heretical theories and their role in the decline of phage prophylaxis in the West. *The Canadian journal of infectious diseases & medical microbiology = Journal canadien des maladies infectieuses et de la microbiologie medicale / AMMI Canada*. 2007;18(1):19-26.
496. Tikhonenko AS. *Ultrastructure of bacterial viruses*. New York,: Plenum Press; 1970. x, 294 p. p.
497. Chanishvili N. Phage therapy--history from Twort and d'Herelle through Soviet experience to current approaches. *Advances in virus research*. 2012;83:3-40.

498. Sillankorva SM, Oliveira H, Azeredo J. Bacteriophages and their role in food safety. *Int J Microbiol.* 2012;2012:863945.
499. Greer GG. Bacteriophage control of foodborne bacteriat. *J Food Prot.* 2005;68(5):1102-11.
500. Thiel K. Old dogma, new tricks--21st Century phage therapy. *Nature biotechnology.* 2004;22(1):31-6.
501. Kutter E, De Vos D, Gvasalia G, Alavidze Z, Gogokhia L, Kuhl S, et al. Phage therapy in clinical practice: treatment of human infections. *Current pharmaceutical biotechnology.* 2010;11(1):69-86.
502. Wright A, Hawkins CH, Anggard EE, Harper DR. A controlled clinical trial of a therapeutic bacteriophage preparation in chronic otitis due to antibiotic-resistant *Pseudomonas aeruginosa*; a preliminary report of efficacy. *Clinical otolaryngology : official journal of ENT-UK ; official journal of Netherlands Society for Oto-Rhino-Laryngology & Cervico-Facial Surgery.* 2009;34(4):349-57.
503. Loc-Carrillo C, Abedon ST. Pros and cons of phage therapy. *Bacteriophage.* 2011;1(2):111-4.
504. Shors T. *Understanding viruses.* Sudbury, Mass.: Jones and Bartlett Publishers; 2009. xxiv, 639 p. p.
505. Nelson D. Phage taxonomy: We agree to disagree. *J Bacteriol.* 2004;186(21):7029-31.
506. Ackermann H-W. Phage Classification and Characterization. In: Clokie MJ, Kropinski A, editors. *Bacteriophages. Methods in Molecular Biology™.* 501: Humana Press; 2009. p. 127-40.
507. Bradley DE. The morphology and physiology of bacteriophages as revealed by the electron microscope. *Journal of the Royal Microscopical Society.* 1965;84(3):257-316.
508. Birge EA. *Bacterial and bacteriophage genetics.* 5th ed. New York: Springer; 2006. 577 p. p.
509. Rossmann MG, Mesyanzhinov VV, Arisaka F, Leiman PG. The bacteriophage T4 DNA injection machine. *Current opinion in structural biology.* 2004;14(2):171-80.
510. Young R. Bacteriophage lysis: mechanism and regulation. *Microbiological reviews.* 1992;56(3):430-81.
511. Shao Y, Wang IN. Bacteriophage adsorption rate and optimal lysis time. *Genetics.* 2008;180(1):471-82.
512. Waldor MK, Mekalanos JJ. Lysogenic conversion by a filamentous phage encoding cholera toxin. *Science.* 1996;272(5270):1910-4.
513. Abedon ST, Lejeune JT. Why bacteriophage encode exotoxins and other virulence factors. *Evolutionary bioinformatics online.* 2005;1:97-110.
514. Gorski A, Wazna E, Dabrowska BW, Dabrowska K, Switala-Jelen K, Miedzybrodzki R. Bacteriophage translocation. *FEMS immunology and medical microbiology.* 2006;46(3):313-9.
515. Dubos RJ, Straus JH, Pierce C. The Multiplication of Bacteriophage in Vivo and Its Protective Effect against an Experimental Infection with *Shigella Dysenteriae*. *The Journal of experimental medicine.* 1943;78(3):161-8.
516. Abedon ST. Phage therapy of pulmonary infections. *Bacteriophage.* 2015;5(1):e1020260.
517. Fastier LB. A Bacteriophage for *Pseudomonas pyocyanea* (*Pseudomonas aeruginosa*). *J Bacteriol.* 1945;50(3):301-3.
518. Strateva T, Yordanov D. *Pseudomonas aeruginosa* - a phenomenon of bacterial resistance. *Journal of medical microbiology.* 2009;58(Pt 9):1133-48.
519. Soothill JS. Bacteriophage prevents destruction of skin grafts by *Pseudomonas aeruginosa*. *Burns : journal of the International Society for Burn Injuries.* 1994;20(3):209-11.
520. Wang J, Hu B, Xu M, Yan Q, Liu S, Zhu X, et al. Use of bacteriophage in the treatment of experimental animal bacteremia from imipenem-resistant *Pseudomonas aeruginosa*. *International journal of molecular medicine.* 2006;17(2):309-17.
521. Tiwari BR, Kim S, Rahman M, Kim J. Antibacterial efficacy of lytic *Pseudomonas* bacteriophage in normal and neutropenic mice models. *Journal of microbiology.* 2011;49(6):994-9.
522. Vinodkumar CS, Kalsurmath S, Neelagund YF. Utility of lytic bacteriophage in the treatment of multidrug-resistant *Pseudomonas aeruginosa* septicemia in mice. *Indian journal of pathology & microbiology.* 2008;51(3):360-6.

523. Debarbieux L, Leduc D, Maura D, Morello E, Criscuolo A, Grossi O, et al. Bacteriophages Can Treat and Prevent *Pseudomonas aeruginosa* Lung Infections. *J Infect Dis.* 2010;201(7):1096-104.
524. Morello E, Sausseure E, Maura D, Huerre M, Touqui L, Debarbieux L. Pulmonary bacteriophage therapy on *Pseudomonas aeruginosa* cystic fibrosis strains: first steps towards treatment and prevention. *PloS one.* 2011;6(2):e16963.
525. Alemayehu D, Casey PG, McAuliffe O, Guinane CM, Martin JG, Shanahan F, et al. Bacteriophages phiMR299-2 and phiNH-4 can eliminate *Pseudomonas aeruginosa* in the murine lung and on cystic fibrosis lung airway cells. *mBio.* 2012;3(2):e00029-12.
526. Soothill J. Use of bacteriophages in the treatment of *Pseudomonas aeruginosa* infections. *Expert Rev Anti-Infe.* 2013;11(9):909-15.
527. Khawaldeh A, Morales S, Dillon B, Alavidze Z, Ginn AN, Thomas L, et al. Bacteriophage therapy for refractory *Pseudomonas aeruginosa* urinary tract infection. *Journal of medical microbiology.* 2011;60(Pt 11):1697-700.
528. Abul-Hassan HS E-TMB, Gomaa R. Bacteriophage therapy of *Pseudomonas* burn wound sepsis. *Annals of the Mediterranean Burns Club.* 1990;3(4):262-4.
529. Golshahi L, Seed KD, Dennis JJ, Finlay WH. Toward modern inhalational bacteriophage therapy: nebulization of bacteriophages of *Burkholderia cepacia* complex. *Journal of aerosol medicine and pulmonary drug delivery.* 2008;21(4):351-60.
530. Hraiech S, Brégeon F, Rolain JM. Bacteriophage-based therapy in cystic fibrosis-associated *Pseudomonas aeruginosa* infections: rationale and current status. *Drug Des Devel Ther.* 2015;9:3653-63.
531. Wittebole X, De Roock S, Opal SM. A historical overview of bacteriophage therapy as an alternative to antibiotics for the treatment of bacterial pathogens. *Virulence.* 2014;5(1):226-35.
532. Hoiby N, Bjarnsholt T, Givskov M, Molin S, Ciofu O. Antibiotic resistance of bacterial biofilms. *International journal of antimicrobial agents.* 2010;35(4):322-32.
533. Azeredo J, Sutherland IW. The use of phages for the removal of infectious biofilms. *Current pharmaceutical biotechnology.* 2008;9(4):261-6.
534. Sillankorva S, Azeredo J. Bacteriophage attack as an anti-biofilm strategy. *Methods in molecular biology.* 2014;1147:277-85.
535. Stratton CW. Dead bugs don't mutate: susceptibility issues in the emergence of bacterial resistance. *Emerging infectious diseases.* 2003;9(1):10-6.
536. Hyman P, Abedon ST. Bacteriophage host range and bacterial resistance. *Advances in applied microbiology.* 2010;70:217-48.
537. Abedon ST, Thomas-Abedon C. Phage therapy pharmacology. *Current pharmaceutical biotechnology.* 2010;11(1):28-47.
538. Chan BK, Abedon ST. Phage therapy pharmacology phage cocktails. *Advances in applied microbiology.* 2012;78:1-23.
539. Skurnik M, Pajunen M, Kiljunen S. Biotechnological challenges of phage therapy. *Biotechnology letters.* 2007;29(7):995-1003.
540. Inal JM. Phage therapy: a reappraisal of bacteriophages as antibiotics. *Archivum immunologiae et therapiae experimentalis.* 2003;51(4):237-44.
541. Thiel K. Old dogma, new tricks - 21st century phage therapy. *Nature biotechnology.* 2004;22(1):31-6.
542. Miller RV, Rubero VJ. Mucoïd conversion by phages of *Pseudomonas aeruginosa* strains from patients with cystic fibrosis. *Journal of clinical microbiology.* 1984;19(5):717-9.
543. Scanlan PD, Buckling A. Co-evolution with lytic phage selects for the mucoïd phenotype of *Pseudomonas fluorescens* SBW25. *The ISME journal.* 2012;6(6):1148-58.
544. Willner D, Furlan M, Haynes M, Schmieder R, Angly FE, Silva J, et al. Metagenomic Analysis of Respiratory Tract DNA Viral Communities in Cystic Fibrosis and Non-Cystic Fibrosis Individuals. *PloS one.* 2009;4(10).

545. Gorski A, Miedzybrodzki R, Borysowski J, Dabrowska K, Wierzbicki P, Ohams M, et al. Phage as a Modulator of Immune Responses: Practical Implications for Phage Therapy. *Advances in Virus Research*, Vol 83: Bacteriophages, Pt B. 2012;83:41-71.
546. Srivastava AS, Kaido T, Carrier E. Immunological factors that affect the in vivo fate of T7 phage in the mouse. *Journal of virological methods*. 2004;115(1):99-104.
547. Kim KP, Cha JD, Jang EH, Klumpp J, Hagens S, Hardt WD, et al. PEGylation of bacteriophages increases blood circulation time and reduces T-helper type 1 immune response. *Microb Biotechnol*. 2008;1(3):247-57.
548. Lu TK, Collins JJ. Engineered bacteriophage targeting gene networks as adjuvants for antibiotic therapy. *P Natl Acad Sci USA*. 2009;106(12):4629-34.
549. Viertel TM, Ritter K, Horz HP. Viruses versus bacteria-novel approaches to phage therapy as a tool against multidrug-resistant pathogens. *The Journal of antimicrobial chemotherapy*. 2014.
550. Kutter ESA. *Bacteriophages: Biology and Applications*. 1 ed: CRC Press; December 28 2004. 528 p.
551. Abbe E. VII.—On the Estimation of Aperture in the Microscope. *Journal of the Royal Microscopical Society*. 1881;1(3):388-423.
552. Alberts B BD, Lewis J, Raff M, Roberts K, Watson J. *Molecular Biology of the Cell*. 3 ed: Garland Science; 1994 1994.
553. Ruska E. Nobel Lecture - The development of the electron microscope and of electron microscopy 1986 [Available from: http://www.nobelprize.org/nobel_prizes/physics/laureates/1986/ruska-lecture.html].
554. Erni R, Rossell MD, Kisielowski C, Dahmen U. Atomic-Resolution Imaging with a Sub-50-pm Electron Probe. *Phys Rev Lett*. 2009;102(9).
555. Williams D, Carter CB. *The Transmission Electron Microscope*. *Transmission Electron Microscopy*: Springer US; 1996. p. 3-17.
556. Ohi M, Li Y, Cheng Y, Walz T. Negative Staining and Image Classification - Powerful Tools in Modern Electron Microscopy. *Biological procedures online*. 2004;6:23-34.
557. Horne RW, Wildy P. An historical account of the development and applications of the negative staining technique to the electron microscopy of viruses. *Journal of microscopy*. 1979;117(1):103-22.
558. Harris JR. Negative staining of thinly spread biological samples. *Methods in molecular biology*. 2007;369:107-42.
559. Moyes RB, Reynolds J, Breakwell DP. Preliminary staining of bacteria: negative stain. *Current protocols in microbiology*. 2009;Appendix 3:Appendix 3F.
560. Holloway BW. Genetic recombination in *Pseudomonas aeruginosa*. *Journal of general microbiology*. 1955;13(3):572-81.
561. Klockgether J, Munder A, Neugebauer J, Davenport CF, Stanke F, Larbig KD, et al. Genome diversity of *Pseudomonas aeruginosa* PAO1 laboratory strains. *J Bacteriol*. 2010;192(4):1113-21.
562. Marincs F, White DWR. Immobilization of *Escherichia-Coli* Expressing the Lux Genes of *Xenorhabdus-Luminescens*. *Appl Environ Microb*. 1994;60(10):3862-3.
563. Kovach ME, Elzer PH, Hill DS, Robertson GT, Farris MA, Roop RM, et al. 4 New Derivatives of the Broad-Host-Range Cloning Vector Pbb1mcs, Carrying Different Antibiotic-Resistance Cassettes. *Gene*. 1995;166(1):175-6.
564. Esoh C, Blouin Y, Loukou G, Cablanmian A, Lathro S, Kutter E, et al. The susceptibility of *Pseudomonas aeruginosa* strains from cystic fibrosis patients to bacteriophages. *PloS one*. 2013;8(4):e60575.
565. Larche J, Pouillot F, Esoh C, Libisch B, Straut M, Lee JC, et al. Rapid identification of international multidrug-resistant *Pseudomonas aeruginosa* clones by multiple-locus variable number of tandem repeats analysis and investigation of their susceptibility to lytic bacteriophages. *Antimicrobial agents and chemotherapy*. 2012;56(12):6175-80.

566. Miles AA, Misra SS, Irwin JO. The estimation of the bactericidal power of the blood. *The Journal of hygiene*. 1938;38(6):732-49.
567. Filonov GS, Piatkevich KD, Ting LM, Zhang J, Kim K, Verkhusha VV. Bright and stable near-infrared fluorescent protein for in vivo imaging. *Nature biotechnology*. 2011;29(8):757-61.
568. Giraud E, Zappa S, Vuillet L, Adriano JM, Hannibal L, Fardoux J, et al. A new type of bacteriophytochrome acts in tandem with a classical bacteriophytochrome to control the antennae synthesis in *Rhodospseudomonas palustris*. *The Journal of biological chemistry*. 2005;280(37):32389-97.
569. Rolfe MD, Rice CJ, Lucchini S, Pin C, Thompson A, Cameron ADS, et al. Lag Phase Is a Distinct Growth Phase That Prepares Bacteria for Exponential Growth and Involves Transient Metal Accumulation. *J Bacteriol*. 2012;194(3):686-701.
570. Finkel SE. Long-term survival during stationary phase: evolution and the GASP phenotype. *Nat Rev Microbiol*. 2006;4(2):113-20.
571. Paulton RJL. The Bacterial-Growth Curve. *J Biol Educ*. 1991;25(2):92-4.
572. Zwietering MH, Jongenburger I, Rombouts FM, Vantriet K. Modeling of the Bacterial-Growth Curve. *Appl Environ Microb*. 1990;56(6):1875-81.
573. Kolter R, Siegele DA, Tormo A. The stationary phase of the bacterial life cycle. *Annual review of microbiology*. 1993;47:855-74.
574. Lichten CA, White R, Clark IB, Swain PS. Unmixing of fluorescence spectra to resolve quantitative time-series measurements of gene expression in plate readers. *BMC biotechnology*. 2014;14:11.
575. Hazan R, Que YA, Maura D, Rahme LG. A method for high throughput determination of viable bacteria cell counts in 96-well plates. *BMC microbiology*. 2012;12:259.
576. Flecknell PA, Mitchell M. Midazolam and Fentanyl-Fluanisone - Assessment of Anesthetic Effects in Laboratory Rodents and Rabbits. *Lab Anim*. 1984;18(2):143-6.
577. Singer M, Sansonetti PJ. IL-8 is a key chemokine regulating neutrophil recruitment in a new mouse model of *Shigella*-induced colitis. *Journal of immunology*. 2004;173(6):4197-206.
578. De Filippo K, Henderson RB, Laschinger M, Hogg N. Neutrophil chemokines KC and macrophage-inflammatory protein-2 are newly synthesized by tissue macrophages using distinct TLR signaling pathways. *Journal of immunology*. 2008;180(6):4308-15.
579. Heinzl B, Eber E, Oberwaldner B, Haas G, Zach MS. Effects of inhaled gentamicin prophylaxis on acquisition of *Pseudomonas aeruginosa* in children with cystic fibrosis: a pilot study. *Pediatr Pulmonol*. 2002;33(1):32-7.
580. Tramper-Stranders GA, Wolfs TF, van Haren Noman S, van Aalderen WM, Nagelkerke AF, Nuijsink M, et al. Controlled trial of cycled antibiotic prophylaxis to prevent initial *Pseudomonas aeruginosa* infection in children with cystic fibrosis. *Thorax*. 2010;65(10):915-20.
581. Eber E, Zach MS. *Pseudomonas aeruginosa* infection in cystic fibrosis: prevent, eradicate or both? *Thorax*. 2010;65(10):849-51.
582. Hubeau C, Puchelle E, Gaillard D. Distinct pattern of immune cell population in the lung of human fetuses with cystic fibrosis. *The Journal of allergy and clinical immunology*. 2001;108(4):524-9.
583. Rosenfeld M, Gibson RL, McNamara S, Emerson J, Burns JL, Castile R, et al. Early pulmonary infection, inflammation, and clinical outcomes in infants with cystic fibrosis. *Pediatr Pulmonol*. 2001;32(5):356-66.
584. Bessis N, GarciaCozar FJ, Boissier MC. Immune responses to gene therapy vectors: influence on vector function and effector mechanisms. *Gene therapy*. 2004;11 Suppl 1:S10-7.
585. Skurnik M, Strauch E. Phage therapy: facts and fiction. *International journal of medical microbiology : IJMM*. 2006;296(1):5-14.
586. Clark JR, March JB. Bacterial viruses as human vaccines? Expert review of vaccines. 2004;3(4):463-76.

587. Merabishvili M, Pirnay JP, Verbeken G, Chanishvili N, Tediashvili M, Lashkhi N, et al. Quality-controlled small-scale production of a well-defined bacteriophage cocktail for use in human clinical trials. *PLoS One*. 2009;4(3):e4944.
588. Lu TK, Koeris MS. The next generation of bacteriophage therapy. *Curr Opin Microbiol*. 2011;14(5):524-31.
589. Alemayehu D, Ross RP, O'Sullivan O, Coffey A, Stanton C, Fitzgerald GF, et al. Genome of a virulent bacteriophage Lb338-1 that lyses the probiotic *Lactobacillus paracasei* cheese strain. *Gene*. 2009;448(1):29-39.
590. Carmody LA, Gill JJ, Summer EJ, Sajjan US, Gonzalez CF, Young RF, et al. Efficacy of bacteriophage therapy in a model of *Burkholderia cenocepacia* pulmonary infection. *J Infect Dis*. 2010;201(2):264-71.
591. Jones AM, Martin L, Bright-Thomas RJ, Dodd ME, McDowell A, Moffitt KL, et al. Inflammatory markers in cystic fibrosis patients with transmissible *Pseudomonas aeruginosa*. *Eur Respir J*. 2003;22(3):503-6.
592. Morissette C, Skamene E, Gervais F. Endobronchial inflammation following *Pseudomonas aeruginosa* infection in resistant and susceptible strains of mice. *Infection and immunity*. 1995;63(5):1718-24.
593. Anderson BO, Brown JM, Harken AH. Mechanisms of neutrophil-mediated tissue injury. *The Journal of surgical research*. 1991;51(2):170-9.
594. Venaille TJ, Ryan G, Robinson BWS. Epithelial cell damage is induced by neutrophil-derived, not *Pseudomonas*-derived, proteases in cystic fibrosis sputum. *Resp Med*. 1998;92(2):233-40.
595. Hoiby N, Schiøtz PO. Immune-Complex Mediated Tissue-Damage in the Lungs of Cystic-Fibrosis Patients with Chronic *Pseudomonas-Aeruginosa* Infection. *Acta Paediatr Scand*. 1982;63-73.
596. Downey DG, Bell SC, Elborn JS. Neutrophils in cystic fibrosis. *Thorax*. 2009;64(1):81-8.
597. Gifford AM, Chalmers JD. The role of neutrophils in cystic fibrosis. *Curr Opin Hematol*. 2014;21(1):16-22.
598. Segel GB, Halterman MW, Lichtman MA. The paradox of the neutrophil's role in tissue injury. *J Leukocyte Biol*. 2011;89(3):359-72.
599. van Furth R, van Zwet TL, Buisman AM, van Dissel JT. Anti-tumor necrosis factor antibodies inhibit the influx of granulocytes and monocytes into an inflammatory exudate and enhance the growth of *Listeria monocytogenes* in various organs. *The Journal of infectious diseases*. 1994;170(1):234-7.
600. Staugas RE, Harvey DP, Ferrante A, Nandoskar M, Allison AC. Induction of tumor necrosis factor (TNF) and interleukin-1 (IL-1) by *Pseudomonas aeruginosa* and exotoxin A-induced suppression of lymphoproliferation and TNF, lymphotoxin, gamma interferon, and IL-1 production in human leukocytes. *Infection and immunity*. 1992;60(8):3162-8.
601. Hedges S, Svensson M, Svanborg C. Interleukin-6 response of epithelial cell lines to bacterial stimulation in vitro. *Infection and immunity*. 1992;60(4):1295-301.
602. Watford WT, Moriguchi M, Morinobu A, O'Shea JJ. The biology of IL-12: coordinating innate and adaptive immune responses. *Cytokine & growth factor reviews*. 2003;14(5):361-8.
603. Rovai LE, Herschman HR, Smith JB. The murine neutrophil-chemoattractant chemokines LIX, KC, and MIP-2 have distinct induction kinetics, tissue distributions, and tissue-specific sensitivities to glucocorticoid regulation in endotoxemia. *Journal of leukocyte biology*. 1998;64(4):494-502.
604. Couper KN, Blount DG, Riley EM. IL-10: the master regulator of immunity to infection. *Journal of immunology*. 2008;180(9):5771-7.
605. Sanjabi S, Zenewicz LA, Kamanaka M, Flavell RA. Anti-inflammatory and pro-inflammatory roles of TGF-beta, IL-10, and IL-22 in immunity and autoimmunity. *Current opinion in pharmacology*. 2009;9(4):447-53.
606. Kent G, Iles R, Bear CE, Huan LJ, Griesenbach U, McKerlie C, et al. Lung disease in mice with cystic fibrosis. *J Clin Invest*. 1997;100(12):3060-9.

607. Bragonzi A. Murine models of acute and chronic lung infection with cystic fibrosis pathogens. *International journal of medical microbiology : IJMM*. 2010;300(8):584-93.
608. Starke JR, Edwards MS, Langston C, Baker CJ. A Mouse Model of Chronic Pulmonary Infection with *Pseudomonas-Aeruginosa* and *Pseudomonas-Cepacia*. *Pediatr Res*. 1987;22(6):698-702.
609. Stevenson MM, Kondratieva TK, Apt AS, Tam MF, Skamene E. In vitro and in vivo T cell responses in mice during bronchopulmonary infection with mucoid *Pseudomonas aeruginosa*. *Clinical and experimental immunology*. 1995;99(1):98-105.
610. Kukavica-Ibrulj I, Levesque RC. Animal models of chronic lung infection with *Pseudomonas aeruginosa*: useful tools for cystic fibrosis studies. *Lab Anim*. 2008;42(4):389-412.
611. de la Fuente-Nunez C, Reffuveille F, Fernandez L, Hancock RE. Bacterial biofilm development as a multicellular adaptation: antibiotic resistance and new therapeutic strategies. *Current opinion in microbiology*. 2013;16(5):580-9.
612. Stewart PS. Mechanisms of antibiotic resistance in bacterial biofilms. *International journal of medical microbiology : IJMM*. 2002;292(2):107-13.
613. Webb JS, Thompson LS, James S, Charlton T, Tolker-Nielsen T, Koch B, et al. Cell death in *Pseudomonas aeruginosa* biofilm development. *J Bacteriol*. 2003;185(15):4585-92.
614. Donlan RM. Preventing biofilms of clinically relevant organisms using bacteriophage. *Trends Microbiol*. 2009;17(2):66-72.
615. Hughes KA, Sutherland IW, Jones MV. Biofilm susceptibility to bacteriophage attack: the role of phage-borne polysaccharide depolymerase. *Microbiol-Uk*. 1998;144:3039-47.
616. Fu W, Forster T, Mayer O, Curtin JJ, Lehman SM, Donlan RM. Bacteriophage cocktail for the prevention of biofilm formation by *Pseudomonas aeruginosa* on catheters in an in vitro model system. *Antimicrobial agents and chemotherapy*. 2010;54(1):397-404.
617. Knezevic P, Petrovic O. A colorimetric microtiter plate method for assessment of phage effect on *Pseudomonas aeruginosa* biofilm. *Journal of microbiological methods*. 2008;74(2-3):114-8.
618. Doolittle MM, Cooney JJ, Caldwell DE. Tracing the interaction of bacteriophage with bacterial biofilms using fluorescent and chromogenic probes. *J Ind Microbiol*. 1996;16(6):331-41.
619. Wagner T, Soong G, Sokol S, Saiman L, Prince A. Effects of azithromycin on clinical isolates of *Pseudomonas aeruginosa* from cystic fibrosis patients. *Chest*. 2005;128(2):912-9.
620. Ichimiya T, Takeoka K, Hiramatsu K, Hirai K, Yamasaki T, Nasu M. The influence of azithromycin on the biofilm formation of *Pseudomonas aeruginosa* in vitro. *Chemotherapy*. 1996;42(3):186-91.
621. Anwar H, Strap JL, Chen K, Costerton JW. Dynamic Interactions of Biofilms of Mucoid *Pseudomonas-Aeruginosa* with Tobramycin and Piperacillin. *Antimicrobial agents and chemotherapy*. 1992;36(6):1208-14.
622. Ceri H, Olson ME, Stremick C, Read RR, Morck D, Buret A. The Calgary Biofilm Device: New technology for rapid determination of antibiotic susceptibilities of bacterial biofilms. *Journal of clinical microbiology*. 1999;37(6):1771-6.
623. Kaplan JB. Antibiotic-induced biofilm formation. *Int J Artif Organs*. 2011;34(9):737-51.
624. Pirnay JP, De Vos D, Verbeken G, Merabishvili M, Chanishvili N, Vaneechoutte M, et al. The phage therapy paradigm: pret-a-porter or sur-mesure? *Pharmaceutical research*. 2011;28(4):934-7.
625. Griesenbach U, Alton EW. Moving forward: cystic fibrosis gene therapy. *Human molecular genetics*. 2013;22(R1):R52-8.
626. Lusiak-Szelachowska M, Zaczek M, Weber-Dabrowska B, Miedzybrodzki R, Klak M, Fortuna W, et al. Phage Neutralization by Sera of Patients Receiving Phage Therapy. *Viral immunology*. 2014.
627. Lentz YK, Worden LR, Anchordoquy TJ, Lengsfeld CS. Effect of jet nebulization on DNA: identifying the dominant degradation mechanism and mitigation methods. *J Aerosol Sci*. 2005;36(8):973-90.
628. Davison PF. The Effect of Hydrodynamic Shear on the Deoxyribonucleic Acid from T(2) and T(4) Bacteriophages. *Proc Natl Acad Sci U S A*. 1959;45(11):1560-8.

629. Manunta MD, McAnulty RJ, Tagalakis AD, Bottoms SE, Campbell F, Hailes HC, et al. Nebulisation of receptor-targeted nanocomplexes for gene delivery to the airway epithelium. *PLoS one*. 2011;6(10):e26768.
630. Ari A, de Andrade AD, Sheard M, AlHamad B, Fink JB. Performance Comparisons of Jet and Mesh Nebulizers Using Different Interfaces in Simulated Spontaneously Breathing Adults and Children. *Journal of aerosol medicine and pulmonary drug delivery*. 2015;28(4):281-9.
631. Cooper CJ, Denyer SP, Maillard JY. Stability and purity of a bacteriophage cocktail preparation for nebulizer delivery. *Letters in applied microbiology*. 2014;58(2):118-22.
632. Sahota JS, Smith CM, Radhakrishnan P, Winstanley C, Goderdzishvili M, Chanishvili N, et al. Bacteriophage Delivery by Nebulization and Efficacy Against Phenotypically Diverse *Pseudomonas aeruginosa* from Cystic Fibrosis Patients. *J Aerosol Med Pulm Drug Deliv*. 2015;28(5):353-60.
633. Williams OW, Sharafkhaneh A, Kim V, Dickey BF, Evans CM. Airway mucus: From production to secretion. *American journal of respiratory cell and molecular biology*. 2006;34(5):527-36.
634. Verkman AS, Song Y, Thiagarajah JR. Role of airway surface liquid and submucosal glands in cystic fibrosis lung disease. *American journal of physiology Cell physiology*. 2003;284(1):C2-15.
635. Labiris NR, Dolovich MB. Pulmonary drug delivery. Part I: physiological factors affecting therapeutic effectiveness of aerosolized medications. *Br J Clin Pharmacol*. 2003;56(6):588-99.
636. Sanders NN, De Smedt SC, Van Rompaey E, Simoens P, De Baets F, Demeester J. Cystic fibrosis sputum: a barrier to the transport of nanospheres. *Am J Respir Crit Care Med*. 2000;162(5):1905-11.
637. Proesmans M, Balinska-Miskiewicz W, Dupont L, Bossuyt X, Verhaegen J, Hoiby N, et al. Evaluating the "Leeds criteria" for *Pseudomonas aeruginosa* infection in a cystic fibrosis centre. *The European respiratory journal : official journal of the European Society for Clinical Respiratory Physiology*. 2006;27(5):937-43.
638. Sausseureau E, Vachier I, Chiron R, Godbert B, Sermet I, Dufour N, et al. Effectiveness of bacteriophages in the sputum of cystic fibrosis patients. *Clin Microbiol Infect*. 2014;20(12):O983-90.
639. Spilker T, Coenye T, Vandamme P, LiPuma JJ. PCR-based assay for differentiation of *Pseudomonas aeruginosa* from other *Pseudomonas* species recovered from cystic fibrosis patients. *Journal of clinical microbiology*. 2004;42(5):2074-9.
640. Foweraker JE, Loughton CR, Brown DF, Bilton D. Phenotypic variability of *Pseudomonas aeruginosa* in sputa from patients with acute infective exacerbation of cystic fibrosis and its impact on the validity of antimicrobial susceptibility testing. *The Journal of antimicrobial chemotherapy*. 2005;55(6):921-7.
641. Govan JR. Multidrug-resistant pulmonary infection in cystic fibrosis--what does 'resistant' mean? *Journal of medical microbiology*. 2006;55(Pt 12):1615-7.
642. Henry M, Lavigne R, Debarbieux L. Predicting In Vivo Efficacy of Therapeutic Bacteriophages Used To Treat Pulmonary Infections. *Antimicrobial agents and chemotherapy*. 2013;57(12):5961-8.
643. Treggiari MM, Retsch-Bogart G, Mayer-Hamblett N, Khan U, Kulich M, Kronmal R, et al. Comparative efficacy and safety of 4 randomized regimens to treat early *Pseudomonas aeruginosa* infection in children with cystic fibrosis. *Archives of pediatrics & adolescent medicine*. 2011;165(9):847-56.
644. Kumar S, Huang J, Abbassi-Ghadi N, Mackenzie HA, Veselkov KA, Hoare JM, et al. Mass Spectrometric Analysis of Exhaled Breath for the Identification of Volatile Organic Compound Biomarkers in Esophageal and Gastric Adenocarcinoma. *Annals of surgery*. 2015.
645. UK CR. Oesophageal cancer survival statistics2014. Available from: <http://www.cancerresearchuk.org/health-professional/cancer-statistics/statistics-by-cancer-type/oesophageal-cancer/survival#heading-Zero>.
646. Taverna G, Tidu L, Grizzi F, Torri V, Mandressi A, Sardella P, et al. Olfactory system of highly trained dogs detects prostate cancer in urine samples. *The Journal of urology*. 2015;193(4):1382-7.

647. McCulloch M, Jezierski T, Broffman M, Hubbard A, Turner K, Janecki T. Diagnostic accuracy of canine scent detection in early- and late-stage lung and breast cancers. *Integrative cancer therapies*. 2006;5(1):30-9.
648. Church J, Williams H. Another sniffer dog for the clinic? *Lancet*. 2001;358(9285):930-.
649. Rooney NJ, Morant S, Guest C. Investigation into the Value of Trained Glycaemia Alert Dogs to Clients with Type I Diabetes. *PloS one*. 2013;8(8).
650. van Heeckeren AM, Schluchter MD. Murine models of chronic *Pseudomonas aeruginosa* lung infection. *Lab Anim*. 2002;36(3):291-312.
651. Hoffmann N, Rasmussen TB, Jensen PO, Stub C, Hentzer M, Molin S, et al. Novel mouse model of chronic *Pseudomonas aeruginosa* lung infection mimicking cystic fibrosis. *Infection and immunity*. 2005;73(4):2504-14.

Appendix

A1: Consent form for Collection of Exhaled Breath and Sputum (Version 4 – 04/FEB/2014)

Study Number:

Patient Identification Number for this study:

PATIENT CONSENT FORM

Title of Project: Non-invasive physiological biomarkers in health and disease

Chief Investigator: Professor Andrew Bush

Please initial boxes

1. I confirm that I have read and understood the information sheet dated 04/FEB/2014 (Version 4) for the above study. I have had the opportunity to consider the information, ask questions and have had these answered satisfactorily.
2. I understand that my participation is voluntary and that I am free to withdraw at any time, without giving any reason, without my medical care or legal rights being affected.
3. I understand that sections of any of my medical notes may be looked at by responsible individuals from regulatory authorities where it is relevant to my taking part in research. I give permission for these individuals to have access to my records.
4. I understand that samples from the study will be stored for up to 10 years and may be used in the future for similar tests. Any remaining samples (e.g. sputum) at the end of this period may be transferred to an approved tissue bank.
5. I agree to my GP being informed of my participation in the study.
6. I agree to take part in the above study.

Name of Patient

Date

Signature

Name of Person taking consent

Date

Signature

When completed, 1 for patient; 1 for researcher site file; 1 (original) to be kept in medical notes

A2: Absorbance and Fluorescence of iRFP and Wild Type PAO1 with and without Phage Treatment

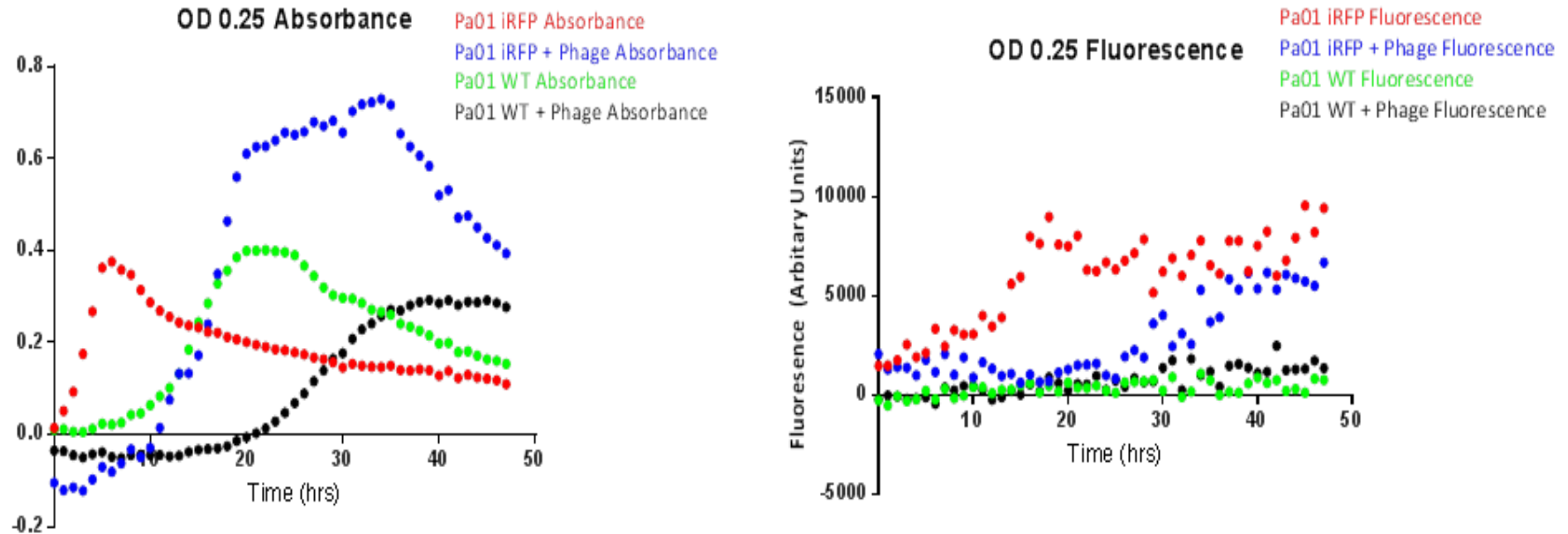


Figure A2.1: Graph showing absorbance and fluorescence over time for wild type (WT) PaO1 and iRFP PaO1 with a starting optical density of 0.25. Note that, although fluorescence of iRFP is reduced over the entire 48hr period when phage is added (blue line compared to red line), indicating impairment of growth by phage, absorbance of iRFP PaO1 is paradoxically higher. This again suggests, as with lower starting optical densities (Figure 11.2.4.1), that absorbance is not an accurate proxy measure of bacterial density. Furthermore, it is concerning that the peak fluorescence of non-treated PaO1 iRFP is only around 10000 when starting optical density is 0.25, compared to 17796 when starting OD was 0.05 and almost 15000 when starting OD was 0.1 (Figure 11.2.4.1); if fluorescence is an accurate and linear proxy measure of bacterial density, this suggests that there is significantly less growth in the wells where starting optical density was 0.25. This might be explained by the fact that, at higher starting optical densities, there is more competition for limited nutrients and bacterial growth may therefore be reduced. However, if that was the case, lower fluorescence would be expected with even higher starting optical densities and, as shown in Figure A2.2 (overleaf), peak optical density of PaO1 iRFP with a starting optical density of 0.5 exceeds that of PaO1 iRFP with a starting optical density of 0.25. These findings raise concerns about the feasibility of using PaO1 iRFP as a non-invasive measure of phage activity as they indicate that the relationship between fluorescence and bacterial density may not be linear.

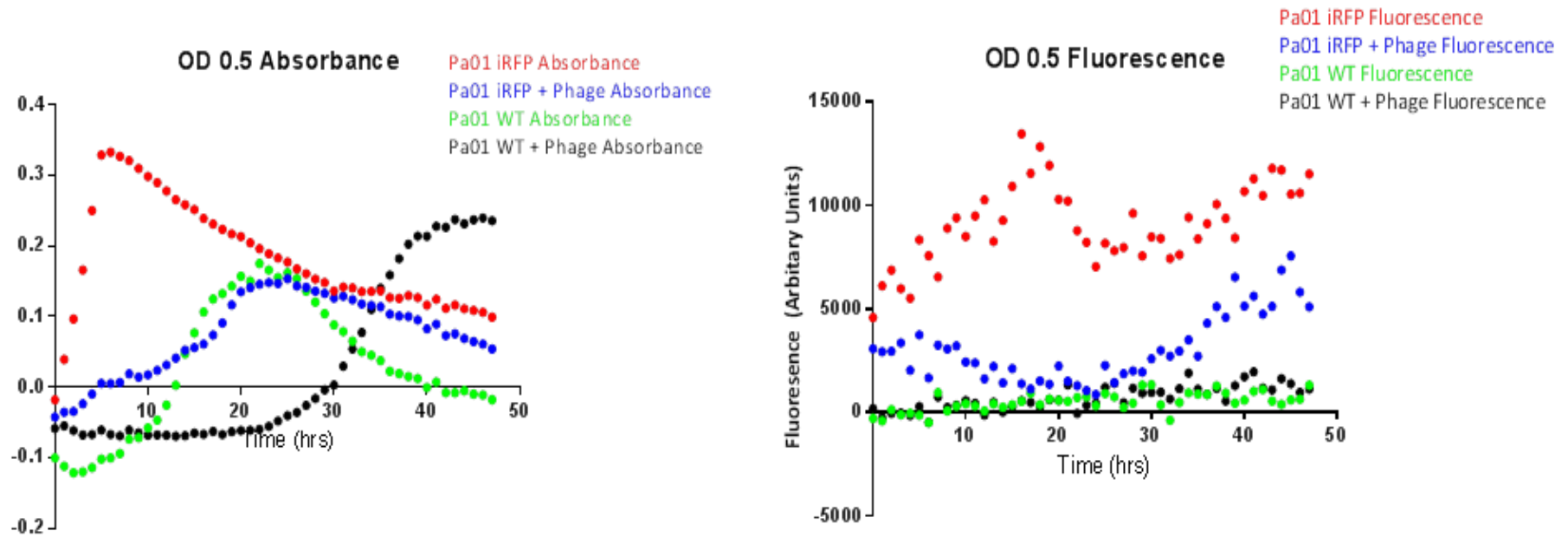


Figure A2.2: Graph showing absorbance and fluorescence over time for wild type (WT) Pa01 and iRFP Pa01 with a starting optical density of 0.5. As with lower starting optical densities, fluorescence of iRFP Pa01 is reduced in phage-treated wells. However, unlike in previous graphs, absorbance is also lower, although the curves do not mirror the shape of the fluorescence curves. This is most notable for iRFP + Phage (blue line) where fluorescence is increasing from around 24hrs, suggesting ongoing growth, whilst absorbance is decreasing which paradoxically indicates reduced bacterial density. As discussed in Figure A2.1, it is difficult to account for the difference in magnitude of peak fluorescence observed at each of the starting optical densities; the peak for 0.05 and 0.1 exceeds that of 0.25 and 0.5 and, whilst this might be explained by increased competition for nutrients at higher starting optical densities, it would be reasonable to expect that all wells (containing the same amount of liquid culture medium) could sustain growth to a critical point (signified by comparable peak fluorescence) before dropping off. This appears not to be the case as fluorescence peaks at significantly lower levels in wells where starting optical density was higher, suggesting that using iRFP Pa01 fluorescence alone as a proxy measure of bacterial density is an overly simplistic approach that lacks accuracy.

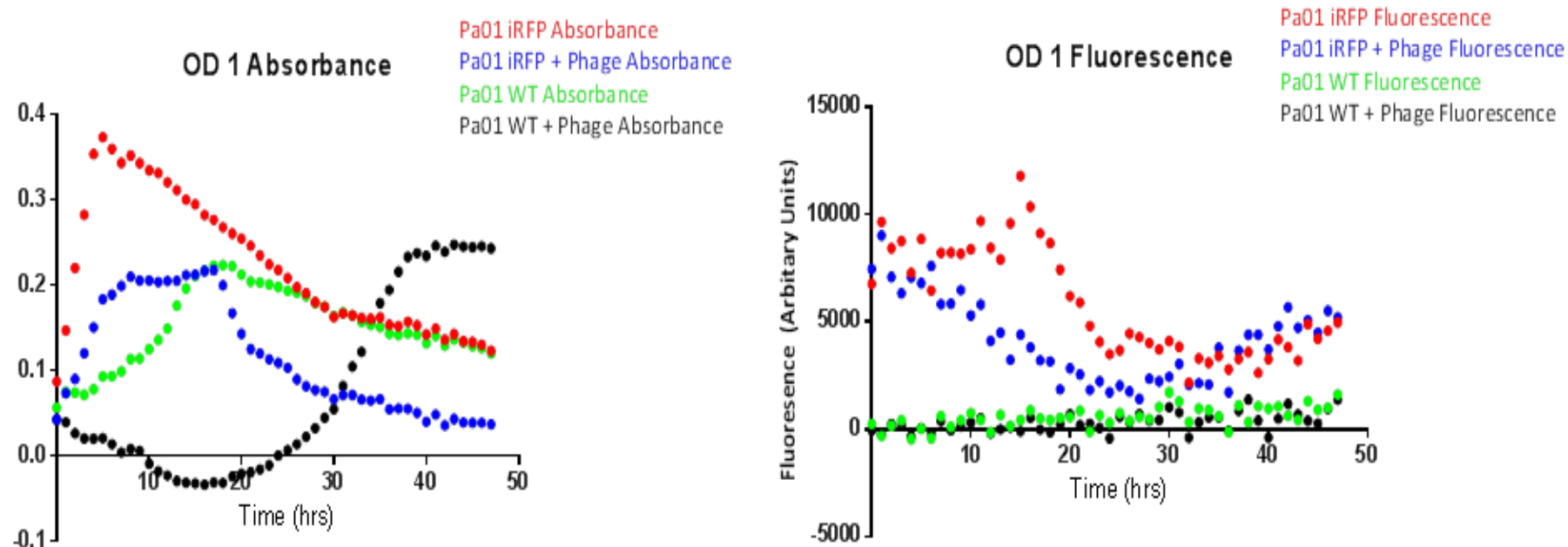


Figure A2.3: Graph showing absorbance and fluorescence over time for wild type (WT) Pa01 and iRFP Pa01 with a starting optical density of 1.0. As with lower starting optical densities, fluorescence of iRFP Pa01 is reduced in phage-treated wells. However, unlike in graphs for starting OD of 0.05, 0.1 and 0.25, absorbance is also lower, although the curves do not mirror the fluorescence curves. This is most notable for iRFP + Phage (blue line) where fluorescence is increasing from around 20hrs, suggesting ongoing growth, whilst absorbance is decreasing which indicates reduced bacterial density. As discussed in Figure A2.1, it is difficult to account for the difference in magnitude of peak fluorescence observed at each of the starting optical densities; the peak for 0.05 and 0.1 exceeds that of 0.25, 0.5 and 1.0 and, whilst this might be explained by increased competition for nutrients at higher starting optical densities, it would be reasonable to expect that all wells (containing the same amount of liquid culture medium) could sustain growth to a critical point (signified by comparable peak fluorescence) before dropping off. This appears not to be the case as fluorescence peaks at significantly lower levels in wells where starting optical density was higher, suggesting that using iRFP Pa01 fluorescence alone as a proxy measure of bacterial density is an overly simplistic approach that lacks accuracy.

[A3: Insert from MesoScale Discovery Multiplex Kit for Cytokine Measurements](#)

MSD[®] MULTI-SPOT Assay System

Mouse Pro-Inflammatory 7-Plex
Ultra-Sensitive Kit

1-Plate Kit	K15012C-1
5-Plate Kit	K15012C-2
25-Plate Kit	K15012C-4



www.mesoscale.com[®]

MSD Biomarker Assays

Mouse ProInflammatory 7-Plex Ultra-Sensitive Kit

IL-1 β , IL-12p70, IFN- γ , IL-6, KC/GRO, IL-10, TNF- α

This package insert must be read in its entirety before using this product.

FOR RESEARCH USE ONLY.

NOT FOR USE IN DIAGNOSTIC PROCEDURES.

Meso Scale Discovery

A division of Meso Scale Diagnostics, LLC.

9238 Gaither Road

Gaithersburg, MD 20877 USA

www.mesoscale.com

Meso Scale Discovery, Meso Scale Diagnostics, www.mesoscale.com, MSD, MSD (design), Discovery Workbench, Quickplex, Multi-Array, Multi-Spot, Sulfo-Tag and Sector are trademarks and/or service marks of Meso Scale Diagnostics, LLC.

© 2010 Meso Scale Discovery a division of Meso Scale Diagnostics, LLC. All rights reserved.

Table of Contents

Introduction	271
Principle of the Assay	272
Reagents Supplied	273
Required Material and Equipment (not supplied)	273
Safety	273
Reagent Preparation	274
Assay Protocol	276
Analysis of Results	276
Typical Standard Curve	277
Sensitivity	278
Assay Components	278
Summary Protocol	279
Plate Diagrams	280

Ordering Information

MSD Customer Service

Phone: 1-301-947-2085
Fax: 1-301-990-2776
Email: CustomerService@mesoscale.com

MSD Scientific Support

Phone: 1-301-947-2025
Fax: 1-240-632-2219 attn: Scientific Support
Email: ScientificSupport@mesoscale.com

Introduction

Inflammatory processes are involved in many physiological events, including infection, the healing response, and other disease states such as autoimmunity. Cytokines and chemokines are small, soluble proteins that can help mediate both acute and chronic inflammatory responses.

Interleukin (IL)-1 β is produced by dendritic cells, monocytes, macrophages and certain epithelial cells. IL-1 β is produced in response to infection induced inflammation. It induces the production of adhesion molecules that enable the transmigration of leukocytes into inflamed tissues. IL-1 β also participates in fever induction by the hypothalamus.

IL-12p70 is the active heterodimer of IL-12, consisting of the p40 and p35 subunits. IL-12 participates in the differentiation of naïve T cells in Th1 cells. It stimulates the secretion of IFN- γ and TNF- α and inhibits IL-4 induced proliferation of lymphocytes. IL-12 plays an important role in the mediation of the cytotoxic activity of NK cells and CD8⁺ cytotoxic T cells. It is produced by dendritic cells, monocytes, macrophages, and B-cells in response to intra-cellular pathogens.

Interferon- γ (IFN- γ), also known as type two interferon, plays a role in the recruitment of leukocytes to the site of infection. IFN- γ is produced by Th1 cells and NK cells. IFN- γ activates macrophages by increasing the expression of major histocompatibility complex (MHC) molecules and antigen processing components. It has also been shown to contribute to immunoglobulin (Ig) class switching and suppress Th2 responses. IFN- γ enhances the effects of type one interferons, such as IFN- β .

IL-6 is a proinflammatory cytokine secreted by monocytes, macrophages and certain non-lymphoid cell types in response to tissue damage or infection. It plays a role in the acute phase response, the regulation of fever, and the generation of plasma B cells. IL-6 has been recently shown to act in concert with TGF- β to induce the differentiation of IL-17 producing helper T cells from naïve progenitors.

KC/GRO (keratinocyte chemoattractant; keratinocyte-derived chemokine/growth related oncogene) also known as CXCL1, GRO α , GRO1, NAP-3, and CINC (rat) is a small cytokine belonging to the C-X-C family of chemokines. KC/GRO is produced by macrophages, neutrophils and epithelial cells, and is involved in neutrophil chemoattractant activity. It plays a role in spinal cord development, angiogenesis, tumorigenesis and inflammation.

IL-10 inhibits the production of proinflammatory cytokines by T cells, and it is a potent suppressor of monocyte and macrophage functions. As such, it plays an important role in the regulation and termination of inflammatory responses. IL-10 also plays an important role in the growth and differentiation of B cells, NK cells, Th cells, and cytotoxic T cells. IL-10 is produced by macrophages and certain T cell subsets, including CD4⁺CD25⁺Foxp3⁺ regulatory T cells.

Tumor Necrosis Factor- α (TNF- α) plays a key role in the acute phase reaction and systemic inflammation. TNF- α is primarily produced by activated macrophages, but it is also secreted by a variety of other cell types under pathogenic conditions. Upon receptor binding, it has been shown to trigger diverse cell signaling pathways including apoptosis, proliferation, differentiation, chemoattraction, hypothalamic regulation, and cytokine production. TNF- α can also contribute to tumorigenesis and viral replication.

Principle of the Assay

MSD assays provide a rapid and convenient method for measuring the levels of protein targets within a single small-volume sample. The assays are available in both singleplex and multiplex formats. In a singleplex assay, an antibody for a specific protein target is coated on one electrode (or “spot”) per well. In a multiplex assay, an array of capture antibodies against different targets is patterned on distinct spots in the same well. The Mouse ProInflammatory 7-Plex Assay detects IL-1 β , IL-12p70, IFN- γ , IL-6, KC/GRO, IL-10, and TNF- α in a sandwich immunoassay format (Figure 1). MSD provides a plate that has been pre-coated with capture antibody on spatially distinct spots – antibodies for IL-1 β , IL-12p70, IFN- γ , IL-6, KC/GRO, IL-10, and TNF- α . The user adds the sample and a solution containing the labeled detection antibodies— anti-IL-1 β , anti-IL-12p70, anti-IFN- γ , anti-IL-6, anti-KC/GRO, anti-IL-10, and anti-TNF- α labeled with an electrochemiluminescent compound, MSD SULFO-TAG™ label—over the course of one or more incubation periods. Analytes in the sample bind to capture antibodies immobilized on the working electrode surface; recruitment of the labeled detection antibodies by bound analytes completes the sandwich. The user adds an MSD read buffer that provides the appropriate chemical environment for electrochemiluminescence and loads the plate into an MSD SECTOR® instrument for analysis. Inside the SECTOR instrument, a voltage applied to the plate electrodes causes the labels bound to the electrode surface to emit light. The instrument measures intensity of emitted light to afford a quantitative measure of IL-1 β , IL-12p70, IFN- γ , IL-6, KC/GRO, IL-10, and TNF- α present in the sample.

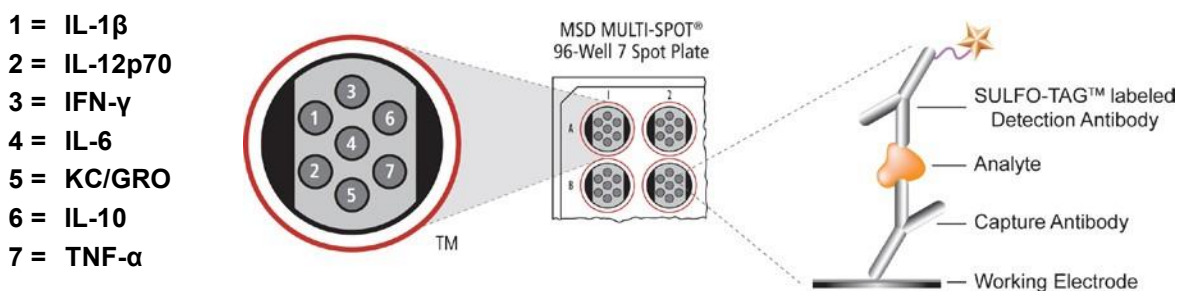


Figure 1. Spot diagram showing placement of analyte capture antibody. The numbering convention for the different spots is maintained in the software visualization tools, on the plate packaging, and in the data files. A unique bar code label on each plate allows complete traceability back to MSD manufacturing records.

Reagents Supplied

Product Description	Storage	Quantity per Kit		
		K15012C-1	K15012C-2	K15012C-4
MULTI-SPOT® 96-well 7-Spot Mouse ProInflammatory 7-Plex Plate N75012B-1	2–8°C	1 plate	5 plates	25 plates
SULFO-TAG Detection Antibody Blend ¹ (50X)	2–8°C	1 vial (75 µL)	1 vial (375 µL)	5 vials (375 µL ea)
Mouse ProInflammatory 7-Plex Calibrator Blend (1 µg/mL of each)	≤-70°C	1 vial (15 µL)	5 vials (15 µL ea)	25 vials (15 µL ea)
Diluent 4 R52BB-4 (8 mL) R52BB-3 (40 mL)	≤-10°C	1 bottle (8 mL)	1 bottle (40 mL)	5 bottles (40 mL ea)
Diluent 5 R52BA-4 (5 mL) R52BA-5 (25 mL)	≤-10°C	1 bottle (5 mL)	1 bottle (25 mL)	5 bottles (25 mL ea)
Read Buffer T (4X) R92TC-3 (50 mL) R92TC-2 (200 mL)	RT	1 bottle (50 mL)	1 bottle (50 mL)	2 bottles (200 mL ea)

Required Materials and Equipment - not supplied

- Deionized water for diluting concentrated buffers
- 50 mL tubes for reagent preparation
- 15 mL tubes for reagent preparation
- Microcentrifuge tubes for preparing serial dilutions
- Phosphate buffered saline plus 0.05% Tween-20 (PBS-T) for plate washing
- Appropriate liquid handling equipment for desired throughput, capable of dispensing 10 to 150 µL into a 96-well microtiter plate
- Plate washing equipment: automated plate washer or multichannel pipette
- Adhesive plate seals
- Microtiter plate shaker

Safety

Safe laboratory practices and personal protective equipment such as gloves, safety glasses, and lab coats should be used at all times during the handling of all kit components. All hazardous samples should be handled and disposed of properly, in accordance with local, state, and federal guidelines.

¹ SULFO-TAG conjugated detection antibodies should be stored in the dark.

Reagent Preparation

Bring all reagents to room temperature and thaw the Calibrator stock on ice.

Important: Upon first thaw, separate Diluent 4 and Diluent 5 into aliquots appropriate to the size of your assay needs. These diluents can go through up to three freeze-thaw cycles without significantly affecting the performance of the assay.

Prepare Calibrator and Control Solutions

MSD recommends the preparation of an 8-point standard curve consisting of at least 2 replicates of each point. Each well requires 25 μ L of Calibrator. For the assay, MSD recommends 4-fold serial dilution steps and Diluent 4 alone for the 8th point:

Standard	Mouse ProInflammatory 7-Plex Calibrator Blend (pg/mL)	Dilution Factor
100X Stock	1000000	
STD-01	10000	100
STD-02	2500	4
STD-03	625	4
STD-04	156	4
STD-05	39	4
STD-06	9.8	4
STD-07	2.4	4
STD-08	0	n/a

To prepare this 8-point standard curve for up to 4 replicates:

- 1) Prepare the highest Calibrator point (STD-01) by adding 10 μ L of the Mouse ProInflammatory 7-Plex Calibrator Blend to 990 μ L Diluent 4.
- 2) Prepare the next Calibrator by transferring 50 μ L of the Mouse ProInflammatory diluted Calibrator to 150 μ L Diluent 4. Repeat 4-fold serial dilutions 5 additional times to generate 7 Calibrators.
- 3) The recommended 8th Standard is Diluent 4 (i.e. zero Calibrator).

Notes:

- a. Alternatively, Calibrators can be prepared in the sample matrix or diluent of choice to verify acceptable performance in these matrices. In general, the presence of some protein (for example, 1% BSA) in the sample matrix is helpful for preventing loss of analyte by adsorption onto the sides of tubes, pipette tips, and other surfaces. If your sample matrix is serum-free tissue culture media, then the addition of 10% FBS or 1% BSA is recommended.
- b. The standard curve can be modified as necessary to meet specific assay requirements.

Dilution of Samples

Serum and Plasma

All solid material should be removed by centrifugation. Plasma prepared in heparin tubes commonly displays additional clotting following the thawing of the sample. Remove any additional clotted material by centrifugation. Avoid multiple freeze/thaw cycles for serum and plasma samples. Normal serum or plasma samples may not require a dilution prior to being used in the MSD Mouse ProInflammatory 7-Plex Assay. Serum or plasma with high levels of these analytes may require a dilution.

Tissue Culture

Tissue culture supernatant samples may not require dilution prior to being used in the MSD Mouse ProInflammatory 7-Plex Assay. If using serum-free medium, the presence of carrier protein (e.g., 1% BSA) in the solution is helpful to prevent loss of analyte to the labware. Samples from experimental conditions with extremely high levels of cytokines may require a dilution.

Other Matrices

Information on preparing samples in other matrices, including sputum, CSF, and tissue homogenates can be obtained by contacting MSD Scientific Support at 1-301-947-2025 or ScientificSupport@mesoscale.com.

Prepare Detection Antibody Solution

The Detection Antibody Blend is provided at 50X stock solution. The final concentration of the working Detection Antibody Solution should be at 1X. For each plate used, dilute a 60 μ L aliquot of the stock Detection Antibody Blend into 2.94 mL of Diluent 5.

Prepare Read Buffer

The Read Buffer should be diluted 2-fold in deionized water to make a final concentration of 2X Read Buffer T. Add 10 mL of 4X Read Buffer T to 10 mL of deionized water for each plate.

Prepare MSD Plate

This plate has been pre-coated with antibody for the analyte shown in Figure 1. The plate can be used as delivered; no additional preparation (e.g., pre-wetting) is required. The plate has also been exposed to a proprietary stabilizing treatment to ensure the integrity and stability of the immobilized antibodies.

Assay Protocol

- 1. Addition of Diluent 4:** Dispense 25 μL of Diluent 4 into each well. Seal the plate with an adhesive plate seal and incubate for 30 min with vigorous shaking (300–1000 rpm) at room temperature.
- 2. Addition of the Sample or Calibrator:** Dispense 25 μL of sample or Calibrator into separate wells of the MSD plate. Seal the plate with an adhesive plate seal and incubate for 2 hours with vigorous shaking (300–1000 rpm) at room temperature.
- 3. Wash and Addition of the Detection Antibody**
Solution: Wash the plate 3 times with PBS-T. Dispense 25 μL of the 1X Detection Antibody Solution into each well of the MSD plate. Seal the plate and incubate for 2 hours with vigorous shaking (300–1000 rpm) at room temperature.
- 4. Wash and Read:** Wash the plate 3 times with PBS-T. Add 150 μL of 2X Read Buffer T to each well of the MSD plate. Analyze the plate on the SECTOR Imager. Plates may be read immediately after the addition of Read Buffer.

Notes

Shaking a 96-well MSD plate typically accelerates capture at the working electrode.

Lower sample volumes such as 10 μL are feasible, but it may reduce assay sensitivity. If lower sample volume is utilized, then the volume of the Calibrators / Standard Curve should be adjusted in parallel.

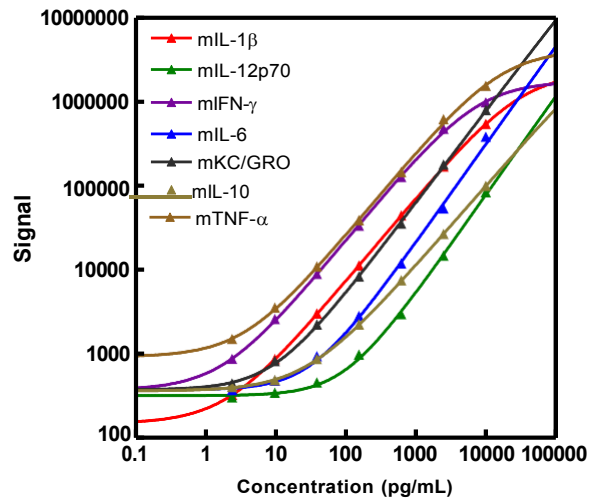
Bubbles in the fluid will interfere with reliable reading of plate. Use reverse pipetting techniques to insure bubbles are not created when dispensing the Read Buffer.

Analysis of Results

The Calibrators should be run in duplicate to generate a standard curve. The standard curve is modeled using least squares fitting algorithms so that signals from samples with known levels of the analyte of interest can be used to calculate the concentration of analyte in the sample. The assays have a wide dynamic range (3–4 logs) which allows accurate quantitation in many samples without the need for dilution. The MSD DISCOVERY WORKBENCH[®] analysis software utilizes a 4-parameter logistic model (or sigmoidal dose-response) and includes a $1/Y^2$ weighting function. The weighting function is important because it provides a better fit of data over a wide dynamic range, particularly at the low end of the standard curve.

Typical Standard Curve

The following standard curves are an example of the dynamic range of the assay. The actual signals may vary and a standard curve should be run for each set of samples and on each plate for the best quantitation of unknown samples.



IL-1 β		
Conc. (pg/mL)	Average Signal	%CV
0	163	8.4
2.4	324	3.8
9.8	861	2.6
39	2995	2.8
156	11104	1.8
625	43777	1.9
2500	166088	2.5
10000	534299	3.2

IL-12p70		
Conc. (pg/mL)	Average Signal	%CV
0	287	8.2
2.4	302	4.1
9.8	343	1.1
39	455	5.7
156	972	2.3
625	2938	4.8
2500	14542	2.0
10000	82687	4.4

IFN- γ		
Conc. (pg/mL)	Average Signal	%CV
0	303	7.3
2.4	868	3.0
9.8	2571	1.0
39	8831	1.0
156	33039	2.6
625	125242	2.1
2500	469071	1.5
10000	966829	2.9

IL-6		
Conc. (pg/mL)	Average Signal	%CV
0	310	2.8
2.4	369	4.4
9.8	479	7.8
39	932	6.8
156	2792	5.8
625	11793	8.6
2500	52767	5.8
10000	376903	4.0

KC/GRO		
Conc. (pg/mL)	Average Signal	%CV
0	320	7.8
2.4	443	3.8
9.8	813	5.4
39	2217	5.7
156	8220	8.3
625	34903	5.2
2500	175986	6.3
10000	780038	2.8

IL-10		
Conc. (pg/mL)	Average Signal	%CV
0	370	4.3
2.4	403	2.7
9.8	484	4.3
39	863	1.1
156	2215	3.2
625	7419	1.7
2500	26352	5.8
10000	98572	3.6

TNF- α		
Conc. (pg/mL)	Average Signal	%CV
0	826	9.0
2.4	1494	1.9
9.8	3519	3.6
39	10808	3.4
156	38325	4.5
625	143460	3.9
2500	607294	3.5
10000	1522508	2.6

Sensitivity

The lower limit of detection (LLOD) is the calculated concentration of the signal that is 2.5 standard deviations over the zero Calibrator. The values below represent the average LLOD over multiple kit lots.

	IL-1 β	IL-12p70	IFN- γ	IL-6	KC/GRO	IL-10	TNF- α
LLOD (pg/mL)	0.75	35	0.38	4.5	3.3	11	0.85

Assay Components

The mouse IL-1 β , IL-12p70, IFN- γ , IL-6, KC/GRO, IL-10, and TNF- α capture and detection antibodies used in this assay are listed below.

Analyte	Source species	
	MSD Capture Antibody	MSD Detection Antibody
mIL-1 β	Mouse Monoclonal	Goat Polyclonal
mIL-12p70	Rat Monoclonal	Goat Polyclonal
mIFN- γ	Rat Monoclonal	Rat Monoclonal
mIL-6	Rat Monoclonal	Goat Polyclonal
mKC/GRO	Rat Monoclonal	Goat Polyclonal
mIL-10	Rat Monoclonal	Goat Polyclonal
mTNF- α	Rat Monoclonal	Rat Monoclonal

Summary Protocol

MSD 96-well MULTI-SPOT Mouse ProInflammatory 7-Plex Ultra-Sensitive Kit

MSD provides this summary protocol for your convenience. Please read the entire detailed protocol prior to performing the MSD Mouse ProInflammatory 7-Plex Assay.

Sample and Reagent Preparation

Bring all reagents to room temperature and thaw the Calibrator stock on ice. If necessary, samples should be diluted in Diluent 4. Prepare Calibrator solutions and standard curve.

Use the 100X Calibrator stock to prepare an 8-point standard curve by diluting in Diluent 4.

Note: The standard curve can be modified as necessary to meet specific assay requirements.

Prepare Detection Antibody Solution by diluting Detection Antibody Blend to 1X in a final volume of 3.0 mL Diluent 5 per plate.

Prepare 20 mL of 2X Read Buffer T by diluting 4X Read Buffer T with deionized water.

SERUM OR PLASMA SAMPLES

Step 1: Add Diluent 4

Dispense 25 μ L/well Diluent 4.

Incubate at room temperature with vigorous shaking (300-1000 rpm) for 30 minutes.

Step 2: Add Sample or Calibrator

Dispense 25 μ L/well Calibrator or sample.

Incubate at room temperature with vigorous shaking (300-1000 rpm) for 2 hours.

Step 3: Wash and Add Detection Antibody Solution

Wash plate 3 times with PBS-T.

Dispense 25 μ L/well 1X Detection Antibody Solution.

Incubate at room temperature with vigorous shaking (300-1000 rpm) for 2 hours.

Step 4: Wash and Read Plate

Wash plate 3 times with

PBS-T. Dispense 150

μ L/well 2X Read Buffer T.

Analyze plate on SECTOR Imager instrument.

t.

	1	2	3	4	5	6	7	8	9	10	11	12
A	<input type="checkbox"/>	<input type="checkbox"/>	<input type="checkbox"/>	<input type="checkbox"/>	<input type="checkbox"/>	<input type="checkbox"/>	<input type="checkbox"/>	<input type="checkbox"/>	<input type="checkbox"/>	<input type="checkbox"/>	<input type="checkbox"/>	<input type="checkbox"/>
B	<input type="checkbox"/>	<input type="checkbox"/>	<input type="checkbox"/>	<input type="checkbox"/>	<input type="checkbox"/>	<input type="checkbox"/>	<input type="checkbox"/>	<input type="checkbox"/>	<input type="checkbox"/>	<input type="checkbox"/>	<input type="checkbox"/>	<input type="checkbox"/>
C	<input type="checkbox"/>	<input type="checkbox"/>	<input type="checkbox"/>	<input type="checkbox"/>	<input type="checkbox"/>	<input type="checkbox"/>	<input type="checkbox"/>	<input type="checkbox"/>	<input type="checkbox"/>	<input type="checkbox"/>	<input type="checkbox"/>	<input type="checkbox"/>
D	<input type="checkbox"/>	<input type="checkbox"/>	<input type="checkbox"/>	<input type="checkbox"/>	<input type="checkbox"/>	<input type="checkbox"/>	<input type="checkbox"/>	<input type="checkbox"/>	<input type="checkbox"/>	<input type="checkbox"/>	<input type="checkbox"/>	<input type="checkbox"/>
E	<input type="checkbox"/>	<input type="checkbox"/>	<input type="checkbox"/>	<input type="checkbox"/>	<input type="checkbox"/>	<input type="checkbox"/>	<input type="checkbox"/>	<input type="checkbox"/>	<input type="checkbox"/>	<input type="checkbox"/>	<input type="checkbox"/>	<input type="checkbox"/>
F	<input type="checkbox"/>	<input type="checkbox"/>	<input type="checkbox"/>	<input type="checkbox"/>	<input type="checkbox"/>	<input type="checkbox"/>	<input type="checkbox"/>	<input type="checkbox"/>	<input type="checkbox"/>	<input type="checkbox"/>	<input type="checkbox"/>	<input type="checkbox"/>
G	<input type="checkbox"/>	<input type="checkbox"/>	<input type="checkbox"/>	<input type="checkbox"/>	<input type="checkbox"/>	<input type="checkbox"/>	<input type="checkbox"/>	<input type="checkbox"/>	<input type="checkbox"/>	<input type="checkbox"/>	<input type="checkbox"/>	<input type="checkbox"/>
H	<input type="checkbox"/>	<input type="checkbox"/>	<input type="checkbox"/>	<input type="checkbox"/>	<input type="checkbox"/>	<input type="checkbox"/>	<input type="checkbox"/>	<input type="checkbox"/>	<input type="checkbox"/>	<input type="checkbox"/>	<input type="checkbox"/>	<input type="checkbox"/>

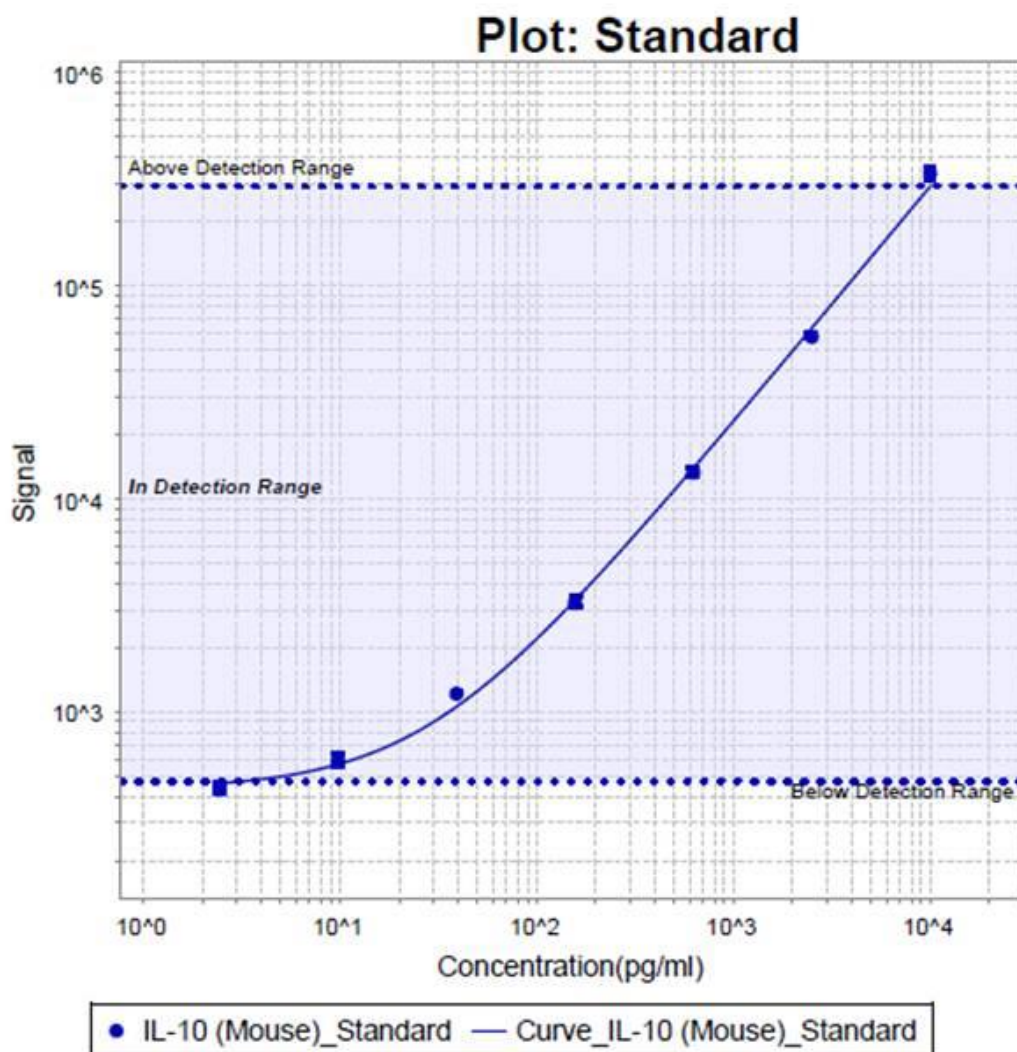
	1	2	3	4	5	6	7	8	9	10	11	12
A	<input type="checkbox"/>	<input type="checkbox"/>	<input type="checkbox"/>	<input type="checkbox"/>	<input type="checkbox"/>	<input type="checkbox"/>	<input type="checkbox"/>	<input type="checkbox"/>	<input type="checkbox"/>	<input type="checkbox"/>	<input type="checkbox"/>	<input type="checkbox"/>
B	<input type="checkbox"/>	<input type="checkbox"/>	<input type="checkbox"/>	<input type="checkbox"/>	<input type="checkbox"/>	<input type="checkbox"/>	<input type="checkbox"/>	<input type="checkbox"/>	<input type="checkbox"/>	<input type="checkbox"/>	<input type="checkbox"/>	<input type="checkbox"/>
C	<input type="checkbox"/>	<input type="checkbox"/>	<input type="checkbox"/>	<input type="checkbox"/>	<input type="checkbox"/>	<input type="checkbox"/>	<input type="checkbox"/>	<input type="checkbox"/>	<input type="checkbox"/>	<input type="checkbox"/>	<input type="checkbox"/>	<input type="checkbox"/>
D	<input type="checkbox"/>	<input type="checkbox"/>	<input type="checkbox"/>	<input type="checkbox"/>	<input type="checkbox"/>	<input type="checkbox"/>	<input type="checkbox"/>	<input type="checkbox"/>	<input type="checkbox"/>	<input type="checkbox"/>	<input type="checkbox"/>	<input type="checkbox"/>
E	<input type="checkbox"/>	<input type="checkbox"/>	<input type="checkbox"/>	<input type="checkbox"/>	<input type="checkbox"/>	<input type="checkbox"/>	<input type="checkbox"/>	<input type="checkbox"/>	<input type="checkbox"/>	<input type="checkbox"/>	<input type="checkbox"/>	<input type="checkbox"/>
F	<input type="checkbox"/>	<input type="checkbox"/>	<input type="checkbox"/>	<input type="checkbox"/>	<input type="checkbox"/>	<input type="checkbox"/>	<input type="checkbox"/>	<input type="checkbox"/>	<input type="checkbox"/>	<input type="checkbox"/>	<input type="checkbox"/>	<input type="checkbox"/>
G	<input type="checkbox"/>	<input type="checkbox"/>	<input type="checkbox"/>	<input type="checkbox"/>	<input type="checkbox"/>	<input type="checkbox"/>	<input type="checkbox"/>	<input type="checkbox"/>	<input type="checkbox"/>	<input type="checkbox"/>	<input type="checkbox"/>	<input type="checkbox"/>
H	<input type="checkbox"/>	<input type="checkbox"/>	<input type="checkbox"/>	<input type="checkbox"/>	<input type="checkbox"/>	<input type="checkbox"/>	<input type="checkbox"/>	<input type="checkbox"/>	<input type="checkbox"/>	<input type="checkbox"/>	<input type="checkbox"/>	<input type="checkbox"/>

A4: Examples of Standard Curves Generated from MesoScale Discovery Plates October 2012

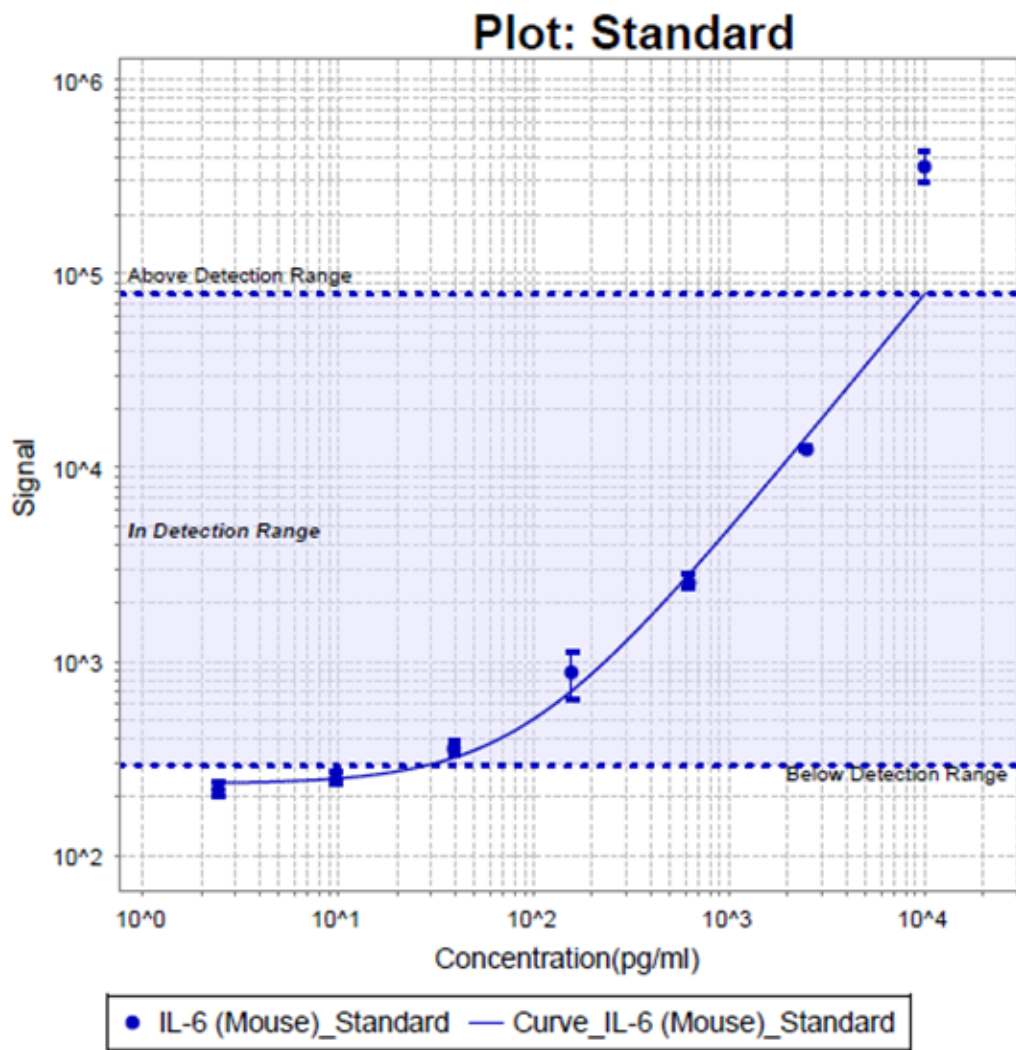
Experiment_20121030170927

30-Oct-2012

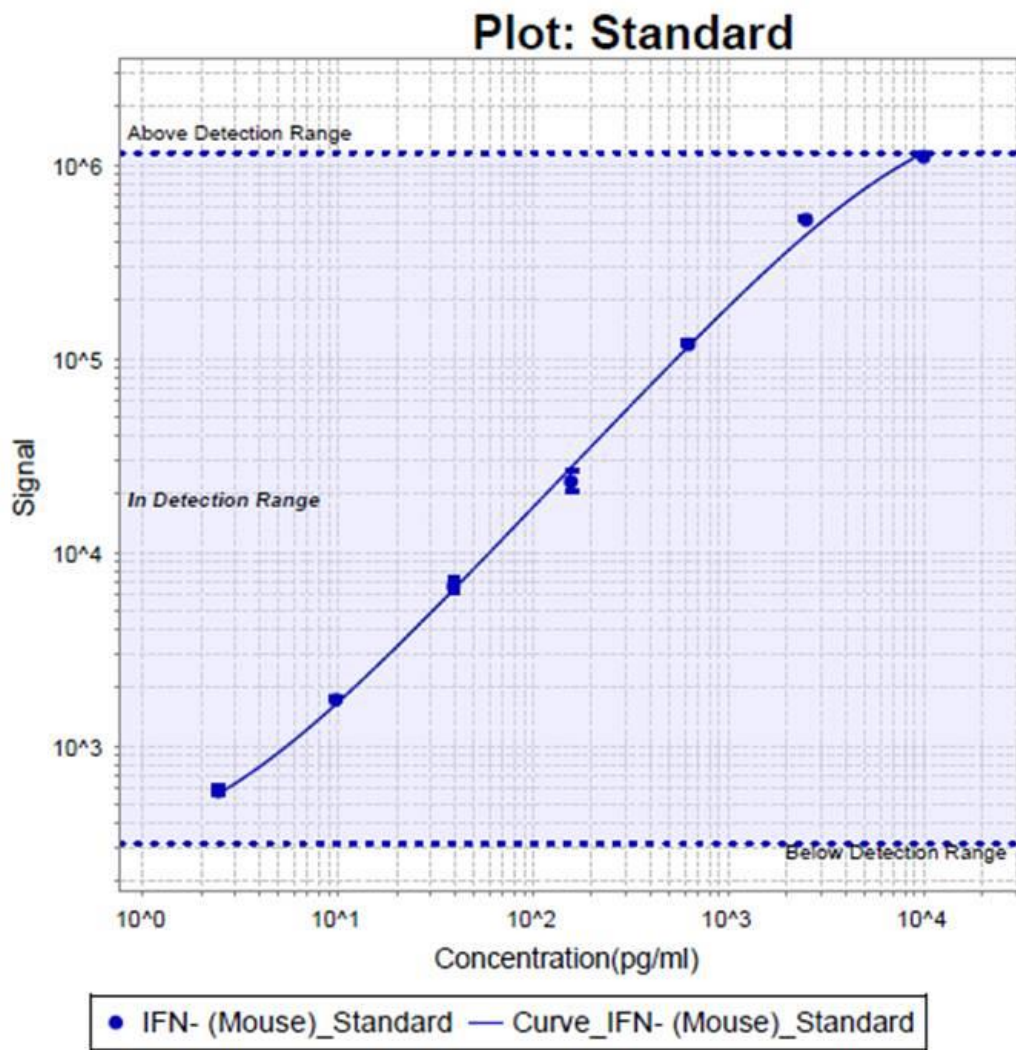
Plot: Standard



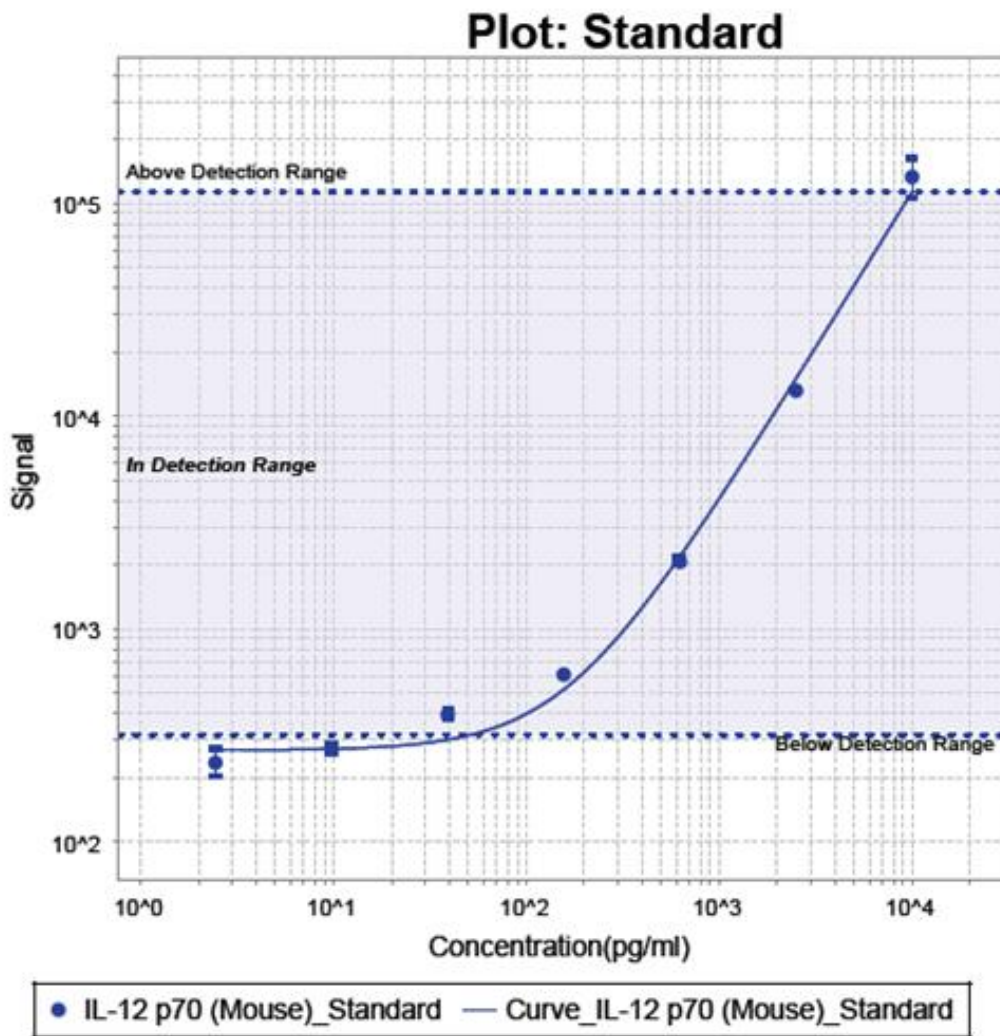
Plot: Standard



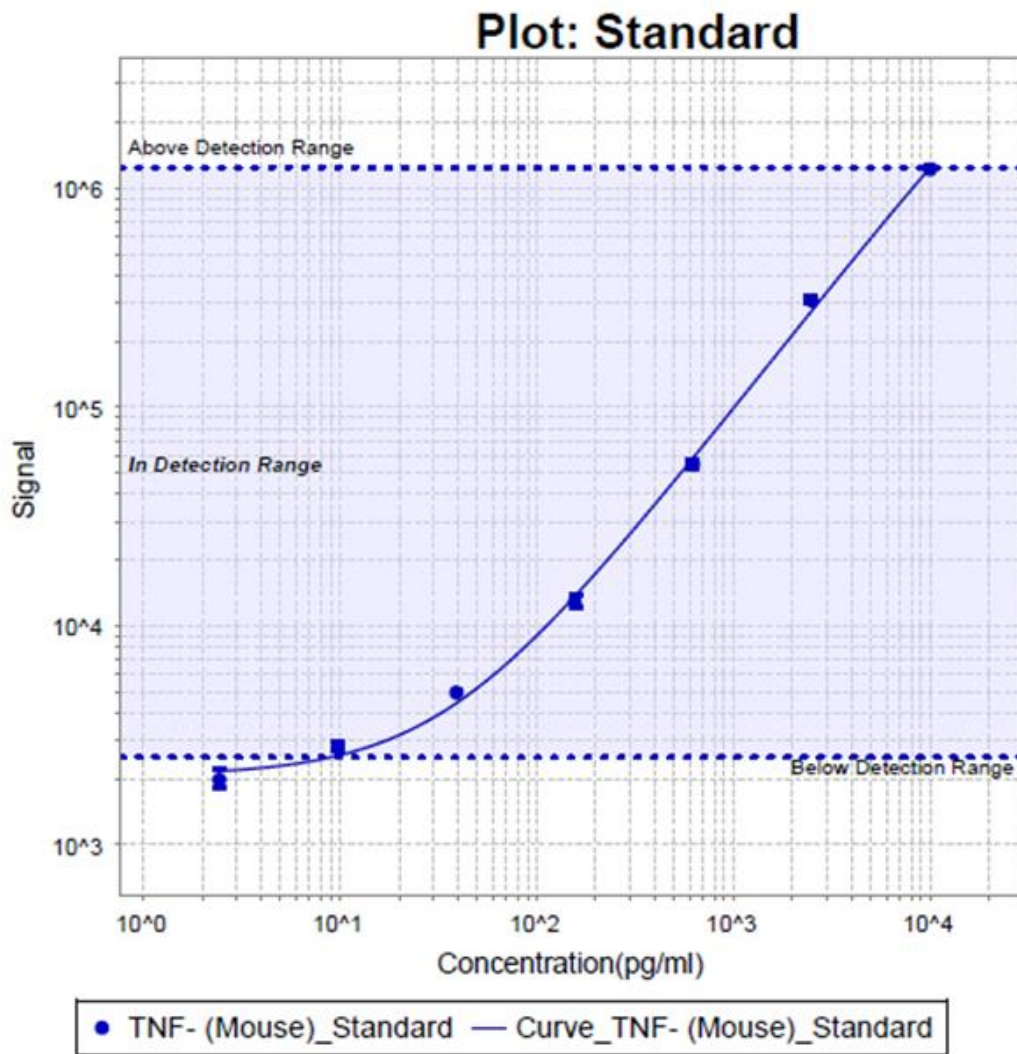
Plot: Standard



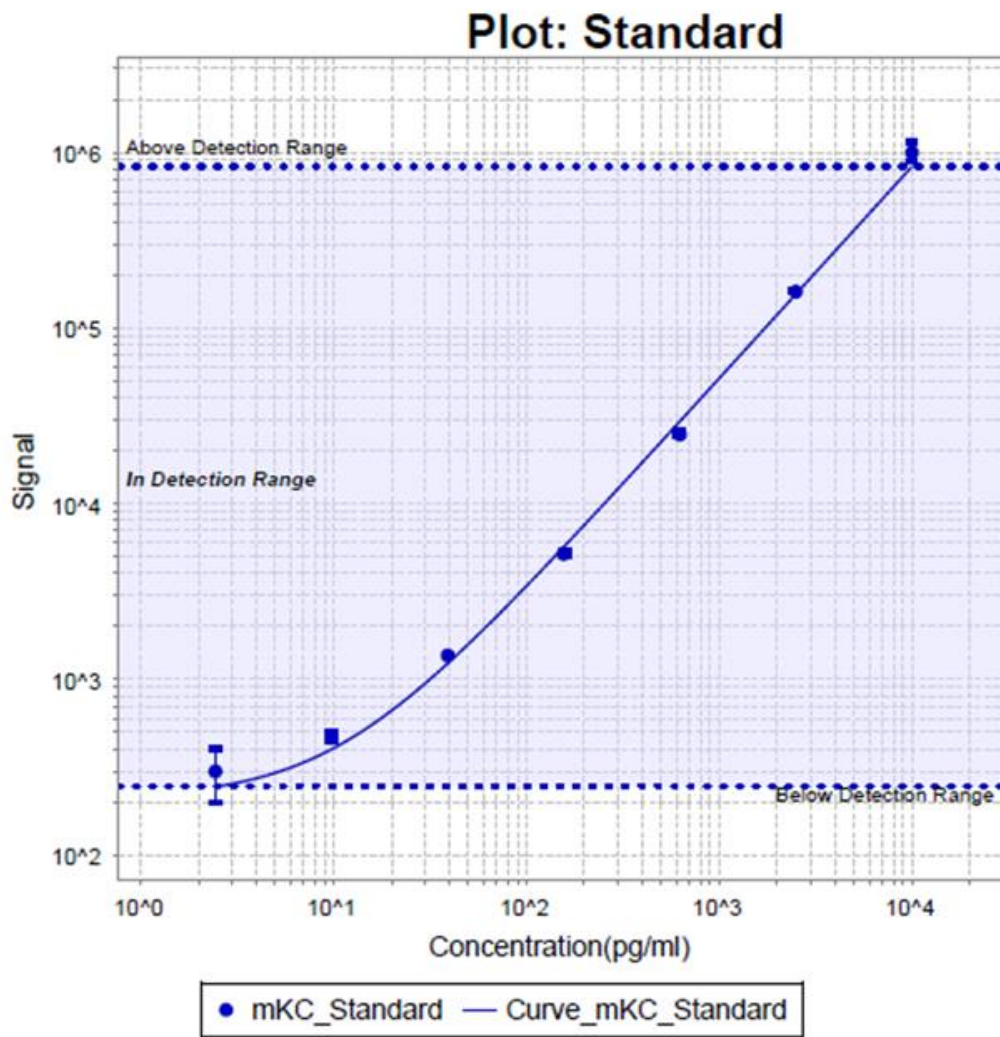
Plot: Standard



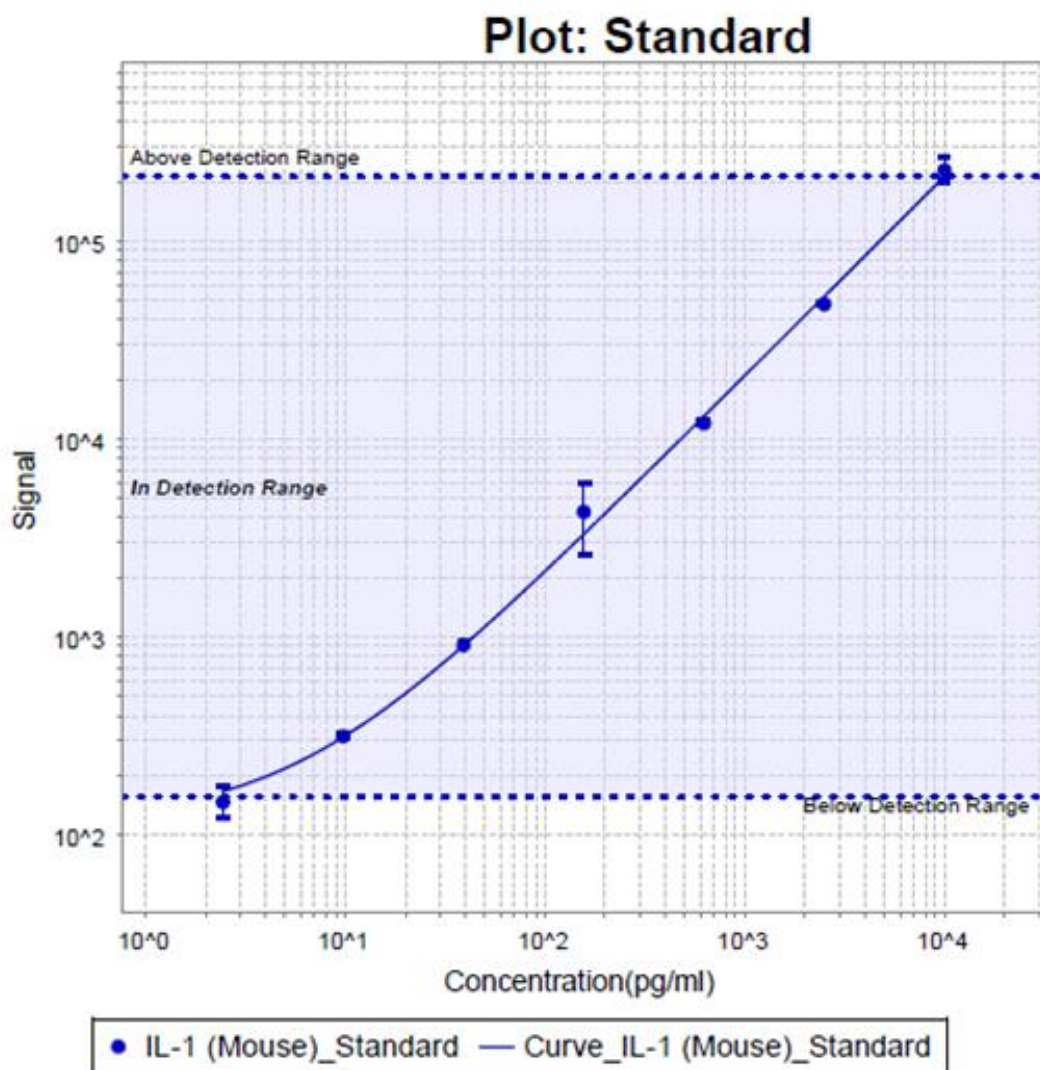
Plot: Standard



Plot: Standard



Plot: Standard



A5: SOP for Absolute Quantification of Bacteriophage Following Nebulisation



Standard Operating Procedures / Standardni Operativni Postopki

1. PURPOSE / NAMEN

This SOP provides information necessary to perform a spot test method for the titration of lytic bacteriophages.

2. SCOPE / PODROČJE UPORABE

The plaque assay method is used for measurement of potency/bioassay of bacteriophage samples.

3. RESPONSIBILITIES / ODGOVORNOSTI

The person who is working in Process Development (PD) Laboratory is responsible for complying with this procedure. Reading and understanding the SOP is required to perform this method.

4. DEFINITIONS / DEFINICIJE

4.1. VPB – Vegetable Peptone Broth

4.2. PFU – Plaque Forming Units

5. EQUIPMENT, MATERIALS, AND REAGENTS / OPREMA, MATERIALI IN REAGENTI

5.1. Equipment

- 5.1.1. Class 2 Biologic Safety Cabinet (PD-0008 or equivalent)
- 5.1.2. Spectrophotometer (PD-0010 or equivalent)
- 5.1.3. Incubator (PD-0016 or equivalent)
- 5.1.4. Water bath (PD-50058 / PD-50059 / PD-50060 or equivalent)
- 5.1.5. Pipette – 200 μ L (PD-0048 / PD-0054 or equivalent)
- 5.1.6. Pipette – 1000 μ L (PD-0053 / PD-0049 or equivalent)

5.2. Materials

- 5.2.1. Sterile disposable Inoculation loop (PN 50043 or equivalent)
- 5.2.2. 125 mL sterile Erlenmeyer flask with a cap (PN 90004 or equivalent)
- 5.2.3. Sterile 1.5 / 2 mL microcentrifuge tubes (PN 90008 / 90009 or equivalent)
- 5.2.4. Cuvettes (PN 90087 or equivalent)

Spot Test for Titration of Bacteriophages / Spot test za titracijo bakteriofagov
SOP-SPD-001 Version Original
Effective Date: 24 Jul 2014
Page 3 of 7

CONFIDENTIAL – DO NOT COPY OR DUPLICATE / ZAUPNO - NE KOPIRAJ

5.2.5. 15 mL falcon tubes (PN 50059 or equivalent)

5.2.6. 70 % alcohol (PN 50077 or equivalent)

5.3. Reagents

N/A

6. PROCEDURE / POSTOPKI

NOTE: Every step of the procedure when handling with bacteria or phage has to be done at performed sterile conditions under aseptic conditions in a BSC.

6.1. Preparation of Bacteria Culture Suspension

6.1.1. Prepare bacterial culture suspension as per SOP-SPD-003.

6.2. Preparation of Solid Agar Plates

6.2.1. Prepare solid agar plates as per SOP-SPD-006 or use purchased plates.

6.3. Preparation of Top Agar

6.3.1. Prepare Top Agar as per SOP-SPD-005.

6.3.2. Let Top-agar cool down to $50\text{ }^{\circ}\text{C} \pm 2\text{ }^{\circ}\text{C}$ in a water bath set at for 30 min (you should be able to pick up the jar without a glove).

6.3.3. Aliquot 3 mL of Top Agar into 15 mL sterile falcon tube.

6.3.4. Put falcon tube into Water bath set at $50\text{ }^{\circ}\text{C}$ until used for plaque assay

6.4. Dilution Buffer

6.4.1. Use VPB prepared as per SOP-SPD-005 as dilution buffer.

6.5. Preparation of Serial Dilutions of Phages

NOTE: Serial dilution is prepared according to expected number of phages in a sample. For example if expected PFU/mL is 1×10^8 PFU/mL then serial dilution is prepared up to dilution 10^7 . Dilutions 10^5 , 10^6 and 10^7 are plated.

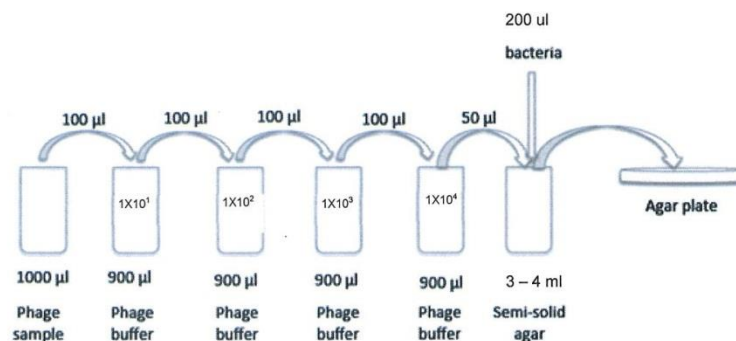
NOTE: During preparation of dilution series, buffer/media is pipetted first then follows pipetting sample.

Standard Operating Procedures / Standardni Operativni Postopki

NOTE: When sample is transferred from one vial to another vial or from vial to top agar, tips needs to go inside of second vial/top agar before the sample is pressed out into the dilution buffer/top agar. This pressing and releasing the pipette button has to be repeated 2-3 times in order to assure that no sample is left inside of the tips.

- 6.5.1. Use 1.5 mL sterile microcentrifuge tubes for preparation of serial dilution.
- 6.5.2. Use Vegetable peptone broth as dilution buffer (Prepared in section 6.4).
- 6.5.3. Dispense 900 μ L of VPB into each 1.5 mL sterile microcentrifuge tube.
- 6.5.4. Deposit 100 μ L of phage sample into first microcentrifuge tube labelled 10^{-1} . Recap tube.
- 6.5.5. Efficiently mix content of microcentrifuge tube by quickly inverting it 10 times.
- 6.5.6. Tap the tube to remove the liquid from the lid.
- 6.5.7. Remove 100 μ L from first microcentrifuge tube and deposit it into second microcentrifuge tube.
- 6.5.8. Repeat this dilution procedure until the desired dilution is reached.
- 6.5.9. An illustration of the sample dilution method is presented in Figure 1.

Figure 1: Sample Dilution Method



6.6. Preparation of Bacterial Overlay in Top Agar

- 6.6.1. Add 200 μ L of appropriate bacteria prepared in section 6.1. into the top agar prepared in section 6.3.
- 6.6.2. Mix gently by inverting the tube two to three times to avoid bubbles.

Standard Operating Procedures / Standardni Operativni Postopki

- 6.6.3. Pour the top agar media to agar plate and gently mix the plate.
 6.6.4. Leave plates at room temperature for 20 minutes to solidify.

6.7. Plating of Phage Dilutions

- 6.7.1. Spot 3 µL of phage dilutions onto the bacterial overlay, e.g. as shown in Attachment 1. Don't touch the pipette tip to the agar; just hold the tip slightly above the top agar, and push the droplet out slowly.
 6.7.2. Allow the spots to dry/sink into the overlay before moving the plate. Incubate the plate in the biosafety cabinet with the lid slightly open if required
 6.7.3. Leave plates at room temperature for 20 ± 5 min.
 6.7.4. Incubate plates. See incubation conditions in a table below

ID of working bacterial culture	Temperature	Time
Staphylococcus aureus (SPS 1216/ SPS1226)	37± 2 °C	20 ± 4 h
Pseudomonas aeruginosa (BC00629)	37± 2 °C	20 ± 4 h
Pseudomonas aeruginosa (SPS1430)	37± 2 °C	6 ± 1 h

6.8. Count of Plaque Forming Units (PFU) and Calculation of Phage Titer

- 6.8.1. After incubation, remove plates from the incubator.
 6.8.2. Count PFU on plates. To be able to see plaque you have to hold the plate up to the light. The acceptance criteria for PFU count is 5-100 PFU/spot. If the count is outside this range, the value is not used for calculation of titer. If only one value is inside of range then associated plaque dilution may not be used.
 6.8.3. If all phage dilutions of the series yield counts outside the acceptance range, the assay may be repeated by adjusting the dilutions.
 6.8.4. Calculate the number of phages per mL of diluted sample for all plates with valid plaque number (5-100 PFU/plate) using following equation:

$$\frac{PFU}{mL} = \frac{X}{0.003} \times D$$

Standard Operating Procedures / Standardni Operativni Postopki

Legend:

X: Average of the plate counts

D: Dilution

0.003: Amount of sample deposit on plate (mL)

6.8.5. If necessary Calculate the RSD

$$\%RSD = \frac{s}{\bar{x}} \times 100$$

where s is equal to the standard deviation, and \bar{x} is equal to the mean

7. DOCUMENT MANAGEMENT / UPRAVLJANJE Z DOKUMENTI

7.1. Paper Records Management

All result will be recorded in Laboratory notebook.

7.2. Electronic Records Management

There are no electronic records associated with this procedure.

8. REFERENCES / REFERENCE

8.1. SOPs

8.1.1. SOP-SPD-003 Preparation of bacterial culture suspension / Priprava bakterijske kulture

8.1.2. SOP-SPD-005 Media and Reagent preparation / Priprava gojišč in reagentov

8.1.3. SOP-SPD-006 Solid agar plates preparation / Priprava trdnih plošč

9. ATTACHMENTS / PRILOGE

N/A

A6: Abstracts arising from Thesis

Anti-Pseudomonal Bacteriophage Reduces Inflammatory Responses in the Murine Lung

Pabary R, Singh C, Morales S, Bush A, Alshafi K, Bilton D, Alton EFWF, Smithyman A and Davies JC

- Poster Presentation, North American CF Conference, Orlando, 2012
- Oral Presentation, UK CF Microbiology Consortium, Liverpool, November 2012
- Oral Presentation, British Thoracic Society Winter Meeting, London, December 2012
- Oral Presentation, European CF Conference, Lisbon, June 2013

SIFT-MS Analysis as a Non-Invasive Determinant of *Pseudomonas aeruginosa* Infection in CF Patients

Pabary R, Huang J, Kumar S, Alton EFWF, Bush A, Hanna GB, and Davies JC

- Poster Presentation, North American CF Conference, Salt Lake City, October 2013
- Oral Presentation, British Thoracic Society Winter Meeting, London, December 2013
- Oral Presentation, 9th CF Young Investigator Meeting, Paris, February 2014
- Oral Presentation, European CF Conference, Gothenburg, June 2014

Towards the Clinical Application of Anti-Pseudomonal Bacteriophages: Activity is Retained Following Nebulisation with a Range of Commercially Available Nebuliser Systems

Pabary R, Alegro A, Alton EFWF, Bilton D, Morales S, Smrekar F and Davies JC

- Poster Presentation, European CF Conference, Brussels, June 2015
- Oral Presentation, British Thoracic Society Winter Meeting, London, December 2015

Variability in Susceptibility to Antibiotics and Bacteriophages between Individual Colonies of *Pseudomonas aeruginosa* from cystic fibrosis sputum samples: Implications for Future Clinical Trial Design

Khoo V, Pabary R, Lund-Palau H, Turnbull A, Madden N, Schelenz S, Jones A, Morales S, Alton EFWF and Davies JC

- Oral Presentation, British Thoracic Society Winter Meeting, London, December 2015

A7: Papers arising from Thesis

1. Pabary R, Huang J, Kumar S, Alton EW, Bush A, Hanna GB and Davies JC. Does mass spectrometric breath analysis detect *Pseudomonas aeruginosa* in cystic fibrosis? *Eur Respir J* 2016 Mar; 47 (3): 994-7
2. Pabary R, Singh C, Morales S, Bush A, Alshafi K, Bilton D, Alton EW, Smithyman A and Davies JC. Antipseudomonal bacteriophage reduces infective burden and inflammatory response in murine lung. *Antimicrob Agents Chemother* 2015 Nov 16; 60 (2): 744-51